AFOSR SCIENTIFIC REPORT
AFOSR 70-2395TR

NATIONAL BUREAU OF STANDARDS REPORT

10 326

INTERIM REPORT ON THE THERMODYNAMICS OF CHEMICAL SPECIES IMPORTANT TO ROCKET TECHNOLOGY

(The previous reports in this series have the NBS Report Nos. 6297, 6484, 6645, 6928, 7093, 7192, 7437, 7587, 7796 8033, 8186, 8504, 8628, 8919, 9028, 9389, 9500, 9601, 9803, 9905, 10004, and 10074.)

U.S. DEPARTMENT OF COMMERCE
NATIONAL BUREAU OF STANDARDS

Qualified requestors may obtain additional copies from the Defense Documentation Center. All others should apply to the National Technical Information Service.

NATIONAL BUREAU OF STANDARDS REPORT

NBS PROJECT

232-0423
316-0401
316-0403
316-0405
316-0426

1 July 1970

NBS REPORT

10 326

INTERIM REPORT ON THE THERMODYNAMICS OF CHEMICAL SPECIES IMPORTANT TO ROCKET TECHNOLOGY

(The previous reports in this series have the NBS Report Nos. 6297, 6484, 6645, 6928, 7093, 7192, 7437, 7587, 7796, 8033, 8186, 8504, 8628, 8919, 9028, 9389, 9500, 9601, 9803, 9905, 10004 and 10074.)

Reference: U. S. Air Force, Office of Scientific Research, Agreement No. AFOSR-ISSA-69-001, Project No. 9750-01

NBS

U.S. DEPARTMENT OF COMMERCE

NATIONAL BUREAU OF STANDARDS

FOREWORD

Structure, propulsion, and guidance of new or improved weapons delivery systems are dependent in crucial areas of design on the availability of accurate thermodynamic data. Data on high-temperature materials, new rocket propellant ingredients, and combustion products (including exhaust ions) are, in many cases, lacking or unreliable. This broad integrated research program at the National Bureau of Standards supplies new or more reliable thermodynamic properties essential in several major phases of current propulsion development and application. Measured are compounds of those several chemical elements important in efficient propulsion fuels; those substances most affecting ion concentrations in such advanced propulsion concepts as ion propulsion; and the transition and other refractory metals (and their pertinent compounds) which may be suitable as construction materials for rocket motors, rocket nozzles, and nose cones that will be durable under extreme conditions of high temperature and corrosive environment. The properties determined extend in temperature up to 6000 degrees Kelvin. The principal research activities are experimental, and involve developing new measurement techniques and apparatus, as well as measuring heats of reaction, of fusion, and of vaporization; specific heats; equilibria involving gases; fast processes at very high temperatures; spectra of the infrared, matrix-isolation, microwave, and electronic types; and mass spectra. Some of these techniques, by relating thermodynamic properties to molecular or crystal structures, make it possible to tabulate reliably these properties over far wider ranges of temperature and pressure than those actually employed in the basic investigations.

ABSTRACT

This report presents in detail the results and critical analyses of several recently completed NBS experimental investigations, literature surveys, and developments of new measurement methods. The heat of formation of $C\ell F$ was measured by burning it with H_2 in a flame calorimeter; the result is shown to favor the new lower dissociation energy of F_2, 32.0 kcal per mol, but not unambiguously owing to uncertain interpretations of necessary auxiliary data. A transpiration search for chemical reaction between HF and gaseous $A\ell F_3$ revealed none detectable, near 1200 K and up to 0.75 atm of HF, beyond the sensitivity of the method (1-2%). Selected values of the standard heats, free energies, and entropies of formation of a number of niobium compounds resulting from an up-to-date critical review of the literature are discussed and tabulated. The heat capacity, electrical resistivity, and hemispherical total and normal spectral emittances of tantalum metal were measured by an accurate high-speed pulse technique from 1900 to 3200 K; the spectral emittance (at a wavelength of 650 nm) was found to decrease approximately 3.5% during the initial one-third of the melting period. The pulse heating technique is adapted to measuring the melting points of thin-wire electrical conductors above 2000 K, and checked by finding 2044 K (estimated uncertainty, $\pm$ 5 K) for platinum (accepted value, 2045 K). In designing a transpiration technique for seeking unknown higher gaseous hydrates of beryllia above 2000 K, the results of detailed calculations are presented which show that sufficiently accurate temperature measurement, dubious by pyrometer, can probably be met by comparison

with the volatility of gold and application of several corrections. The results of several investigations of barium and one of its compounds are presented. Accurate heat-capacity and enthalpy measurements on the metal from 18 to 1173 K show several anomalies, unusually high heat capacities, and a heat of fusion which is thought to reflect solubility of BaO impurity in the liquid metal. Based on these new thermal data, a "third-law" analysis was made of the existing vapor-pressure data, leading to a heat of sublimation of the metal whose uncertainty is believed to be due largely to uncertainties in the published vapor pressures. Atomic barium, deposited in solid-argon matrices containing isotopic varieties of O_2, yielded infrared values for two stretching frequencies of several isotopic forms of the BaO_2 molecule; the (much weaker) O-O stretching frequency is interpreted as evidence that the molecule is essentially $Ba^+ O_2^-$.

Thomas B. Douglas

Charles W. Beckett

TABLE OF CONTENTS

Chapter 1

THE ENTHALPY OF FORMATION OF CHLORINE MONOFLUORIDE AND ITS APPLICATION TO THE DISSOCIATION ENERGY OF FLUORINE

R L. Nuttall and G. T. Armstrong

Introduction

The enthalpy of the reaction

$$ClF(g) + H_2(g) + 100\ H_2O(\ell) = [HCl + HF + 100\ H_2O](\ell) \qquad (1)$$

was measured in a flame calorimeter. From the results of these measurements the enthalpy of formation, ΔH_f° (ClF), of chlorine monofluoride was calculated. The application of these results to the determination of the dissociation energy of fluorine is discussed.

Apparatus

The apparatus used is a flame calorimeter which has been developed and used in this laboratory over a period of several years. The latest version of the calorimeter was described in great detail by King and Armstrong [1]. The system used for these measurements is essentially the same as theirs. The calorimeter contains a combustion chamber in which the oxidizer, ClF, is burned in excess hydrogen. The combustion product gases then flow through two solution vessels in series where the soluble HCl and HF are absorbed. The excess hydrogen then flows out of the calorimeter through a heat exchanger which tempers the incoming gases. The hydrogen entering the calorimeter is saturated with water.

Materials

The chlorine monofluoride sample was obtained from Ozark-Mahoning Company, and is from the same lot of material as was used by Dibeler, Walker, and McCulloh [2] in their recent dissociative photoionization study. The sample contained 1.5 mole percent chlorine, as determined mass spectrometrically by Dibeler, et al. While the purity of the sample was less than desirable for thermochemical work, the effect of the chlorine impurity was small, because its participation in the reaction led to a thermal effect very close to that of the ClF, on a molar basis. No other impurities were detected in the mass spectrometric examination.

The hydrogen was from the same cylinder as was used by King and Armstrong. They report an analysis, in mole percent, as follows: H_2, 99.9; H_2O, 0.04±0.02; and N_2, 0.05±0.01.

Oxygen was a commercial high purity grade and is the same as used in this laboratory for bomb combustion experiments. The supplier reported a purity of better than 99.99 percent O_2. It was passed over CuO at 500°C and then through Ascarite in filling the sample bulb.

Calibration

The calorimeter was calibrated with electrical energy. The mean energy equivalent found from five experiments was

$$E_{cal} = 216969 \text{ J ohm}^{-1}$$

with a standard deviation of the mean of 15 J ohm^{-1}.

For these experiments the calorimeter was the same as used for the combustion experiments, with water in the solution vessels and gas flowing out of the calorimeter at the same rates.

The heater was the same one used by King and Armstrong [1] in their F_2O - H_2 - H_2O reaction study. The electrical measuring station was reassembled following the move of the laboratory, from Washington, D. C. to Gaithersburg, using the same instruments. The standard cells were replaced with a new set. They were calibrated after the move. The volt box and other standard resistors were also recalibrated after the move. These calibration experiments were interspersed with the combustion experiments. For the combustion experiments the energy equivalent was adjusted for the mass of reactants that entered and remained in the calorimeter to give the energy equivalent E, appropriate to the reaction energy measurements.

Oxygen - Hydrogen Experiments

Four experiments were made in which oxygen was burned in excess hydrogen. For these experiments the solution vessels were filled with water and the hydrogen was saturated with water before entering the calorimeter. The amount of reaction was determined from the amount of oxygen introduced as determined by weighing the sample bulb before and after the experiment. The oxygen was assumed to be 100% pure.

The results of these experiments gave as heats for the reaction

$$H_2(g) + 1/2\ O_2(g) = H_2O(\ell)$$

284331, 285635, 285252, 285667 J mol^{-1}

The mean value is $-\Delta H = 285.22$ kJ mol^{-1} with a standard deviation of the mean of 0.31 kJ mol^{-1} at the mean reaction temperature of 302.4 K. Adjustment to 298.15 K gives

$$-\Delta H_{298} = 285.36 \text{ kJ mol}^{-1}$$

This value can be compared with the value of 285.83 kJ mol^{-1} calculated from the selected value for the enthalpy of formation of water [3]. The difference is small enough to suggest that no gross systematic errors are present in our results.

Chlorine Monofluoride - Hydrogen - Water Experiments

Six experiments were made in which the enthalpy of reaction (1)

$$ClF(g) + H_2(g) + 100\ H_2O(\ell) \rightarrow [HCl + HF + 100\ H_2O](\ell) \qquad (1)$$

was measured. The procedures used were similar to those described in detail by King and Armstrong [1]. The sample of ClF was contained under pressure in a monel bulb and the amount used was determined by weighing the bulb before and after each experiment. The total acid formed in the reaction was measured by analyzing the solutions in the solution vessels. This gives another measure of the amount of reaction. As was found in previous studies [1] the total acid formed was less than calculated from the mass of sample. The deficiencies ranged from about one to about three percent. This deficiency is attributed to a side

reaction in which the combustion chamber and the burner tip react to form NiF_2. The deficiency of acid is used as a measure of the amount of this corrosion reaction. Because the heat evolved by the corrosion reaction is nearly the same as that by the main reaction (1), the corrected value for the energy of reaction (1) differs only very slightly from the value that would be obtained if all the ClF entering were presumed to have participated in reaction (1).

The results of these experiments are summarized in table 1. The items tabulated by line are: (1) Experiment number; (2) m_s is the mass of sample; (3) n_{ClF} is the number of moles of ClF determined from mass of sample and analysis of 98.5 mol percent; (4) n_{Cl_2} is the number of moles of Cl_2 in the sample calculated as 1.5 molepercent of sample; (5) n_{H^+}(calc) is the number of moles of acid expected if all the ClF reacted according to equation (1); (6) n_{H^+}(obs) is the number of moles of acid found by titrating the product solutions; (7) Δn_{H^+}(calc-obs) is the deficiency in acid, line (5) - line (6); (8) ΔR_c is the temperature rise of the calorimeter corrected for heat exchange with the jacket; (9) q(obs) is the observed heat evolved by the reaction (q(obs) = ΔR_c x E); (10) q(ign) is the heat generated by the spark used to ignite the flame; (11) $q(Cl_2)$ is the heat generated by n_{Cl_2} moles of Cl_2 reacting with H_2 to give $HCl \cdot 50H_2O$; (12) q(vap) is the heat liberated by condensation of the water vapor carried into the calorimeter by the reacting hydrogen; (13) q(temp) is the heat required to temper the reacting gases entering the calorimeter from room temperature; (14) q(corros) is the heat attributed to reaction with the burner and combustion chamber walls to form NiF_2.

It is calculated from the enthalpy of the hypothetical reaction $HF(aq,50\ H_2O) + 1/2Ni \rightarrow 1/2NiF_2 + 1/2H_2$ $\Delta H = \Delta H(corros)$ $q(corros) = \Delta H(corros) x$ $\Delta n_{H^+}(calc-obs)$; (15) q_r is the heat of n_{ClF} reacting according to equation (1). $q_r = q(obs) - q(ign) - q(Cl_2) - q(vap) - q(temp) - q(corros)$; (16)- $\Delta H_r = q_r$ (line(15))/n_{ClF} (line(3)); (17) - ΔH_r(mean) is the average of the values in line 16 and is the negative enthalpy of reaction (1); (18) Std dev of mean is the measure of precision of the measurements of ΔH_r in line (17) and is equal to

$$\sqrt{\frac{\Sigma_i(\Delta H_{ri} - \Delta H_r(mean))^2}{5 \times 6}}$$

The value of the enthalpy of reaction, -426.74 kJ mol^{-1}, given in table (1) refers to the temperature of 303 K. Adjustment to 298 K gives

$$\Delta H(298\ K) = -426.00\ kJ\ mol^{-1}$$
$$= -101.81\ kcal\ mol^{-1}$$

This value of the enthalpy of reaction (1) was combined with enthalpies of reactions (2), (3), and (4), which follow.

$$ClF(g) + H_2(g) + 100\ H_2O(\ell) = [HCl + HF + 100\ H_2O](\ell) \quad (1)$$
$$\Delta H = -426.00\ kJ\ mol^{-1}$$

$$1/2H_2(g) + 1/2Cl_2(g) + 50\ H_2O(\ell) = [HCl + 50\ H_2O](\ell) \quad (2)$$
$$\Delta H = -165.36 \pm 0.8\ kJ\ mol^{-1}$$

$$1/2H_2(g) + 1/2F_2(g) + 50\ H_2O(\ell) = [HF + 50\ H_2O](\ell) \quad (3)$$
$$\Delta H = -320.83 \pm 0.4\ kJ\ mol^{-1}$$

$$[HCl + 50\ H_2O](\ell) + [HF + 50\ H_2O](\ell) = [HCl + HF + 100\ H_2O](\ell) \quad (4)$$
$$\Delta H = 0.0 \pm 0.4\ kJ\ mol^{-1}$$

to give the enthalpy of formation of chlorine monofluoride

$$\Delta Hf_{298}\ (ClF) = -60.19\ kJ\ mol^{-1}$$

$$= -14.39\ kcal\ mol^{-1}$$

The value of the enthalpy of reaction (2) is from Wagman et al. [3], that for reaction (3) from King and Armstrong [1]. The enthalpy of reaction (4) is estimated.

The standard deviation of the mean enthalpy of reaction (1) given in table 1 is 452 J mol^{-1} taking double this as an uncertainty interval gives ±0.90 kJ mol^{-1}. Significant errors may exist in the calibration of the calorimeter and in the analysis of the sample. We estimate the uncertainty from these sources as: Calibration 0.1 percent or 0.43 kJ mol^{-1}; analysis 0.7 percent or 2.99 kJ mol^{-1}. These three values are combined by summing their squares to give an estimate the uncertainty interval of ±3.15 kJ mol^{-1}. Thus for reaction (1) we obtain

$$\Delta H_{r298} = -426.00 \pm 3.15\ kJ\ mol^{-1}$$

This value combined with the enthalpies of reactions (2), (3) and (4) gives for the enthalpy of formation of chlorine monofluoride (reaction 5)

$$\Delta Hf_{298}(ClF) = -60.2 \pm 3.3\ kJ\ mol^{-1}$$

$$= -14.4 \pm 0.8\ kcal\ mol^{-1}$$

Table 1. Calorimetric measurements of ClF - H_2 - H_2O reaction

	Expt. No.		1	2	3	4	5	6
(1)	m_s	g	3.3061	3.1177	2.5707	3.0677	3.1435	3.1096
(2)	n_{ClF}	mol	0.059536	0.056144	0.046293	0.055243	0.056608	0.055998
(3)	nCl_2	mol	0.00091	0.00085	0.00070	0.00084	0.00086	0.00085
(4)	n_{H^+}(calc)	mol	.12088	.11400	.09400	.11217	.11494	.11370
(5)	n_{H^+}(obs)	mol	.11928	.1106	.09205	.11113	.112	.11038
(6)	Δn_{H^+}(calc-obs)	mol	.00160	.00340	.00195	.00104	.00294	.00332
(7)	ΔR_c	Ω	.119203	.112864	.09329	.110626	.113372	.112266
(8)	q(obs)	J	25814.2	24441.5	20202.6	23956.8	24551.5	24312.
(9)	q(ign)	J	50	47	66	58	63	98
(10)	$q(Cl_2)$	J	295.2	278.4	229.5	273.9	280.7	277.7
(11)	q(vap)	J	87.4	82.4	68.0	81.1	83.1	82.2
(12)	q(temp)	J	-3.6	-3.4	-2.8	-3.4	-3.4	-3.4
(13)	q(corros)	J	7.72	16.34	9.35873	4.99	14.1	15.97
(14)	q_r	J	25377.5	24020.8	19832.6	23542.2	24114.	23841.6
(15)	$-\Delta H_r$	J mol^{-1}	426254.	427846.	428412.	426156.	425981.	425760.
(16)	$-\Delta H_r$(mean)	J mol^{-1}	426735.					
(17)	Std dev of mean	J mol^{-1}		452				

Application to the dissociation energy of fluorine

The dissociation energies of ClF, Cl_2 and F_2 are related to the enthalpy of formation ΔHf_0° of ClF by the following series of reactions.

(1) $ClF(g) \rightarrow Cl(g) + F(g)$ $\Delta H_0^\circ(1) = D_0^\circ(ClF)$ (6)

(2) $1/2Cl_2(g) \rightarrow Cl(g)$ $\Delta H_0^\circ(2) = 1/2D_0^\circ(Cl_2)$ (7)

(3) $1/2F_2(g) \rightarrow F(g)$ $\Delta H_0^\circ(3) = 1/2D_0^\circ(F_2)$ (8)

---

(4) $1/2Cl_2(g) + 1/2F_2(g) = ClF(g)$ $\Delta H_0^\circ(4) = \Delta Hf_0^\circ(ClF)$ (5)

$$\Delta H_0^\circ(4) = \Delta H_0^\circ(2) + \Delta H_0^\circ(3) - \Delta H_0^\circ(1)$$

We present here a resumé of the existing data, which, while not exhaustive, indicates the degree of confidence with which data for reactions (6), (7), and (5) can be used to calculate $\Delta H_0^\circ(8)$, the dissociation energy of fluorine.

Data applicable to an evaluation of the above process which will be considered here are (1) the dissociation energy of chlorine, (2) the ionization potential of chlorine atom, (3) the dissociation energy of ClF, (4) the dissociative ionization energy of ClF, (5) the enthalpy of reaction of chlorine and fluorine, (6) the equilibrium involving ClF_3, ClF, and F_2, (7) reactions of ClF and F_2 with NaCl, and (8) the reaction between ClF and hydrogen in the presence of water.

The dissociation energy of Cl_2

$$Cl_2 \rightarrow 2Cl \qquad (7a)$$

Values cited by Herzberg [4], the JANAF tables [5], and Wagman et al. [3] are listed in table 2 along with two recent determinations, by Rao and Venkateswarlu (1962) [6] and Douglas, Mueller and Stoicheff [7] (1963). The assignment of 881 cm^{-1} to the excitation energy of $Cl(^2P\ 1/2)$ is applied in the work of Douglas et al., but not in the work of Rao et al. The latter studies a novel resonance spectrum which gave information about the ground state potential energy curve. The difference of 63 cm^{-1} between their work and that of Douglas et al. is ascribed by Douglas et al. to a possible maximum in the ground state potential energy curve, or to some error caused by the difficulty of the resonance-spectrum experiment.

The present best value for the dissociation energy of Cl_2 seems to be that derived from the work of Douglas et al. which leads to $\Delta Hf^\circ_0[Cl] = 28.59$ kcal mol^{-1}. We assign an uncertainty approximately equal to the difference between the latter two determinations.

Ionization potential of Cl

$$Cl \rightarrow Cl^+ + e \qquad (9)$$

The energy of this process was assigned the value 104991 cm^{-1} by Sitterly (1949) [8]. It was redetermined with progressively greater accuracy by Hoffman, Larrabee and Tanaka (1967) [9] and by Radziemski and Kaufman (1969) [10]. In her most recent review, Sitterly (1970) [11] selects 104591 cm^{-1} (12.967 e.v.), the value determined by Radziemski and Kaufman. This value is about 1.0 kcal mol^{-1} lower than her previous selection. See table 3 for a summary.

Table 2

Zero-point Dissociation Energy of Chlorine (Cl_2)

$Cl_2 \rightarrow 2Cl$			
cm^{-1}	e.v.	$\Delta Hf^\circ_0[Cl]$	
	2.475	28.54	(1)
19950 ± 20[a]		28.52 ± 2(±0.03)	(2)
20062 ± 10	2.4873 ± 0.0012	28.68	(3)
19999 ± 2[a]	2.4795 ± 0.0003	28.59	(4)
		28.68	(5)
		28.59 ± 0.10	(6)

[a] $Cl(^2P\ 1/2) \rightarrow Cl(^2P\ 3/2)$ 881 cm^{-1}

This energy change was applied to the observed spectroscopic dissociation limit.

(1) Herzberg, Diatomic Molecules (1950) [4].

(2) Stull et al., JANAF tables (1961) [5].

(3) Rao and Venkateswarlu, J. Mol. Spectroscopy 9, 173-190 (1962) [6].

(4) Douglas, Moeller and Stoicheff, Can. J. Phys. 41, 1174 (1963) [7].

(5) Wagman et al., NBS Tech. Note 270-3 (1968) [3].

(6) Used in this work.

Table 3

Ionization Potential of Cl

$$Cl \rightarrow Cl^{+} + e$$

cm^{-1}	e.v.	$kcal\ mol^{-1}$	
104991	13.01(7)	300.18	(1)
104588 ± 10	12.9669	299.03	(2)
104591.0 ± 0.3	12.9673 ± 0.0004	299.04	(3)
104591.0	12.967	299.04	(4)

(1) Sitterly, NBS Circ. 467 (1949).

(2) Hoffman, Larrabee and Tanaka, J. Chem. Phys. 47, 856-857 (1967).

(3) Radziemski and Kaufman, J. Optical Soc. 59, 424-443 (1969).

(4) Sitterly, J. Research NBS (in press, 1970).

Dissociation of ClF

Spectroscopic studies of the dissociation of ClF lead to products whose energy states are ambiguous. Referring to the energy states of Cl and F respectively as X and Y we have for the spectroscopic dissociation process reaction 6a.

$$ClF \rightarrow Cl(X) + F(Y) \qquad (6a)$$

It is generally accepted that the products will be either $Cl(^2P\ 1/2) + F(^2P\ 3/2)$ or $Cl(^2P\ 3/2) + F(^2P\ 1/2)$. To reduce the products to the ground state ($Cl(^2P\ 3/2) + F(^2P\ 3/2)$), the energies are generally accepted (Sitterly, 1949) to be 881 cm^{-1} or 404 cm^{-1} depending on whether chlorine or fluorine is in the excited state.

The relevant applicable data available are listed in table 4. Wahrhaftig (1942) [12] observed a dissociation energy (reaction 6a) of 21508±2 cm^{-1}. Schmitz and Schumacher (1947) [13] calculated three dissociation limits among which they made no selection. However, Schumacher, Schmitz and Broderson (1950) [14] reported 21512±5 cm^{-1}. Stricker (1966) [15] reported 21514±2 cm^{-1}. As the available data are not in disagreement with the last determined value, this is taken as the best value. The dissociation to ground state atoms (reaction 6) is therefore very probably either 2.558 or 2.617 electron volts. The former is preferred for reasons described in the next section.

Table 4

Spectroscopic Dissociation Limits of ClF(g)

	$ClF \rightarrow Cl(x) + F(y)$		
	cm^{-1}	e.v.	e.v.
(1)	21508 ± 2		
(2)	21323 21522 21622		
(3)	21512 ± 5		
(4)	21514 ± 2		
Selected	21514 ± 2	2.6673 ± 0.0003	2.6673 ± 0.0003
	$Cl(^2P1/2) \rightarrow Cl(^2P3/2)$		
	881	.1092	
	$F(^2P1/2) \rightarrow F(^2P3/2)$		
	404		.0501
	$ClF \rightarrow Cl + F$		
		2.558	2.617

(1) L. Wahrhaftig, J. Chem. Phys. 10, 248 (1942) [12].

(2) Schmitz and Schumacher, Z. Naturforsch. 29, 359 (1947) [13].

(3) Schumacher, Schmitz and Broderson, Anales asoc. quim Argentina 38, 98 (1950) [14].

(4) Stricker, Deutsch Luft u. Raumfahrt Report 66-06 (1966) [15].

Dissociative ionization of ClF

The dissociative ionization reaction (10) was carried out by Dibeler, Walker and McCullough [2], who observed the onset of dissociation (adjusted) at 80.0 nm (15.50±0.04 e.v.)

$$ClF \rightarrow Cl^+ + F + e \qquad (10)$$

When combined with the energy of reaction (9) their value can be used to calculate the energy of reaction (6). The value thus found is 2.53±0.04 e.v. This definitely appears to favor 2.558 e.v. as the better of two possible spectroscopic values for this energy.

The near coincidence of the calculated onset of dissociative ionization of Cl_2 (reaction 11) which would lead to the same

$$Cl_2 \rightarrow Cl^+ + Cl + e \qquad (11)$$

observed ion (Cl^+) as in the ClF work, is discounted as an interference because of the low concentration of Cl_2 in the ClF sample. The argument for interference would be that the tailing-off observed in the ClF work might be accounted for by almost complete dissociative ionization of the 1 to 1.5% Cl_2 present in the ClF. If such interference occurred it could conceivable obscure an onset of dissociation at 79.5 nm (corresponding to 2.617 e.v. for reaction (6)), and weaken the argument for selecting 2.558 e.v. preferential to 2.617 e.v. for reaction (6). The relevant numbers are: for reaction (11), 80.16 nm; for reaction (10) leading to 2.558 for reaction (6), 79.86 nm; for reaction (10) leading to 2.617 e.v. for reaction (6), 79.56 nm; observed onset of Cl^+, 80.0 nm, subject to some interpretation of the beginning of deviations from the base line.

Table 5

Summary of Data Leading to Dissociative Ionization of ClF

		cm^{-1}	e.v.	e.v.
(Stricker)[15]	$ClF \rightarrow Cl(x) + F(y)$	21514 ± 2	2.66733	2.66733
(Sitterly)[8]	$Cl(^2P1/2) \rightarrow Cl(^2P3/2)$	881	.10923	
(Sitterly)[8]	$F(^2P1/2) \rightarrow F(^2P3/2)$	404		.05009
Calculated	$ClF \rightarrow Cl + F$		2.558	2.617
	$Cl \rightarrow Cl^+ + e$		12.967	12.967
	$ClF \rightarrow Cl^+ + F + e$		15.525	15.584
	Dibeler, Walker, & McCulloh [2]		15.50 ± 0.04	

Evidence from equilibrium measurements

Reaction (12) was the subject of an equilibrium study by Schmitz and Schumacher [16], and also by Schäfer and Wicke [17]. Reanalysis of their data give ΔH°_0 = 24.83 and 25.15 respectively

$$ClF_3 = F_2 + ClF \qquad (12)$$

for this reaction from the two sets of data. We assign an uncertainty of 1.0 kcal mol^{-1} to each of these data. When the recent work of King and Armstrong [18] on the enthalpy of formation of ClF_3 ($\Delta H^\circ_{f_{298}}$ = -39.35± 1.23, ΔHf°_0 = -38.35±1.23 kcal mol^{-1}), these data lead to ΔHf°_0 = -13.52± 1.6 and -13.20±1.6 kcal mol^{-1} respectively. These numbers are not in disagreement with the new work reported in this paper beyond the limits of error assigned.

In table 6 we give several values calculated for $D^\circ_0(F_2)$ on the basis of the preceeding reported values. The preferred value from these calculations is 32.0 kcal mol^{-1}. Numbers in parentheses follow from the less preferred dissociation energy of ClF. It will be noted that even discounting all previous determinations of ΔH_f[ClF] we still find within the 95% confidence limits values for D°_0[F] ranging from $\sim$ 30 to $\sim$ 37 kcal mol^{-1} provided we do not exclude the uncertainty as to the choice of dissociation energy of ClF.

Table 6

Dissociation Energy of F_2 as Derived from $\Delta Hf^\circ_0[ClF]$

Source	Process	e.v.	kcal mol^{-1}	$D^\circ_0(F_2)$
(Stricker)[15]	$ClF \rightarrow Cl + F$	2.558	58.99	
		(2.617)	(60.35)	
(Douglas et al.)[7]	$1/2\ Cl_2 \rightarrow Cl$	1.240	28.59	
	$ClF \rightarrow 1/2\ Cl_2 + F$		30.40	
			(31.76)	
	$1/2\ Cl_2 + 1/2\ F_2 \rightarrow ClF$		ΔHf°_0	
(Wicke)[19]	direct		-11.6	37.6 (40.3)
(Wicke & Friz)[20]	direct		-11.7	37.4 (40.1)
(Schmitz & Schumacher)[16]	Equilibrium with ClF_3 and F_2		-13.49±1.6	33.8±3.2 (36.5)
(Schaefer & Wicke)[17]	Equilibrium with ClF_3 and F_2		-13.17±1.6	34.5±3.2 (37.2)
(Schmitz & Schumacher)[21]	reaction of ClF with NaCl		-14.34	32.1 (34.8)
(Schmitz & Schumacher)[21]	reaction of ClF and F_2 with NaCl		-15.0	30.8 (33.5)
This Work			-14.4±0.8	32.0±1.6 (34.7)

References

[1] R. C. King and G. T. Armstrong, J. Research NBS 72A, 113 (1968).

[2] V. H. Dibeler, J. A. Walker and K. E. McCulloh, J. Chem. Phys. (in press).

[3] D. D. Wagman, W. H. Evans, V. B. Parker, I. Halow, S. M. Bailey, and R. H. Schumm, NBS Tech. Note 270-3 (January, 1968).

[4] G. Herzberg, "Diatomic Molecules" (1950).

[5] Stull et al., JANAF Thermochemical Tables (1961).

[6] Rao and Venkataswerlu, J. Mol. Spectroscopy 9, 173-190 (1962).

[7] Douglas,Mueller and Stoicheff, Can. J. Phys. 41, 1174 (1963).

[8] Sitterly, NBS Circ. 467 (1949).

[9] Hoffman, Larrabee and Tanaka, J. Chem. Phys. 47, 856-857 (1967).

[10] Radziemski and Kaufman, J. Optical Soc. 59, 424-443 (1969).

[11] Sitterly, J. Research NBS (in press, 1970).

[12] Wahrhaftig, J. Chem. Phys. 10, 248 (1942).

[13] Schmitz and Schumacher, Z. Naturforsch. 2a, 359 (1947).

[14] Schumacher, Schmitz and Broderson, Anales asoc. quim. Argentina 38, 98 (1950).

[15] Stricker, Deutsch Luft- u. Raumfahrt Report 66-06 (1966).

[16] Schmitz and Schumacher, Z. Naturforsch 2a, 362 (column 1) (1947).

[17] Schäfer and Wicke, Z. Elektrochem. 52, 205-209 (1948).

[18] R. C. King and G. T. Armstrong, J. Research NBS (in press).

[19] Wicke, Nachr. Akad Wiss. Gottingen, Math.-Phys. Chem. Abt. 1946, 89-90.

[20] Wicke and Friz, Z. Elektrochem. 57, 9-16 (1953).

[21] Schmitz and Schumacher, Z. Naturforsch. 2a, 362 (column 2) (1947).

Chapter 2

HEAT CAPACITY AND THERMODYNAMIC PROPERTIES OF BARIUM METAL FROM 18 to 370 K

George T. Furukawa and Shigeru Ishihara

I. Introduction

The results of heat-capacity measurements of barium metal presented between 18 and 370 K in this paper have been obtained in connection with a continuing research program at the National Bureau of Standards to provide accurate thermodynamic data on substances that are of interest to science and technology. The accuracy of the data reported here is, unfortunately, limited by the low purity (95.6 mole percent) of the available sample. In connection with this program, the measurements of high-temperature enthalpy, relative to 0°C at temperatures up to 900°C, on the barium sample are reported in Chapter 3.

Three heat measurements have previously been published in the temperature region of this paper. Nordmeyer and Bernoulli (1907) [1][1] reported the mean heat capacity between -185 and 20°C obtained using a liquid air vaporization calorimeter. Dewar (1913) [2] reported the mean heat capacity between 20 and 80 K obtained using a liquid hydrogen vaporization calorimeter. Roberts (1957) [3] reported measurements between 1.5 and 20 K employing a vacuum isothermal-jacket type calorimeter. The data of only Roberts [3] were considered for comparison with the measurements presented in this paper.

II. Apparatus and Method

The heat-capacity measurements on the barium metal sample were conducted in the adiabatic calorimeter described previously [4]. Descriptions of methods and procedures used for the measurements of temperature, power, and time interval of heating and calibration information on the temperature scale and electrical instruments are given in the above reference. A manually operated Mueller bridge was used exclusively in the measurements with barium.

---

[1] Figures in brackets indicate the literature references at the end of the chapter.

The 1961 atomic weights, based on carbon-12 were used to convert the mass of sample investigated to gram formula weight basis [5]. The energy measurements were in terms of the MKSA unit of energy, the joule, and wherever conversion to calorie was made, the relation used was:

1 calorie = 4.1840 joule.

III. Sample

The barium sample used in the investigation was obtained from Varlacoid Chemical Company, Elizabeth, New Jersey, in the form of oil coated rods about 0.86" in diameter. The information from the supplier indicated that the vacuum distilled metal was melted and cast in fused silica tubes under argon atmosphere, the material solidifying in about 30 to 45 minutes. Because of the relatively short time for complete solidification, any impurity segregation was probably small. Except for the outer surface of the rod, the sample was considered homogeneous and specimens for analysis were taken accordingly.

In order to fill the calorimeter sample vessel [6] through its 5/16"-opening, the rod was cut into small cubes of about 3 mm on the edge. The sample from one rod was enough for both low-temperature heat capacity measurements reported here, for the high-temperature measurements reported in Chapter 3, and for the chemical analyses. The cutting process was carried out in a controlled atmosphere box containing dry argon (dew point: -80°C). The outer surface of the barium rod was first scraped to remove any oxides and thoroughly rinsed in mineral oil (Marcol) dried with sodium. The rod was then sawed into 3-mm thick wafers, the wafers being stored in mineral oil containing sodium until enough were cut. The wafers were then cut with a compound shears into 3-mm cubes and finally soaked and rinsed about eight times with reagent-grade benzene dried with sodium. The barium sample was transferred into the sample vessel containing dried benzene and the screw cap was sealed. The auxiliary 1/16" tube on the sample vessel [6] was equipped with a valve and, by connecting to an external mechanical pump and dry-ice trap system, most of the benzene was removed. After filling with dried argon, the vessel was enclosed in a polyethylene bag and remove from the controlled atmosphere box. The valve was then connected to a high-vacuum system to remove the remaining small quantity of benzene. The polyethylene bag around the sample vessel was maintained at a slightly positive pressure of dried nitrogen until all of the benzene was removed

and the screw-cap seal helium-leak tested. The vessel was filled with dried helium gas and pumped to a high vacuum four times and finally the 1/16" auxiliary tube was sealed with 48 torr of helium gas in the vessel to enhance the temperature equilibration during the heat measurements.

One of the wafers was examined by qualitative spectrochemical analysis. The elements that were detected are listed in Table 1. Aluminum may have been the reducing agent in the preparation of metallic barium; iron may have been introduced from the saw used in cutting the barium rod. The weight loss of the saw blade was 0.8 mg for the entire cutting operation, most of which probably being incorporated in the discarded "saw dust." These impurities are, however, relatively low and will contribute very little to the heat capacity of the sample.

Chemical analysis was made for calcium, strontium, and magnesium by flame emission and atomic absorption spectrometry. The results are given in Table 2.

For the analysis of oxygen in the barium sample, two rods approximately 1/2" diameter and 2" long were prepared and sealed in polyethylene vials which were in turn sealed in glass ampoules to preserve the samples until the analysis was ready to be performed. The barium samples were analyzed inside the polyethylene vials using a comparative 14-MEV neutron activation technique. The analysis for the two samples are given in Table 3. The oxygen impurity on the weight basis seems relatively small, but on the molar basis the figure corresponds to 2.98 mole-percent.

Barium forms the nitride, Ba_3N_2. The nitride was analyzed by the Kjeldahl method. The results on two specimens, given in Table 4, show that the sample contains very little nitride.

The heat-capacity data obtained were adjusted by taking the oxygen to be combined as barium oxide (BaO) and the magnesium, calcium, and strontium as free metals and by assuming their heat capacities to be additive. In addition, calcium, strontium, and barium were assumed to follow the Dulong and Petit law of specific heats, i.e., the atomic heat is the same for all substances. The results of the present measurements indicate, however, that at 298 K the atomic heat of barium is higher than that of calcium.

Table 5 summarizes the chemical composition of the barium sample taken for the analysis of heat-capacity data obtained.

IV. Heat-Capacity Measurements and Results

The heat measurements between 18 and 370 K on the calorimeter vessel plus sample (gross) totaled 94 "points." The measurements on the empty vessel (tare) were those obtained during the investigation of beryllium nitride (Be_3N_2) [4]. An adjustment was made for the small differences in the mass of copper and solder of the vessel between the two measurements. A small correction was also made for the heat capacity of helium gas used.

The procedure followed in analyzing the experimental observations were similar to those used with the data obtained on beryllium nitride [4]. The measured energy increments (ΔQ) and the associated thermometer resistances (R) before and after heating for the tare and the gross measurements were analyzed to obtain

$$d\,Q/dR = f(R), \tag{1}$$

first for the empty vessel and then for the sample only. The procedure was to obtain a suitable equation (Eq 1) to represent the data on the empty vessel, then the energy increments for sample only (net) were calculated for each gross observation according to:

$$\Delta Q_{R_i R_j}(\text{net}) = \Delta Q_{R_i R_j}(\text{gross}) - \Delta Q_{R_i R_j}(\text{tare}). \tag{2}$$

Next, the values of $\Delta Q_{R_i R_j}$ (net) were analyzed to obtain

$$dQ/dR \quad (\text{net}) = f(R). \tag{3}$$

The values of heat capacity dQ/dT were then obtained at integral equally-spaced temperatures from the relation

$$dQ/dT = (dQ/dR)\,(dR/dT). \tag{4}$$

From the thermometer calibration, R corresponding to an integral temperature T was obtained and dQ/dR at R (Eq 3) calculated, which was in turn multiplied by dR/dT at T to obtain dQ/dT.

Figure 1 shows the deviation of $\Delta Q_{R_i R_j}$ (net) (Eq. 2) from the fitted equation (3) converted to terms of temperatures employing the thermometer calibration. For every $\Delta Q_{R_i R_j}$ (net, obs), $\Delta Q_{T_i T_j}$ (net, obs) was first calculated, then from equations 3 and 4, $\Delta Q_{T_i T_j}$ (net, calcd) was evaluated to yield

$$\frac{\Delta Q_{T_i T_j}(\text{net,obs}) - \Delta Q_{T_i T_j}(\text{net, calcd})}{T_j - T_i} \times 100 \qquad (5)$$

of Figure 1. The precision of the measurements is shown to be well within $\pm$0.025 percent. The $\pm$0.025 percent boundary curve narrows at the lower temperatures because the heat capacity of the barium metal sample relative to that of the sample vessel is greater at the lower temperatures.

In the region 44 to 66 K an anomaly in the heat capacity was observed. Figure 2 shows the deviation from the normal heat-capacity curve. The anomaly indicated immediately the possibility of air in the sample vessel; the melting point of oxygen is 54 K and that of nitrogen is 63 K. The enthalpy above the normal heat-capacity curve corresponds to 4.216 joules which in turn corresponds to 0.0063 mole of air. The available space in the sample vessel would, however, accommodate only 0.0041 mole at 1 atm and 25°C. These figures indicate, therefore, that the anomaly is associated with the barium sample or possibly a combination of air and a property of the sample.

In the analysis of the data to obtain thermodynamic properties, the anomaly was considered a property of barium and the anomalous energy was added to the thermodynamic property at 57 K. (See Table 6.) The values of thermodynamic properties given up to 57 K "follow" the normal heat-capacity curve. Above 57 K, the values of thermodynamic properties reflect the "adjustment."

The measurements of Roberts [3] between 1.5 and 20 K were employed for extrapolating below the experimental temperature limit of the present work to obtain smoothed values of heat capacity down to 0 K. Figure 3 shows how the extrapolation compares with the present work and with the data reported by Roberts [3]. By combining the present measurements with those of Roberts [3] tabular values of heat capacity at 1 K intervals from 0 to 370 K were obtained and smoothed by nine-point cubic smoothing [7]. The derived

thermodynamic properties were calculated from the smoothed values of heat capacity according to

$$H_T^o - H_0^c = \int_0^T C\, dT, \tag{6}$$

$$S_T^o - S_0^c = \int_0^T (C/T)\, dT, \tag{7}$$

$$G_T^o - H_0^c = \int_0^T (S_T^o - S_0^c)\, dT - TS_0^o \tag{8}$$

The values of $H_T^o - H_0^c/T$ and $(G_T^o - H_0^c/T$ were obtained by dividing the values of equations (6) and (8), respectively, by the corresponding temperature T. The internal consistency of the calculation was checked by evaluating the Gibbs energy by equation (8) and by the equivalent relation:

$$G_T^o - H_0^c = (H_T^o - H_0^c) - T(S_T^o - S_0^c) - TS_0^o \tag{9}$$

The equations were evaluated by stepwise numerical integration employing five-point Lagrangian integration coefficients [8].

V. References

[1] Nordmeyer, P., and Bernoulli, A. L., Verh. deut. physik. Ges. 9, 175 (1907)

[2] Dewar, J., Proc. Roy, Soc. 89A, 158 (1913)

[3] Roberts, L. M., Proc. Phys. Soc. (London) 70B, 738 (1957).

[4] Furukawa, G. T., and Reilly, M. L., publication pending.

[5] Cameron, A. E., and Wichers, E., J.Am.Chem. Soc. 84, 4175 (1962)

[6] Furukawa, G. T., Reilly, M. L., and Piccirelli, J. H., J. Research NBS 68A (Phys. and Chem.) No. 4, 381 (1964).

[7] Whittaker, E., and Robinson, G., The Calculus of Observations. A Treatise on Numerical Mathematics. 4th ed., (Blackie and Son, Ltd., London, 1944) pp. 285-316.

[8] United States National Bureau of Standards, National Applied Mathematics Laboratories, Computation Laboratory, Tables of Lagrangian Interpolation Coefficients (Columbia University Press, New York, 1944).

Table 1

SPECTROCHEMICAL ANALYSIS OF BARIUM METAL[a]

Element	Percentage Limit	Element	Percentage Limit
Al	0.001-0.01	Mg	0.01-01
Ba	> 10	Mn	0.001-0.01
Ca	0.1 - 1	Pb	0.001-0.01
Cu	< 0.001	Si	< 0.001
Fe	0.001-0.01	Sn	0.001-0.01
Li	< 0.001	Sr	0.1 - 1

[a]Analysis by Virginia C. Stewart,
Spectrochemical Analysis Section, NBS

Table 2

CHEMICAL ANALYSIS OF BARIUM METAL BY FLAME EMISSION AND ATOMIC ABSORPTION SPECTROMETRY[a]

Element	Analysis, mg/g[b]
Ca	0.605 ± 0.01
Sr	6.81 ± 0.01
Mg	0.045 ± 0.001

[a]Analysis by T. A. Rush and T. C. Rains, Analytical Coordination Chemistry Section, NBS

[b]Milligram per gram of sample.

Table 3

NEUTRON ACTIVATION ANALYSIS OF BARIUM METAL FOR OXYGEN[a]

	Weight-Percent Oxygen
Sample 1	0.356 ± 0.007[b]
Sample 2	0.358 ± 0.007[b]

[a]Analysis by S. S. Nargolwalla and J. E. Suddueth, Activation Analysis Section, N.B.S.

[b]Weighted mean standard error of the weighted mean based on Poisson counting statistics, Activation Analysis Section, N.B.S.

Table 4

ANALYSIS OF BARIUM METAL FOR NITRIDE[a]

Mass of Sample, g	Weight Percent Nitrogen
1.48	0.004
3.66	0.002

[a]Analysis by R. A. Paulson,
Microchemical Analysis Section, N.B.S.

Table 5

ASSIGNMENT OF CHEMICAL COMPOSITION
OF THE BARIUM METAL SAMPLE
BASED ON THE CHEMICAL ANALYSIS

Component	Weight Percent	Mole Percent
Ba Metal	95.8_{32}	95.6_{44}
BaO	3.4_{22}	3.0_{59}
Ca Metal	0.0605	0.207
Sr Metal	0.681	1.06_{5}
Mg Metal	0.0045	0.025
Total	100.000	100.000

Mass of sample used = 147.8314 g

Apparent number of moles of barium metal in sample including Ca and Sr metal = 1.045_{25}

TABLE 6

MOLAR THERMODYNAMIC FUNCTIONS FOR BARIUM METAL

SOLID PHASE WITH OBSERVED TRANSITION AT 57 K

1 MOL = 0.13734 KG 1 CAL = 4.1840 J

K = 273.15 + °C

T	C_p	$(H_T^O-H_0^C)$	$(H_T^O-H_0^C)/T$	$(S_T^O-S_0^C)$	$-(G_T^O-H_0^C)$	$-(G_T^O-H_0^C)/T$
K	J/K	J	J/K	J/K	J	J/K
.00	.000	.000	.000	.000	.000	.000
5.00	.249	.309	.062	.084	.114	.023
10.00	1.930	4.974	.497	.666	1.689	.169
15.00	5.293	22.479	1.499	2.040	8.119	.541
20.00	9.261	58.955	2.948	4.111	23.266	1.163
25.00	12.512	113.77	4.551	6.544	49.827	1.993
30.00	15.028	182.87	6.096	9.057	88.828	2.961
35.00	16.983	263.12	7.518	11.527	140.32	4.009
40.00	18.488	351.95	8.799	13.897	203.93	5.098
45.00	19.674	447.47	9.944	16.146	279.09	6.202
50.00	20.607	548.27	10.965	18.269	365.17	7.303
55.00	21.333	653.20	11.876	20.268	461.57	8.392
57.00	21.578	696.11	12.213	21.035	502.87	8.822
57.00	21.578	700.15	12.283	21.106	502.87	8.822
60.00	21.906	765.38	12.756	22.221	567.87	9.465
65.00	22.377	876.12	13.479	23.993	683.45	10.515
70.00	22.777	989.03	14.129	25.667	807.64	11.538
75.00	23.124	1103.8	14.717	27.250	939.97	12.533
80.00	23.427	1220.2	15.252	28.753	1080.0	13.500
85.00	23.690	1338.0	15.741	30.181	1227.4	14.440
90.00	23.920	1457.0	16.189	31.542	1381.7	15.352
95.00	24.121	1577.2	16.602	32.840	1542.7	16.239
100.00	24.300	1698.2	16.982	34.082	1710.0	17.100
105.00	24.459	1820.1	17.334	35.272	1883.4	17.937
110.00	24.603	1942.8	17.662	36.413	2062.7	18.751
115.00	24.735	2066.1	17.966	37.510	2247.5	19.543
120.00	24.858	2190.1	18.251	38.565	2437.7	20.314
125.00	24.975	2314.7	18.518	39.582	2633.1	21.065
130.00	25.086	2439.8	18.768	40.564	2833.4	21.796
135.00	25.193	2565.5	19.004	41.513	3038.6	22.509
140.00	25.296	2691.8	19.227	42.431	3248.5	23.204
145.00	25.397	2818.5	19.438	43.320	3462.9	23.882
150.00	25.495	2945.7	19.638	44.183	3681.7	24.544
155.00	25.591	3073.5	19.829	45.020	3904.7	25.192
160.00	25.685	3201.6	20.010	45.834	4131.8	25.824
165.00	25.776	3330.3	20.184	46.626	4363.0	26.442
170.00	25.866	3459.4	20.349	47.397	4598.1	27.047
175.00	25.954	3589.0	20.508	48.148	4836.9	27.640
180.00	26.041	3718.9	20.661	48.880	5079.5	28.220
185.00	26.126	3849.4	20.807	49.595	5325.7	28.788
190.00	26.209	3980.2	20.948	50.293	5575.4	29.344
195.00	26.289	4111.4	21.084	50.975	5828.6	29.890
200.00	26.369	4243.1	21.215	51.641	6085.2	30.426
205.00	26.449	4375.1	21.342	52.293	6345.0	30.951
210.00	26.529	4507.6	21.465	52.932	6608.1	31.467
215.00	26.609	4640.4	21.583	53.557	6874.3	31.973
220.00	26.691	4773.7	21.699	54.169	7143.6	32.471
225.00	26.774	4907.3	21.810	54.770	7416.0	32.960
230.00	26.858	5041.4	21.919	55.360	7691.3	33.440
235.00	26.942	5175.9	22.025	55.938	7969.5	33.913
240.00	27.026	5310.8	22.129	56.506	8250.7	34.378
245.00	27.111	5446.2	22.229	57.064	8534.6	34.835
250.00	27.196	5582.0	22.328	57.613	8821.3	35.285
255.00	27.282	5718.2	22.424	58.152	9110.7	35.728
260.00	27.368	5854.8	22.518	58.683	9402.8	36.165
265.00	27.455	5991.8	22.611	59.205	9697.5	36.594
270.00	27.544	6129.3	22.701	59.719	9994.8	37.018
273.15	27.600	6216.2	22.757	60.039	10183.	37.282
275.00	27.634	6267.3	22.790	60.225	10294.	37.435
280.00	27.726	6405.7	22.877	60.724	10597.	37.847
285.00	27.821	6544.5	22.963	61.216	10901.	38.252
290.00	27.919	6683.9	23.048	61.700	11209.	38.652
295.00	28.022	6823.7	23.131	62.179	11518.	39.047
298.15	28.089	6912.1	23.183	62.476	11715.	39.293
300.00	28.129	6964.1	23.214	62.650	11831.	39.437
305.00	28.242	7105.0	23.295	63.116	12145.	39.821
310.00	28.360	7246.5	23.376	63.576	12462.	40.200
315.00	28.486	7388.7	23.456	64.031	12781.	40.575
320.00	28.618	7531.4	23.536	64.481	13102.	40.945
325.00	28.757	7674.8	23.615	64.926	13426.	41.311
330.00	28.904	7819.0	23.694	65.366	13751.	41.672
335.00	29.058	7963.9	23.773	65.802	14079.	42.029
340.00	29.219	8109.6	23.852	66.233	14409.	42.381
345.00	29.385	8256.1	23.931	66.661	14741.	42.730
350.00	29.557	8403.4	24.010	67.085	15076.	43.075
355.00	29.732	8551.7	24.089	67.506	15412.	43.416
360.00	29.910	8700.8	24.169	67.923	15751.	43.754
365.00	30.086	8850.8	24.249	68.336	16092.	44.088
370.00	30.260	9001.6	24.329	68.747	16434.	44.418
373.15	30.366	9097.1	24.379	69.004	16651.	44.625
375.00	30.427	9153.4	24.409	69.154	16779.	44.745

H_0^C AND S_0^C APPLY TO THE REFERENCE STATE OF THE SOLID AT ZERO DEG K.

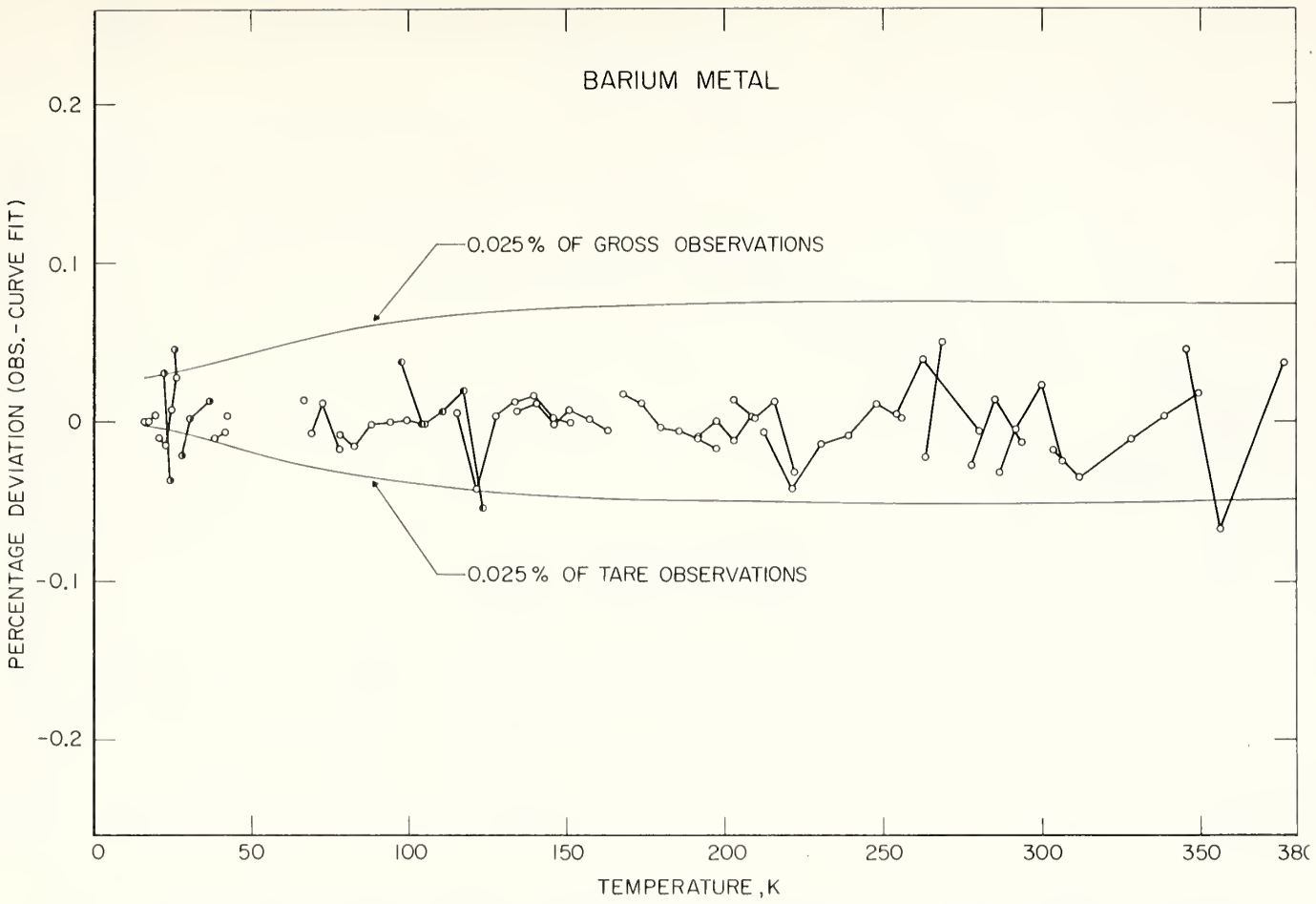

Figure 1. Percentage deviation of the barium metal sample heat capacity (net) from the fitted equation. The boundary curves represent the effect on the final smoothed values (base line) of a change of 0.025 percent in the values of the heat-capacity measurements for the empty and filled sample vessel. Consecutive measurements obtained during the day are connected by lines.

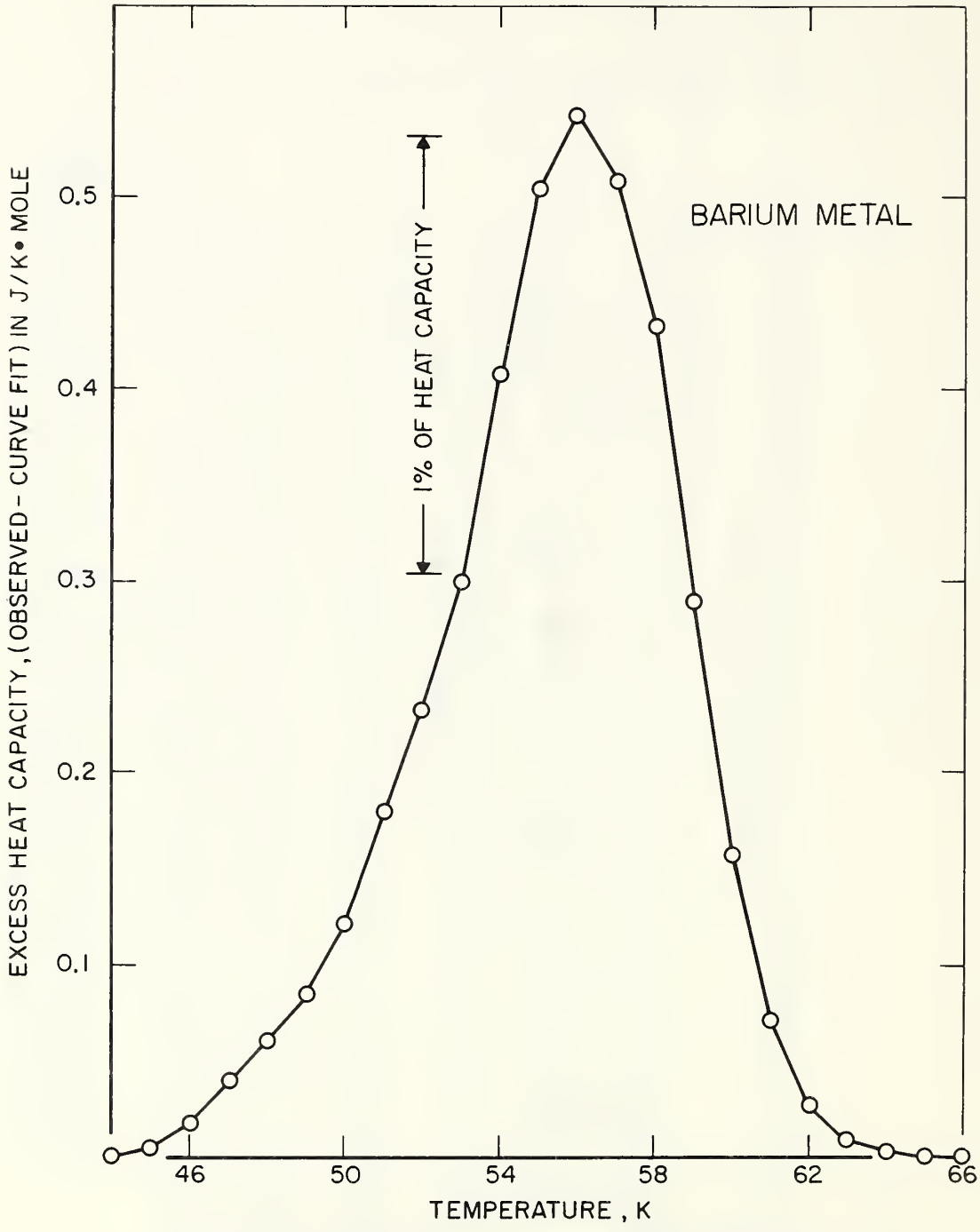

Figure 2. Observed excess heat capacity of barium metal in the range 45 to 66 K. The base line is the estimated normal heat-capacity curve.

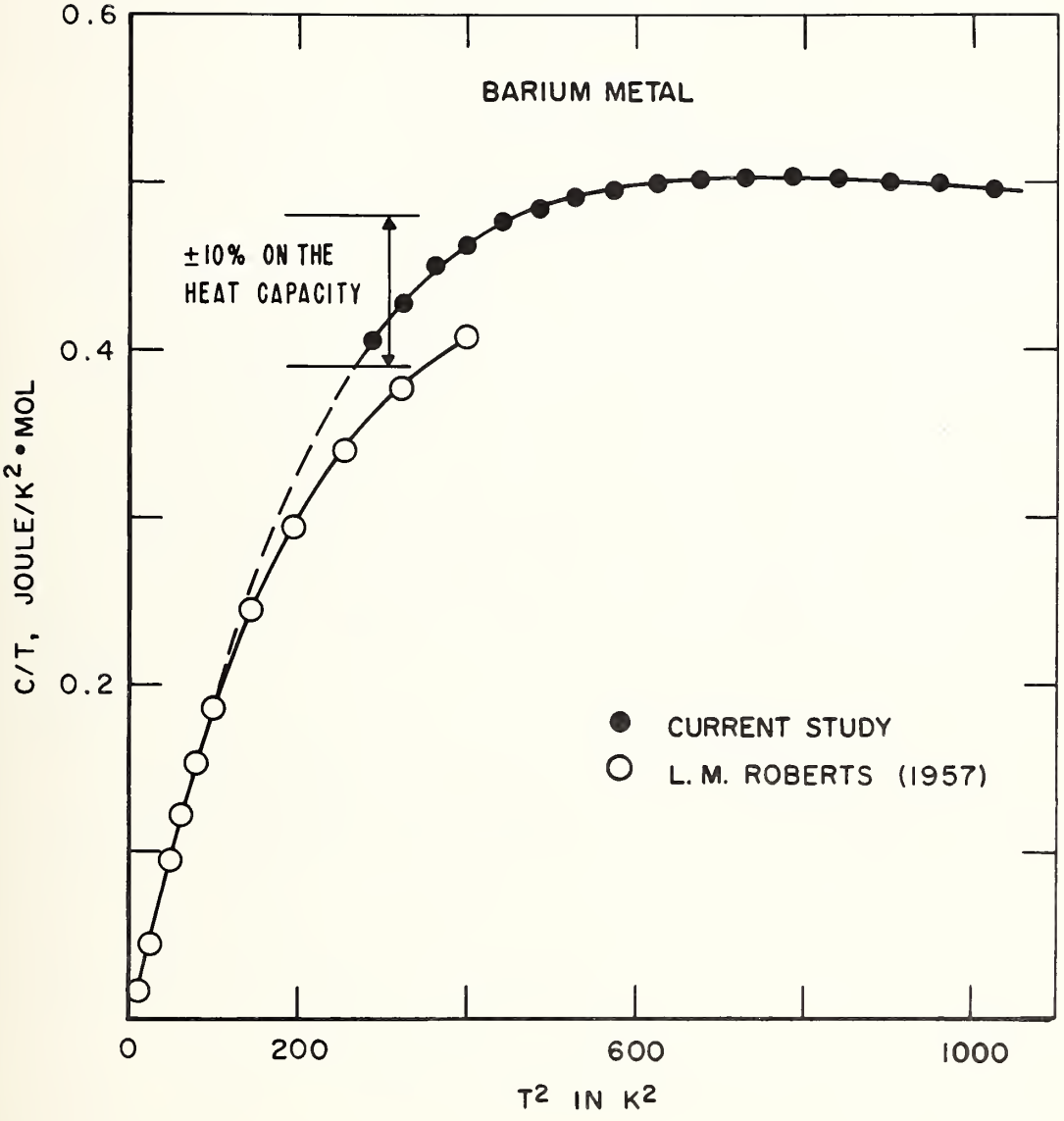

Figure 3. Comparison of the present measurements with those reported by Roberts [3] and the extrapolation to 0 K.

Chapter 3

THE ENTHALPY OF SOLID AND LIQUID BARIUM FROM 273.15 TO 1200 K

D. A. Ditmars and T. B. Douglas

Abstract

The enthalpy of barium relative to 273.15 K has been measured with a precision Bunsen ice calorimeter in the range 273.15 to 1173.15 K. The melting point of the specimen measured was found to be consistent with values previously reported for barium, and, from the data obtained, its heat of fusion was chosen as 7975 J/mol, K at 991. K. The heat effects due to all impurities were accounted for except for one effect of barium oxide in the premelting and liquid region, where the presence of this impurity is estimated to have enhanced (due to its heat of solution in liquid barium) the heat of fusion and liquid enthalpies a few percent. The unusually high heat capacities observed for barium are in essential agreement with the results of earlier workers and are thought to be attributable to high-temperature electronic contributions. Thermodynamic functions of barium in the range 273.15 to 1200 K based on the present work and the NBS low-temperature calorimetry reported in Chapter 2 are presented.

Introduction

The need for improved thermophysical data on barium arose from interest in its effect upon certain ion processes arising in propulsion applications. Available literature data on its vapor pressure and heat capacity have been recently re-examined at the NBS. The vapor pressure data have been subjected to a critical analysis described in Chapter 4 of this report. The heat capacity data, completely lacking between 20 and 273.15 K and in a dubious state above 273.15 K, were felt to be inadequate for reliable calculations. Only two series of high-temperature enthalpy measurements, due to Jauch [1, 2, 3][1] and Kagan [4, 16], were found in the literature. Besides having a scatter of up to 2 or 3 percent, the enthalpy measurements of these investigators differ by as much as 10% from each other. It was therefore

[1] Numbers in brackets refer to literature references at the end of this chapter.

decided to remeasure the heat capacity and enthalpy of barium up to 1173.15 K. The low-temperature heat capacity results are described in Chapter 2. The present chapter describes measurements made, with a precision Bunsen ice calorimeter, of the relative enthalpy of barium from 273.15 to 1173.15 K.

Experimental Procedure

Sample

Barium was obtained from the Varlacoid Chemical Co. of Elizabeth, N. J. in the form of three cast rods about an inch in diameter and a foot long. A section was removed from the middle of one rod and machined under dried mineral oil to a circular cylinder .406 in. in diameter and 1.250 in. long. Other specimens were taken at the same time from this rod and the other rods for the purpose of chemical analyses. The specimen for the high-temperature enthalpy measurements was stored in dry mineral oil and thereafter, because of its great chemical reactivity, the utmost care was observed to prevent its exposure to oxygen or water. It was cleaned with dry benzene and weighed (mass = 8.8076 g, corrected to vacuum) in a dry box containing an argon atmosphere. It was then encapsulated under high vacuum in a container of stainless steel 347 using an electron-beam welding technique. The stainless steel container was in turn sealed along with helium gas at 1/4 atmosphere pressure in a capsule of pt-Pt10Rh alloy in order to avoid possible reaction with the atmosphere of the calorimeter furnace. At the same time, a composite capsule duplicating the sample capsule in materials and dimensions, but devoid of barium, was fabricated to serve as a "blank."

Chemical analyses were carried out at the NBS on the six barium specimens reserved for that purpose. One specimen was examined spectrochemically for metallic constituents in the NBS Spectrochemical Analysis Section. Another was examined specifically for Ca, Mg and Sr by flame emmission and atomic absorption spectrometry in the NBS Analytical Chemistry Division. Two specimens were subjected to a quantitative analysis for nitrogen in the NBS Microchemical Analysis Section and two others were analyzed for oxygen using a comparative 14-MeV neutron activation technique in the NBS Activation Analysis Section. For detailed quantitative results of these analyses, see Chapter 2.

The oxygen and nitrogen identified in the above analyses were assumed to occur in combination with barium as the simplest known oxide and nitride. Under this supposition and using the results of all analyses, the sample composition was calculated and is shown in Table 1, expressed on a molar basis. Additive corrections to the measured heat values were based on this composition.

Table 1

Barium Sample composition based on four analytical techniques (see text).

Component	Mole %	Component	Mole %
Ba (metallic)	95.6	Mg	0.03
BaO	3.0	Ba_3N_2	0.01
Sr	1.1	10 other metals	<0.01 each
Ca	0.2		

Enthalpy Measurements

All enthalpy measurements were made using a calorimetric technique which has been described in exhaustive detail in prior publications [5, 6] and is briefly as follows: After having reached a predetermined constant temperature in an isothermal zone of a high-temperature furnace, the capsule (either one containing a sample or a "blank" capsule) is allowed to fall into a Bunsen ice calorimeter. There, under conditions which preclude direct radiation or convection loss from the capsule out of the calorimeter, the heat evolved by the capsule as it cools to the (constant) calorimeter temperature is precisely measured. The difference between the heat values for two similar capsules, one containing a sample and one empty ("blank"), yields the heat evolved by the sample alone.

Results

The correct functioning of the calorimeter and furnace was first affirmed by measuring the relative enthalpy of pure α-aluminum oxide (a calorimetric heat capacity standard) at 500°C. Enthalpy values were obtained which reproduced previous accurate measurements on this substance at the NBS [5] to 0.01%.

Table 2

Enthalpy measurements on empty composite capsule[a]

Furnace temperature[b]	Measured heat	Smoothed heat	Measured - Smoothed heat
°C	J	J	J
50.	243.20 242.79	243.70	- .50 - .91
100.	492.80 492.86	493.29	- .49 - .43
150.	748.01 747.82	747.75	+ .26 + .07
200.	1006.52 1007.01	1006.49	+ .03 + .52
250.	1270.33 1269.46	1269.17	+ 1.16 + .29
300.	1534.71 1535.27	1535.55	- .84 - .28
350.	1805.79 1805.33	1805.49	+ .30 - .16
400.	2080.85 2080.58	2078.87	+ 1.98 + 1.71
450.	2352.83 2353.86	2355.62	- 2.79 - 1.76
500.	2636.49 2637.03	2635.69	+ .80 + 1.34
600.	3206.09 3205.44	3205.67	+ .42 - .23
625.	3349.69 3348.67	3350.19	- .50 - 1.52
650.	3494.95 3494.51	3495.52	- .57 - 1.01
675.	3640.74 3640.88	3641.66	- .92 - .78
700.	3788.05 3788.67	3788.60	- .55 + .07
725.	3935.79 3935.93	3936.35	- .56 - .42
750.	4085.70 4086.91	4084.90	+ .80 + 2.01

Table 2 (Continued)

Furnace temperature[b]	Measured heat	Smoothed heat	Measured - Smoothed heat
°C	J	J	J
775.	4236.25 4236.28	4234.25	+ 2.00 + 2.03
800	4385.05 4384.16	4384.41	+ .64 - .25
900	4992.08 4992.11	4993.05	- .97 - .94

a. Pt 10 Rh capsule containing one of SS 347 plus some He. (SS 347 capsule is evacuated.)

b. International Practical Temperature Scale of 1968 [9].

c. Smoothed heats were calculated from the following equation:

$$H_t - H_{0°C} = At + Bt^2 + Ct^3 + D\frac{t}{T}$$

$A = 5.0599000$ H, [J]

$B = 5.9733774 \times 10^{-4}$ t °C IPTS - 68

$C = 1.2069774 \times 10^{-8}$ T K IPTS - 68

$D = -69.736320$ T,K = t °C + 273.15

which was obtained by fitting the data of Col. 2 by the method of least squares.

Two series of enthalpy measurements were then made, one on the blank capsule and one of the capsule containing barium. Table 2 summarizes the results of these measurements on the blank capsule at twenty temperatures in the range 50 to 900 °C. The measured heat values of column 2 have been corrected (using published specific heat data on the capsule materials [7, 8]) by small amounts averaging 0.05% to account for the slight differences between the actual temperatures at which measurements were made and the even temperatures of column 1. The values in column 2 were then smoothed by a least squares procedure (see footnote to table 2). Column 4, giving the difference between the measured and smoothed heat values for the temperatures of column 1, illustrates an oft-observed characteristic of this calorimeter; namely, that the absolute precision is essentially temperature-independent.

The results of the enthalpy measurements on the barium-containing capsule are given as Table 3. As in the enthalpy measurements on the blank capsule, the gross observed heats (column 4) have been adjusted by small amounts to correspond to the even temperatures of column 1. No such adjustment has been made to the measurements falling within the "premelting" region of the sample (between 600 and 730 °C), however, due to uncertainty as to the effective specimen heat capacity. Column 2 indicates the order in which the measurements were made, duplicate measurements at a single temperature having been made for the most part consecutively on the same day. (For exceptions to this, see Discussion, below.) In six instances (indicated by footnote) the final temperature (column 1) was approached through higher temperatures immediately after the specimen had been allowed to equilibrate for about an hour at a temperature safely within the range of the adjacent higher-temperature phase. All other temperatures (column 1) were approached "from below."

In all instances, the time entered in column 3 corresponds to the resident time of the capsule within the furnace maintained at the equilibrium temperature of column 1.

The net observed heats (column 5) were obtained by subtracting from column 4 the corresponding smoothed blank enthalpies calculated from the equation given in footnote c, table 2. These blank enthalpy values were on the average 2/3 of the gross observed heats. All observed specimen heat values were then corrected for the additive contribution of the impurities listed in Table 1. In making this correction, the barium oxide enthalpy was chosen from published data [7] whereas the effect of all other metallic impurities was accounted for by considering them to have made equal contributions to the specimen enthalpy on a gram-atom basis. This correction averaged about 1% from 50 to 900 °C and did not exceed 2.3%.

Data Analysis and Discussion

Smoothing the Data

The enthalpy data lent itself most conveniently to smoothing in four separate temperature ranges corresponding apparently (column 9) to three solid phases and a liquid phase. The following equations are applicable in the indicated temperature ranges and were derived from the present high-

Table 3

Relative enthalpy of barium(s,ℓ), $H_t - H_{0°C}$

Temperature[a]	Order of Experiment	Time in Furnace	Observed Heats Uncorrected For Impurities		Net Sample Heat Corrected for Impurities on Additive Basis			Phases Assumed Present
			Sample plus Container	Sample	Observed	Smoothed[f]	Observed minus Smoothed	
°C		Min.	J	J/mol[c]	J/mol	J/mol	J/mol	
50.	1	68	339.22	1489.48	1458.38	1468.06	- 9.7	
	2	78	339.28	1490.41	1459.34	"	- 8.7	
100.	3	68	687.50	3028.38	2965.25	2964.38	+ .9	
	4	67	687.34	3025.89	2962.69	"	- 1.7	
150.	5	82	1051.18	4731.49	4639.47	4621.13	+ 16.1	
	6	66	1051.04	4729.31	4637.22	"	+ 18.3	
200.	7	68	1431.54	6627.95	6511.39	6514.61	- 3.2	α(s)
	8	70	1431.54	6627.95	6511.39	"	- 3.2	
250.	9	60	1831.57	8769.70	8634.75	8691.92	- 57.2	
	10	62	1833.49	8799.64	8665.58	"	- 26.3	
	32	86	1832.16	8778.90	8644.23	"	- 47.7	
260.	16	32	1925.48	9407.78	9275.29	9164.35	+ 110.9	
270.	17	81	2006.63	9844.70	9708.62	9649.58	+ 59.0	
280.[b]	15	48	2083.15	10207.10	10065.2	10147.8	- 82.6	
290.[b]	14	33	2175.25	10810.24	10669.6	10659.1	+ 10.5	
300.	11	61	2263.81	11356.01	11214.9	11183.8	+ 31.1	
310.	13	48	2349.31	11851.72	11708.6	11708.2	+ .4	
350.	12	62	2654.86	13244.52	13075.5	13076.4	- .9	β(s)
400.	18	36	3051.96	15173.73	14977.1	14976.2	+ .9	
450.	19	55	3465.41	17305.34	17086.4	17086.6	- .2	
500.	20	47	3893.11	19607.39	19370.4	19361.2	+ 9.2	
	25	74	3893.43	19612.38	19375.5	"	+ 14.3	
550.	21	48	4300.52	21541.74	21274.9	21314.4	- 39.5	
	26	55	4302.52	21572.93	21307.0	"	- 7.4	γ(s)
600.	22	43	4748.86[e]	-	-	-	-	
	27	49	4718.32	23587.28	23293.2	23267.6	+ 25.6	
	29	79	4716.59	23560.30	23265.5	"	- 2.1	
650.02	23	48	5141.38	25662.60	25341.5	25221.6[d]	+ 119.9	
650.09	28	58	5140.29	25639.21	25317.3	25224.4[d]	+ 92.9	
699.81	48	142	5692.69	29708.61	29419.0	27166.7[d]	+2252.3	
700.05[b]	49	186	5729.90	30266.69	29993.4	27176.0[d]	+2817.4	γ(s)
700.22	24	68	5598.78	28206.50	27871.3	27182.7[d]	+ 688.6	Liq.
704.72[b]	47	97	5844.97	31631.58	31390.6	27358.5[d]	+4032.1	
704.85	46	88	5814.52	31102.65	30845.6	27363.5[d]	+3482.1	("Premelting region")
710.22[b]	44	50	6019.64	33849.11	33664.4	27573.3[d]	+6091.1	
710.31	43	110	5992.84	33422.79	33225.2	27576.8[d]	+5648.4	
710.32[b]	45	72	6025.87	33937.06	33754.8	27577.2[d]	+6177.6	
730.	30	52	6308.39	36525.71	36385.2	36373.3	+ 11.9	
	31	49	6307.18	36506.84	36365.8	"	- 7.5	
750.	33	60	6480.67	37358.08	37206.2	37236.6	- 30.4	
	34	56	6483.16	37396.91	37246.2	"	+ 9.6	
775.	35	107	6702.28	38484.86	38321.2	38308.8	+ 12.4	
	36	38	6701.63	38474.72	38310.8	"	+ 2.0	Liq.
800.	37	43	6922.11	39571.24	39394.4	39373.2	+ 21.2	
	38	58	6920.57	39547.23	39369.7	"	- 3.5	
850.	39	66	7359.41	41669.80	41464.8	41479.0	- 14.2	
	40	46	7359.76	41675.26	41469.5	"	- 9.5	
900.	41	71	7801.26	43789.40	43554.4	43553.8	+ .6	
	42	46	7801.69	43796.11	43561.3	"	+ 7.5	

a. International Practical Temperature Scale of 1968 [9].
b. These temperatures approached "from above" (see text).
c. Molecular weight = 137.34
d. These smooth values correspond to the gamma phase, which is assumed to be the equilibrium phase in the absence of impurities.
e. This measurement not included in smoothing gamma phase due to fault in mercury accounting.
f. From equations (1), (2), (3), and (4), (see text).

temperature data by the method of least squares, weighting equally all NBS barium enthalpy data within a given range.

alpha(s):

$$H_t - H_{273.15} = A_1 t^2 + B_1 t + C_1\left(\frac{t}{T}\right) \qquad (1)$$

$$273.15 \leq T \leq 582.53 \text{ K}$$

$$A_1 = +8.0216372 \times 10^{-2}$$

$$B_1 = -2.4726564$$

$$C_1 = +8.9909895 \times 10^{3}$$

beta(s):

$$H_T - H_{273.15} = A_2 T^2 + B_2 T + C_2 \qquad (2)$$

$$582.53 \leq T \leq 768.13 \text{ K}$$

$$A_2 = +4.2118189 \times 10^{-2}$$

$$B_2 = -1.6601921 \times 10^{1}$$

$$C_2 = +7.0667702 \times 10^{3}$$

gamma(s):

$$H_T - H_{273.15} = A_3 T + B_3 \qquad (3)$$

$$768.13 \leq T \leq 991 \text{ K}$$

$$A_3 = +3.9064399 \times 10^{1}$$

$$B_3 = -1.0841444 \times 10^{4}$$

liquid:

$$H_T - H_{273.15} = A_4 T^2 + B_4 T + C_4 \qquad (4)$$

$$T \geq 991 \text{ K}$$

$$A_4 = -6.1773602 \times 10^{-3}$$

$$B_4 = +5.5681880 \times 10^{1}$$

$$C_4 = -1.3267603 \times 10^{4}$$

H, J/mol ; T, K = t °C + 273.15 , IPTS-68

Transitions and Hysteresis Effects

It was from these equations that the smoothed entries of column 7 were derived. Instances of duplicate enthalpy measurements at a given temperature listed in this column indicate a precision of enthalpy measurement better than 0.1% except in the vicinity of 300 °C and in the premelting region. Both of these regions are ones in which impurities could reasonably be expected to have contributed to composition hysteresis effects. In the course of the current series of measurements, attempts were made to detect effects of thermal history

on the measured enthalpy values. Thus, for example, experiments Nos. 20 & 25 and Nos. 9, 10 & 32 indicate that enthalpy measurements of a given phase are reproducible even if the sample has been quenched from a higher temperature phase between the repeated measurements.

Although the present barium enthalpy data (Table 3) can be interpreted as indicating the presence of two solid-solid phase transitions, it seems unsafe to draw conclusions concerning the nature of these transitions because conceivably they may have resulted wholly from the impurities and not be characteristic of pure barium at all. No solid-solid latent heats have been observed, the enthalpy-temperature function having shown two "corners" rather than well-defined "steps." These corners appear 65 K below and 120 K above the transition temperature previously derived by Rinck [10] from electrical resistivity measurements on pure barium.

The impurities in the sample (Table 1) also contributed to a considerable premelting effect extending probably as much as 70 K below the true melting point of pure Ba. Unsuccessful attempts were made to derive a credible melting temperature for pure barium from the present enthalpy data in the premelting range. The melting temperature for pure barium (991 K) was chosen as a weighted average of results reported by previous investigators [2, 4, 10] and must be regarded as uncertain by 5 K or more. In order to derive a heat of fusion for pure barium, the straight line chosen to represent the gamma phase data has been extrapolated 120 K to the melting point, neglecting all possible premonitory rises such as might arise from lattice defects. The heat of fusion reported below (7975. J/mol) was obtained as the difference at the melting point between the fits to the enthalpy data of the liquid range and the gamma (solid) range.

If eqs (3) and (4) were exactly correct, the uncertainty in the heat of fusion due to uncertainty in the melting point would be 0.05% per Kelvin However, a vastly greater source of error (discussed below) arises from a suspected heat of solution effect connected with the (assumed) presence of BaO as an impurity phase, and this may place the true heat of fusion as much as several percent below the reported value. This would be consistent with the values reported by Jauch [2] (7657. $\pm$ 335. J/mol) and Kagan [4, 16] (7758 J/mol). It should pointed out, nevertheless, that apparently these two investigators never analyzed their barium samples for oxygen.

Thermal Effects of any Ba - BaO Miscibility

All impurity corrections to the NBS high-temperature enthalpy data have been made on a strictly additive basis assuming, notably, that the 3 mole per cent of barium oxide (m.p.≈1923 °C) present, existed only as a distinct solid phase throughout the temperature range of these experiments. Any miscibility of BaO with liquid or solid barium might further alter significantly the NBS enthalpy data (Table 3, Column 6). Furthermore, in the practical generation of barium vapor as a photoionization device, BaO is formed and miscibility of this compound with barium would certainly affect the thermodynamic properties of the system. Fortunately, some data on the Ba-BaO system does exist in the literature. These are summarized in some detail below because of their major significance for the NBS data as well as for their application to thermodynamic calculations on systems containing both Ba and BaO.

Summary of One Investigation of Ba - BaO Miscibility

Schriel [14], in an attempt to verify the existence of the suboxide, Ba_2O, claimed earlier by Guntz and Benoit [15], has reported four types of experiments. These led him to the conclusion that the considerable solubility of BaO in liquid Ba rather than the formation of a suboxide was responsible for his and Guntz's results. Schriel's four experiments were as follows:

I : The first was an attempt to reproduce the reported experiment of Guntz and Benoit [15] in which Ba (m.p.≈717 °C) and BaO (m.p.≈1923 °C) were heated together in a vacuum at 1150 °C for an hour. Various cooling rates for the melt were tried (even quenching to liquid introgen temperatures). Nevertheless, Schriel never obtained the "homogeneous" mixture reported by Guntz and Benoit. Rather, he observed in each instance a reddish-brown, glassy substance on top of his solidified melt and, distributed uniformly throughout it, small (.15 mm) crystals of apparently the same substance. Quantitative chemical analysis later showed the composition of these crystals to correspond to BaO with no more than 1.3% excess Ba.

II : Next, Schriel carried out a crude differential thermal analysis of a mixture of Ba and BaO heated to 1150 °C in an argon atmosphere. No heat effect which would be expected to correspond to the heat of formation of Ba_2O was observed. A rough value for the melting point of Ba was obtained.

III : Schriel's third experiment was essentially a Langmuir-type vaporization experiment in which Ba was distilled into vacuum from a series of Ba-rich, Ba-BaO mixtures. He obtained data yielding the time variation of the composition of each mixture.

These results indicated that if a suboxide were formed, it must be Ba_3O, not Ba_2O. However, microscopic examination of the solidified melts indicated that the appearance of a BaO layer over the molten Ba was a more credible explanation for the results of these experiments.

IV : At this point, Schriel evidently suspected that BaO was soluble in liquid Ba and designed his fourth experiment, in which Ba and BaO were heated together in an argon atmosphere at several temperatures in the range 725 - 1250 °C. At each temperature, the crystalline BaO portion of the initial mixture was systematically increased by the experimenter. Also, the crystalline BaO portion of the initial mixture was spatially confined by wire mesh cloth in the melts. Analysis of those portions of the melts which could have received BaO only through its solution in liquid Ba and diffusion through the iron-mesh retaining wall showed the following: The BaO content of the solidified melt, provided sufficient BaO were present at the start, was clearly a function of temperature. From these data, Schriel derived a solubility curve for BaO in Ba which indicates an almost linear increase in solubility from 20% (by weight) at 725 °C to 50% at 1250 °C.

Significance of Ba-BaO Miscibility for NBS Thermal Data.

If the simple assumption is made (based on Schriel's study described above) that the BaO in our barium sample remained as a separate phase while the barium was solid, but all dissolved in the barium as soon as the latter became liquid, a further correction of the thermal values for impurity should have been made by subtracting from the enthalpy of the liquid (relative to the enthalpy of the solid) a constant amount (at every temperature above the melting point) corresponding to the heat of solution of the BaO in the liquid barium.

We have not applied the above correction to our data because we know no basis for doing so accurately. We hope to add a known amount of BaO to our sample and then measure the enthalpy increases above the additive amounts. Meanwhile, one can try to estimate very roughly the heat of solution of BaO in liquid barium from Schriel's solubility data. The average for the two samples of BaO he used is well reproduced from 725° to 1200 °C by

$$\ell n\left(N_{BaO}\right) = -2720/T + 0.93, \qquad (5)$$

where N_{BaO} is the mol-fraction solubility of BaO at temperature T,(K). If we ignore the fact that the solution at hand is not an ideal one, the numerical coefficient of -1/T gives a not unreasonable estimate for the heat of solution, which in turn furnishes the estimate that the BaO in our sample dissolved in the

liquid barium with an absorption of 0.16 kcal per mole of barium. This figure is about 8.4% of the heat of fusion reflected in Table 4. Note also that it is of about the same magnitude as the reproducibility of the NBS enthalpy data (Table 3, Column 6) in the premelting region. Further consequences of such an error are estimated in Chapter 4.

Comparison With Other Published Results.

A comparison of the present NBS high-temperature barium thermal data with those of previous investigators is given in Figures 1 and 2. Figure 1, which compares the enthalpy data, illustrates the superior precision of the NBS data (over half the NBS points represent duplicate measurements which differ from one another by less than 0.2%) and the considerable difference between the three sets of results. This difference is perhaps attributable to differences in sample composition, though the agreement between the NBS results and those of Kagan [4, 16] in the liquid range would appear to belie this explanation. Apparently, Jauch [1, 2, 3] never measured the enthalpy of the room-temperature α phase.

Figure 2 compares the heat capacity results expressed in units of R (gas constant). Again, the NBS results show vastly superior precision. The three sets of results (Jauch's individual data were not available and only his published C_p function [3] could be plotted) probably agree within what one might expect from the samples measured. Jauch's solid-phase data, however, does seem to be improbably high, a fact which has induced more than one reviewer to cast a skeptical eye upon it [3, 11, 12].

The Unusually Large Heat Capacity of Barium.

The most remarkable feature of the thermal behavior of barium (aside from the apparent transitions, at whose causes we can but guess) is the unusually large values of heat capacity which it exhibits. Even after accounting for the low-temperature electronic contribution determined by Roberts [13] (see also Chapter 2 of this report), and then converting to C_V (by the Nernst-Lindemann approximation), it appears that the residual C_v exceeds 3R (per gram-atom) above about 150 K and 4R at the melting point (near 1000 K).

These "excesses" over the anticipated limiting value of 3R appear not to be attributable to transitions, lattice vacancies, or to any reasonable contribution to the lattice vibrations (which might have the opposite sign anyhow). It may be suspected that they are due to the impurity in our sample

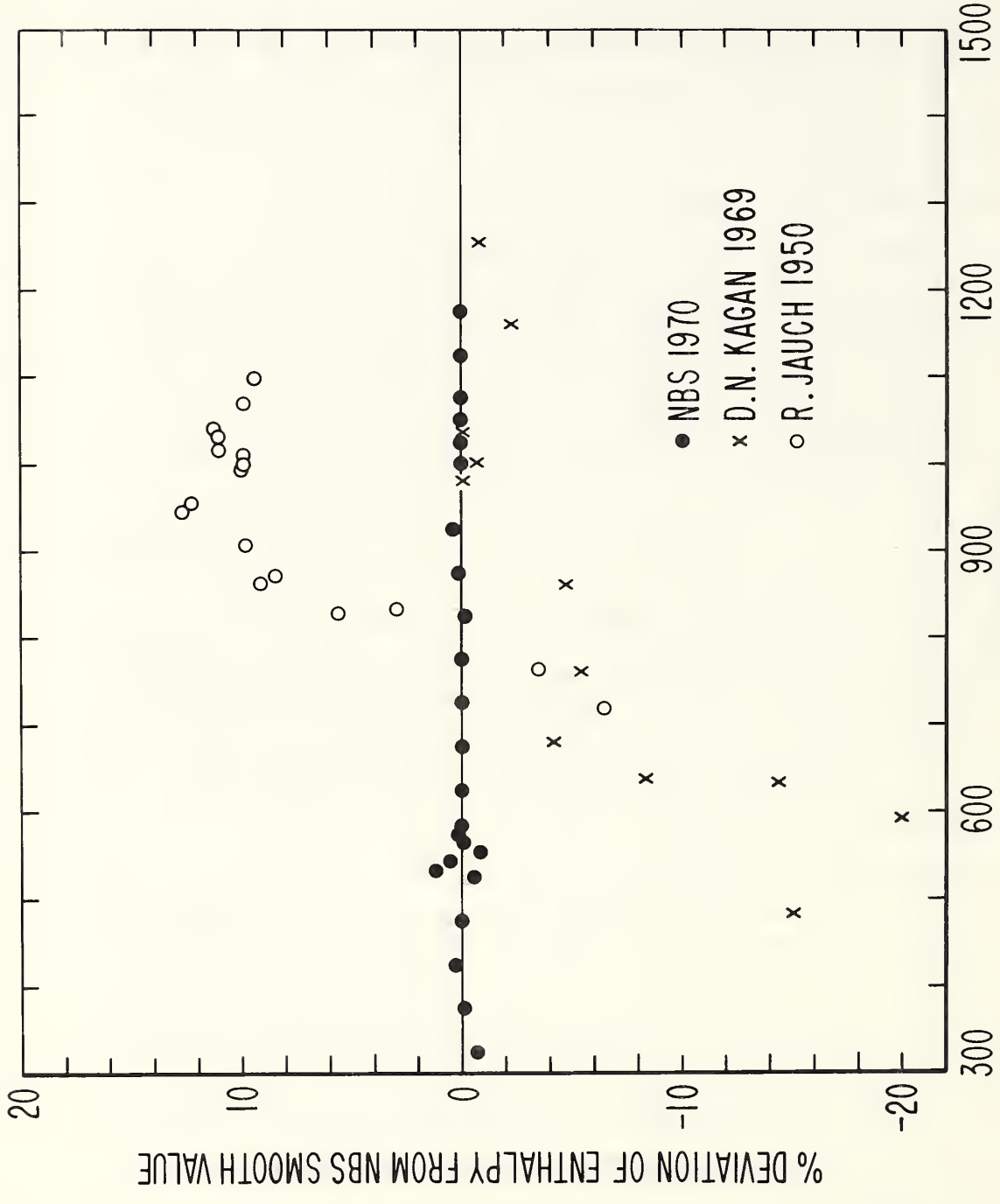

Figure 1. Comparison of barium enthalpy measurements of two investigators, with NBS high-temperature enthalpy data.

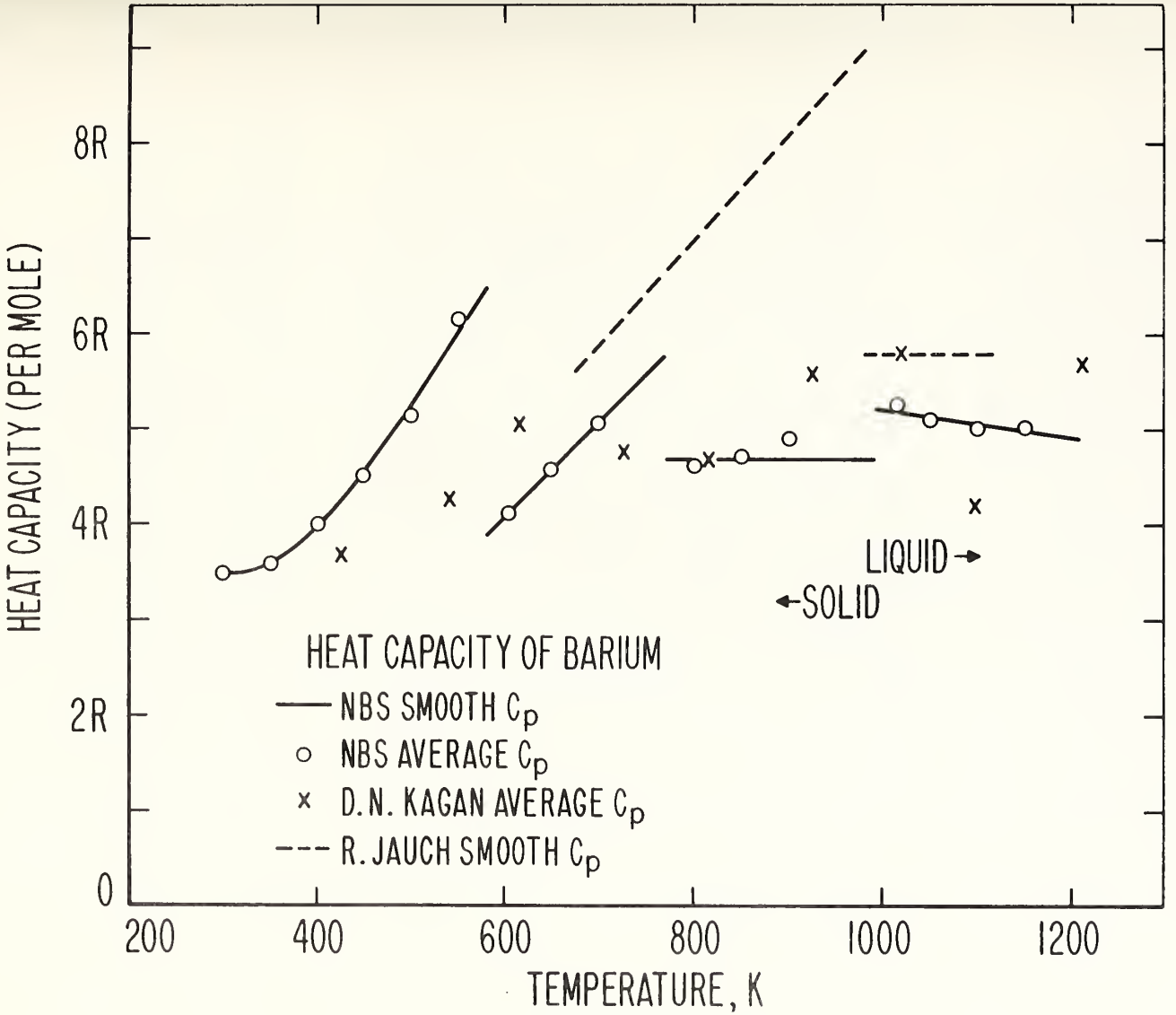

Figure 2. Comparison of barium high-temperature heat capacity according to two investigators, with NBS results.

(since it contained 3 mole % of BaO), but, in line with our conclusion (see above)from Schriel's study of the Ba-BaO system, we do not think so. The most likely explanation for the unexpected largeness of the heat capacity of barium may be a considerable contribution from the "inner" electrons of the atom, whose electronic terms begin contributing to the heat capacity of the gas at probably a lower temperature (about 1000 K) than for any other metal for which precise condensed-phase heat capacity data are available. (For a comparison of the heat capacity of liquid barium to that of other liquid metals, see Table I of Chapter 4.)

Thermodynamic Functions of Barium

The heat-capacity-vs.-temperature curve for barium given by the data of the present chapter does not join the corresponding curve from the "low-temperature" thermal data (Chapter 2), as it should, but lies between 1 and 2 percent higher but with roughly the same slope. This discrepancy is many times that encountered in the numerous previous cases in which a material was measured by both techniques at NBS, and hence begs for an explanation. We believe that the most likely explanation is as follows. The barium specimen for the "high-temperature" thermal measurements, unlike that for the "low-temperature" measurements, represented only the part of the (previously cast) sample rods near the axis, and hence may have contained more insoluble impurity which, if fully corrected for, would lower all the high-temperature heats still more and make the two curves join much more smoothly. We expect to investigate this possibility. Actually, the analysis of the barium sample that was made may correspond more closely to the "high-temperature" than to the "low temperature" specimen; see the discussion in Chapter 2.

Thermodynamic functions for barium were computed on a UNIVAC 1108 computer programmed in FORTRAN, using as input all the smoothed NBS specific-heat data for barium. Practically, the low-temperature specific-heat data (Chapter 2) were accepted up to 295 K. Between 295 and 345 K, an expanded-scale plot was used to obtain specific heat values smoothly merging the low- and high-temperature results. Above 345 K, the high-temperature heat capacities derived from equations (1), (2), (3) and (4) were used.

The thermodynamic functions appear in Table 4 (joules) and Table 5 (calories). In Table 6 are given selected values of the thermodynamic functions which resulted from a preliminary smoothing and integration; these selected values are included here since it is upon them that the calculations of Chapter 4 were based. It should be pointed out that the consequence of using Table 6 instead of Table 4 or 5, in Chapter 4, is well within the uncertainty of all the vapor-pressure data treated in Chapter 4.

For an estimate of the uncertainty in the thermodynamic functions below 295 K, see Chapter 2. Above 295 K, systematic errors arising from impurity effects already discussed above are felt to exceed by a factor of perhaps 10, any errors inherent in the measuring technique. The heat capacity and enthalpy values above 295 K, as well as the heat of fusion, must be considered uncertain by as much as 5% due to these causes.

TABLE 4

MOLAR THERMODYNAMIC FUNCTIONS FOR BARIUM (S,L)

1 MOL = 0.13734 KG K = 273.15 + C

T	C_p	$(H_T^O-H_0^C)$	$(H_T^O-H_0^C)/T$	$(S_T^O-S_0^C)$	$-(G_T^O-H_0^C)$	$-(G_T^O-H_0^C)/T$
K	J/K	J	J/K	J/K	J	J/K
273.15	27.600	6216.3	22.757	60.039	10183.	37.282
275.00	27.634	6267.3	22.790	60.225	10294.	37.435
280.00	27.726	6405.7	22.877	60.724	10597.	37.847
285.00	27.821	6544.5	22.963	61.216	10901.	38.252
290.00	27.919	6683.7	23.048	61.700	11209.	38.653
295.00	28.022	6823.7	23.131	62.179	11518.	39.047
298.15	28.095	6912.1	23.183	62.477	11715.	39.293
300.00	28.140	6964.1	23.214	62.651	11831.	39.437
305.00	28.267	7105.2	23.296	63.117	12145.	39.821
310.00	28.405	7246.8	23.377	63.577	12462.	40.201
315.00	28.553	7389.2	23.458	64.033	12781.	40.575
320.00	28.710	7532.4	23.539	64.484	13102.	40.945
325.00	28.888	7676.4	23.620	64.930	13426.	41.311
330.00	29.075	7821.3	23.701	65.373	13751.	41.672
335.00	29.263	7967.1	23.782	65.812	14079.	42.029
340.00	29.470	8113.9	23.865	66.247	14409.	42.382
345.00	29.688	8261.8	23.947	66.678	14742.	42.731
350.00	29.905	8410.8	24.031	67.107	15076.	43.076
355.00	30.146	8560.9	24.115	67.533	15413.	43.418
360.00	30.411	8712.2	24.201	67.956	15752.	43.756
365.00	30.697	8865.1	24.288	68.378	16092.	44.090
370.00	31.005	9019.3	24.377	68.798	16435.	44.421
373.15	31.208	9117.3	24.433	69.061	16652.	44.628
375.00	31.332	9175.1	24.467	69.216	16780.	44.749
380.00	31.677	9332.7	24.560	69.633	17127.	45.074
390.00	32.420	9653.1	24.751	70.465	17828.	45.714
400.00	33.227	9981.3	24.953	71.296	18537.	46.343
410.00	34.092	10317.	25.165	72.127	19254.	46.962
420.00	35.009	10663.	25.389	72.960	19979.	47.571
430.00	35.973	11018.	25.624	73.795	20713.	48.171
440.00	36.981	11382.	25.870	74.633	21455.	48.763
450.00	38.028	11757.	26.129	75.476	22206.	49.347
460.00	39.110	12143.	26.399	76.324	22965.	49.924
470.00	40.226	12540.	26.681	77.177	23732.	50.495
480.00	41.372	12948.	26.975	78.035	24508.	51.060
490.00	42.546	13367.	27.281	78.900	25293.	51.619
500.00	43.745	13799.	27.598	79.772	26086.	52.174
510.00	44.968	14242.	27.927	80.650	26888.	52.723
520.00	46.213	14698.	28.267	81.536	27699.	53.269
530.00	47.477	15167.	28.617	82.428	28519.	53.811
540.00	48.761	15648.	28.978	83.327	29348.	54.349
550.00	50.062	16142.	29.350	84.234	30186.	54.884
560.00	51.379	16649.	29.731	85.148	31033.	55.416
570.00	52.711	17170.	30.123	86.069	31889.	55.946
580.00	54.057	17703.	30.524	86.997	32754.	56.473
582.53	54.399	17841.	30.627	87.233	32974.	56.606
582.53	32.468	17841.	30.627	87.233	32974.	56.606
590.00	33.097	18085.	30.654	87.651	33628.	56.997
600.00	33.940	18421.	30.702	88.214	34507.	57.512
610.00	34.782	13764.	30.762	88.782	35392.	58.020
620.00	35.625	19116.	30.833	89.355	36283.	58.521
630.00	36.467	19477.	30.916	89.931	37179.	59.015
640.00	37.309	19846.	31.009	90.512	38081.	59.503
650.00	38.152	20223.	31.113	91.097	38989.	59.984
660.00	38.994	20609.	31.226	91.686	39903.	60.460
670.00	39.837	21003.	31.348	92.279	40823.	60.931
680.00	40.679	21405.	31.479	92.875	41749.	61.396
690.00	41.521	21816.	31.619	93.475	42681.	61.857
700.00	42.364	22236.	31.766	94.079	43618.	62.313
720.00	44.048	23100.	32.084	95.296	45512.	63.212
740.00	45.733	23998.	32.430	96.526	47430.	64.096
760.00	47.418	24929.	32.802	97.767	49373.	64.965
768.13	48.103	25318.	32.961	98.276	50170.	65.315
768.13	39.064	25318.	32.961	98.276	50170.	65.315
780.00	39.064	25781.	33.053	98.875	51340.	65.821
800.00	39.064	26562.	33.204	99.864	53328.	66.660
820.00	39.064	27344.	33.347	100.83	55335.	67.482
840.00	39.064	28125.	33.483	101.77	57361.	68.287
860.00	39.064	28906.	33.613	102.69	59405.	69.076
880.00	39.064	29688.	33.736	103.59	61468.	69.850
900.00	39.064	30469.	33.855	104.46	63549.	70.610
920.00	39.064	31250.	33.968	105.32	65646.	71.355
940.00	39.064	32032.	34.077	106.16	67761.	72.087
960.00	39.064	32813.	34.180	106.99	69893.	72.806
980.00	39.064	33594.	34.280	107.79	72041.	73.511
991.00	39.064	34024.	34.333	108.23	73229.	73.894
991.00	43.438	41999.	42.381	116.28	73229.	73.894
1000.00	43.327	42389.	42.390	116.67	74277.	74.277
1020.00	43.080	43253.	42.406	117.52	76619.	75.117
1040.00	42.833	44113.	42.416	118.36	78978.	75.941
1060.00	42.586	44967.	42.422	119.17	81353.	76.749
1080.00	42.339	45816.	42.423	119.96	83744.	77.542
1100.00	42.092	46660.	42.419	120.74	86152.	78.320
1120.00	41.845	47500.	42.411	121.50	88574.	79.084
1140.00	41.597	48334.	42.399	122.23	91011.	79.835
1160.00	41.350	49164.	42.383	122.95	93463.	80.572
1180.00	41.103	49988.	42.363	123.66	95929.	81.296
1200.00	40.856	50808.	42.340	124.35	98409.	82.008

H_0^C AND S_0^C APPLY TO THE REFERENCE STATE OF THE SOLID AT ZERO DEG K.

TABLE 5

MOLAR THERMODYNAMIC FUNCTIONS FOR BARIUM (S,L)

1 MOL = 0.13734 KG
1 CAL = 4.1840 ABS J

K = 273.15 + C

T	C_p	$(H_T^O-H_0^C)$	$(H_T^O-H_0^C)/T$	$(S_T^O-S_0^C)$	$-(G_T^O-H_0^C)$	$-(G_T^O-H_0^C)/T$
K	CAL/K	CAL	CAL/K	CAL/K	CAL	CAL/K
273.15	6.597	1485.7	5.439	14.350	2433.9	8.911
275.00	6.605	1497.0	5.447	14.394	2460.5	8.947
280.00	6.627	1531.0	5.468	14.513	2532.8	9.046
285.00	6.649	1564.2	5.488	14.631	2605.6	9.143
290.00	6.673	1597.5	5.509	14.747	2679.1	9.238
295.00	6.697	1630.9	5.529	14.861	2753.1	9.333
298.15	6.715	1652.3	5.541	14.932	2800.0	9.391
300.00	6.726	1664.5	5.548	14.974	2827.7	9.426
305.00	6.756	1698.2	5.568	15.085	2902.8	9.517
310.00	6.789	1732.0	5.587	15.195	2978.5	9.608
315.00	6.824	1766.1	5.607	15.304	3054.8	9.698
320.00	6.862	1800.3	5.626	15.412	3131.6	9.786
325.00	6.904	1834.7	5.645	15.519	3208.9	9.874
330.00	6.949	1869.3	5.665	15.625	3286.8	9.960
335.00	6.994	1904.2	5.684	15.729	3365.1	10.045
340.00	7.043	1939.3	5.704	15.833	3444.0	10.130
345.00	7.096	1974.6	5.724	15.937	3523.5	10.213
350.00	7.147	2010.2	5.744	16.039	3603.4	10.295
355.00	7.205	2046.1	5.764	16.141	3683.9	10.377
360.00	7.268	2082.3	5.784	16.242	3764.8	10.458
365.00	7.337	2118.8	5.805	16.343	3846.3	10.538
370.00	7.410	2155.7	5.826	16.443	3928.2	10.617
373.15	7.459	2179.1	5.840	16.506	3980.1	10.666
375.00	7.488	2192.9	5.848	16.543	4010.7	10.695
380.00	7.571	2230.6	5.870	16.643	4093.7	10.773
390.00	7.749	2307.1	5.916	16.842	4261.1	10.926
400.00	7.942	2385.6	5.964	17.040	4430.5	11.076
410.00	8.148	2466.0	6.015	17.239	4601.9	11.224
420.00	8.367	2548.6	6.068	17.438	4775.3	11.370
430.00	8.598	2633.4	6.124	17.637	4950.7	11.513
440.00	8.839	2720.6	6.183	17.838	5128.0	11.655
450.00	9.089	2810.2	6.245	18.039	5307.4	11.794
460.00	9.348	2902.4	6.310	18.242	5488.8	11.932
470.00	9.614	2997.2	6.377	18.446	5672.3	12.069
480.00	9.888	3094.7	6.447	18.651	5857.7	12.204
490.00	10.169	3195.0	6.520	18.858	6045.3	12.337
500.00	**10.455**	**3298.1**	**6.596**	**19.066**	**6234.9**	**12.470**
510.00	10.748	3404.1	6.675	19.276	6426.6	12.601
520.00	11.045	3513.1	6.756	19.487	6620.4	12.732
530.00	11.347	3625.0	6.840	19.701	6816.4	12.861
540.00	11.654	3740.0	6.926	19.916	7014.4	12.990
550.00	11.965	3858.1	7.015	20.132	7214.7	13.118
560.00	12.280	3979.3	7.106	20.351	7417.1	13.245
570.00	12.598	4103.7	7.200	20.571	7621.7	13.371
580.00	12.920	4231.3	7.295	20.793	7828.5	13.497
582.53	13.002	4264.1	7.320	20.849	7881.2	13.529
582.53	7.760	4264.1	7.320	20.849	7881.2	13.529
590.00	7.910	4322.6	7.326	20.949	8037.3	13.623
600.00	8.112	4402.7	7.338	21.084	8247.5	13.746
610.00	8.313	4484.9	7.352	21.219	8459.0	13.867
620.00	8.514	4569.0	7.369	21.356	8671.9	13.987
630.00	8.716	4655.2	7.389	21.494	8886.1	14.105
640.00	8.917	4743.3	7.411	21.633	9101.8	14.221
650.00	9.118	4833.5	7.436	21.773	9318.8	14.337
660.00	9.320	4925.7	7.463	21.913	9537.2	14.450
670.00	9.521	5019.9	7.492	22.055	9757.1	14.563
680.00	9.722	5116.1	7.524	22.198	9978.3	14.674
690.00	9.924	5214.3	7.557	22.341	10201.	14.784
700.00	10.125	5314.6	7.592	22.485	10425.	14.893
720.00	10.528	5521.1	7.668	22.776	10877.	15.108
740.00	10.930	5735.7	7.751	23.070	11336.	15.319
760.00	11.333	5958.3	7.840	23.367	11800.	15.527
768.13	11.497	6051.1	7.878	23.488	11991.	15.611
768.13	9.337	6051.1	7.878	23.488	11991.	15.611
780.00	9.337	6162.0	7.900	23.632	12270.	15.732
800.00	9.337	6348.7	7.936	23.868	12745.	15.932
820.00	9.337	6535.4	7.970	24.099	13225.	16.129
840.00	9.337	6722.2	8.003	24.324	13709.	16.321
860.00	9.337	6908.9	8.034	24.543	14198.	16.510
880.00	9.337	7095.6	8.063	24.758	14691.	16.695
900.00	9.337	7282.4	8.092	24.968	15188.	16.876
920.00	9.337	7469.1	8.119	25.173	15690.	17.054
940.00	9.337	7655.8	8.144	25.374	16195.	17.229
960.00	9.337	7842.6	8.169	25.570	16704.	17.401
980.00	9.337	8029.3	8.193	25.763	17218.	17.570
991.00	9.337	8132.0	8.206	25.867	17502.	17.661
991.00	10.382	10038.	10.129	27.790	17502.	17.661
1000.00	10.355	10131.	10.131	27.884	17752.	17.753
1020.00	10.296	10337.	10.135	28.089	18312.	17.953
1040.00	10.237	10543.	10.138	28.288	18876.	18.150
1060.00	10.178	10747.	10.139	28.482	19444.	18.343
1080.00	10.119	10950.	10.139	28.672	20015.	18.533
1100.00	10.060	11152.	10.138	28.857	20590.	18.719
1120.00	10.001	11352.	10.136	29.038	21169.	18.902
1140.00	9.942	11552.	10.134	29.215	21752.	19.081
1160.00	9.883	11750.	10.130	29.387	22338.	19.257
1180.00	9.824	11947.	10.125	29.555	22927.	19.430
1200.00	9.765	12143.	10.120	29.720	23520.	19.600

H_0^C AND S_0^C APPLY TO THE REFERENCE STATE OF THE SOLID AT ZERO DEG K.

TABLE 6

MOLAR THERMODYNAMIC FUNCTIONS FOR BARIUM (S,L)

(PROVISIONAL VALUES)

1 MOL = 0.13734 KG K = 273.15 + C

T	C_p	$(H_T^O-H_U^C)$	$(H_T^O-H_O^C)/T$	$(S_T^O-S_O^C)$	$-(G_T^O-H_O^C)$	$-(G_T^O-H_O^C)/T$
K	J/K	J	J/K	J/K	J	J/K
298.15	28.073	6909.0	23.173	62.340	11677.	39.167
980.00	39.064	33591.	34.277	112.246	76410.	77.969
991.00	39.064	34021.	34.330	112.682	77647.	78.352
991.00	43.438	41996.	42.377	120.729	77647.	78.352
1080.00	42.339	45813.	42.419	124.418	88559.	81.999
1180.00	41.103	49985.	42.360	128.114	101189.	85.753

H_O^C AND S_O^C APPLY TO THE REFERENCE STATE OF THE SOLID AT ZERO DEG K.

Bibliography

1. Jauch, R., Diplomarbeit, Techn. Hochschule, Stuttgart, 1946. (Cited by Kubaschewski, Refs. 2, 3 below.)
2. Kubaschewski, O., Zeit. f. Elektrochemie, 54, 275 (1950).
3. Kubaschewski, O., Zeit. f. Metallkunde, 41, 445 (1950).
4. Kagan, D. N., Dissert., Akad. Nauk SSSR, Inst. Vys. Temp., Moscow, 1969.
5. Furukawa, G. T., Douglas, T. B., McCoskey, R. E. and Ginnings, D. C., J.Res. NBS 56, 67 (1956) RP2694.
6. Douglas, T. B. and King, E. G., "High Temperature Drop Calorimetry" (chap. 8 in "Experimental Thermodaynamics V.I," Butterworths, London, 1968.)
7. Kelley, K. K., Bulletin 584, Bureau of Mines, 1960.
8. Douglas, T. B., and Dever, J. L., J. Res. NBS 54, 15 (1955) RP 2560.
9. The International Practical Temperature Scale of 1968, Metrologia 5, 35 (1969).
10. Rinck, E., Ann. de Chim. 18, 510 (1932).
11. Hultgren, R. et al, "Selected Values of Thermodynamic Properties of Metals and Alloys," Wiley, 1963, P. 43.
12. Stull, D. R. and Sinke, G. C., "Thermodynamic Properties of the Elements," Am. Chem. Soc., 1956, P. 11.
13. Roberts, L. M., Proc. Phys. Soc. (London) 70B, 738 (1957).
14. Schriel, M., Zeit. anorg. allg. Chem., 231, 313 (1937).
15. Guntz, A., Benoit, F., Bull.Soc. Chim. 35, 709 (1924).
16. Shpil'rain, É. É. and Kagan, D. N., Institute of High Temperatures, Academy of Sciences of the USSR 7 [3], 525-527 (1969) (translated from Teplofizika Vysokikh Temperatur, Vol. 7, No. 3, pp. 577-579 (1969)).

Chapter 4

A THIRD-LAW ANALYSIS OF THE VAPOR-PRESSURE DATA FOR BARIUM METAL

By

Thomas B. Douglas and Ralph F. Krause, Jr.

Introduction

The published data on the vapor pressure of barium metal cover the temperature range 730-2027K (pressure range, approximately 10^{-8} to about 1 atm) and consist of the work of several groups of authors using a variety of experimental techniques (details are given below). Although several thermodynamic analyses of some of these sets of data have been made previously, these have been largely second-law analyses owing to the lack of thermal measurements on the condensed phases that would have provided free-energy functions for the solid and the liquid. Chapters 2 and 3 of this report describe recently completed measurements of the heat capacity and enthalpy of barium from 15 to 1173K. Although the adequacy of correcting these thermal data for the effects of the sample impurities is open to some question (see discussion in the cited chapters), the precision of the data is high and leaves little to be desired in this respect. Consequently, free-energy functions for the solid and liquid have been evaluated from these thermal data, and with their use a third-law analysis of the vapor-pressure data is given in this chapter. At the end of the chapter is a discussion of possible causes of the considerable thermodynamic inconsistency found.

Extrapolation of the Free-Energy Function of Liquid Barium from the Melting Point to 2027K

In Chapter 3 the basis of somewhat arbitrarily assuming the melting point of barium to be 991K is described. Suffice it to say here that the free-energy function of the condensed phases is a continuous function at the melting point, and the uncertainty in the value assumed for that temperature has a negligible effect compared with the uncertainties in the available vapor-pressure values.

In the treatment presented in this chapter, the values of the thermodynamic functions used for Ba(c) up to 991K and for Ba(ℓ) at 991K are given in a table of Chapter 3. For Ba(ℓ) at higher temperatures (up to 2027K),

the free-energy functions used are those resulting from an extrapolated heat-capacity, temperature function for the liquid, derived as follows.

The heat capacities (C_p) of several liquid metals have been measured over considerable temperature ranges and with sufficient accuracy to show the shapes of their C_p (T) curves and to show that these are similar to one another on some reasonable corresponding-state basis (Hg, [1][1]; Pb, [2]; Li, [3]; Na, [4]; K, [5]; Cs [6]). For these six liquid metals and liquid barium, the smoothed observed heat capacities give approximately the values listed in Table I ("M P"= melting point; "B P" = normal boiling point; "T_{min}" = temp., in K, where C_p is a minimum).

Table I

Some Approximate Values Derived from the Heat Capacities of Liquid Metals

Metal	$\frac{dC_p/dT}{C_p/(T_{BP}-T_{MP})}$ at MP	$\frac{T_{min}-T_{MP}}{T_{BP}-T_{MP}}$	C_p/R (mol^{-1})		
			At MP	Minimum	At BP
Hg	-0.08	0.857	3.4	3.3	3.3
Pb	-0.14	-	3.7	<3.4	-
Li	-0.22	-	3.7	<3.4	-
Na	-0.25	0.659	3.8	3.5	3.6
K	-0.22	0.630	3.9	3.6	3.7
Cs	-0.18	0.738	3.9	3.7	3.7
Ba	-0.26	(0.738)	5.2	(4.6)	(4.7)

The parenthesized values are assumed in the absence of any observed values.

The rate of decrease of the heat capacity of barium (taken from the measurements of Chapter 3) is reasonable in comparison with the other metals.

A quadratic function of temperature fits the heat capacities of most of the other metals well, and was assumed for liquid barium also, the coefficients of

[1] Numbers in brackets denote references at the end of this chapter.

the equation being determined from the three conditions: (a) C_p, 43.438 J mol^{-1} K^{-1} at 991 K (tabulated in Chapter 3), (b) C_p, 41.103 J $mol^{-1}K^{-1}$ at 1180 K (tabulated in Chapter 3), and (c) C_p a minimum at 1670 K (corresponding to Table I, Column 3). The resulting provisional equation for Ba(ℓ) (991-2027 K) is (in J mol^{-1} K^{-1}):

$$C_p = 68.04 - 0.03530\ T + 1.0568(10^{-5})\ T^2 \ . \qquad (1)$$

Despite the fact that the derivation of Eq (1) may seem reasonable as an extrapolation, it is highly advisable to warn the reader that it should not be used or cited without recognizing its uncertain nature and explicitly calling attention to this. The equation closely reproduces the observed heat capacities in the approximate temperature range of actual measurement, 1000 to 1200 K, yet the extrapolation is over a range of more than 800 degrees.

Numerical Equations for the Third-Law Heat of Sublimation of Barium

Unlike the alkali metals, some of whose saturated vapors are considerably dimerized near their normal boiling points, the ground electronic state of the barium atom is singlet ($^1S_0$), so formation of Ba_2 should be considerably less extensive. By analogy to an estimated value for the dissociation energy of Ca_2, that of Ba_2 has been estimated as 0.22 eV (5 kcal mol^{-1}) [7]. Using this value, the mol fraction of Ba_2 in the saturated vapor must increase with temperature; we estimated less than 0.1% dimer at 2000 K. Neglecting gas imperfection of all other types, it should be safe to assume that saturated barium vapor is an ideal monatomic gas in the range of the reported vapor-pressure measurements ($T \leq 2027$ K), to well within the experimental uncertainties of these measurements.

The ideal-gas thermodynamic properties of monatomic barium are accurately known from the atomic spectrum [8]. Since it was desired to avoid interpolation in the computer calculations, $C_p(T)$ of Ba(g) as tabulated was fit to empirical equations:

$$800\text{-}1000\text{K}: \quad C_p^0 = 20.786 + 8.368(10^{-7})(T-800)^2 \ \text{J mol}^{-1}\ \text{K}^{-1} \qquad (2)$$

$$800\text{-}2000\text{K}: \quad C_p^0 = 20.79 + 1.25(10^{-6})(T-800)^2 + 3(10^{-12})(T-800)^4 \ \text{J mol}^{-1}\text{K}^{-1} \qquad (3)$$

Using Eqs (2) and (3) respectively (actually, only Eq (3) is needed), the following two numerical equations were derived for the heat of sublimation of Ba(c) in kcal mol^{-1} at 298.15K (see the equation in Table IV below) (T in K; P, the vapor pressure, in atm; "ln" = $\log_e$; 1 kcal = 4184.0J):

$$T \leq 991K: \quad \Delta H_{298}^{subl} = -0.0019872\ T\ \ln P - 1.385 + 0.054425T - 0.0043685\ T\ \ln T - 1.600(10^{-7})\ T^2 + 3.33\ (10^{-11})\ T^3 \qquad (4)$$

$$T \geq 991K: \quad \Delta H_{298}^{subl} = -0.0019872\ T\ \ln P - 2.919 + 0.097121T - 0.0108081\ T\ \ln T + 3.2451(10^{-6})\ T^2 + 8.77(10^{-11})\ T^3 - 1.912(10^{-13})\ T^4 + 3.585(10^{-17})\ T^5 \qquad (5)$$

Reported Vapor Pressures of Barium, and Calculated Third-Law ΔH_{298}^{subl}

The various authors who have reported vapor-pressure values for barium, the experimental methods they used to measure the vapor pressure, and the temperature range each covered are summarized in Table II.

Table II

Sets of Vapor-Pressure Data on Barium Reported

Authors (Year)	Reference	Experimental Method	Temperature Range (in K)
Hinnov & Ohlendorf (1969)	[9]	Vapor density by resonance fluorescence	730-1200
Rudberg & Lempert (1935)	[10]	Effusion rate	798-1024
Zavitsanos (1968)	[11]	Time-of-flight mass spectrometry	1064-1255
Zavitsanos (1968)	[11]	Recoil force	1103-1216
Zavitsanos (1968)	[11]	Effusion rate	1120-1210
Ruff & Hartmann (1924)	[12]	Boiling-point method	1204-1404
Hartmann & Schneider (1929)	[13]	Boiling-point method	1334-1421
Bohdansky & Schins (1967)	[14]	A dynamic boiling-point method	1498-2027

Hinnov and Ohlendorf assigned large tolerances to their vapor-pressure values, which within those tolerances generally agree with the data of Rudberg and Lempert for solid barium, and which would apparently have agreed for liquid barium also, had Hinnov and Ohlendorf not failed to take into account the reduction of the temperature coefficient of vapor pressure above the melting point equivalent to a reasonable estimated heat of fusion. Thus the equation they give to represent their data, $\log_{10}P(atm)=3.92-8800/T$, is applicable only below the melting point. Apparently Zavitsanos did not evaluate the factor which would convert his mass-spectrometric data to absolute pressures, so his results obtained by this technique are not really subject to a third-law analysis.

Omitting the two sets of measurements of vapor pressures of barium discussed in the preceding paragraph, we subjected the remaining six sets of Table II to a third-law analysis by calculating ΔH_{298}^{subl} for each reported value of vapor pressure by Eq (4) or (5), depending on the temperature. The reported vapor pressures and the values of ΔH_{298}^{subl} so calculated are listed in Table III. The temperatures reported for these measurements have been assumed to be on the International Practical Temperature Scale of 1948, and have been converted to the IPTS of 1968, which is known to be closer to the true thermodynamic temperature scale [15].

Table III

Reported Vapor Pressures of Barium, and Corresponding Third-Law Values of ΔH_{298}^{subl} Calculated from Equations (4) and (5)

Temperature (K)	Vapor Pressure (torr)	ΔH_{298}^{subl} (kcal mol^{-1})	Temperature (K)	Vapor Pressure (torr)	ΔH_{298}^{subl} (kcal mol^{-1})
Rudberg and Lempert [10]					
798.1	$5.34(10^{-5})$	44.79	923.3	$1.44(10^{-3})$	45.39
823.1	$1.31(10^{-4})$	44.66	923.3	$1.57(10^{-3})$	45.23
823.1	$1.52(10^{-4})$	44.41	948.3	$2.97(10^{-3})$	45.18
848.1	$2.32(10^{-4})$	44.98	973.4	$6.01(10^{-3})$	44.94
873.2	$5.22(10^{-4})$	44.83	973.4	$6.94(10^{-3})$	44.66
883.2	$8.65(10^{-4})$	44.43	998.5	$8.86(10^{-3})$	45.23
898.2	$9.65(10^{-4})$	44.94	1023.5	$1.81(10^{-2})$	44.79
923.3	$1.22(10^{-3})$	45.70			

Table III (Continued)

Temperature (K)	Vapor Pressure (torr)	ΔH^{sub1}_{298} (kcal mol^{-1})	Temperature (K)	Vapor Pressure (torr)	ΔH^{sub1}_{298} (kcal mol^{-1})
Zavitsanos (recoil force)[11]					
1102.7	0.266	41.96	1138.8	0.399	42.24
1102.7	0.119	43.73	1139.9	0.399	42.27
1113.8	0.399	41.43	1140.9	0.466	41.95
1122.8	0.506	41.19	1147.9	0.207	44.03
1125.8	0.612	40.86	1156.9	0.266	43.75
1125.8	0.443	41.59	1162.9	0.399	43.01
1126.8	0.320	42.34	1164.9	0.612	42.08
1128.8	0.532	41.27	1166.9	0.700	41.84
1134.8	0.248	43.18	1216.1	1.13	42.20
Zavitsanos (effusion rate) [11]					
1119.8	0.276	42.44	1144.9	0.372	42.60
1120.8	0.241	42.78	1144.9	0.367	42.62
1138.8	0.170	44.16	1164.9	0.649	41.95
1144.9	0.346	42.76	1210.0	1.57	41.22
Ruff and Hartmann [12]					
1204.0	3.5	39.13	1289.3	27	36.23
1218.1	5	38.65	1301.3	42	35.37
1229.1	8	37.80	1353.5	216	32.12
1246.1	11	37.45	1383.5	298	31.80
1270.2	15	37.27	1404.5	603	30.21
Hartmann and Schneider [13]					
1334.4	12.5	39.32	1406.5	23.5	39.32
1366.5	15.5	39.52	1412.5	26.5	39.12
1373.5	19.5	39.06	1420.6	26.5	39.30
1378.5	17.5	39.48			
Bohdansky and Schins [14]					
1497.7	20	41.89	1812.2	200	40.77
1601.9	50	41.37	1986.6	500	40.24
1704.1	100	41.17	2026.7	600	40.14

The values of ΔH^{subl}_{298} from the work of Ruff and Hartmann show much the largest trend with temperature, and may be eliminated from further consideration on the basis of probably being subject to large systematic errors. The remaining five sets of Table III are plotted in Fig. 1.

Discussion

The general degree of thermodynamic consistency among the thermal and vapor-pressure data for barium treated in this chapter may be most readily assessed by an examination of Fig. 1, bearing in mind the following facts about this graph.

(a) Since the ordinate is temperature-independent, complete thermodynamic consistency would require that all points lie on a common horizontal line.

(b) For any one group of vapor-pressure points, the vertical scatter (about the best straight line through the data) is a measure of the precision of those vapor-pressure measurements.

(c) For any group of points or for all the points, the second-law and third-law values of ΔH^{subl}_{298} will agree if and only if the best straight line through the points is horizontal. Furthermore, the greater the slope of this line, the greater the second- and third-law discrepancy.

Although only the points of Bohdansky and Schins in Fig. 1 are precise enough to show a definite temperature trend among themselves, there is clearly a distinct trend in comparing two or more different sets of points. In fact, so great are these trends that it is impossible to select a unique *prima facie* "best" third-law value of ΔH^{subl}_{298} from a mere examination of Fig.1. It is therefore appropriate to examine the plausible sources of systematic error semi-quantitatively in an effort to see which ones cannot be ruled out as major sources of error.

Previously, without benefit of the vapor-pressure data of Zavitsanos or the NBS thermal data reported in Chapters 2 and 3, we made a second-law analysis of the remaining sets of vapor-pressure data (assuming "conventional" estimates for the heat of fusion and liquid-heat-capacity for barium). The data of Rudberg and Lempert and those of Bohdansky and Schins were found to give the smallest standard error of all the possible *pairs* of data sets, and the

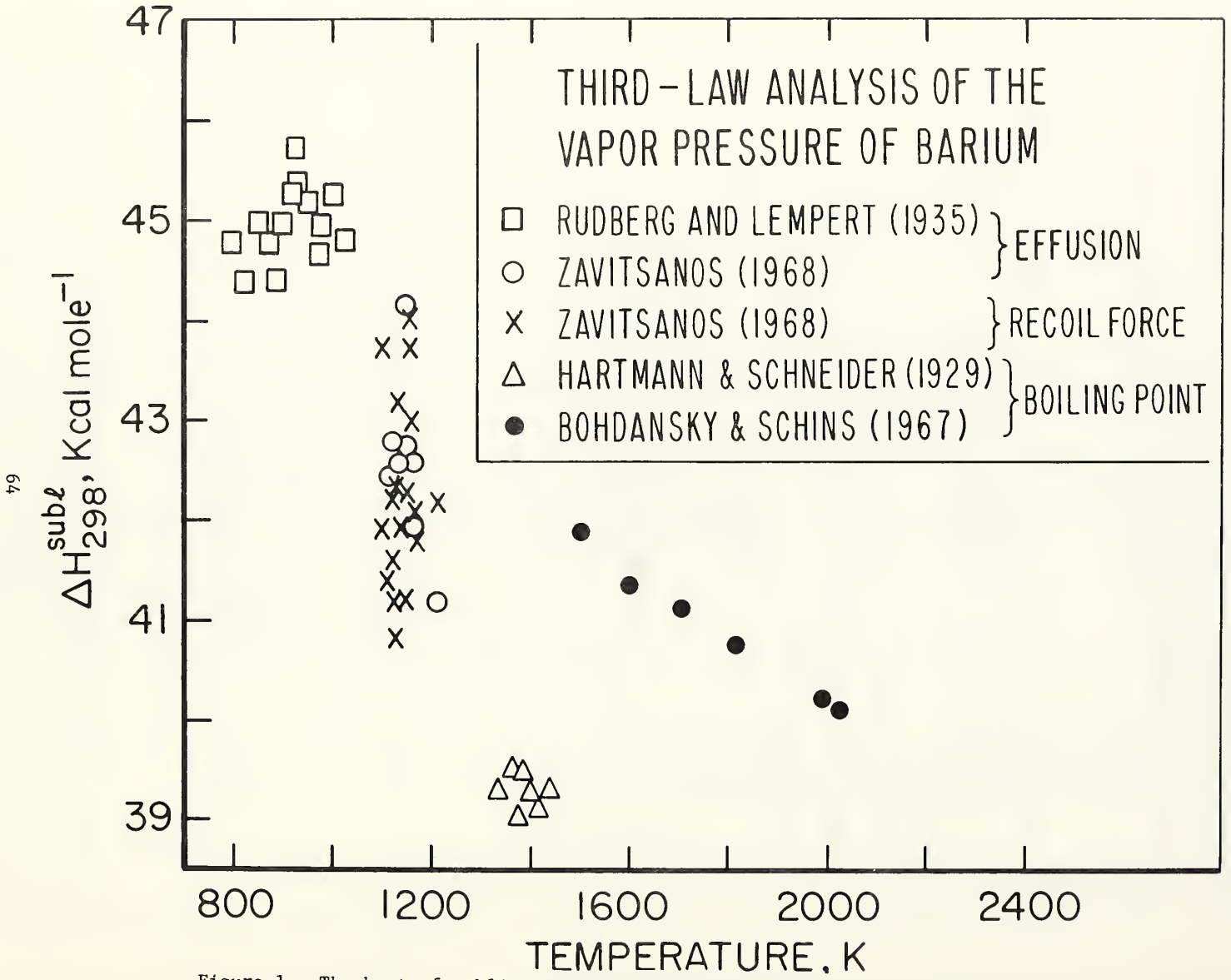

Figure 1. The heat of sublimination of barium at 298.15 K as calculated from five sets of published vapor-pressure data and recent unpublished NBS thermal measurements.

resulting values for the heat of sublimation of barium at the melting point (which may be approximated here as 1000 K) were ΔH^{o} = 45.1 kcal mol^{-1} and ΔS^{o} = 23.3 cal K^{-1} mol^{-1}. Since S^{o}_{1000} for Ba(g) is 46.7, this result gives S^{o}_{1000} of Ba(c) = 23.4; the calorimetric result, however, (see table in Chapter 3) is 27.0 cal $K^{-1}mol^{-1}$, or 3.6 cal K^{-1} mol^{-1} greater.

The trend in Fig. 1 through the points of Rudberg and Lempert and of Bohdansky and Schins may be taken as an exemplary basis for a more thorough search for a single source of experimental error that might plausibly have caused the trend. Table IV shows first the thermodynamic equation by which third-law values of ΔH^{subl}_{298} may be calculated--with the right-hand side decomposed into separate contributions such that the first term represents the vapor pressure, the second term is the product of T and the gas free-energy function, and the sum of the third (representing the low-temperature calorimetry) and the fourth (representing the high-temperature calorimetry) is the product of -T and the condensed-phase free-energy function. Below the equation is given the approximate contribution of each term, at each of three temperatures, to the calculated value of ΔH^{subl}_{298} in kcal mol^{1}. Obviously the multiplication of one of these values by the assumed fractional error in that term gives the effect on the calculated value of ΔH^{subl}_{298}.

Table IV

Individual Contributions (in kcal mol^{-1}) to the Third-Law ΔH^{subl}_{298} for Barium

$$\Delta H^{subl}_{298} = -0.0019872\ T \ln P(atm) + T\left[-\left(\frac{G^{o} - H^{o}_{298}}{T}\right)\right]_{g} - T\int_{298}^{T} \frac{(H^{o}-H^{o})}{T^{2}}\,dT - TS^{o}_{298(c)}$$

800 K	-1.6 ln P	+34	-3	-12
1400 K	-2.8 ln P	+62	-12	-21
2000 K	-4.0 ln P	+92	-23	-30

A 10-deg error in T associated with P falsifies ΔH^{subl}_{298} by 0.5 to 0.15 kcal mol^{-1}.

In this way the following roughly quantitative conclusions were drawn as to what one individual source of error would produce a trend in Fig. 1 of -3.5 kcal mol^{-1} per 1000 K, and how credible such an error seemed.

1. Though the gas free-energy functions make large contributions, these should be reliable. (The degree of dimerization of the vapor is believed to be negligible, as discussed above.)
2. $S^{o}_{298(c)}$ too high by some 20% (very unlikely).
3. High-temperature enthalpies too high by some 20% overall. (Not unequivocally excluded, but considered unlikely in view of the discussions in Chapter 3 and below.)

   The three values for the heat capacity of liquid barium in Table I (last three columns), which correspond to Eq (1) and approximately cover the range 1000 to 2000 K, are all greater than for the other six metals by approximately R. If this "excess" at the melting point is due to some electronic contribution peculiar to barium, it is not known whether this contribution would be twice as great or would even be smaller at 2000 K than at 1000 K. If as a simple example we were to assume that Eq (1) is too high by R at all temperatures above 1000 K, then at 1500 K this would lead to a calculated value of vapor pressure which is too low by 7% or, alternatively, third-law heat of sublimination which is too low by 0.2 kcal mol^{-1}. The errors at 2000 K would be greater: too low by 18% or 0.8 kcal mol^{-1}, respectively. (In contrast, an error of +0.16 kcal/mole in the heat of fusion of barium, postulated in Chapter 2 as due to heat of solution of the BaO in liquid barium, would lead to smaller errors in the calculated ΔH^{subl}_{298} : -0.2 kcal mol^{-1} at 2000 K.)
4. Vapor pressures in error by up to a factor as great as 2. (Considered possible, particularly in the case of more volative impurities or of superheating the sample. Compare, e.g., the data of Ruff and Hartmann with those of Hartmann and Schneider in the same temperature range in Table III.)

5. Temperatures associated with vapor pressures in error by amounts up to 200 degrees. (Too great an error for even only moderately reliable thermometry. But unsuspected large temperature gradients at the higher temperatures that could lead to such errors are not unprecedented.)

A year ago the NBS Thermochemical Data Center reviewed the data on barium [16]. The NBS thermal data were not then available, but those of Kagan were. As a compromise between conflicting second- and third-law values, they chose ΔH^{subl}_{298} = 44 kcal mol^{-1}, but may later revise that value in the light of the more recent pertinent data. We do not here recommend a definite value; but in view of the evidence described in the present chapter, we favor a lower value than 44-- at least as low as 42--on the basis of giving definitely more weight to the third-law results--including the values of Hartmann and Schneider, for several reasons: (a) Vapor pressures of several torr are inherently measurable with a smaller percentage error than much smaller pressures. (b) The precision of their measurements on barium was fair, and there is no temperature trend of their points in Fig. 1. (c) Their apparatus and method resulted from a careful improvement over that of Ruff and Hartmann. (d) Using the same method, Hartmann and Schneider simultaneously measured vapor pressures of lithium metal at comparable temperatures and pressures [13], obtaining results of comparable precision and lack of trend for that metal also [3]. However, Hartmann and Schneider's barium showed a lower melting point than most observers have reported for this metal, and this apparently "indifferent" purity leaves some question as to their vapor-pressure accuracy.

References

[1] T. B. Douglas, A.F.Ball, and D. C. Ginnings, J. Research Nat'l Bur. Standards 46, 334 (1951) (R P 2204).

[2] T. B. Douglas and J. L. Dever, J. Amer. Chem. Soc. 76, 4824 (1954).

[3] T. B. Douglas, L. F. Epstein, J. L. Dever, and W. H. Howland, J. Amer. Chem. Soc. 77, 2144 (1955).

[4] D. C. Ginnings, T. B. Douglas, and A. F. Ball, J. Research Nat'l Bur. Standards 45, 23 (1950) (RP 2110).

References (Continued)

[5] T. B. Douglas, A. F. Ball, D. C. Ginnings, and W. D. Davis, J. Amer. Chem. Soc. 74, 2472 (1952).

[6] Several authors. See JANAF Thermochemical Tables, Third Addendum, PB 168 370-3, Clearinghouse, U. S. Dept. of Commerce, Springfield, Va. (table for Cs(l), dated June 30, 1968).

[7] K. A. Gingerich and H. C. Finkbeiner, J. Chem. Phys. 52, 2956 (1970).

[8] R. R. Hultgren, R. L. Orr, P. D. Anderson, and K. K. Kelley, "Selected Values of Thermodynamic Properties of Metals and Alloys," Supplement of Feb. 1968 for Ba, Hearst Mining Bldg., Univ. of Calif., Berkeley, Calif.

[9] E. Hinnov and W. Ohlendorf, J. Chem. Phys. 50, 3005 (1969).

[10] E. Rudberg and J. Lempert, J. Chem. Phys. 3, 627 (1935).

[11] P. D. Zavitsanos, G. E. Technical Report 68 SO 331, General Electric Co., Valley Forge, Pa., Nov. 1968.

[12] O. Ruff and H. Hartmann, Z. anorg. allgem. Chem. 133, 29 (1924).

[13] H. Hartmann and R. Schneider, Z. anorg. allgem. Chem. 180, 275 (1929).

[14] J. Bohdansky and H. E. J. Schins, J. Phys. Chem. 71, 215 (1967).

[15] T. B. Douglas, J. Research Nat'l Bur. Standards 73A, 451 (1969).

[16] V. B. Parker, Chap. 9, "The Status of the Thermochemical Data on Some Barium Compounds," NBS Report 10074, 1 July 1969, pp. 164-192.

Chapter 5

THE INFRARED SPECTRUM OF MATRIX ISOLATED BaO_2

S. Abramowitz, N. Acquista

Abstract

The infrared spectra of matrix isolated BaO_2 has been observed. Ba atoms were allowed to react with an argon oxygen mixture and condensed on a liquid hydrogen cooled surface. The observed spectra of normal $^{16}O_2$ and spectra observed using $^{18}O_2$ and $^{16}O^{18}O$ confirm this assignment.

Introduction

The reaction of O_2 with barium in the gas phase has been studied by several workers (1,2). This reaction is thought to go through an intermediate step to form BaO_2 (1), even though mass spectrometric evidence for this species is not available. Because of the importance of such an intermediate species, particularly in connection with the recent use of barium releases in the atmosphere to form BaO and Ba clouds it was decided to study the products of this reaction using matrix isolation techniques.

Experimental

A beam of barium atoms was evaporated from either a stainless steel Knudsen cell or a heated stainless steel small diameter tube and allowed to codeposit with an O_2/Ar onto a liquid hydrogen cooled CSI window. The electron beam furnace used for heating the Knudsen cell, the Air Products Cryotip and the Perkin Elmer 301 spectrophotometer has been described previously (3,4). In other experiments a Beckmann IR-7 with a CSI interchange and a conventional cryostat was used. Higher resolution spectra were obtained using a Perkin Elmer 99G

monochromator equipped with interference filters and suitable diffraction gratings. A chromel alumel thermocouple inserted into a .030" hole drilled halfway up the wall of the Knudsen cell, was used to measure the temperature of the effusing gas. The recent vapor pressure data of Hinnov and Ohlendorf for barium was utilized (5). A vapor pressure of barium of about 1μ was allowed to effuse through a 2 mm orifice in the Knudsen cell. This atomic beam was then reacted with an O_2/Ar mixture and the products of this reaction were condensed on the liquid hydrogen cooled CSI window. Deposition times varied from 3 to 37 hrs. Essentially identical experiments were also done with the barium beam from the resisitively heated steel tube.

Results and Discussion

Initial results obtained by codepositing barium at a vapor pressure of about 10^{-3} torr with an argon oxygen mixture indicated a prominent absorption band in the region of 570 cm^{-1}. The multiplet structure of this band as shown in Figure 1 varies with concentration of oxygen to argon. Scan (a) is for a 1/300 O_2/Ar concentration while scan (b) and (c) are for concentrations of 1/100 and 1/50 respectively. This indicates that these multiplet structures are not due to isotopic effects (barium has five naturally occurring isotopes with abundances greater than 2%). They could possibly due to molecular complexes with oxygen neighbors, since the oxygen concentration is about 10 times that of the barium in the matrix. Alternatively they could be ascribed to a matrix effect which is concentration dependent. In any event the feature at 570 cm^{-1} certainly becomes more prominent as the concentration of Ar/O_2 and Ba/O_2 increases. The reaction of Ba + $^{18}O_2$ was then studied. The spectrum shown in Figure 2(b) is for about an $^{18}O_2$/Ar of 200. The same number of features were observed as in

the $^{16}O_2$/Ar experiments. The relative intensities of these features is comparable to similar concentrations of $^{16}O_2$/Ar. It is perhaps interesting that the ratio of the frequencies of the corresponding features for $^{16}O_2$ and $^{18}O_2$ are the same within the experimental error for all four of the observed features for each species. Curve (a) is for $^{16}O_2$/Ar of 1/300 and is shown for comparison purposes. Curve (c) shows a Ba + $^{16}O_2$ + $^{18}O_2$ experiment. In this experiment the $^{16}O_2$ and $^{18}O_2$ were at a concentration of 1/100 yielding a total O_2/Ar of 1/50. It seen from this experiment that the observed spectrum (d) is a supposition of spectra (a) and (b) neglecting relative intensities of the various features within each of the two multiplets. There is no absorption between or midway between corresponding pairs of bands indicating all these features are due to one oxygen molecule per species. In spectrum (c) Ba has been codeposited with $^{16}O_2$ + $^{16}O^{18}O$ + $^{18}O_2$. The ratio fo the $^{16}O_2/^{18}O_2$ in the sample, which was then discharged electrically with a Tesla coil to scramble the oxygen sample was about 2/1. The observed spectra contains all the features which are found in spectrum (d). In addition to these features there are lines in between which correspond on a one to one basis with those due to $^{16}O_2$ and $^{18}O_2$. These lines are about midway between the oxygen 16 and 18 lines.

It was then decided to try to obtain spectra of Ba + O_2 with about equal concentrations of both in the matrix. Figure 3 shows such spectra. The barium was heated resistively in a stainless steel tube with about a 5 mm orifice yielding roughly 6 times the barium (at the same pressure)

as the Knudsen cell. Also the orifice was closer to the CSI low temperature surface. In these experiments only one prominent feature is found for Ba + $^{16}O_2$ and Ba + $^{18}O_2$ at 570 and 545 cm^{-1} respectively (An $^{16}O^{18}O$ impurity is present in the $^{18}O_2$). An experiment with the scrambled isotopic constitution shows features at 570 and 545 cm^{-1} and another at 559 cm^{-1} due to $Ba^{16}O^{18}O$. This result verifies our initial results indicating that the species responsible for this absorption has two oxygen atoms or one O_2 unit per barium atom. While definitive spectroscopic proof of one barium atom per molecule has not been obtained in this study, any other conclusion doesn't seem warranted. Mass spectral, Knudsen, and optical data indicate that barium evaporates as an atom. Also the only group 2 diatomic molecule spectroscopically found to date is Mg_2 (6) which has a dissociation energy of about 400 cm^{-1}. Reports in the Russian literature purporting to show the existence of Ca_2 are most probably misinterpreted (7). More likely emitters for the species are thought to be either CaC or CaN because of the ωe, Be and extrapolated De values reported.

Rather long extensive runs of duration of 36 - 40 hours were necessary to produce the spectra shown in Figure 4. This is the region of O-O stretching mode for a proposed BaO_2 molecule. This mode is found at 1066 cm^{-1} for the $Ba^{16}O_2$ and at 1004 cm^{-1} for $Ba^{18}O_2$. These spectra as those shown in Figure 3 were obtained with the Perkin Elmer 99G monochromator. Unfortunately it was not possible to obtain spectra of the mixed isotope in this region (because of the large amount of sample needed). Attempts at longer runs were unsuccessful because of loss of thermal contact between the liquid

hydrogen surface and the cryostat's low temperature window, or increased scattering of the argon/O_2/Ba film so that transmission and therefore in effect S/N ratio was adversely affected. The results and assignment for the BaO_2 species are summarized in Table 1.

Conclusions

The product of the reaction of barium atoms and oxygen can be trapped out in an argon matrix at liquid hydrogen temperatures. Isotopic results using $^{18}O_2$ and $^{16}O^{18}O$ in addition to $^{16}O_2$ ~~are~~ confirm the existence of such a species, despite the fact that the reaction

$$Ba + O_2 \rightarrow BaO + O$$

is exothermic to the extent of about 0.6 ev (8) no BaO was observed in these experiments. The $Ba^{16}O$ fundamental was recently found at 632 cm^{-1} in an argon matrix by Linevsky (9).

The intensity of the O-O stretching mode is very weak compared to the Ba-O stretching mode found at 570 cm^{-1} for $Ba^{16}O_2$. This low intensity coupled with a frequency which is similar to the O_2^- fundamental frequency reported on by several workers found in solids such as O_2^- doped alkali halide single crystals (10,11) tends to support a charge transfer type structure consisting of $Ba^+ + O_2^-$. A complete charge separation would yield an O-O bond which would indeed not be active. Crude attempts to observe fluorescence spectra of the O_2^- by using Hg 2537 A line were not successful possibly because of the low fluorescence yield or the scattering of the matrix.

Unfortunately the other BaO stretching mode has not been observed as yet. It is not at all clear why the intensity of this mode is weak compared to the other BaO stretching mode. Weak features have been found in the $Ba^{16}O_2$ spectra, however comparable bands in the $Ba^{18}O_2$ have not been found. Without these data it is not possible to assign the 570 and 545 cm^{-1} in $Ba^{16}O_2$ and $Ba^{18}O_2$ to the symmetric or asymmetric stretch of BaO_2.

References

1. K. Sakurai, S.E. Johnson, H.P. Broida, J. Chem. Phys. 52, 1625 (1970).
2. R.S. Newbury, G.W. Balton Jr., A.W. Searcy, J. Chem. Phys. 48, 793 (1968).
3. D.E. Mann, G.V. Calder, K.S. Seshadri, D. White, M.J. Linevsky, J. Chem. Phys. 46, 1138 (1967).
4. Certain commercial instruments are identified in this paper to specify completely the experimental procedure. In no case does such identification imply a recommendation or endorsement by the National Bureau of Standards.
5. E. Hinnov, W. Ohlendorf, J. Chem. Phys, 50, 3005 (1969).
6. W.J. Balfour, A.E. Douglas, Can. J. Phys. 48, 901 (1970).
7. G.V. Kovalenok, V.A. Sokolov, Izvestia Vysshikh, Uchebnykh, Zavedenii Fizika, 3, 27 (1968).
8. K. Sakurai, H.P. Broida, J. Chem. Phys. 50, 2404 (1969).
9. M.J. Linevsky, Private communication.
10. W. Holzer, W.F. Murphy, A.J. Bernstein, J. Mol. Spectroscopy 32, 13 (1969).
11. J. Rolfe, W. Holzer, W.F. Murphy, H.T. Bernstein, J. Chem. Phys. 49, 963 (1968).

Table 1

Observed Fundamental Modes for BaO_2

Assignment	$Ba^{16}O_2$	$Ba^{18}O_2$	$Ba^{16}O^{18}O$
Ba-O Stretch	570	545	559
O-O Stretch	1066	1004	

Figure 1. The Infrared Spectra of Ba + O_2/Ar
a) O_2/Ar = 1/300, b) O_2/Ar = 1/100
c) O_2/Ar = 1/50

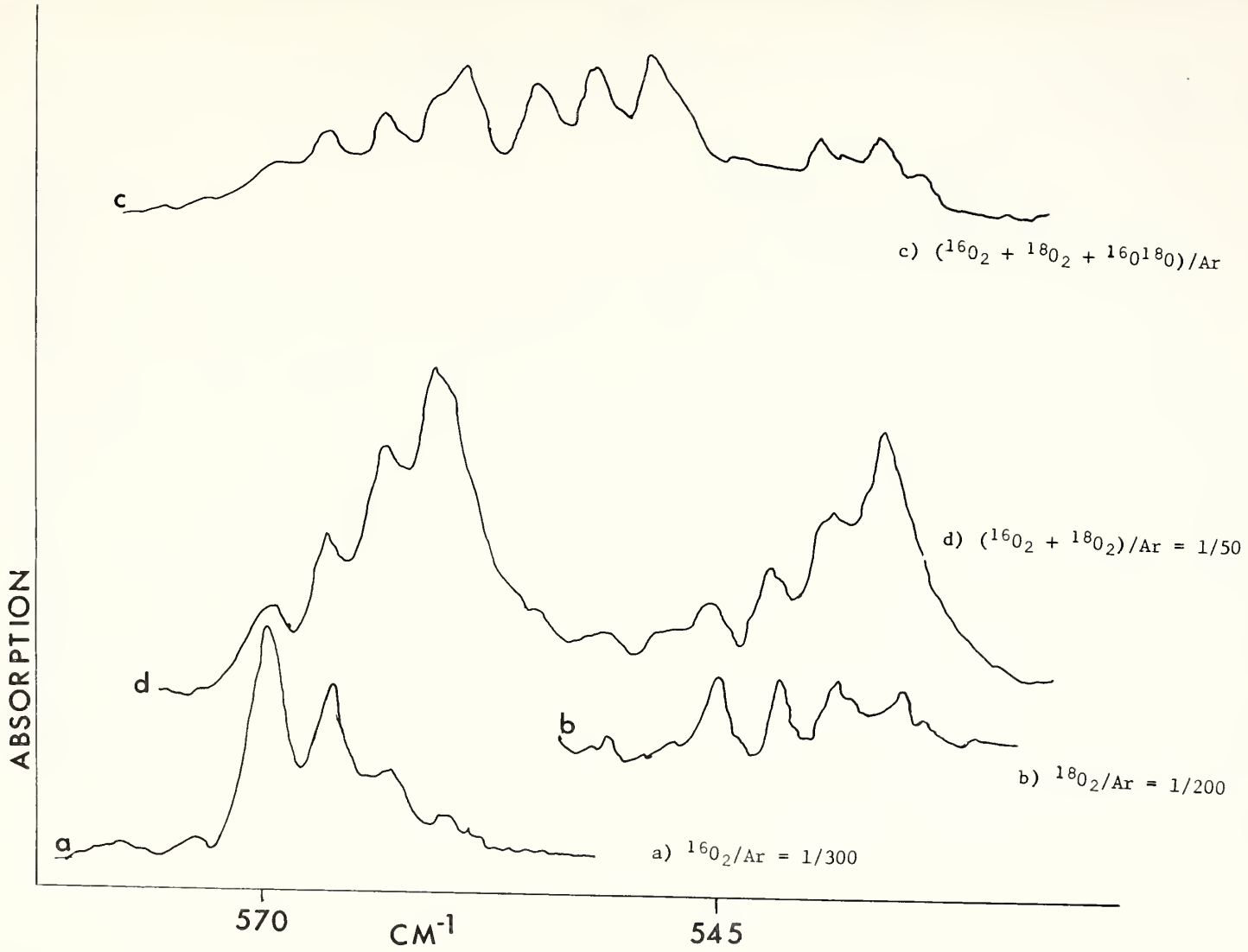

Figure 2. The Infrared Spectra of Ba + O_2/Ar

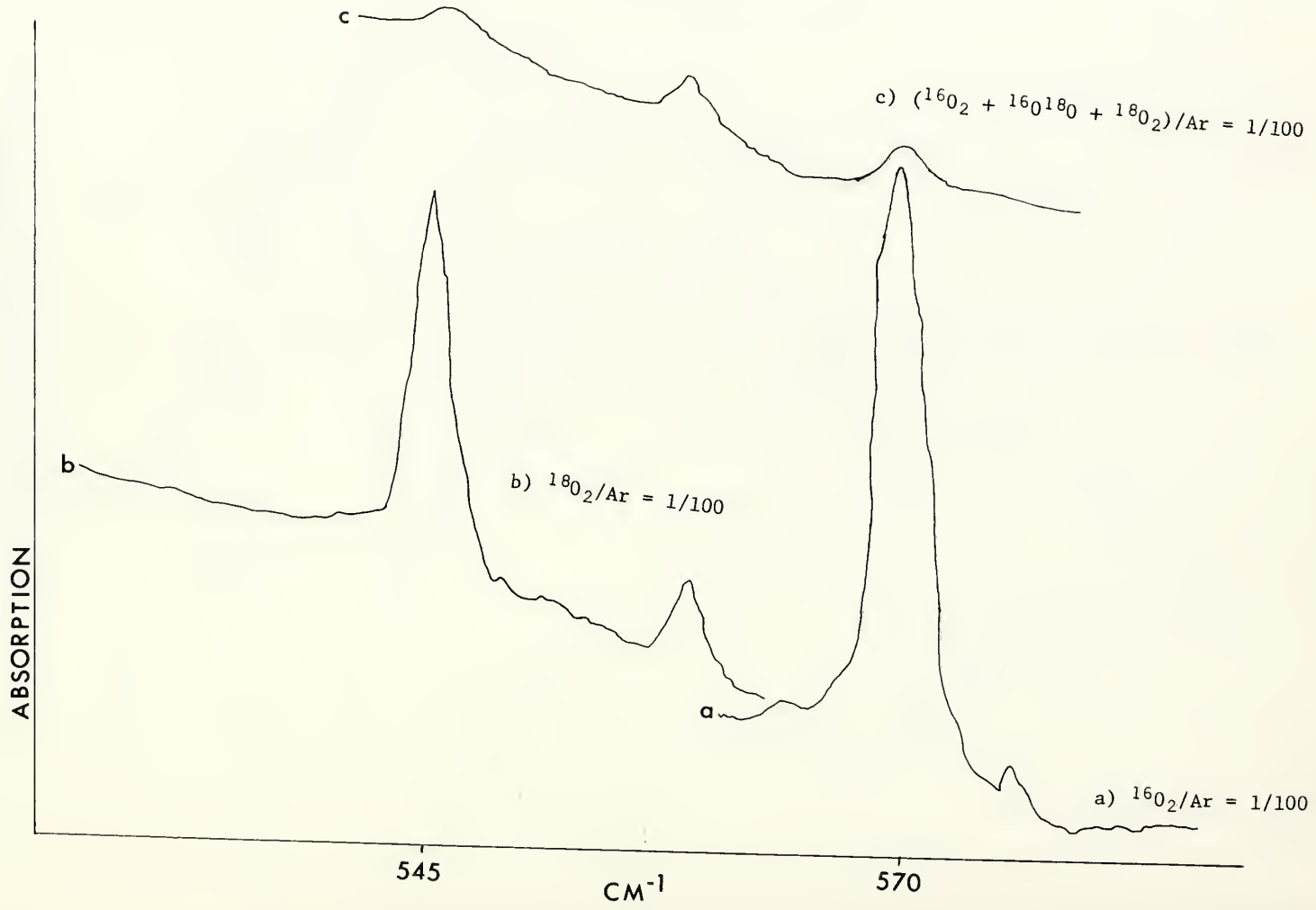

Figure 3. The Infrared Spectra of Ba + O_2/Ar

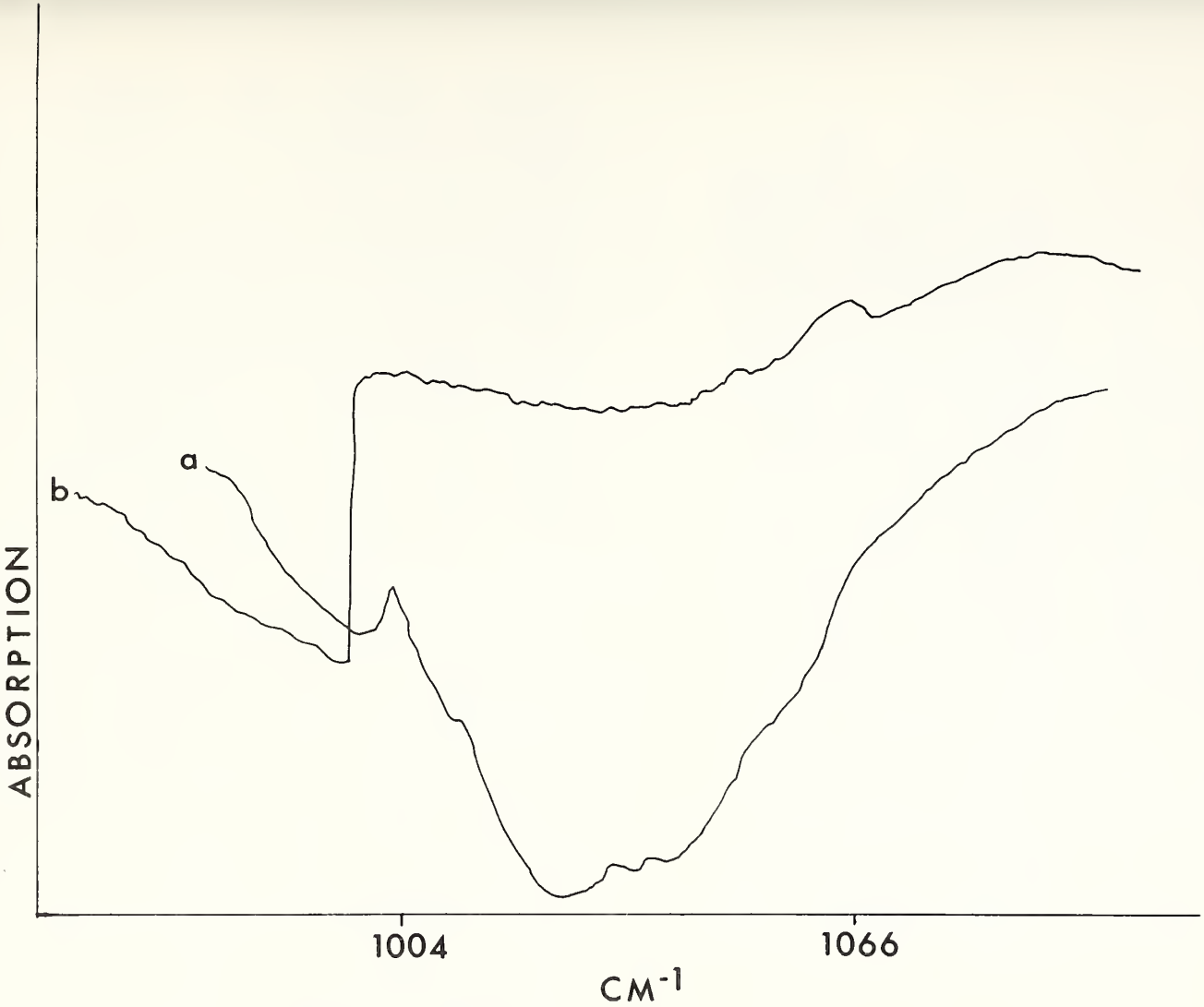

Figure 4. The Infrared Spectra of Ba + O_2/Ar
a) $^{18}O_2$/Ar = 1/100
b) $^{16}O_2$/Ar = 1/100

Chapter 6

A TRANSPIRATION INVESTIGATION OF THE REACTIVITY BETWEEN HF AND GASEOUS AlF_3 NEAR 1200 K

Thomas B. Douglas and Ralph F. Krause, Jr.

Gaseous HF, at partial pressures of approximately 0.02 and 0.76 atm and mixed with argon was passed under approximately equilibrium conditions over crystalline AlF_3 near 1200 K. Within the experimental error, the vapor pressure of AlF_3 was found to be the same as in similar experiments in which HF was absent, indicating a far lower reactivity of AlF_3 with HF than with gaseous LiF or NaF at this temperature. Even after estimating the entropies of two postulated structures for a hypothetical molecule $HAlF_4$, it is concluded that the precision of the transpiration results, though fairly high, does not permit a more exact conclusion than that the heat of decomposing this molecule into HF and gaseous AlF_3 is less than 35 kcal per mole, and that some spectroscopic technique would be required to detect and measure any molecule formed by combining HF and AlF_3.

Introduction

Several years ago we developed a precise apparatus for using the transpiration (or entrainment) method up to about 1500 K, and used it to measure the vapor pressure of pure aluminum trifluoride, AlF_3, near 1200 K [1].[1] This method is also an accurate means of measuring the equilibrium constants of chemical reactions between a transpiring gas and an evaporating solid or liquid --to the extent that ambiguity as to the reactants and products can be eliminated or is immaterial. The use of the method for this purpose rests on the exact fact that at equilibrium the thermodynamic activity of every vapor species produced by the evaporation of a pure solid or liquid, at a given temperature, is independent of what other gaseous species are present. By evaporating AlF_3 in the presence of gaseous $AlCl_3$, we made this type of application of our apparatus to measure successfully the heats of formation of AlF_2Cl and $AlFCl_2$ [7]. These two gases had not previously been investigated experimentally, but they are present in the combustion gases of every fuel formulation containing these three chemical elements.

[1] Numbers in brackets indicate literature references at the end of this chapter.

The present chapter reports the results of an additional investigation, in which AlF_3 was evaporated at temperatures near 1200 K, but this time in the presence of HF. Our purpose was to detect any appreciable formation of gaseous species from these two components ($HAlF_4$ would be the formula of the simplest and most likely one) and, if one were formed in measurable amounts, to determine from the data some of its thermodynamic properties. The most likely reaction would be

$$AlF_3(g) + HF(g) = HAlF_4(g) \qquad (1)$$

From thermodynamic data now available [8], the formally analogous reactions

$$AlF_3(g) + LiF(g) = LiAlF_4(g) \qquad (2)$$

and

$$AlF_3(g) + NaF(g) = NaAlF_4(g) \qquad (3)$$

are known to proceed very nearly to completion under comparable conditions. However, it is immediately recognized that hydrogen is far from analogous to the alkali elements in many important respects. And, in fact, the attempts of the present investigation to detect any appreciable reactivity such as by Reaction (1) were completely negative. However, oftentimes negative results give useful positive information. Along this line, the experimental data are used in a later section of this chapter to set an upper limit to the heat of decomposition of the hypothetical gas $HAlF_4$.

Experimental Details

This work involved nearly saturating a flow of argon with HF in one cell at dry-ice or ice temperature, and passing the mixture through another cell which contained AlF_3 at a temperature between 1200 and 1262 K. When the gas phase was subsequently cooled, the sublimed AlF_3 was condensed downstream, the HF vapor was absorbed by solid NaF, and the argon was collected in a tank for subsequently measuring its volume. The essential features of the apparatus are those described in our paper reporting the vaporization of AlF_3 in an inert medium [1].

Some attachments to the original apparatus were made to handle the HF. Three special weighing tubes were made from monel to account for the loss and gain of HF in an experiment. Each tube had a miniature 4-way teflon-packed valve welded to a teflon-gasketed flange, the total weight being about 220 g empty. One tube was designed for bubbling argon through a liquid HF sample. The other two were initially loaded with solid $NaHF_2$ and heated in a tube furnace near 350 °C while a stream of argon entrained the evolving HF vapor (in this process of producing "activated" NaF) to a waste-disposal tube containing soda-lime. These special tubes were held in a line of monel tubing by stainless-steel (Type 316) fittings using teflon ferrules, and were connected to the high-temperature cell by monel diaphragm valves. After a flush of HF conditioned the surfaces of the monel lines, a portion of a commercial source of anhydrous liquid HF, which the manufacturer reported as 99.9 mol % pure, was distilled at room temperature and condensed at dry-ice temperature into the first special tube. Using the 4-way valves to bypass the contents of the special tubes, the apparent mass of HF, vaporized from the first tube and absorved by the activated NaF in the other two tubes, was determined by weight differences. Estimated corrections were added, respectively, for the mass of argon which replaced HF or which was displaced by $NaHF_2$ (because the latter is less dense than NaF).

Argon which the manufacturer reported as 99.996 mol % pure served as the carrier gas. Water vapor in the flowing gas was removed to a high degree by molecular sieves which the manufacturer said could achieve dew points of -73 °C (1.5 ppm by volume). The quantity of argon involved in a given experiment was measured by a volumetric gasometer and corrected for differences in the initial and final barometric pressures and room temperatures. The total pressure of the gas mixture in the high-temperature cell was taken as the time average of the barometric pressure plus an observed head pressure minus an estimated correction for the average height of liquid HF in the special weighing tube.

The sample of fine crystals of AlF_3 was taken from the same source as the earlier work [1], where it showed by chemical analysis 32.15% Al and 67.8% F (theoretical, 32.13% Al and 67.87% F). The sample, which was contained in Pt/Rh boats and tubes, was baked several hours under vacuum (10^{-5} torr) near 900 K before an experiment. The mass of sublimed sample was taken as the mean of the sample-boat loss and the gain of the condenser-tube, the latter having a total weight near 137 g.

Table 1. Data and Results of Subliming AlF_3 in the Absence or Presence of HF Gas

Property	Units	Run Number 2	3	4	5	6	7	8	10	11	12	13*	14	15
P(baro)	torr	755.2	753.2	746.5	748.7	752.0	751.7	746.6	756.7	750.8	751.6	748.5	753.6	751.0
ΔP(mano)	torr	3.7	4.3	5.7	1.5	5.0	14	14.2	10.5	3.0	11.9	10.5	8.4	13.0
ΔP(HF liq)	torr	-1.1	-1.1	-1.0		-0.7	-5.5	-4.5	02.3			-1.6		-5.6
V (Ar)	ℓ	14.868	10.850	15.054	43.886	46.446	0.849	1.000	2.000	7.416	15.181	2.500	17.663	3.133
Δ V (corr)	ℓ	-.084	-.056	-.038	+.004	-.020	-.001	+.003	-.020	-.007	-.006	-.043	-.034	-.031
n (Ar)	mmol	605.1	441.8	609.5	1788.1	1895.7	34.6	40.8	81.7	303.8	622.6	100.2	724.1	126.6
						HF								
T	°C	-78.5	-78.5	-78.5		-78.5	0.0	0.0	0.0			0.0		0.0
wt. loss	g	0.2439	0.1737	0.2428		0.7614	2.1454	2.5128	5.4110			6.6688		8.6504
loss corr.	g	.0004	.0003	.0004		.0014	.0038	.0045	.0096			.0119		.0154
wt. gain	g	0.2444	0.1697	0.2416		0.7513	2.1464	2.5122	5.4017			6.6471		8.6388
gain corr.	g	.0008	.0006	.0008		.0026	.0074	.0086	.0182			.0228		.0295
net(loss-gain)	%	-0.4	+2.1	+0.3		+1.17	-0.21	-0.14	+0.013			-0.12		-0.03
flow	ml/sec	0.387	0.407	0.438		0.428	1.073	1.115	0.690			0.691		0.664
assoc.factor	HF/mol	3.76	3.62	3.67		3.71	3.54	3.45	3.79			3.74		3.84
						AlF_3								
wt. loss	mg			121.6	272.8	320.4			243.0	184.4	338.6	312.4	363.1	340.2
wt. gain	mg			123.0	272.0	324.1			242.6	183.5	337.2	314.4	362.5	344.2
excess	mg			28.8		32.4			60.6			69.6		54.3
(loss-gain)/av.	%			-1.15	+0.29	-1.15			+0.16	+0.54	+0.41	-0.64	+0.16	-1.2
						Reaction Cell								
T	K	~800	~1200	1200.5	1201.2	1201.2	~820	~850	1256.0	1262.1	1258.1	1257.8	1254.3	1255.4
flow	ml/sec			2.744	2.580	2.687			7.407	2.336	5.962	7.326	6.294	7.176
P(HF)obs	matm			19.26		19.47			768.4			757.5		763.6
$P(AlF_3)$obs	matm			1.767	1.787	1.773			6.155	7.103	6.451	6.617	5.946	6.075
(obs/calc-1)‡	%			+0.8	+0.28	-0.5			-1.25	-0.17	-1.13	+2.07	-1.00	-1.27

* Some argon accidentally rushed into the evacuated Pt/Rh tubes at the start, so some AlF_3 may have been lost. Hence this run was discarded.

‡ Calculated values were interpolated from the previously determined vapor pressure of AlF_3 [1].

The observed data are tabulated in Table 1.

Some experiments excluded HF, others $A\ell F_3$; but in those which involved both, a measured excess of argon bypassed the HF-generation cell at the end of each run, and swept the HF vapor remaining in the flow path through the $A\ell F_3$ sublimation cell into the NaF absorbers. This was done in order not to neglect the $A\ell F_3$ which sublimed before the HF reached the $A\ell F_3$ sublimation cell, and at the same time to account for all the HF that had passed through this cell. The corresponding $A\ell F_3$ correction was taken to be that accurately calculated from the earlier vapor-pressure data [1] and the excess argon. The temperature of an experiment (IPTS-68 [9]) was taken as the time average at the $A\ell F_3$ sublimation-cell exit.

Experimental Results

Assuming the gas mixture in the high-temperature vapor cell to consist of HF, $A\ell F_3$, and Ar only (it was convenient to count each mole of $A\ell_2F_6$ as two moles of $A\ell F_3$), the partial pressure of each component was taken to be its mole fraction multiplied by the total pressure. These partial pressures in the runs in which $A\ell F_3$ was sublimed in the absence or presence of HF are shown in Table 1 at nine independently measured temperatures. The average gas flow also shown refers to the total gas mixture at the temperature of the vapor cell. The last line of the table compares the observed value of the partial pressure of $A\ell F_3$ with that calculated from the previous measurements [1] of the vapor pressure of $A\ell F_3$. (Runs 2, 3, 7, and 8, in which no $A\ell F_3$ was present, served to test the accountability for HF.)

These results indicate that any supposed enhancement of the volatility of $A\ell F_3$ in the presence of HF cannot be detected within the limits of precision of this work. Runs 5 and 11 served as a verification test of the earlier work [1], in which there was a 0.15% standard deviation in $\underline{P}$ for a least-squares fit of a 2-coefficient equation to 8 sets of $\underline{P}$ and $\underline{T}$ data. Although the difference between Runs 4 and 6, in which $A\ell F_3$ was sublimed in the presence of about 19 matm of HF, is a little greater than expected, the percent differences of Runs 10 and 15, in which HF was about 40 times more concentrated, seem to indicate a distinct negative trend. However, Runs 12 and 14 show that this trend is probably merely an indication of undersaturation of $A\ell F_3$ in the gas flow, which in <u>these</u> experiments ranged from about 6.0 to 7.4 mℓ/sec while the flow of the earlier work ranged from 1.0 to 2.0 mℓ/sec. The effect of

the higher flow is reflected by the greater pressure drop through the small-tube restriction at the vapor cell exit; compare the differences in Table 1 between ΔP (mano) and ΔP (HF liq). (This apparent lack of saturation at the higher flow rates will be examined more quantitatively in a later section.)

Concerning the Degree of Association of Saturated HF Vapor at Low Temperatures

Incidental to the main purpose of this work was an inspection of the degree of association of HF vapor at the temperature of its generation. Using Claussen and Hildebrand's [2] measurements of the vapor pressure of HF, the ratio of the observed number of moles of HF to the calculated number of moles was determined and is shown in Table 1. This ratio, which is the degree of association, appears sensitive to the gas flow through the HF generation tube; but no attempts were made to insure an approach to saturation because it was obviously not necessary for the main purpose of this work. The average ratio for the last three experiments gives a molecular weight of 75.8 for the saturated vapor at 273 K. Simons and Hildebrand [3] observed 67.6, and calculated 72.1 based on their model of association. Fredenhagen [4] observed values from 73.09 to 74.57. Jarry and Davis [5] calculated the degree of association as 4.717 (molecular weight 94.39) from their vapor-density measurements between 0 and 105°C; but Yabroff, Smith, and Lightcap [6] have concluded that Jarry and Davis' values at temperatures below 60 °C are not reliable. It is to be noted that the values from the present work can claim no high accuracy, because they depend on the cited vapor-pressure data used in their calculation and because no systematic effort was made to ensure that the vapor in the present case was saturated.

Upper Limits to $\Delta G°$ of Reaction (1) (from the Data)

Runs 4-6 detected no reactivity between $A\ell F_3$ and HF, so experiments more favorable for positive results (Runs 10-15) were then undertaken. In these cases the HF pressures were approximately 40 times as great, so that there should have been about 40 times as great a fraction of the $A\ell F_3$ converted to the new species (if this is represented by Reaction (1)). As noted earlier from Table 1, the evaporated $A\ell F_3$ in Runs 10, 12, 14, and 15 probably

came out low (last line) because of the unusually high flow rates, and an attempt will be made to correct the results of these runs to equilibrium before attempting to conclude limiting values from them.

If the simple assumption is made that under comparable conditions the rate of sublimation is proportional to the degree of unsaturation of the vapor, then it is easy to derive

$$k = v \log [P/(P-p)], \qquad (4)$$

where k is a constant, v is the gas-flow rate, P is the real saturation pressure, and p is the apparent saturation pressure from an experiment at v. The data of Table 1 give the values in Table 2 for Runs 10-12, 14, and 15. (Run 13 was discarded for the reason stated in a footnote of Table 1.)

Table 2

Dependence of $A\ell F_3$ Sublimation on Rate of Gas Flow

Run No.	HF Present?	v(ml/sec)	(P-p)/P	k[from Eq (4)]
11	No	2.34	0.0017	6.5
12	"	5.96	.0113	11.6
14	"	6.29	.0100	12.6
15	Yes	7.18	.0127	13.6
10	"	7.41	.0125	14.1

The values of k in Table 2 show a definite drift with v, which indicates that Eq (4) is only roughly valid. However, if in trying to establish an upper limit to (P-p)/P in those runs in which HF was present (Runs 10 and 15) we were to assume k = 12.1 (the average from Runs 12 and 14), the results from Runs 10 and 15 would then indicate approximately a 1% interaction of the $A\ell F_3$ with HF (the latter being present at approximately 0.76 atm, and therefore in great excess). As an upper limit, the 1% was doubled. And from the results for Runs 4 and 6, where the partial pressure of HF was only about 0.02 atm, the upper limit of reactivity was taken as 1.5%.

The estimated upper limits of $\Delta G°$ for Reaction (1) are then calculated to be as follows:

$$T = 1200,\ P(HF) = 0.019\ atm : \Delta G^\circ = -RT\ln K_p \geq + 0.6\ kcal \quad (5)$$

$$T = 1260,\ P(HF) = 0.76\ atm : \Delta G^\circ = -RT\ln K_p \geq + 9.1\ kcal \quad (6)$$

Postulated Molecular Structures of $HAlF_4$

As is commonly realized, a higher entropy tends to favor the abundance of simpler over more complex gaseous molecules under comparable conditions. We shall thus expect that $HAlF_4$--rather than other combinations such as H_2AlF_5 or H_3AlF_6-- is ordinarily the principal product of reaction between AlF_3 and HF. The mass-spectrometric data bear out this relation in the case of the gaseous lithium and sodium "salts" of the above hydrogen compounds [8].

Equations (5) and (6) give estimated upper limits, based on our transpiration results, for the standard free-energy increase, ΔG°, of Reaction (1) under the stated conditions. Since the standard entropies of the reactants are known, a value for the standard entropy of $HAlF_4(g)$ would enable setting an upper limit to the heat of decomposing $HAlF_4$ according to the reverse of Reaction (1).

For the purpose of estimating the entropy, two alternative molecular structures of $HAlF_4$ were assumed, as follows.

Structure I: As has been assumed for the two molecules $LiAlF_4$ and $NaAlF_4$ [8], in $HAlF_4$ the Al was assumed surrounded tetrahedrally by the four F's, with each Al-F distance 1.69 Å. The covalent contribution should be much greater in $HAlF_4$ than in the alkali-metal analogs, so the H was assumed closest to one F, at a distance of 1.0 Å, and with the H-F-Al group linear.

Structure II: This structure is planar, and with the H-F(bond distance, 1.0 Å) attached to an unchanged AlF_3 molecule (FAlF angles each 120°, F-Al distance 1.63 Å) through a hydrogen bond (1.5 Å long) between the H and one of the F's of the AlF_3. (These two H-F distances are the same as has been reported for the hydrogen-bonded gaseous polymers of HF [10].)

Since the present experimental work affords no quantitative information on $HAlF_4$, it would hardly be worthwhile to attempt to make as sophisticated an estimate of the 12 vibrational fundamentals of this molecule as those for

$LiA\ell F_4$ and $NaA\ell F_4$ [8]. The procedure followed was simply to assume for $HA\ell F_4$ approximately the same fundamentals of HF and $A\ell F_3$ [8] [in cm^{-1} and with degeneracies in parentheses: 4000(1), 650(1), 300(1), 940(2), and 260(2)] plus estimated values for the additional one stretching mode and four bending modes of $HA\ell F_4$. These additional fundamentals were taken to be, respectively: For Structure I, 500(1), 300(2), and 800(2); for Structure II, 200(1), 300(2), and 800(2). (The 800 cm^{-1} is for the degenerate bending mode involving, principally, motion of the H atom.)

Using the harmonic-oscillator, rigid-rotor approximation, these structures were calculated to have the moments of inertia and standard-state entropies listed in Table 3.

Table 3

Calculated Moments of Inertia and Entropies of Two Postulated Structures of the Molecule $HA\ell F_4$

Structure	$I_x I_y I_z$	$S^o_{1200\ K}$	$S^o_{1260\ K}$
	$(at.wt.units)^3\ (\AA)^6$	$cal\ K^{-1}\ mol^{-1}$	$cal\ K^{-1}\ mol^{-1}$
I	$3.337\ (10^6)$	109.6	111.0
II	$1.102\ (10^7)$	113.4	114.8

Upper Limits for $\Delta H°$ of $HA\ell F_4$ (g) = HF (g) + $A\ell F_3$ (g); Comparison with Analogous Decompositions of $LiA\ell F_4$ (g) and $NaA\ell F_4$ (g)

Combining the entropy values of Table 3 with those for HF (g) and $A\ell F_3$(g) at the same respective temperatures [8] gives, for $\Delta S°$ for the reverse of Reaction (1), at either 1200 or 1260 K, + 32.4 $cal\ K^{-1}$ for Structure I and +28.6 $cal\ K^{-1}$ for Structure II. These values and those of Eqs (5) and (6) may be substituted into the thermodynamic equation $\Delta H° = \Delta G° + T\Delta S°$ to give

upper limits of ΔH° for the reverse of Reaction (1), adding 1.6 kcal to convert to 298 K. The results are:

$T = 1200$, $P(HF) = 0.019$ atm: $\Delta H^\circ_{298} \leq +40.0$ for I, ≤ 35.5 for II (7)

$T = 1260$, $P(HF) = 0.76$ atm: $\Delta H^\circ_{298} \leq +33.3$ for I, ≤ 28.5 for II (8)

The limits from the transpiration data for the higher pressures of HF [Eq (8)] are a little more definitive than for the lower pressures of HF, and may be compared with corresponding values for the reverse of Reactions (2) and (3) [8] in Table 4.

Table 4

Values of ΔS°_{1260} and ΔH°_{298} for the Decomposition of Gaseous $HA\ell F_4$, $LiA\ell F_4$, and $NaA\ell F_4$

All-Gaseous Reaction	Structure of Reactant	ΔS°_{1260}	ΔH°_{298}
		cal K^{-1}	kcal
$HA\ell F_4 = HF + A\ell F_3$	I	32.4	<33.3
	II	28.6	<28.5
$LiA\ell F_4 = LiF + A\ell F_3$	See [8].	31.7	72.5
$NaA\ell F_4 = NaF + A\ell F_3$	See [8].	31.6	88.1

Discussion

Table 4 shows immediately that the heat of the first reaction (<35 kcal) is considerably less than for the second and third reactions. We may raise the question as to whether this fact could have been reasonably predicted beforehand. For Structure I of $HA\ell F_4$, the answer does not seem clear; perhaps in retrospect the lower energy of the first reaction can be traced principally to the far greater energy of decomposition to ions for HF than for LiF or NaF. For Structure II of $HA\ell F_4$, it is enlightening to examine known energies of other hydrogen bonds, particularly those involving fluorine.

Either H-F bond in the bifluoride ion, HF_2^-, may be considered the simplest hydrogen bond involving fluorine (both H-F distances are equal at 1.13Å in crystalline alkali-metal bifluorides). Defining the hydrogen-bond energy of HF_2^- as ΔH for the reaction

$$HF_2^-(g) = HF(g) + F^-(g), \qquad (9)$$

this energy has been estimated by several semi-experimental and theoretical methods, the values ranging from approximately 27 to 58 kcal. Using thermochemical data[2] and calculated lattice energies of crystalline KHF_2, $RbHF_2$, and $CsHF_2$, Waddington [12] found 58±5 kcal. Later, Harrell and McDaniel [13] claimed that the ΔH value of 37 kcal they obtained for the reaction

$$(CH_3)_4 NHF_2(c) = (CH_3)_4 NF(c) + HF(g) \qquad (10)$$

is identical with ΔH for Reaction (9) to within 1 or 2 kcal, and although this statement has been called "accepted" [14], the basis for such a status is not obvious to us. The several theoretical calculations [of ΔH for Reaction (9)] involve differences between relatively large numbers. Pauling [15] obtained 49.5 kcal from a very simple treatment which, however, involved, as its only assumption, the charge distribution on the atoms. Davies [16] obtained 47.9 kcal, but correction of his treatment to a symmetrical structure for HF_2^- gave Fyfe [17] 57.6 kcal. A treatment of Evans [18], as modified by Waddington [12], gave 57.3 kcal. Recently, by quantum-mechanical calculations, Noble and Kortzeborn [14] obtained 40 kcal, and a H-to-H bond distance in HF_2^- only 0.01 Å different from the experimental value; they claim that the unchanged number of electron pairs in Reaction (9) leads to a high degree of cancellation of error in the correlation energies, which is normally the most serious error in calculations of this kind.

However, the average hydrogen bond energy in the polymers of HF has been found to be much smaller (6.0 kcal/mole, or near the energy of most hydrogen bonds) [10]. In this connection, a statement of Pauling's [10] is significant: "It is interesting that in general fluorine atoms attached to

---

[2] For ΔHf^o_{298} of $F^-(g)$, Waddington rejected the value -79.5 kcal/mol given in NBS Circular 500 (1952) and, instead, used a value (-64.8) almost identical with that in the updated substitute for Circular 500 [11].

carbon do not have significant power to act as proton acceptors in the formation of hydrogen bonds in the way that would be anticipated from the large difference in electronegativity of fluorine and carbon." The electronegativity difference between fluorine and aluminum is still greater, but perhaps an analogous situation obtains for Structure II of $HA\ell F_4$. In summary, our finding that the hydrogen bond energy for Structure II of $HA\ell F_4$ is less than 28.5 kcal (Table 4) does not seem at all surprising.

From a more practical standpoint, the present experimental investigation has shown that gaseous reaction products between HF and $A\ell F_3$ are not important species near 1200 K (except possibly under very high pressures of HF). Nor should they be important species at lower or higher temperatures. Making the reasonable assumption that these species (with respect to HF and $A\ell F_3$) are at least somewhat exothermic, at higher temperatures they will be even more extensively dissociated. And as the temperature falls below 1200 K, they will, by the same token, be less dissociated, but then the vapor pressure of $A\ell F_3$ falls off even faster; in other words, at lower temperatures extensive condensation of $A\ell F_3$ causes their very extensive dissociation. Hence, despite its capability for relatively high precision, the transpiration method is not a promising means of detecting and measuring these particular species. Obviously some discriminatory (spectroscopic) method would be much more promising.

Acknowledgements

Discussions with Charles W. Beckett and Stanley Abramowitz were very helpful in estimating fundamental frequencies for $HA\ell F_4$.

References

[1] R. F. Krause, Jr., and T. B. Douglas, J. Phys. Chem. 72, 475 (1968).

[2] W. H. Claussen and J. H. Hildebrand, J. Amer. Chem. Soc. 56, 1820 (1934).

[3] J. Simons and J. H. Hildebrand, ibid, 46, 2183 (1924).

[4] K. Fredenhagen, Z. anorg. allg. Chem. 210, 210 (1933).

[5] R. L. Jarry and W. Davis Jr., J. Phys. Chem. 57, 600 (1953).

[6] R. M. Yabroff, J. C. Smith, and E. H. Lightcap, J. Chem. Eng. Data 9, 178 (1964).

[7] R. F. Krause, Jr., and T. B. Douglas, J. Phys. Chem. 72, 3444 (1968).

[8] JANAF Thermochemical Tables, Dow Chemical Co., Midland, Mich. Tables for: $A\ell F_3(g)$, June 30, 1970; LiF(g), Dec. 31, 1968; NaF(g), Dec. 31, 1968; $LiA\ell F_4(g)$, June 30, 1970; $NaA\ell F_4(g)$, June 30, 1970; HF(g), Dec. 31, 1968.

[9] "The International Practical Temperature Scale of 1968," Metrologia 5, 35 (1969).

[10] L. Pauling, "The Nature of the Chamical Bond," Cornell University Press, Ithaca, N.Y., 3rd edition, 1960, pp. 460-464.

[11] D. D. Wagman, W. H. Evans, V. B. Parker, I. Halow, S. M. Bailey, and R. H. Schumm, NBS Technical Note 270-3, U.S. Govt. Printing Office, Washington, D. C. January 1968, p. 21.

[12] T. C. Waddington, J. Chem. Soc. 1958, 1708.

[13] S. A Harrell and D.H. McDaniel, J. Amer. Chem. Soc.86, 4497 (1964).

[14] P. N. Noble and R. N. Kortzeborn, J. Chem. Phys. 52, 5375 (1970).

[15] L. Pauling, Proc. Royal Soc. London A114, 181 (1927).

[16] M. Davies, J. Chem. Phys. 15, 739 (1947).

[17] Fyfe, J. Chem. Phys. 21, 2 (1953).

[18] Evans, Dissertation, State Univ. of Iowa, 1946.

Chapter 7

HIGH-SPEED (SUBSECOND) MEASUREMENT OF HEAT CAPACITY, ELECTRICAL RESISTIVITY, AND THERMAL RADIATION PROPERTIES OF TANTALUM IN THE RANGE 1900 TO 3200 K*

A. Cezairliyan, J. L. McClure and C. W. Beckett
National Bureau of Standards
Washington, D. C. 20234

Abstract

Measurements of heat capacity, electrical resistivity, hemispherical total and normal spectral emittances of tantalum above 1900 K by a pulse heating technique are described. Duration of an individual experiment, in which the specimen is heated from room temperature to near its melting point is less than one second. Temperature measurements are made with a photoelectric pyrometer. Experimental quantities are recorded with a digital data acquisition system. Time resolution of the entire system is 0.4 ms. Results on the above properties of tantalum in the range 1900 to 3200 K are reported and are compared with those in the literature. Estimated inaccuracy of measured properties in the above temperature range is: 2 to 3 percent for heat capacity, 0.5 percent for electrical resistivity, 3 percent for hemispherical total emittance and 2 percent for normal spectral emittance.

---

*This work was supported in part by the Propulsion Division of the U. S. Air Force Office of Scientific Research under contract ISSA-69-0001.

1. Introduction

Conventional methods of measuring heat capacity, electrical resistivity, and other thermophysical properties at high temperatures employ "drop", steady-state, and quasi steady-state techniques in which the specimen is exposed to high temperatures for long periods of time, ranging from minutes to hours. Extension of these techniques to temperatures above 2000 K creates problems resulting from increased heat transfer, chemical reactions, evaporation, diffusion, loss of mechanical strength, etc. To overcome these limitations, this laboratory has recently developed a high-speed measurement technique in which the specimen is heated and pertinent quantities required for the determination of properties are measured in short times. The duration of an individual experiment, in which the specimen is heated from room temperature to near its melting point, is less than one second. A millisecond resolution photoelectric pyrometer is used to measure the specimen temperature. The recordings of experimental quantities are made with a high-speed digital data acquisition system which has a time resolution of 0.4 ms. The application of this technique to measurements on molybdenum has been published [1][1]. General reviews on high-speed methods for the measurement of thermophysical properties of electrical conductors have been presented recently [2,17].

In the present study the technique was used to determine the heat capacity and electrical resistivity of tantalum in the temperature range 1900 to 3200 K, and the hemispherical total and normal spectral emittances up to 3000 K.

---

[1] Figures in brackets indicate the literature references at the end of this paper.

2. Method

The method employed in this study is based upon rapid resistive heating of the specimen by the passage of high currents and measuring the pertinent quantities with appropriate time resolution. The required quantities are power imparted to the specimen and temperature of the specimen, both as a function of time. Imparted power is obtained from measurements of current flowing through the specimen and potential difference across the "effective"[2] specimen as a function of time.

The relationship for heat capacity is obtained from power balances for the specimen during the pulse heating and the following free cooling periods. The expression for heat capacity, which was derived in an earlier publication [1], is

$$c_p = \frac{ei - \epsilon\sigma A_s (T^4 - T_o^4)}{m(dT/dt)_h} \qquad (1)$$

where

c_p = heat capacity in J mol^{-1} K^{-1}
e = potential difference across the effective specimen in V
i = current through the specimen in A
ϵ = hemispherical total emittance
σ = Stephan-Boltzmann constant (5.6697×10^{-8} W $m^{-2}K^{-4}$)
A_s = effective specimen surface area in m^2
T = specimen temperature in K
T_o = room temperature in K
m = amount of effective specimen in mol
$(dT/dt)_h$ = heating rate in K s^{-1}

[2] "effective" refers to the portion of the specimen between the knife-edge voltage probes.

The hemispherical total emittance, ϵ, which appears in the radiation loss term of the heat capacity relation, is determined from data collected during the free cooling period. Derived from the power balance relationship during the cooling period and eq (1), the expression for ϵ is

$$\epsilon = \frac{ei}{\sigma A_s (T^4 - T_o^4)(1 + M)} \tag{2}$$

where

$$M = - \frac{(dT/dt)_h}{(dT/dt)_c} \tag{3}$$

$(dT/dt)_c$ = cooling rate in K s^{-1}

Equation (2) is used to compute values for ϵ at selected temperatures which are used to obtain a function for ϵ in terms of temperature. Then, ϵ values from this function are substituted in eq (1) to obtain heat capacity over the entire temperature range.

Data from the heating period is also used to calculate the electrical resistivity with the aid of the equation

$$\rho = \frac{R A_c}{\ell} \tag{4}$$

where

ρ = electrical resistivity in Ω m

R = resistance of effective specimen in Ω

A_c = specimen cross-sectional area in m^2

ℓ = effective specimen length in m.

The normal spectral emittance, $\epsilon_{n,\lambda}$, is obtained from separate pulse experiments in which radiance from the surface of the specimen is measured. The relation for $\epsilon_{n,\lambda}$ is

$$\epsilon_{n,\lambda} = \frac{L_s}{L_b} \tag{5}$$

where

L_s = radiance from surface of specimen as observed by the pyrometer.

L_b = blackbody radiance from sighting hole in specimen as observed by the pyrometer.

In all the above equations, geometrical quantities are corrected for the presence of the sighting hole, and the quantities related to radiation from the sighting hole are corrected for scattered light and departure from blackbody conditions.

3. Apparatus

A functional diagram of the measurement system used in this study is shown in figure 1. The details of the system were described in an earlier publication [1].

The specimen was a tube approximately 100 mm long with a small rectangular hole fabricated in the wall at the middle of its length to approximate blackbody conditions. The knife-edge probes, which were used for potential measurements, were made of tantalum and were placed 50 mm apart on the middle portion of the specimen. The portion between the probes, defined as "effective" specimen, was essentially free of temperature gradients for the duration of an experiment. The specimen and the associated components were contained in a vacuum chamber.

The specimen temperature was measured with a high-speed photoelectric pyrometer [12], which permits 1200 evaluations of the specimen temperature per second. The pyrometer alternately compares the radiance from the blackbody hole in the specimen to that of a reference lamp.

Electrical signals corresponding to voltage, current, and temperature were recorded with a high-speed digital data acquisition system, which consists of a multiplexer, analog-to-digital converter, and a core memory together with various control and interfacing equipment. At the end of each experiment, the data were retrieved

in printed numeric form and on punched paper tape via a teletype-writer. During this retrieval period, data were also sent simultaneously to a time-sharing computer for immediate processing.

Electrical signals corresponding to voltage, current, and temperature were also monitored simultaneously with oscilloscopes.

4. Measurements

Measurements were made on four tantalum specimens. The first two specimens were used for experiments in the temperature interval 1900 to 3000 K. To optimize the operation of the pyrometer, this temperature interval was divided into 3 ranges with 3 experiments per range. These nine experiments are referred to as a series. The temperature ranges were: low, 1900 to 2250 K; medium, 2100 to 2600 K; and high, 2350 to 3000 K.

Two complete series of experiments were conducted on the first specimen (Ta-1). During the second series, two additional experiments were conducted, one in the low range and one in the high range, to measure the surface radiance of the specimen. Before the start of the first series of experiments, the specimen (Ta-1) was subjected to approximately 30 heating pulses (in the range 2200 to 3000 K) in order to anneal the specimen and to determine the optimum heating rate for each temperature range. At the end of the first series of experiments and before the start of the second series, the specimen was pulse heated 15 times to 3000 K. One experiment per temperature range was conducted on the second specimen (Ta-2) without any prior heating pulses.

To obtain heat capacity and electrical resistivity in the temperature range 2950 to 3200 K, two other specimens, (Ta-3) and (Ta-4), were used.

The duration of the current pulses ranged from 280 to 520 ms depending on the temperature. The average heating rate of the specimen was 5700 and 3700 K s^{-1} at 2000 and 3200 K, respectively. At these temperatures, radiative heat losses from the specimen

amounted to approximately 3 and 22 percent of the input power, respectively. All of the experiments were conducted with the specimen in a vacuum environment of approximately 10^{-4} torr.

The data on voltage, current, and temperature were used to obtain third degree polynomial functions for each quantity in terms of time which, then, provided the input information for the equations of section 2.

During the entire set of experiments, the pyrometer was calibrated five times against a tungsten filament standard lamp, which in turn was calibrated against the NBS Temperature Standard. The digital recording system including the differential amplifiers was calibrated three times during the experiments. The details of the calibration procedures were given in an earlier publication [1].

Prior to the start of the experiments, the optical system of the pyrometer was modified to reduce the effect of light scattered from the area around the sighting hole in the specimen. In the present system this effect is approximately one percent. The blackbody quality of the specimen sighting hole was estimated to be 0.99 using DeVos' [13] method. The temperature data from the pyrometer were corrected for both scattered light and departure from blackbody conditions. The details of the methods employed for these corrections were given in an earlier publication [1].

The nominal dimensions of the tubular tantalum specimens were: length = 4 in (101 mm), outside diameter = 0.25 in (6.3 mm), wall thickness = 0.02 in (0.5 mm). The outer surface of each specimen was polished to reduce heat loss due to thermal radiation.

Specimen characterization was made on one specimen (Ta-1) by the following methods: photomicrographic, chemical analyses, and residual resistivity ratio.

Photomicrographs of the specimen before and after the entire set of experiments are shown in figure 2. It may be seen that considerable grain growth has taken place as the result of pulse heating the specimen to high temperatures.

Chemical analyses were made of the specimen before and after the entire set of experiments. Comparison of results does not indicate any detectable change in impurity concentrations. A list of the nature and concentration of impurities in the specimen is given in table 1.

The residual resistivity ratio of the specimen (ratio of electrical resistivity at 273 K to that at 4 K) before and after the entire set of experiments was 22 ± 1. The fact that the value of this ratio remained unchanged indicates that the specimen did not undergo any major chemical or physical changes.

The total mass of the specimen was determined before and after each series of experiments. The "effective" mass of the specimen was calculated from the total mass by ratio of the surface area between voltage probes to total surface area. Length measurements at room temperature were made with a micrometer microscope to the nearest 0.03 mm. The thickness of the cylinder wall was calculated from the mass, surface areas, and density.

Density of tantalum at 298 K was obtained by the water displacement method in a pycnometer. The results of three determinations gave a value of 16.65×10^3 kg m^{-3} with an average deviation of 0.03 percent. This compares favorably with the reported value of 16.6×10^3 kg m^{-3} [16].

5. Experimental Results

This section presents the results on the thermophysical properties determined from the measured quantities. All the results are based on the 1968 International Practical Temperature Scale [14]. The final results on properties at 100 degree temperature intervals are presented in table 2. In all computations, the geometrical quantities are based on their ambient temperature (298 K) dimensions.

5.1 Normal Spectral Emittance

To calculate the normal spectral emittance, two experiments were performed to measure the surface radiance of the Ta-1 specimen during the second heating series. The measurements were made at the effective wavelength of the pyrometer interference filter (650 nm; bandwidth 10 nm). The normal spectral emittance was calculated using the radiance data from each surface experiment together with the data from a previous or later regular blackbody experiment according to eq (5). Since the specimen's true temperature could not be measured directly in a surface experiment, the occurrance of equal temperatures in the two adjacent (surface and blackbody) experiments was calculated by locating times of equal specimen resistance.

A second degree polynomial function for normal spectral emittance was obtained by least squares approximation of the experimental results. The standard deviation (of an individual point) is 0.3 percent. The function which is valid in the temperature range 2000 to 3000 K is:

$$\varepsilon_{n,\lambda} = 0.4892 - 5.644 \times 10^{-5}\ T + 8.734 \times 10^{-9}\ T^2 \quad \text{(second series)} \qquad (6)$$

Normal spectral emittance computed using the above equation is given in table 2. The experimental results are presented in figure 3.

5.2 Hemispherical Total Emittance

The hemispherical total emittance of the Ta-1 specimen was computed with the aid of eq (2) using temperature data taken during both heating and initial free cooling periods in an experiment.

A linear function for hemispherical total emittance for each heating series was obtained by least squares approximation of the individual values. The standard deviation of the points from the function for the first and second heating series were 0.7 and 0.5

percent, respectively. The functions which are valid in the temperature range 2300 to 3000 K are:

$$\epsilon = 0.2197 + 4.146 \times 10^{-5} T \quad \text{(first series)} \quad (7)$$

$$\epsilon = 0.1991 + 4.687 \times 10^{-5} T \quad \text{(second series)} \quad (8)$$

Hemispherical total emittance computed using eq (8) is given in table 2. The experimental results are presented in figure 4.

5.3 Heat Capacity

A third degree polynomial function for heat capacity in terms of temperature for each heating series on Ta-1 was obtained by least squares approximation of results from individual experiments. The standard deviation of the points from the function for the first and second heating series were 0.19 and 0.17 percent, respectively. A similar function was also obtained for the combined results of experiments in first and second series with a standard deviation of 0.18 percent.

Figure 5 shows the deviations of the experimental results from the smooth function for the combined heating series. The figure also shows the deviation of the function for each individual heating series from the heat capacity function for the combined series. Compared to the function for the combined series, the average difference between the functions for the first and second heating series is about 0.1 percent, which is smaller than the standard deviation of the function for the combined series. Therefore, it may be concluded that the measured heat capacity shows no significant difference between the two heating series. The function for the combined series that is valid in the temperature range 1900 to 3000 K is:

$$c_p = -6.549 + 4.583 \times 10^{-2} T - 2.013 \times 10^{-5} T^2 + 3.325 \times 10^{-9} T^3 \quad (9)$$

where T is in K and c_p in J mol^{-1} K^{-1}. Heat capacity up to 3000 K computed using the above equation is given in table 2. In the computations of heat capacity the atomic weight of tantalum was taken as 180.95 [15].

Without any prior heating pulses, three experiments were conducted on a second tantalum specimen (Ta-2). Figure 6 shows the difference in measured heat capacity between Ta-1 and Ta-2. The base line in figure 6 represents the smooth function for heat capacity of Ta-1 given by eq (9). The maximum deviation between the heat capacity results of the two specimens occurs at the lowest temperature and is less than 1 percent. The tendency for the heat capacity of Ta-2 to approach that of Ta-1 as the temperature increases may be due to annealing effects as the temperature range for the Ta-2 specimen was increased.

The preliminary results on heat capacity of tantalum up to 3000 K were reported in an earlier publication [3]. In this study the measurements were extended to 3200 K by performing one experiment each on Ta-3 and Ta-4, and averaging the results. Hemispherical total emittance needed to correct heat capacity above 3000 K was obtained from the extrapolation of the experimental results at lower temperatures. The results of measurements above 3000 K are given in table 2. At 3000 K the heat capacity for this extended temperature range is approximately 0.1 percent lower than the value given by eq (9).

5.4 Electrical Resistivity

The electrical resistivity of the Ta-1 specimen was determined from the same experiments that were used to calculate the heat capacity. A second degree polynomial function for each heating series was obtained by least squares approximation of results from individual experiments. The standard deviation of the points from the function for the first and second heating series are 0.03 and 0.02 percent respectively.

In contrast to the heat capacity results, the electrical resistivity showed a small but significant difference between the two heating series; the results of the second series being lower than those of the first. The combined data from both heating series were fit to a second degree polynomial function. Figure 7 shows the deviations of the experimental results from the smooth function for the combined series. The figure also shows the deviation of the function for each individual heating series from the heat capacity function for the combined series. The average difference between the functions for the first and second heating series is approximately 0.15 percent. The function for the combined series that is valid for the temperature range 1900 to 3000 K is:

$$\rho = 3.671 + 4.292 \times 10^{-2} T - 2.677 \times 10^{-6} T^2 \qquad (10)$$

where T is in K and ρ in 10^{-8} Ω m. Electrical resistivity up to 3000 K computed using the above equation is given in table 2.

The difference between the results on Ta-1 and Ta-2 is presented graphically in figure 6. In contrast to heat capacity, electrical resistivity did not converge as Ta-2 was exposed to high temperatures.

The results of experiments on Ta-3 and Ta-4 were used to compute electrical resistivity above 3000 K. These are included in table 2. At 3000 K electrical resistivity obtained from Ta-3 and Ta-4 was approximately 0.3 percent lower than the value given by eq (10).

In addition, the electrical resistivity of Ta-1 was measured at 293 K under steady state conditions. The resultant value was 14.0×10^{-8} Ω m.

6. Estimate of Errors

Results on imprecision[3] and inaccuracy[4] of measured and computed quantities are given in table 3. Numbers listed under imprecision were obtained from a least squares analysis of experimental results. Numbers listed under inaccuracy were estimated considering the contribution of various items that introduce random and systematic errors in the pertinent quantities. These items are listed below:

(a) In temperature measurements: pyrometer reproducibility, scattered light correction, light source alignment, radiation standard lamp, blackbody quality, specimen temperature uniformity, magnetic fields.

(b) In electrical measurements: skin effect, inductive effects, thermoelectric effects.

(c) In interpretation of results: specimen evaporation, thermionic emission, time synchronization, measurements of length and weight.

Details regarding the estimates of errors and their combination are given in another publication [1]. Specific items in the error analysis were recomputed whenever the present conditions differed from those in the earlier publication.

---

[3] Imprecision refers to the standard deviation of an individual point as computed from the difference between measured and calculated values.

[4] Inaccuracy refers to the estimated maximum error (random and systematic) approximately equivalent to two standard deviations.

7. Discussion

The heat capacity and electrical resistivity results of this work and those in the literature are shown graphically in figures 8 and 9, respectively. Numerical comparisons are given in tables 4 and 5. It may be seen that present results agree favorably with all others at 2000 K and also at higher temperatures, with the exception of heat capacity results of Hoch and Johnston [8]. Estimates of errors in papers cited lead to an estimate of inaccuracies in previously reported heat capacity and electrical resistivity of approximately 5 to 10 and 1 to 3 percent, respectively, in the temperature range considered. Measurements of the electrical resistivity of tantalum corresponding to 293 K, as well as values reported in the literature, are given in table 6.

The results for hemispherical total and normal spectral emittances of this work and those in the literature are presented in figures 10 and 11, respectively. Because of the strong dependence of emittance on surface conditions, considerable deviations exist in the results of various investigators.

Heat capacity results at high temperatures are considerably higher than the Dulong and Petit value of 3R. Some of this departure is due to $c_p - c_v$ and the electronic terms. However, they do not account for the entire departure. Heat capacity above the Debye temperature may be expressed by

$$c_p = A - \frac{B}{T^2} + CT + \Delta c \qquad (11)$$

where the constant term is 3R (24.943 J mol^{-1} K^{-1}), the term in T^{-2} is the first term in the expansion of the Debye function, the term in T represents $c_p - c_v$ and electronic contributions, and the quantity Δc represents excess in measured heat capacity at high temperatures, which is not accounted for by the first three terms. The coefficients B(4.88×10^4) and C(2.59×10^{-3}) were obtained from data on heat capacity at low and moderate temperatures (at 250 and 1000 K) given by Hultgren et al. [11].

Using eq (11) and the heat capacity results of this work, the quantity Δc was computed for temperatures above 1900 K. The results are tabulated in table 7. The estimated uncertainty in the computed Δc may be as high as 1 J mol^{-1} K^{-1}. This was obtained from the combined uncertainties in the coefficients in eq (11) and the measured heat capacities.

Although the mechanisms of vacancy generation become important at high temperatures, it was not possible to attribute the high values entirely to vacancies. To demonstrate this, a crude estimate of the contribution of vacancies to heat capacity was made using the following equation [1]:

$$c_{vac} = \frac{N_A E_f^2}{kT^2} e^{-E_f/kT} \qquad (12)$$

where

N_A = Avogadro's number
k = Boltzmann constant
E_f = vacancy formation energy
A = constant which is obtained from vacancy concentration at the melting point.

If one assumes that vacancy formation energy is approximately proportional to the melting point and considers the value of 3.3 eV reported by Schultz [9] for tungsten, one obtains 2.9 ± 0.5 eV for the vacancy formation energy for tantalum. There are no accurate measurements on tantalum related to vacancy concentrations. Results of quenching experiments on various refractory elements [9,10] have indicated that vacancy concentrations are probably in the range 0.01 to 0.1 percent at their melting points. Estimates corresponding to a vacancy concentration of 0.1 percent at the melting point and a vacancy formation energy of 2.9 eV are given in table 7. The results indicate that vacancy contribution is small, less than 0.7 J mol^{-1} K^{-1} (upper limit) at 3200 K, and does not account for high heat capacity values. A possible contribution

of higher order terms in the electronic heat capacity may partially account for high values of heat capacity at high temperatures.

If the entire deviation of measured heat capacity from the sum of 3R and the linear term at high temperatures is represented by an expression similar to eq (12), one could obtain after rearrangement

$$\ln(T^2 \Delta c) = \ln I - \frac{S}{T} \qquad (13)$$

This equation indicates that a plot of the left side vs 1/T should yield a straight line with slope equal to -S. From the data on tantalum in the range 1900 to 3200 K, a straight line with a standard deviation of 0.8 percent was obtained. However, the parameters obtained through this fit do not seem to have any physical significance. As a crude analogy to vacancy concentration, the computations yielded a value of 1.4 eV for energy and 4.2 percent for concentration at the melting point. Both of these values seem to be unrealistic for tantalum.

In order to give a simple expression for the heat capacity of tantalum over a wide temperature range an empirical term in T^5 for the quantity Δc in eq (11) was substituted. The coefficient of this term was obtained from the results of the present work in conjunction with the values given by Hultgren et al. [11] at temperatures below 1000 K. Then, eq (11) for the range 300 to 3100 K becomes

$$c_p = 24.943 - \frac{4.88 \times 10^4}{T^2} + 2.59 \times 10^{-3} T + 2.85 \times 10^{-17} T^5 \qquad (14)$$

where T is in K and c_p in J mol^{-1} K^{-1}. Average deviation of the individual points from the function over the temperature range considered is 0.4 percent. Equation (14) is presented graphically in figure 12.

The T^{-2} term in eq (14) corresponds to a Debye θ of approximately 200 K for tantalum. This value is somewhat lower than the generally accepted value of 247 K [28]. Such a deviation may be expected since in the above analysis only data above 250 K were considered while determinations reported in the literature were based on more elaborate treatment of lower temperature data.

It was interesting to note that the difference in heat capacity between Ta-1 and Ta-2 was reduced from approximately 1 percent at 1900 K to 0.2 percent at 3000 K. The convergence of the results as Ta-2 was exposed to high temperatures indicates the difference in the initial states of the two specimens; Ta-1 was preheated while Ta-2 was used as received from the manufacturer prior to the start of the measurements.

There was a small, but significant difference in electrical resistivity between the two heating series of Ta-1. The second series results, which were lower than those of the first by approximately 0.15 percent, indicate that the specimen had undergone additional annealing during its exposure to high temperatures.

Unlike most metallic elements, the electrical resistivity of tantalum, in the range of present measurements, showed a negative departure from linearity in the curve of electrical resistivity against temperature. A small Fermi energy is believed to be responsible for some of this negative departure [27].

The experimental results reported in this paper have further substantiated the feasibility of accurate measurement of heat capacity and electrical resistivity of electrical conductors above approximately 2000 K by a pulse method of millisecond resolution. The results also indicated that under proper surface and environmental conditions the technique allows the measurement of hemispherical total and normal spectral emittances.

Acknowledgment

The authors extent their appreciation to M. S. Morse for his contribution in connection with electronic instrumentation which is a vital part of the entire measurement system.

8. References

[1] Cezairliyan, A., M. S. Morse, H. A. Berman, and C. W. Beckett. High-Speed (Subsecond) Measurement of Heat Capacity, Electrical Resistivity, and Thermal Radiation Properties of Molybdenum in the Range 1900 to 2800 K. J. Res. Nat. Bur. Stand. (U.S.), 74A (Phys. and Chem.), 65 (1970).

[2] Cezairliyan, A. High-Speed Methods of Measuring Specific Heat of Electrical Conductors at High Temperatures. High Temp. - High Pres. To be published.

[3] Cezairliyan, A., J. L.McCLure, M. S. Morse, and C. W. Beckett. Measurement of Heat Capacity of Tantalum in the Range 1900 to 3000 K by a Pulse Heating Method. Fifth Symposium on Thermophysical Properties (Boston), ASME, New York (1970).

[4] Lowenthal, G. C. The Specific Heat of Metals Between 1200 K and 2400 K. Australian J. Phys. 16, 47 (1963).

[5] Rasor, N. S., and J. D. McClelland. Thermal Properties of Graphite, Molybdenum, and Tantalum to Their Destruction Temperatures. J. Phys. Chem. Solids, 15, 17 (1960).

[6] Taylor, R. E., and R. A. Finch. The Specific Heats and Resistivities of Molybdenum, Tantalum, and Rhenium. J. Less-Common Metals, 6, 283 (1964).

[7] Jaeger, F. M., and W. A. Veenstra. The Exact Measurement of the Specific Heats of Solid Substances at High Temperatures (Vanadium, Niobium, Tantalum, and Molybdenum). Rec. Trav. Chim. 53, 677 (1934).

[8] Hoch, M., and H. L. Johnston. A High-Temperature Drop Calorimeter. The Heat Capacities of Tantalum and Tungsten Between 1000 and 3000 K. J. Chem. Phys. 65, 855 (1961).

[9] Schultz, H. "Quenching of Vacancies in Tungsten", in Lattice Defects in Quenched Metals, R. M. J. Cotterill, M. Doyama, J. J. Jackson and M. Meshi, eds., Academic Press, New York (1965), p. 761.

[10] Meakin, J. D., A. Lawley, and R. C. Koo. "Vacancy Loops in Quenched Molybdenum", in Lattice Defects in Quenched Metals, R. M. J. Cotterill, M. Doyama, J. J. Jackson, and M. Meshi, eds., Academic Press, New York (1965), p. 767.

[11] Hultgren, R., R. L. Orr, P. D. Anderson, and K. K. Kelley. Selected Values of Thermodynamic Properties of Metals and Alloys, John Wiley, New York (1963).

[12] Foley, G. M. High-Speed Optical Pyrometer. Rev. Sci. Instr. 41, 827 (1970).

[13] DeVos, J. C. Evaluation of the Quality of A Blackbody. Physica 20, 669 (1954).

[14] International Practical Temperature Scale of 1968. Metrologia 5, 35 (1969).

[15] Compt. Rend. of the 21st Conference of the International Union of Pure and Applied Chemistry, Montreal (1961), Report of the Committee on Atomic Weights, p. 284.

[16] Tietz, T. E., and J. W. Wilson. Behavior and Properties of Refractory Metals. Stanford University Press, California (1965), p. 28.

[17] Cezairliyan, A., High-Speed Methods of Measuring Thermophysical Properties at High Temperatures. Rev. Int. Hautes Temper. et Refract., 1970. To be published.

[18] Worthing, A. G. Physical Properties of Well Seasoned Molybdenum and Tantalum as a Function of Temperature. Phys. Rev. 28, 190 (1926).

[19] Malter, L., and D. B. Langmuir. Resistance, Emissivities and Melting Point of Tantalum. Phys. Rev. 55, 743 (1939).

[20] Hörz, G. Emissionsvermögen und elektrischer Widerstand von Tantal bei hohen Temperaturen. Z. Metallk. 57, 871 (1966).

[21] Peletskii, V. E., and V. Ya. Voskresenskii. Thermophysical Properties of Tantalum at Temperatures above 1000°C. High Temperature 4, 329 (1966).

[22] Neimark, B. E., and L. K. Voronin. Thermal Conductivity, Specific Electrical Resistivity, and Total Emissivity of Refractory Metals at High Temperatures. High Temperature 6, 999 (1968).

[23] Petrov, V. A., V. Ya. Chekhovskoi, and A. E. Sheindlin. Integral Hemispherical Radiating Power and Specific Electrical Resistance of Tantalum in the Temperature Interval 1200-2800 K. High Temperature 6, 525 (1968).

[24] Allen, R. D., L. F. Glasier, and P. L. Jordan. Spectral Emissivity, Total Emissivity, and Thermal Conductivity of Molybdenum, Tantalum, and Tungsten above 2300 K. J. Appl. Phys. 31, 1382 (1960).

[25] White, G. K., and S. B. Woods. Electrical and Thermal Resistivity of the Transition Elements at Low Temperatures. Phil. Trans. Royal Soc. (London) 251, 273 (1959).

[26] Tye, R. P. Preliminary Measurements on the Thermal and Electrical Conductivities of Molybdenum, Niobium, Tantalum, and Tungsten. J. Less-Common Metals 3, 13 (1961).

[27] Powell, R. W. Thermal Conductivity: A Review of Some Important Developments. Contemp. Phys. 10, 579 (1969).

[28] Gshneidner, K. A. "Physical Properties and Interrelationships of Metallic and Semimetallic Elements", in Solid State Physics, Vol. 16, F. Seitz and D. Turnbull, eds.,Academic Press, New York (1965), p. 275.

TABLE 1

Impurities in tantalum specimen

Impurity	Composition ppm (by weight)
Al	< 5
C	60
Ca	< 5
Cr	< 10
Cu	< 5
Fe	70
Mg	< 5
Mo	10
N	20
Nb	500
O	50
W	< 200

710 < Total < 940

TABLE 2

Heat capacity, electrical resistivity, hemispherical total and normal spectral emittances of tantalum.

Temperature K	c_p J $mol^{-1}K^{-1}$	ρ^a $10^{-8}\Omega m$	ϵ^a	$\epsilon_{N,\lambda}$
1900	30.66	75.56	0.288[b]	0.413[b]
2000	31.19	78.80	0.293[b]	0.411
2100	31.71	82.00	0.298[b]	0.409
2200	32.25	85.14	0.302[b]	0.407
2300	32.83	88.23	0.307	0.406
2400	33.46	91.26	0.312	0.404
2500	34.17	94.24	0.316	0.403
2600	34.97	97.17	0.321	0.401
2700	35.89	100.04	0.326	0.400
2800	36.95	102.86	0.330	0.400
2900	38.16	105.63	0.335	0.399
3000	39.55	108.34	0.340	0.398
3100	41.39	111.00		
3200	44.48	113.60		

[a]Based on ambient temperature (298 K) dimensions.

[b]Extrapolated from higher temperature results.

TABLE 3

Imprecision and inaccuracy of measured and computed quantities

Quantity	Imprecision %	Inaccuracy %
Temperature	0.02 (0.5 K)	0.2 (4 K) at 2000 K 0.3 (10 K) at 3200 K
Voltage	0.02	0.05
Current	0.03	0.06
Power	0.04	0.08
Resistance	0.04	0.08
Length	0.04	0.08
Weight	0.01	0.1
Density	0.03	0.1
Heat Capacity	0.5	2 at 2000 K 3 at 3200 K
Resistivity	0.04	0.05
Hem. Total Emittance	0.7	3
Norm. Spectral Emittance	0.3	3

TABLE 4

Tantalum heat capacity difference (previous literature values minus present work values) in percent

Investigator	Ref.	Year	Method	Temperature, K						
				2000	2200	2400	2600	2800	3000	3200
Jaeger and Veenstra	7	1934	drop	+1.2*						
Rasor and McClelland	5	1960	pulse	+1.3	+1.4	+1.9	+2.4	+3.4	+5.0	+2.0
Hoch and Johnston	8	1961	drop	-3.8	-5.6	-7.6	-10.4	-14.0		
Lowenthal	4	1963	modul.	-0.8	-1.0	-1.3				
Taylor and Finch	6	1964	pulse	-0.9	-1.6	-2.2	-1.9	-0.8	+0.9	

*Extrapolated from 1873 K

TABLE 5

Tantalum electrical resistivity difference (previous literature values minus present work values) in percent

Investigator	Ref.	Year	Temperature, K						
			2000	2200	2400	2600	2800	3000	3200
Worthing	18	1926	+2.3	+2.1	+2.1	+2.2	+2.4		
Malter and Langmuir	19	1939	-1.2	-1.3	-1.5	-1.6	-1.8	-1.9	-2.0
Peletskii and Voskresenskii	21	1966	+0.2	-0.1	-0.1	+0.1	+0.4		
Hörz	20	1966	-1.0	-0.8	-0.4	+0.1	+0.9		
Neimark and Voronin	22	1968	+0.4	+0.2					
Petrov et al.	23	1968	-2.1	-1.8	-1.4	-0.8	-0.1		

TABLE 6

Electrical resistivity of tantalum at 293 K (literature)

Investigator	Ref.	Year	Resistivity $10^{-8}\Omega m$
Worthing	18	1926	14.2
Malter and Langmuir	19	1939	13.5
White and Woods	25	1959	13.1[a]
Tye	26	1961	14.5
Hörz	20	1966	13.4
Peletskii and Voskresenskii	21	1966	13.7
Neimark and Voronin	22	1968	15.0
Present work			14.0

[a]Ideal resistivity

TABLE 7

Excess heat capacity Δc in equation (11) and estimated vacancy contribution to heat capacity of tantalum

T K	Δc J $mol^{-1}K^{-1}$	c_{vac} J $mol^{-1}K^{-1}$
2000	1.08	0.003
2200	1.62	0.01
2400	2.31	0.04
2600	3.30	0.10
2800	4.76	0.21
3000	6.84	0.41
3200	9.70	0.73

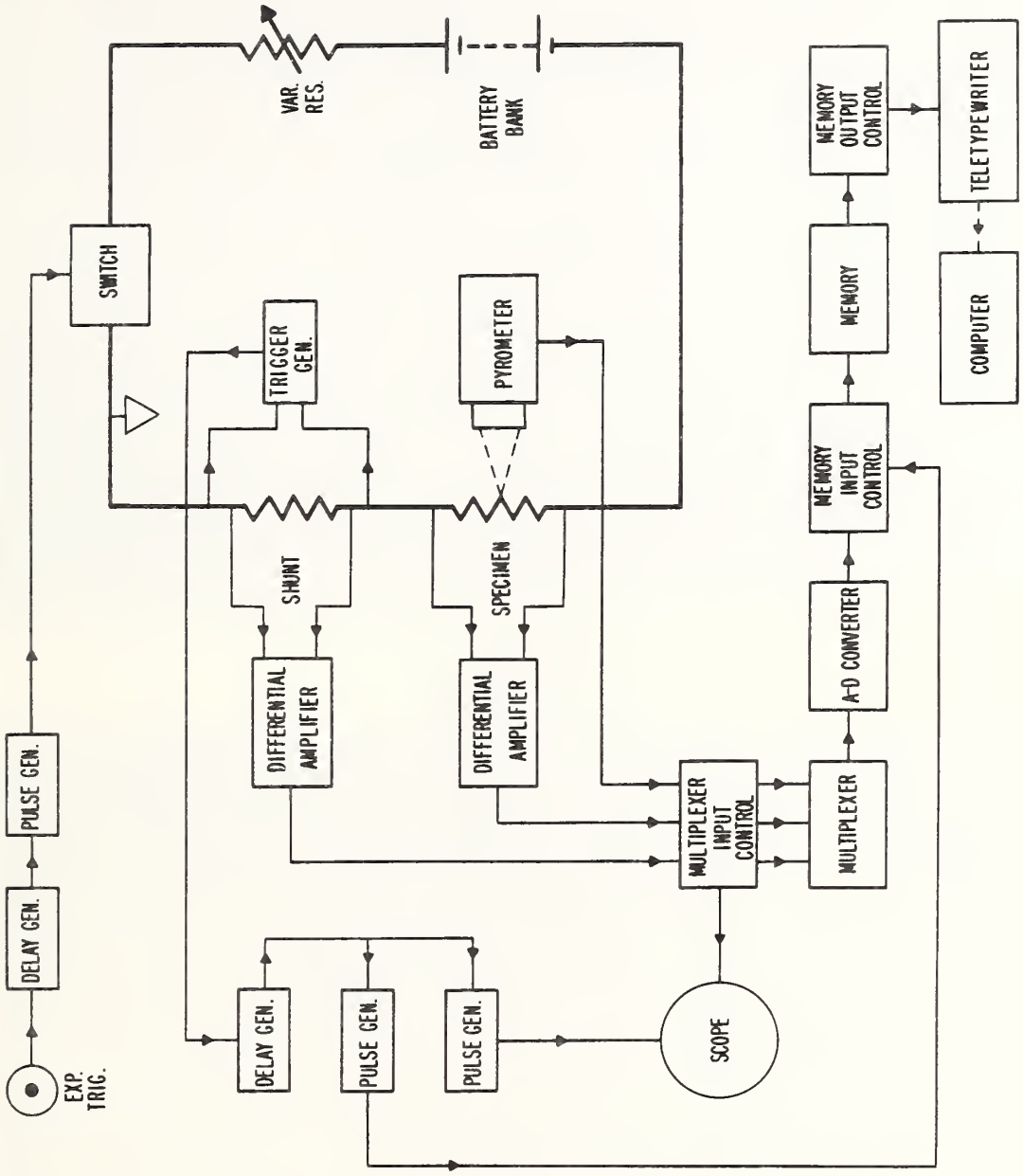

FIGURE 1. Functional diagram of the complete high-speed measurement system.

Combination: Line & Halftone

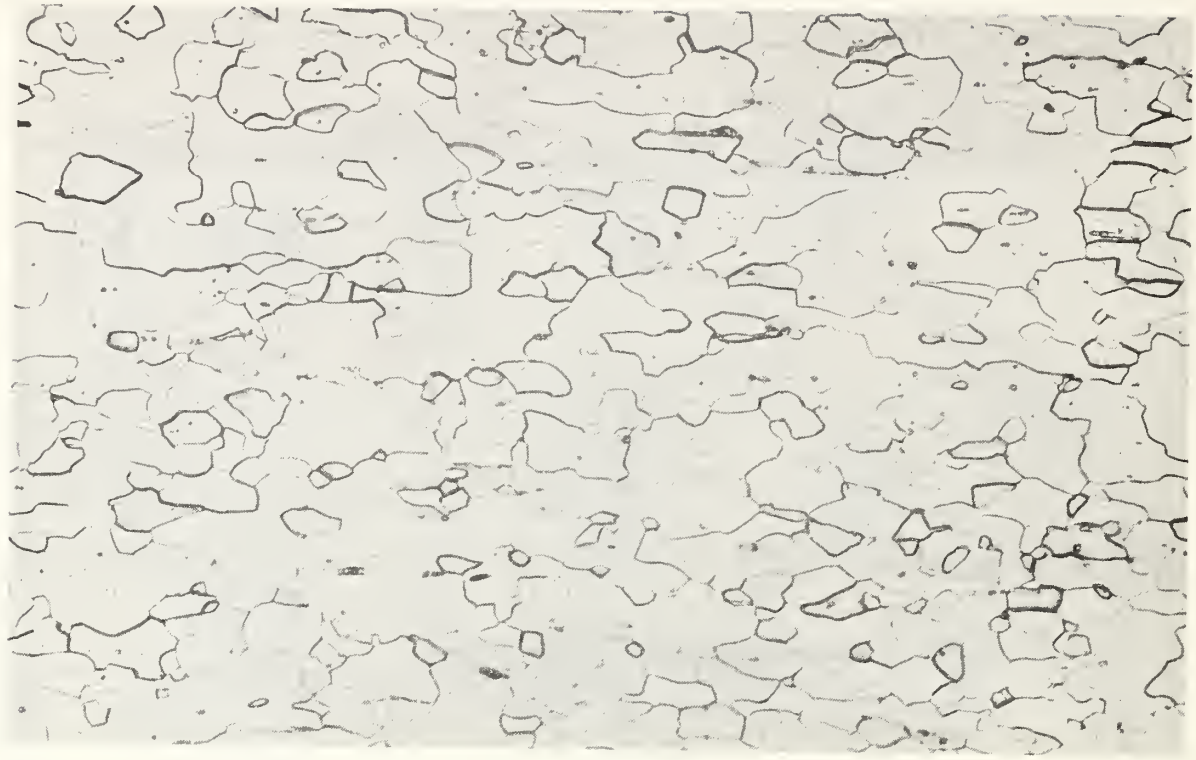

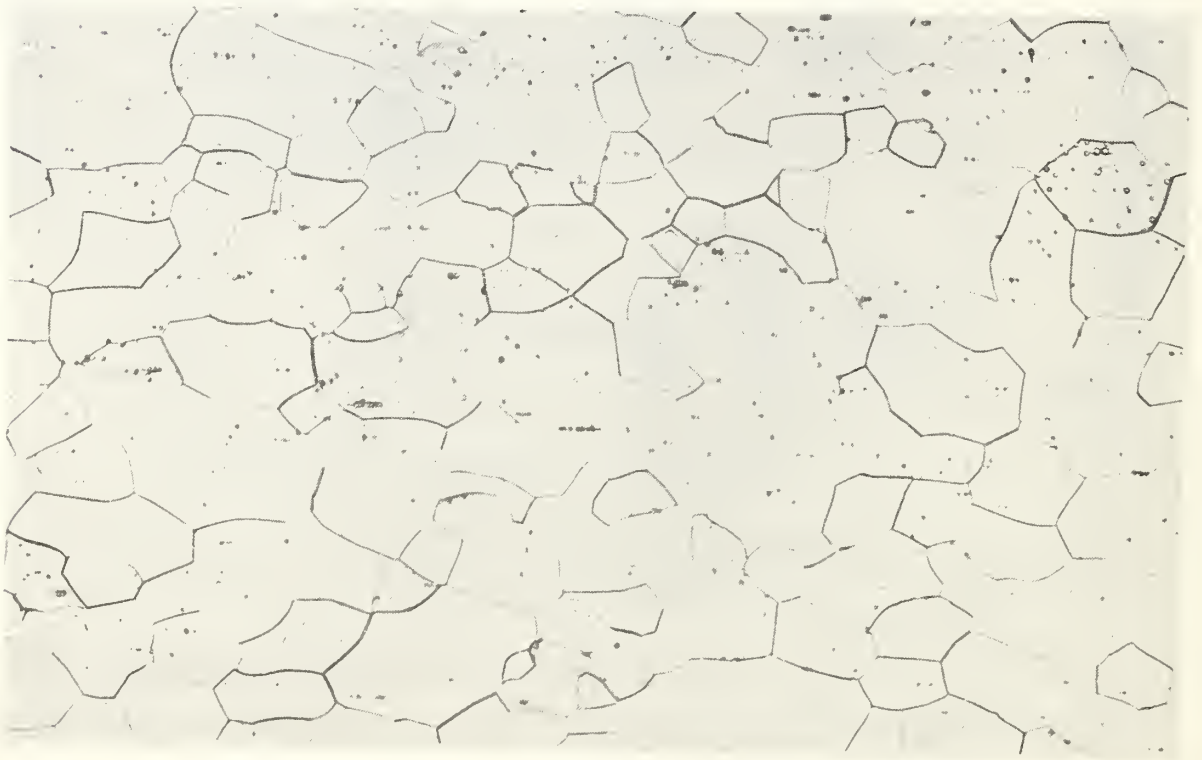

FIGURE 2. Photomicrographs of the tantalum specimen before (upper photograph) and after (lower photograph) the entire set of experiments.

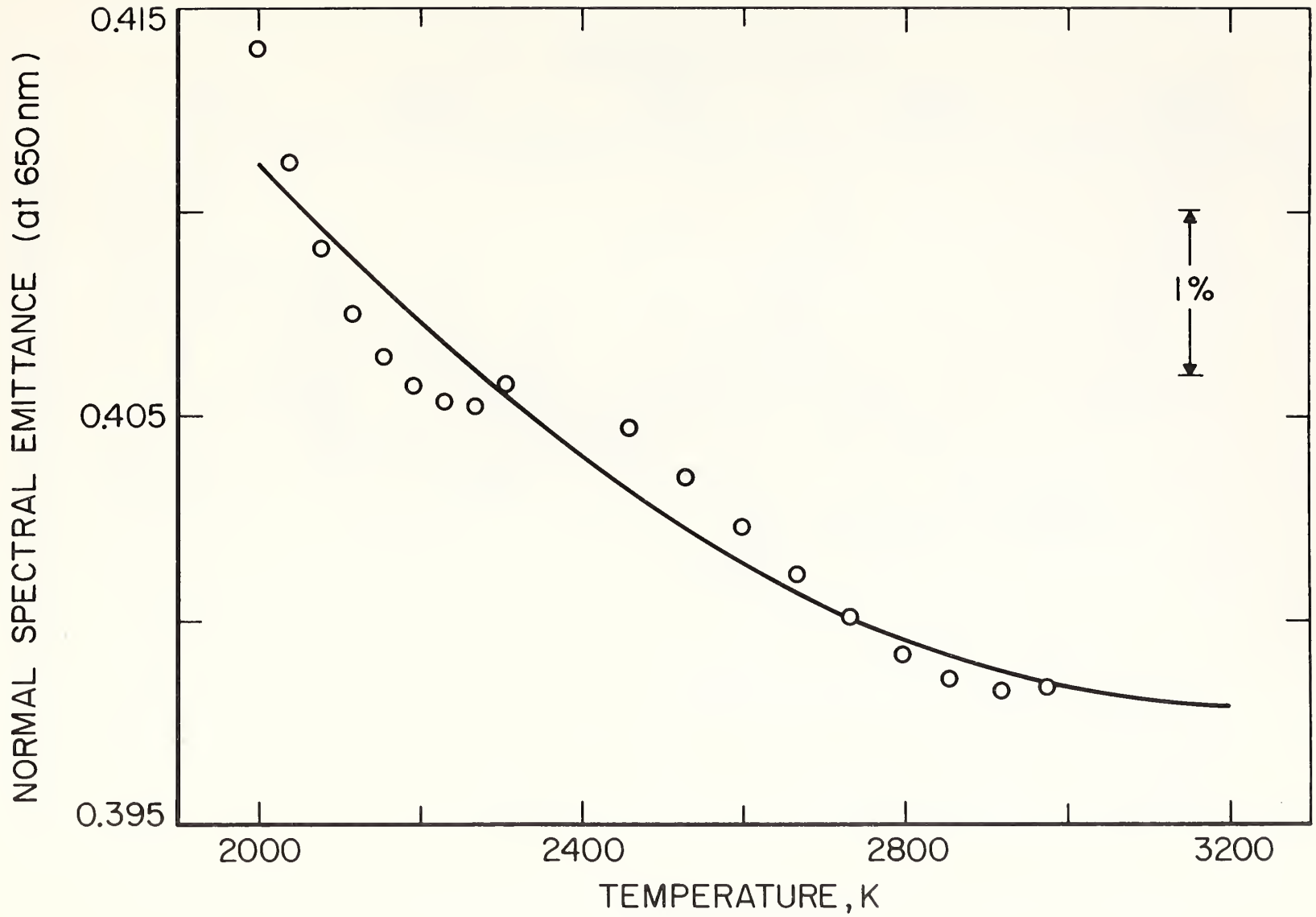

Figure 3. Normal spectral emittance of tantalum at λ=650 nm.

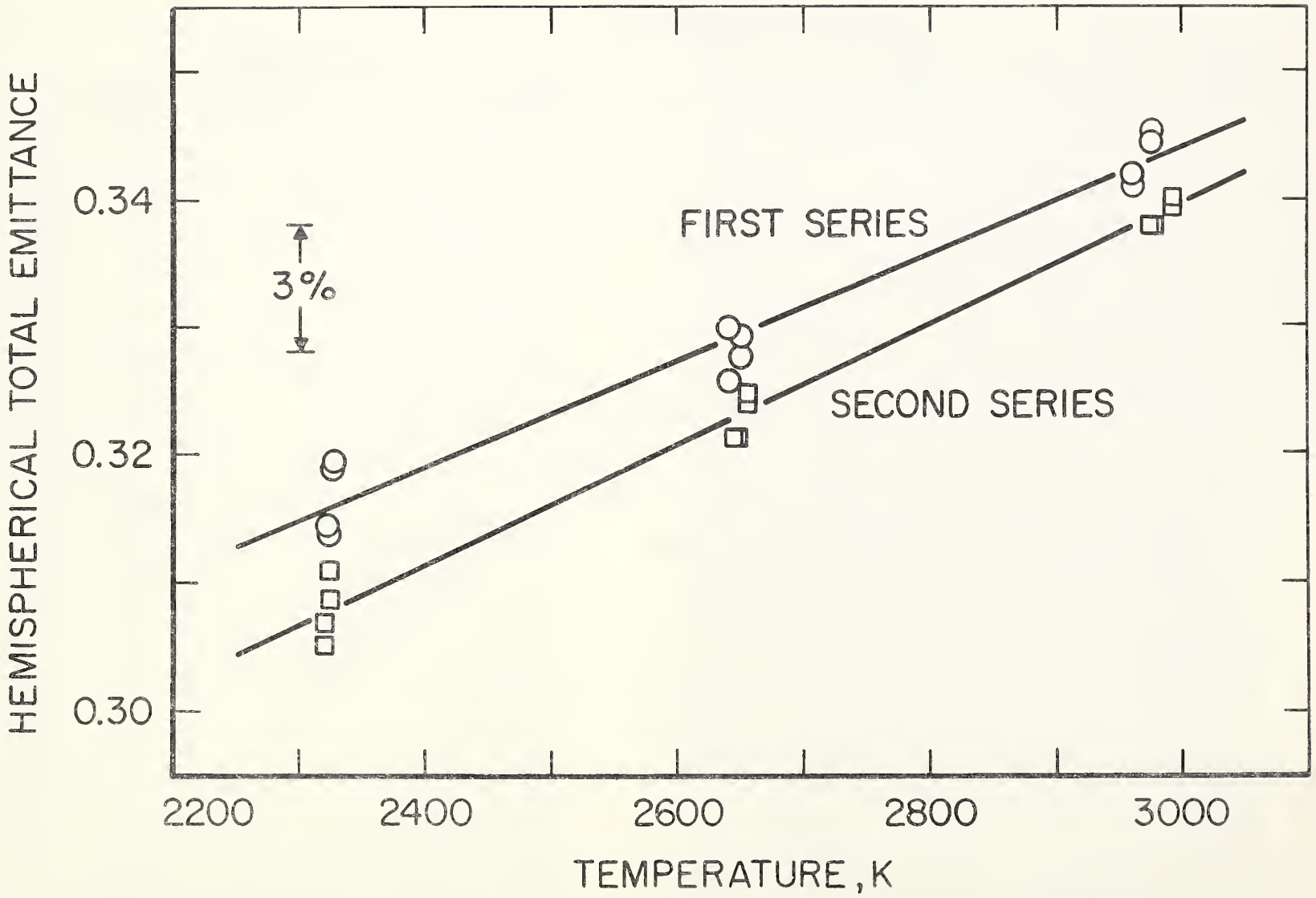

Figure 4. Hemispherical total emittance of tantalum.

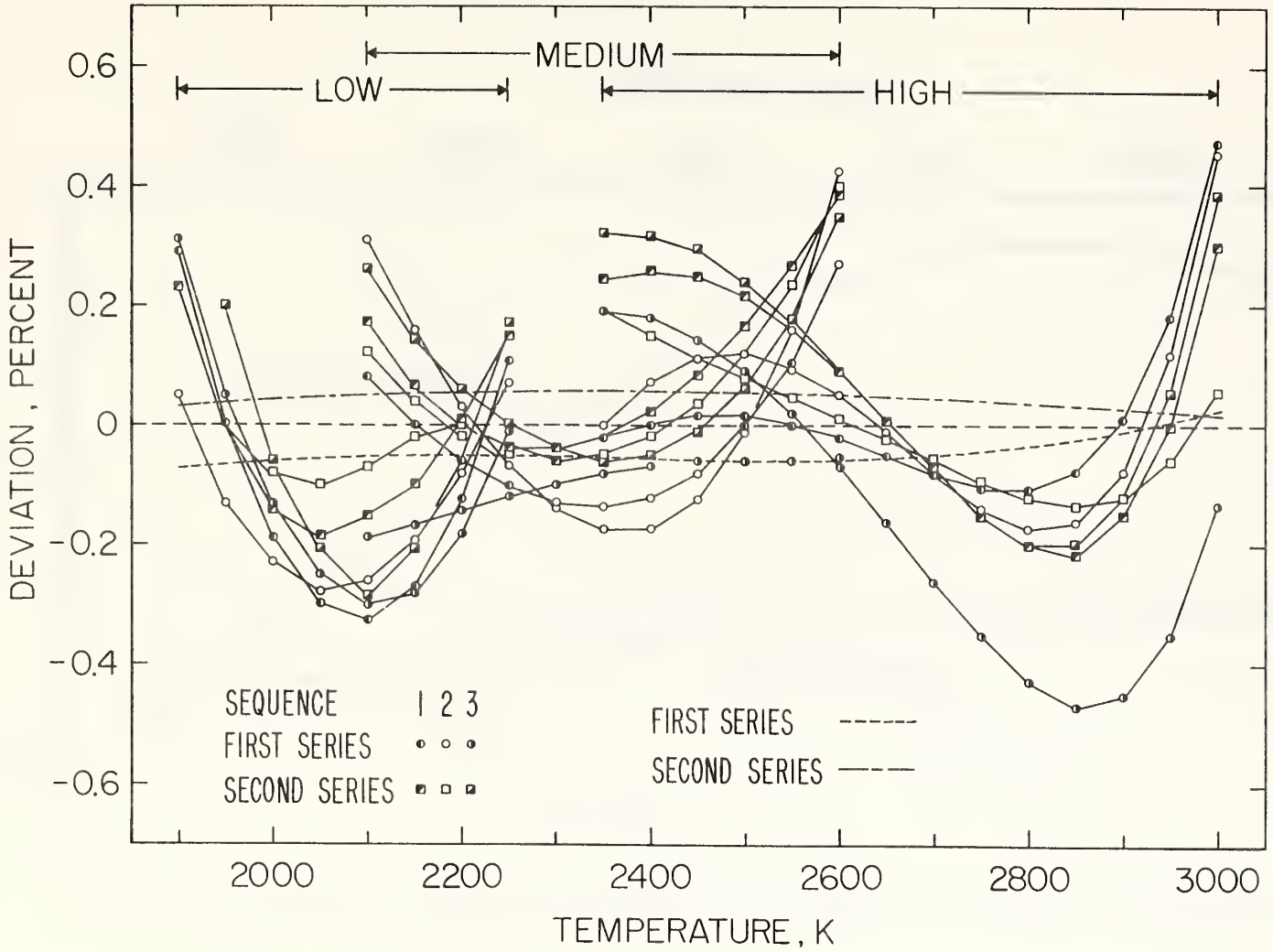

FIGURE 5. Deviation of heat capacity results for tantalum from equation (9).

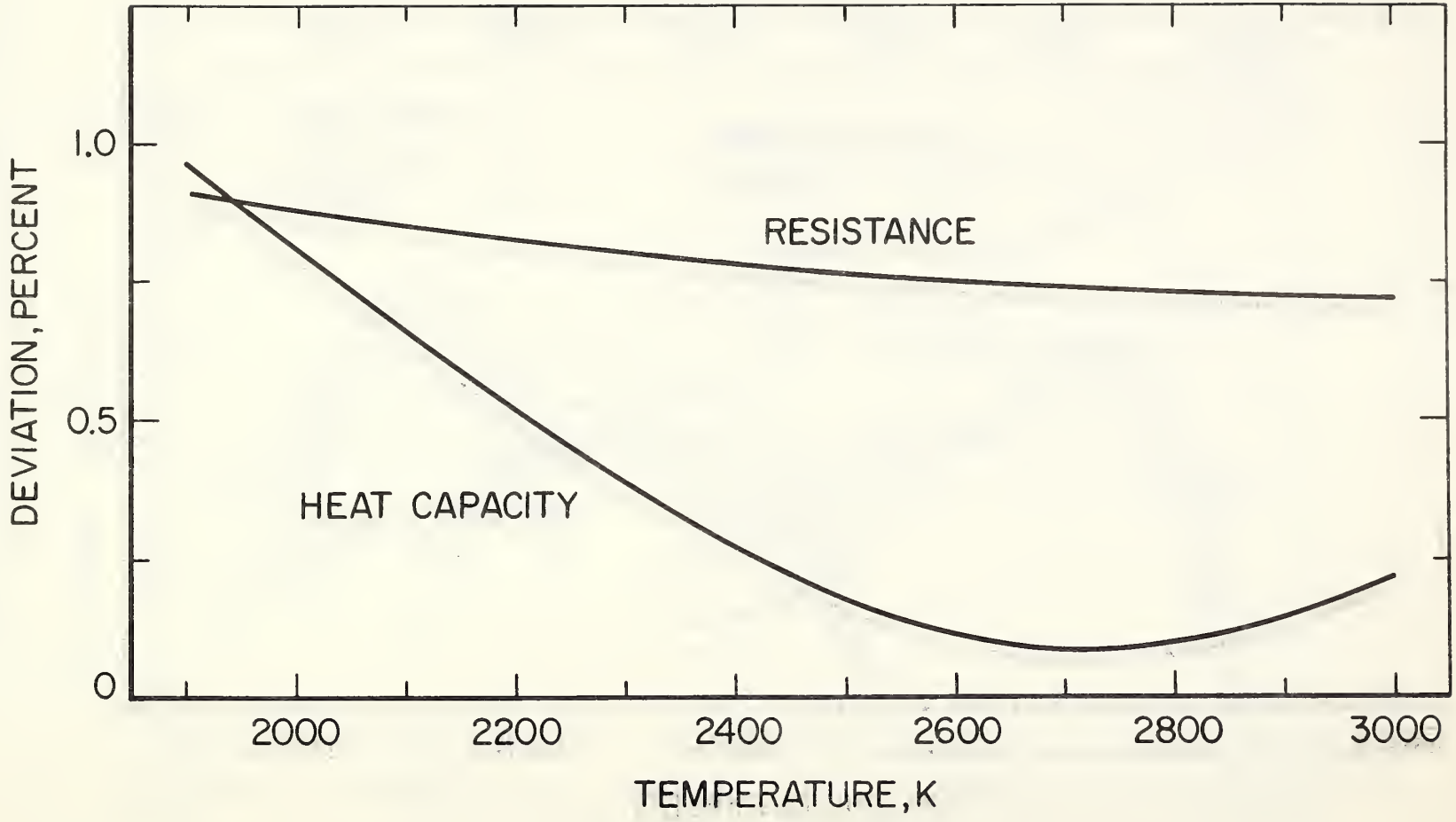

FIGURE 6. Difference in heat capacity and electrical resistivity between two tantalum specimens. Base line represents heat capacity of Ta-1 given by equation (9).

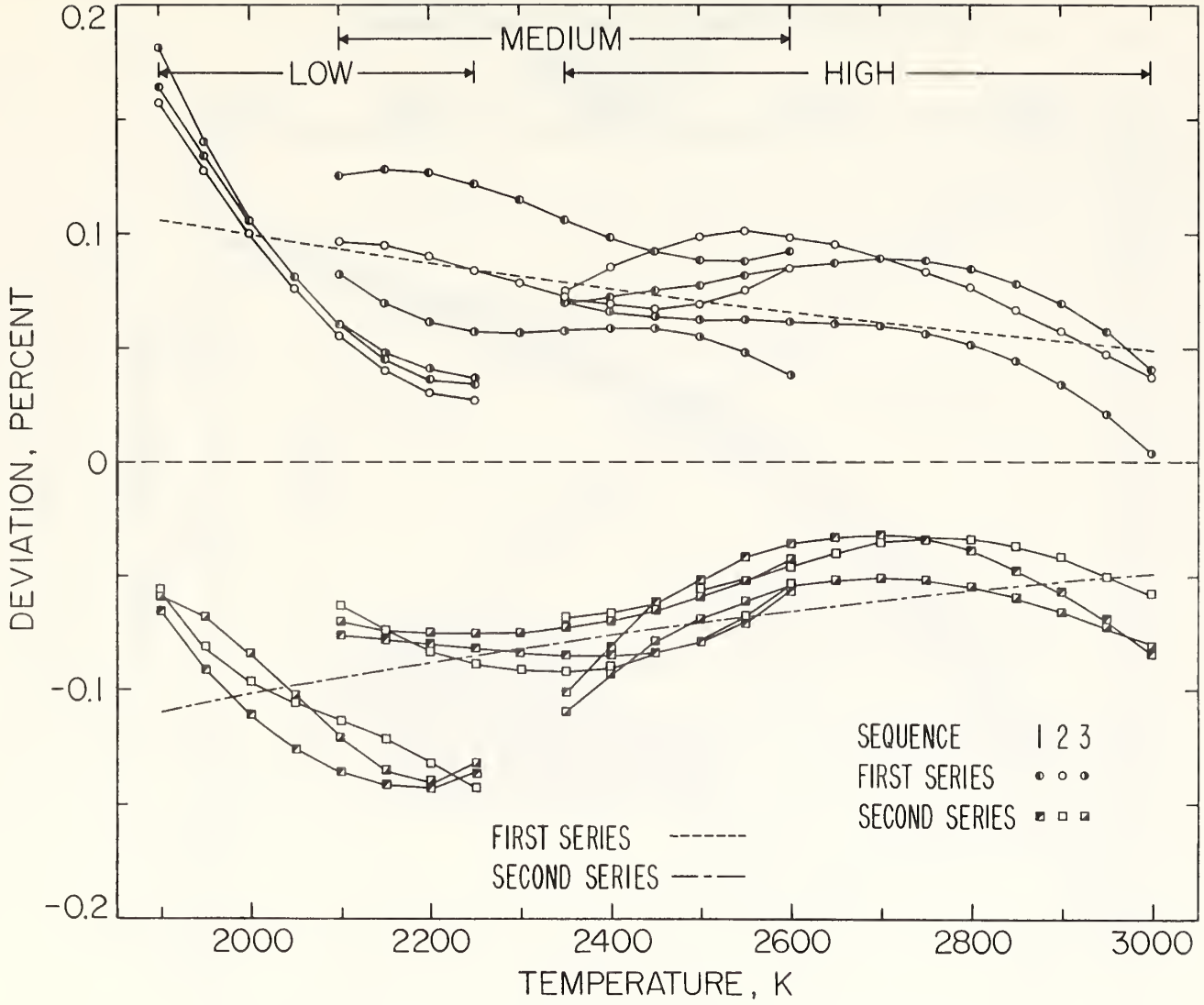

FIGURE 7. Deviation of electrical resistivity results for tantalum from equation (10).

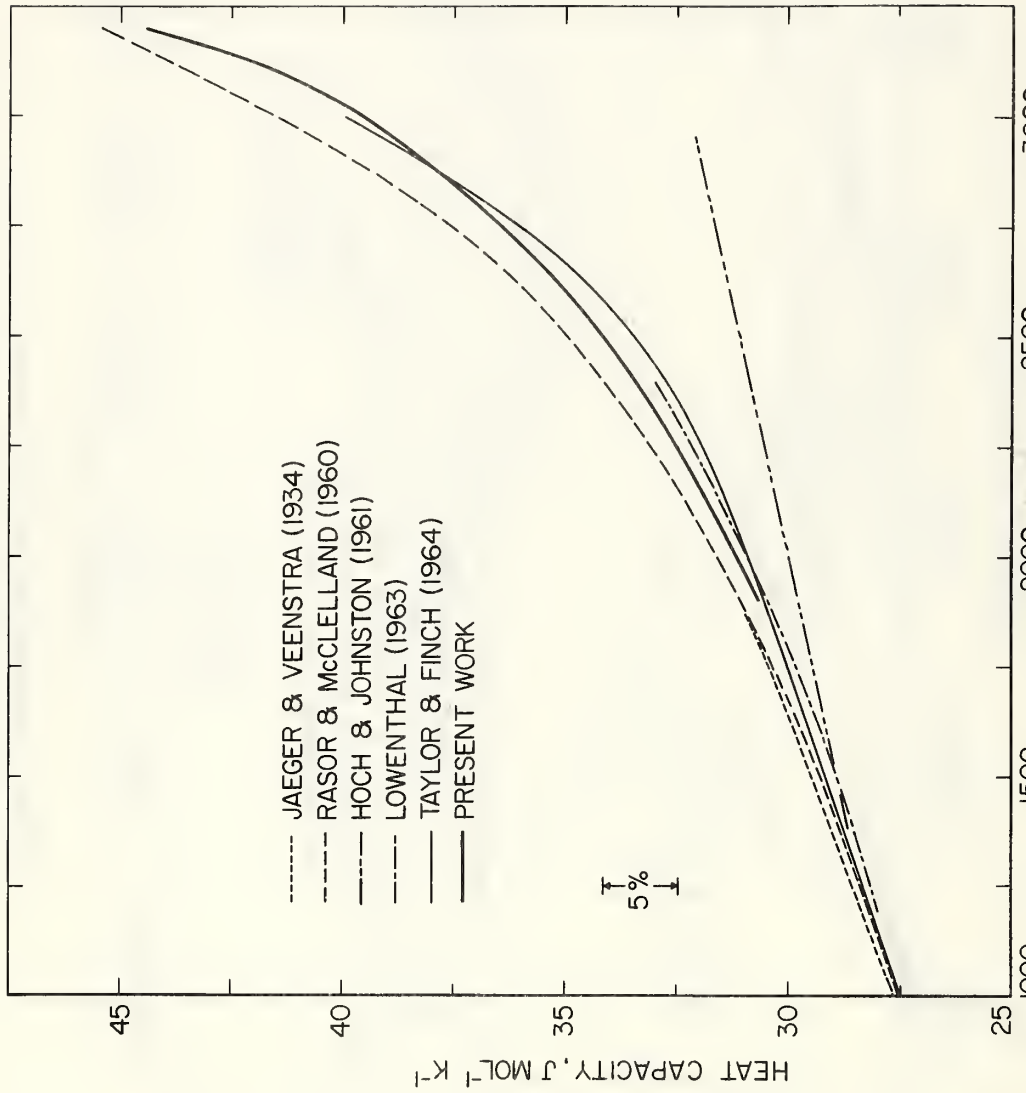

FIGURE 8. Heat capacity of tantalum reported in the literature.

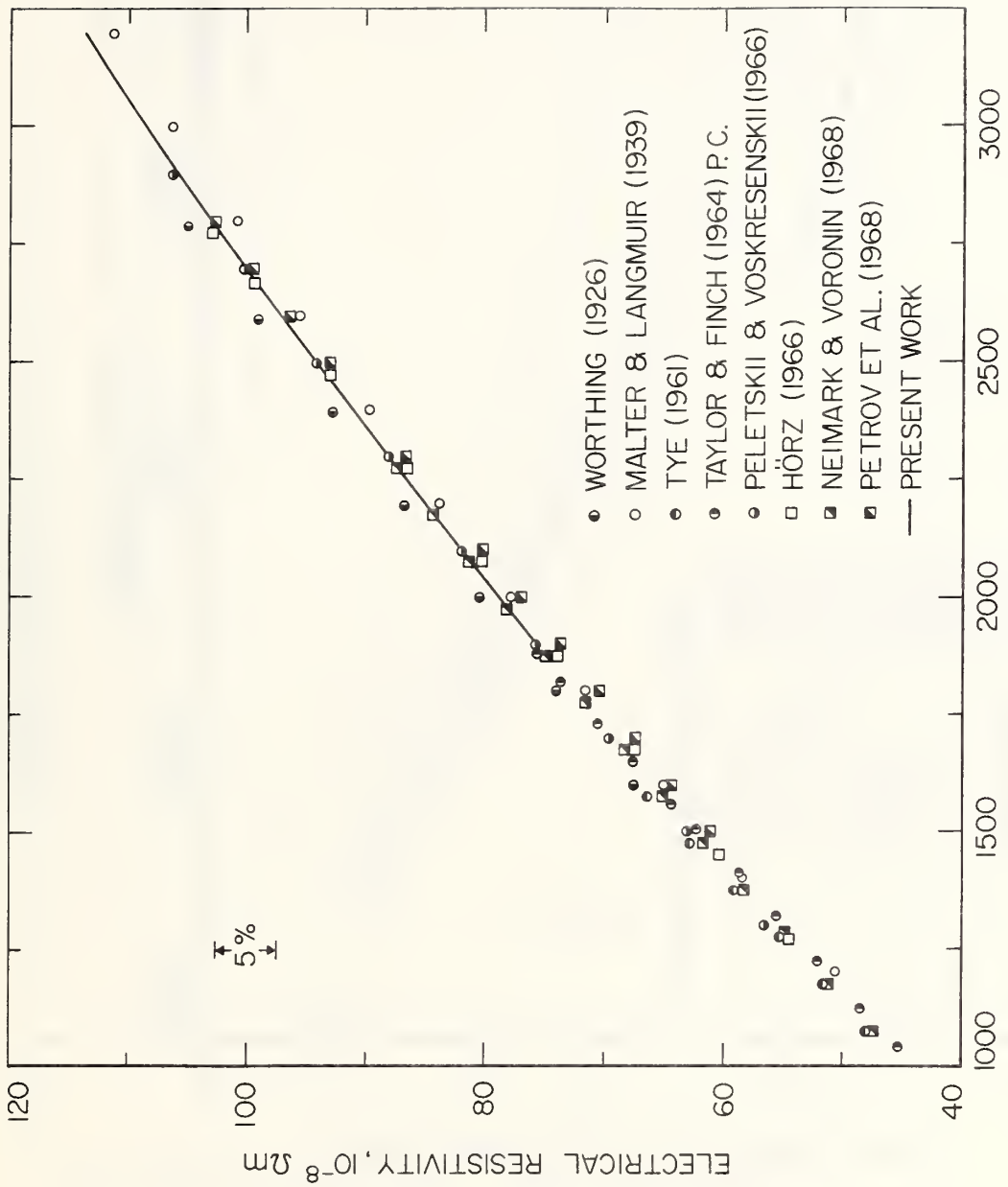

FIGURE 9. Electrical resistivity of tantalum reported in the literature

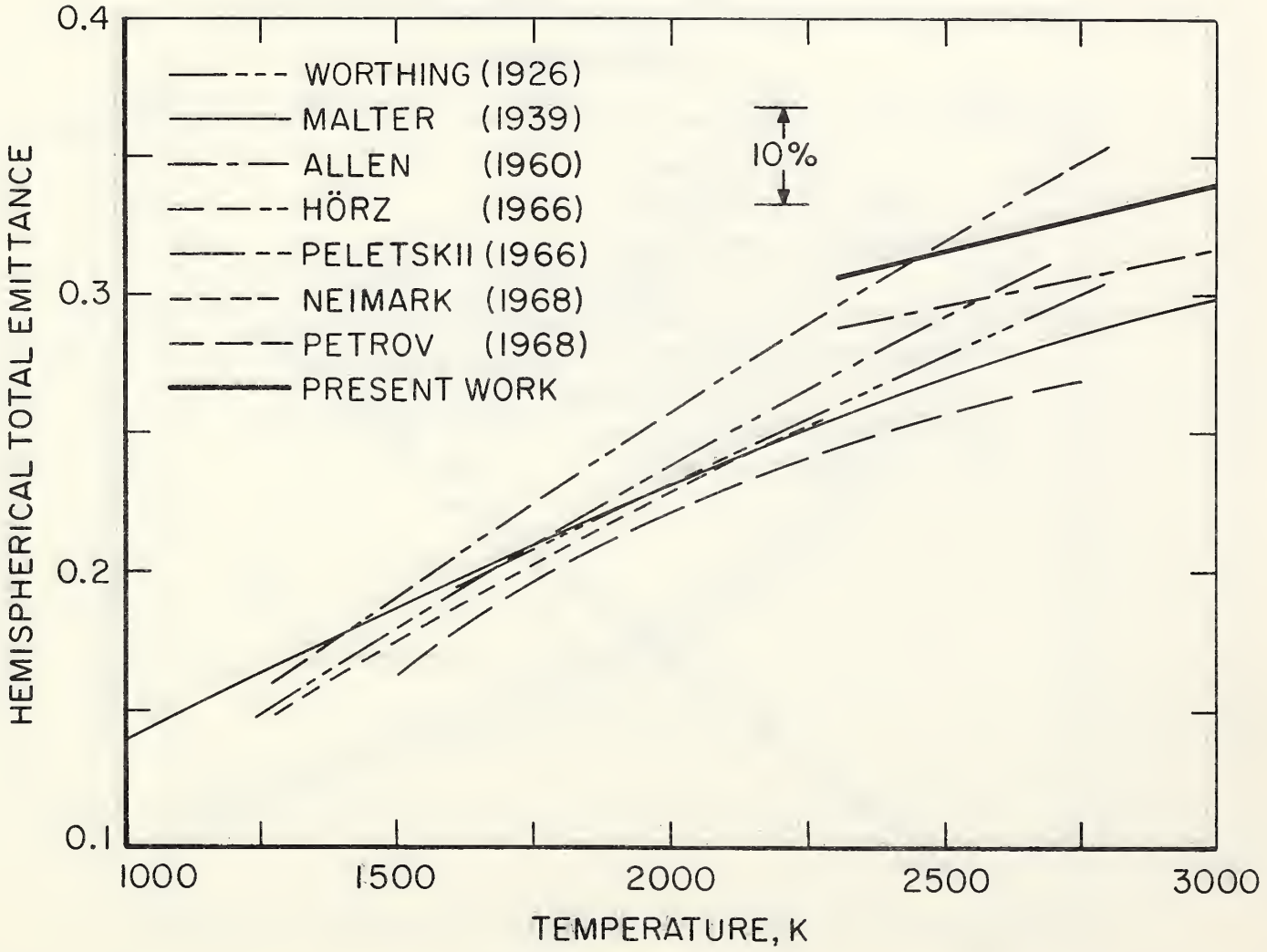

FIGURE 10. Hemispherical total emittance of tantalum reported in the literature.

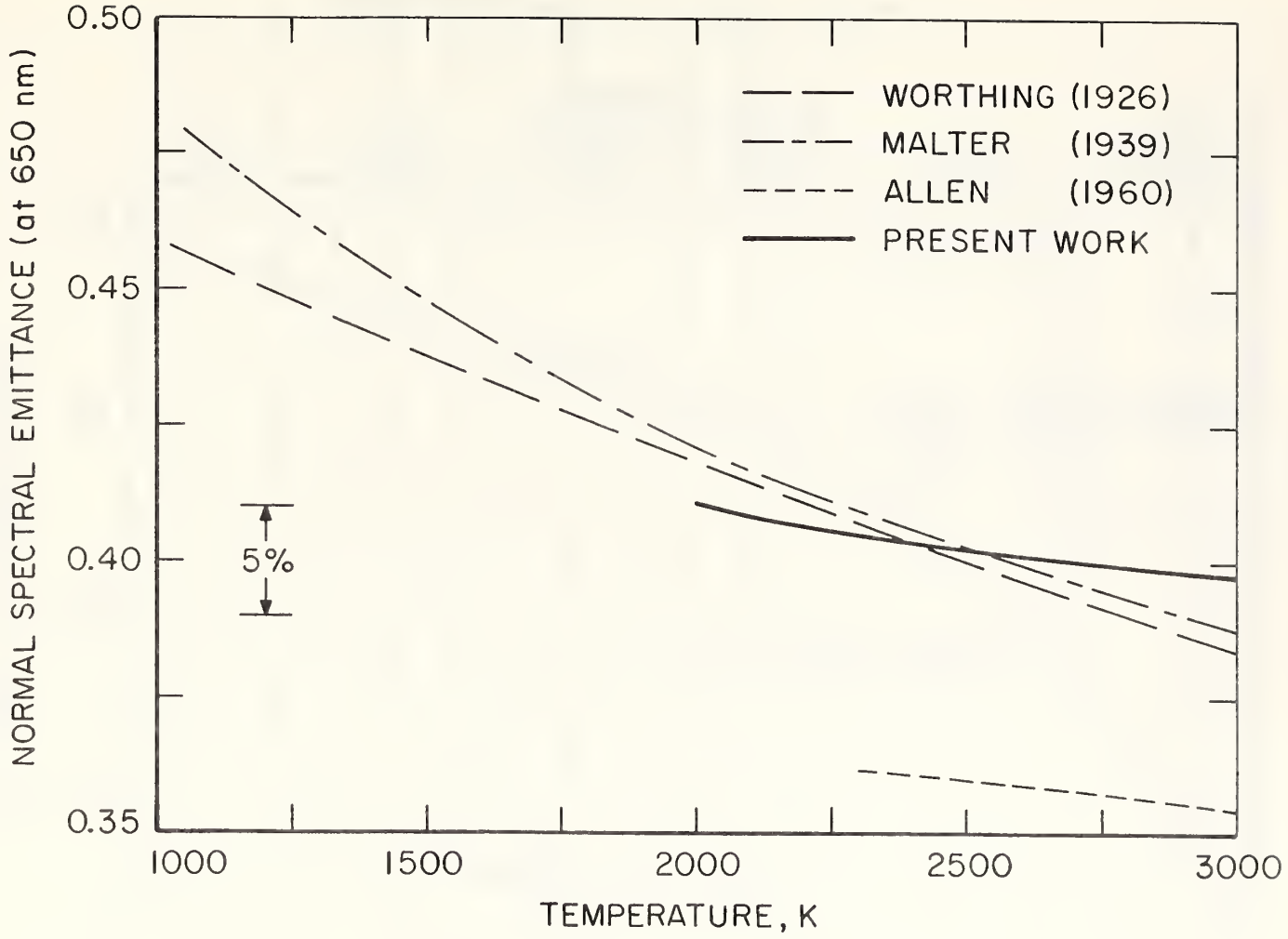

FIGURE 11. Normal spectral emittance of tantalum at λ=650 nm reported in the literature.

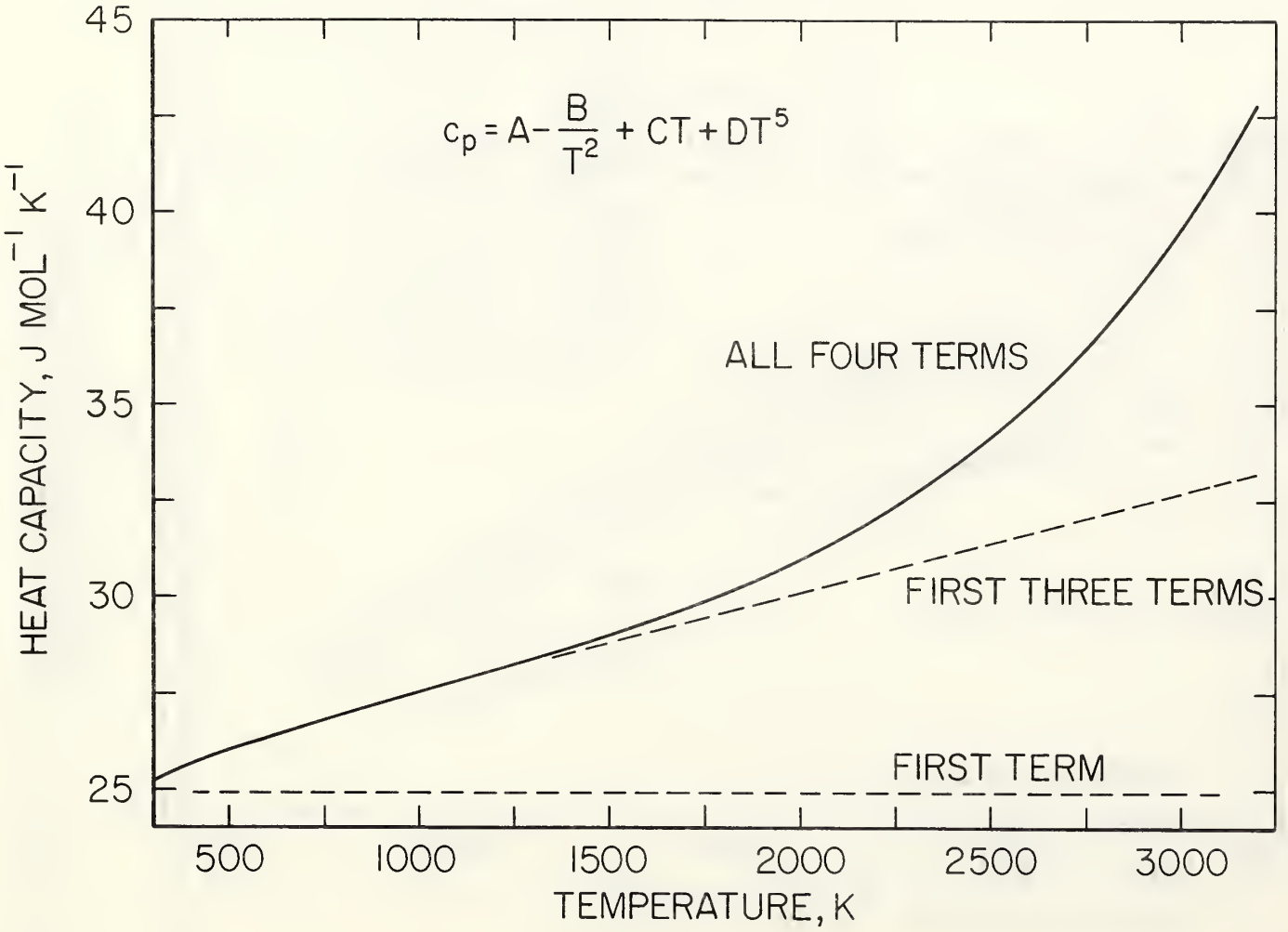

FIGURE 12. Heat capacity of tantalum according to equation (14).

Chapter 8

MEASUREMENT OF VARIATION OF NORMAL SPECTRAL EMITTANCE OF TANTALUM DURING MELTING BY A PULSE HEATING METHOD*

Ared Cezairliyan
National Bureau of Standards
Washington, D.C. 20234

Abstract

A pulse heating method was used to measure the change in normal spectral emittance (at 650 nm) of tantalum as a function of the change in electrical resistance during the initial melting period. Duration of an individual experiment in which the specimen was heated from room temperature to its melting point was approximately 400 ms. The partial melting period was approximately 100 ms. A millisecond resolution photoelectric pyrometer was used for temperature measurements. The recordings of experimental quantities were made with a digital data acquisition system which has a full-scale signal resolution of approximately one part in 8000 and a time resolution of 0.4 ms. It was found that normal spectral emittance decreased by approximately 3.5 percent during the initial one third of the melting period.

---

* This work was supported in part by the Propulsion Division of the U. S. Air Force Office of Scientific Research under Contract ISSA-69-0001.

1. Introduction

In general, normal spectral emittance of metallic elements changes upon melting. It was observed [1] that at 650 nm in some metals (Ag, Au, Co, Cu, Ni, Pd, Pt, Rh, Th, Ti) emittance increases upon melting, in others (Er, Mo, Nb, U, V, Zr) it decreases, and in a few cases (Be, Fe, Mn, Y) no change occurs. The results reported in the literature correspond to conditions of the start and the completion of melting of the specimen. To the best of the author's knowledge, no measurements were described in which emittance was determined during the melting process as a function of a specimen parameter, such as electrical resistance or absorbed energy.

Measurement of normal spectral emittance during melting by steady-state techniques presents serious problems especially at temperatures above 2000 K. These problems are the result of increased chemical reactions, evaporation, heat transfer, loss of mechanical strength, etc. Because of some of the above factors, containment of the specimen during melting becomes very difficult.

In order to eliminate some of the problems inherent to high temperature steady-state experiments, high-speed measurement techniques may be used.

In the present study, a pulse heating method was used for the measurement of the change in normal spectral emittance (at 650 nm) of tantalum as a function of the change in electrical resistance during the initial melting period. Duration of an individual experiment, in

which the specimen was heated from room temperature to its melting point, was approximately 400 ms. The partial melting period was approximately 100 ms. A millisecond resolution photoelectric pyrometer was employed for temperature measurements. The recordings of experimental quantities, temperature, voltage, and current, were made with a millisecond resolution digital data acquisition system.

In the rest of this paper, normal spectral emittance is simply referred to as emittance and is denoted by the symbol ϵ.

2. The Method

The specimen, which was in strip form, was heated in vacuum from room temperature to its melting point by a single heavy-current pulse of subsecond duration. A bank of heavy-duty batteries constituted the pulse power source.

During the pulse period, current flowing through the specimen, potential difference across the specimen, and specimen brightness temperature were measured. Current was measured by measuring potential difference across a standard resistance (0.001 Ω) placed in series with the specimen. The potential difference across the specimen was measured using tantalum knife-edges placed approximately 50 mm apart on the middle portion of the specimen. The knife edges defined an "effective" portion of the specimen which was essentially free of axial temperature gradients for the duration of the experiment.

Temperature was measured with a high-speed photoelectric pyrometer [2] which permitted 1200 evaluations of the specimen brightness temperature per second. The interference filter in the pyrometer had an effective wavelength of 650 nm and a bandwith of 10 nm.

The recordings of voltage, current and temperature were made with a high-speed digital data acquisition system [3] which recorded data with a full-scale signal resolution of approximately one part in 8000 and a time resolution of 0.4 ms. The system consisted of a multiplexer, analog-to-digital converter and core memory together with control and interfacing equipment. The output of the system was a teletypewriter which was connected to a time-sharing computer. Oscilloscopes were used for monitoring purposes only.

Change in emittance during melting may be expressed by the ratio ϵ/ϵ_s, where ϵ is the emittance at a certain stage in melting and ϵ_s is the emittance just before melting starts (subscript "s" refers to "solid"). The quantity ϵ/ϵ_s may be expressed in terms of the ratio R/R_s, where R is the resistance of the specimen at a certain stage in melting and R_s is the resistance just before melting starts.

The quantity ϵ/ϵ_s was determined from measurements of surface brightness temperature. Based on the Wien radiation equation, the relation between emittance and temperature is

$$\epsilon = \frac{1}{\exp\left[\left(\frac{c_2}{\lambda}\right)\left(\frac{1}{T_b} - \frac{1}{T_t}\right)\right]} \qquad (1)$$

where

T_b = specimen surface brightness temperature in K

T_t = specimen true temperature in K

c_2 = second radiation constant (1.4388×10^{-2} mK)

λ = effective wavelength of the pyrometer (650 nm)

For the case where ϵ is equal to ϵ_s, T_b becomes T_{bs}, where T_{bs} is the surface brightness temperature just before melting starts. Using eq (1), the ratio ϵ/ϵ_s becomes

$$\frac{\epsilon}{\epsilon_s} = \exp\left[\left(\frac{c_2}{\lambda}\right)\left(\frac{1}{T_{bs}} - \frac{1}{T_b}\right)\right] \qquad (2)$$

3. The Results

Measurements were made on two tantalum specimens (Ta-1 and Ta-2). They were in strip form with the following nominal dimensions: length = 4 in (102 mm), width = 0.37 in (9.4 mm), thickness = 0.01 in (0.25 mm). The surface of each specimen was polished. Chemical analysis indicated that the specimens were 99.9 percent pure containing the following impurities (all in ppm by weight). Niobium: 500; W: < 200; Fe: 70; Mo: 10; Ca, Mg, Cu, and Aℓ < 5 each; C: 60; O: 50; N: 20.

Each specimen was heated from room temperature to its melting point in approximately 400 ms. The plateau in temperature, which was approximately 100 ms long, indicated the region of solid and liquid

equilibria. It was not possible to follow the entire melting process because the specimen collapsed and opened the main electrical circuit prior to the completion of melting. Variation of the measured surface brightness temperature as a function of time for Ta-1 is shown in figure 1. All the reported results are based on the 1968 International Practical Temperature Scale [8], IPTS-68.

From the measurements of voltage and current resistance of the specimen was computed. Variation of the surface brightness temperature as a function of resistance for Ta-1 during melting is shown in figure 2. A linear function was obtained by least squares approximation of the data. Standard deviation of individual points from the function is 2 and 3 K for Ta-1 and Ta-2, respectively.

Surface brightness temperature of the specimen at the start of melting was obtained from the temperature vs resistance function. The results were 2867 and 2871 K for Ta-1 and Ta-2, respectively. Considering the average of the above two temperatures and taking 0.398 for the emittance (at λ = 650 nm) as reported earlier [5], one obtains 3258 K for the melting point of the specimens. This is 17 degrees lower than the generally accepted value of 3275 K [7], on IPTS-68. Since emittance is a strong function of surface conditions, it is very likely that the literature value used in the above computations may not be representative of the present specimen conditions. At these temperatures, a one percent error in emittance causes an error of approximately 5 K in temperature.

From both figures 1 and 2 it may be seen that surface brightness temperature decreased as melting progressed. Since during melting specimen true temperature remains constant, a decrease in brightness temperature indicates a decrease in emittance.

Variation of ϵ/ϵ_s, given by eq (2), as a function of R/R_s during melting is shown in figure 3. The results were fitted to a linear function by least squares approximation. Standard deviation of the points from the function is 0.6 and 0.9 percent for Ta-1 and Ta-2, respectively. A quadratic function was also tried, but there was no improvement in the standard deviation. This indicates that a linear function represents adequately the present experimental results.

A meaningful parameter for the comparison of the results on the two specimens is the slope of ϵ/ϵ_s vs R/R_s function, which is a measure of the change of emittance with resistance. The value of this slope was found to be -0.22 and -0.21 for Ta-1 and Ta-2, respectively. The reasonably close agreement of the values indicates the reproducibility of the melting process and of the overall measurements. From the results on electrical resistivity and emittance reported earlier [5] at temperatures near the melting point, it is computed that the value of change of emittance with respect to change in resistance during melting is approximately 8 times that of in the premelting region.

From the measurements of voltage and current, power imparted to the specimen was computed. The results of a linear fit of imparted

power as a function of resistance during melting gave a standard deviation of 0.2 percent for both Ta-1 and Ta-2. Integrating imparted power over time one obtains energy imparted to the specimen during melting. In order to compute absorbed energy by the specimen, energy loss due to thermal radiation was subtracted from the measured imparted energy. Energy loss due to thermal radiation was estimated using an extrapolated value (from 3000 K) for hemispherical total emittance of tantalum given in a recent publication [5]. The comparison of the computed absorbed energy with the heat of fusion of tantalum reported in the literature [4] indicates that approximately one third of the specimen was melted before it collapsed and opened the main electrical circuit.

From the measurements of the resistance, R, of the specimen, just before the start of melting electrical resistivity, ρ, was calculated using the relation $\rho = RA/L$, where A is the cross-sectional area and L is the distance between the potential probes. Dimension were based on their room temperature values. Cross-sectional area was determined from measurements of density (16.65×10^{3} kg m^{-3}) and weight. The electrical resistivity results on the two specimens were in agreement within 0.2 percent. Their average value (113.5×10^{-8} Ωm) is 0.6 percent higher than the value reported by Malter and Langmuir [7] at the melting point, and 1.1 percent lower than that obtained by extrapolation of the results from 3200 K reported earlier [5].

4. Estimate of Errors

Results on the imprecision* and the inaccuracy** of measured and computed quantities are given in table 1. Numbers listed under imprecision were obtained from a least squares analysis of the experimental results. Numbers listed under inaccuracy were estimated considering the contribution of various items that introduce random and systematic errors in the pertinent quantities. Details regarding the estimates of errors and their combination are given in another publication [3]. Specific items in the error analysis were recomputed whenever the present conditions differed from those in the earlier publication.

5. Discussion

The experiments reported in this work demonstrated the possibility of measuring, with a high-speed method, the change in normal spectral emittance of electrical conductors during the initial melting process.

---

* Imprecision refers to the standard deviation of an individual point as computed from the difference between measured and calculated values.

** Inaccuracy refers to the estimated maximum error (random and systematic) approximately equivalent to two standard deviations.

The results showed that normal spectral emittance of tantalum decreased linearly with increasing specimen resistance during melting.

Crude estimates indicated that approximately one third of the specimen was melted at the end of the experiment. During this period resistance changed (increased) by approximately 15 percent. The corresponding change (decrease) in normal spectral emittance was approximately 3.5 percent.

A linear extrapolation to complete melting indicates that resistance and emittance may undergo changes of the order of 40 and 10 percent, respectively. No value for the change of resistivity of tantalum on melting has been found in the literature; however, it has been reported [6] that resistivity increase on melting is 23 percent for molybdenum and 40 percent for platinum. Decrease of emittance on melting for molybdenum and niobium has been reported [1] to be 7 and 18 percent, respectively.

The fact that normal spectral emittance is not constant during melting should be an important consideration in certain experiments in which the investigator relies on obtaining temperature calibration points by observing the melting of the specimen from surface radiance measurements.

6. References

[1] Burgess, G. K., and R. G. Waltenberg, Bulletin Nat. Bur. Stand., 11, 591 (1915).

[2] Foley, G. M., Rev. Sci. Instr., 41, 827 (1970).

[3] Cezairliyan, A., M. S. Morse, H. A. Berman, and C. W. Beckett, J. Res. Nat. Bur. Stand. (U.S.), 74A (phys. and chem.), 65 (1970).

[4] Gshneidner, K. A., Physical Properties and Interrelationships of Metallic and Semimetallic Elements, in Solid State Physics, Vol. 16, p. 275, F. Seitz and D. Turnbull, Eds. (Academic Press, New York, 1965).

[5] Cezairliyan, A., J. L. McClure, and C. W. Beckett, High-Speed (Subsecond) Measurement of Heat Capacity, Electrical Resistivity and Thermal Radiation Properties of Tantalum in the Range 1900 to 3200 K, J. Res. Nat. Bur. Stand. (U.S.), to be published.

[6] Ubbelohde, A. R., Melting and Crystal Structure, p. 179 (Clarendon Press, Oxford, 1965).

[7] Malter, L., and D. B. Langmuir, Phys. Rev., 55, 743 (1939).

[8] International Practical Temperature Scale of 1968, Metrologia, 5, 35 (1969).

TABLE 1

Imprecision and inaccuracy of measured and computed quantities

Quantity	Imprecision	Inaccuracy
Brightness Temperature	0.5 K[a], 3 K[b]	10 K
Voltage	0.02 %	0.05 %
Current	0.03 %	0.06 %
Power	0.03 %	0.08 %
Resistance	0.03 %	0.08 %
Length	0.04 %	0.08 %
Weight	0.01 %	0.1 %
Density	0.02 %	0.1 %
Resistivity	0.03 %	0.5 %
Emittance	0.8 %	3 %

[a]for solid surface

[b]during melting

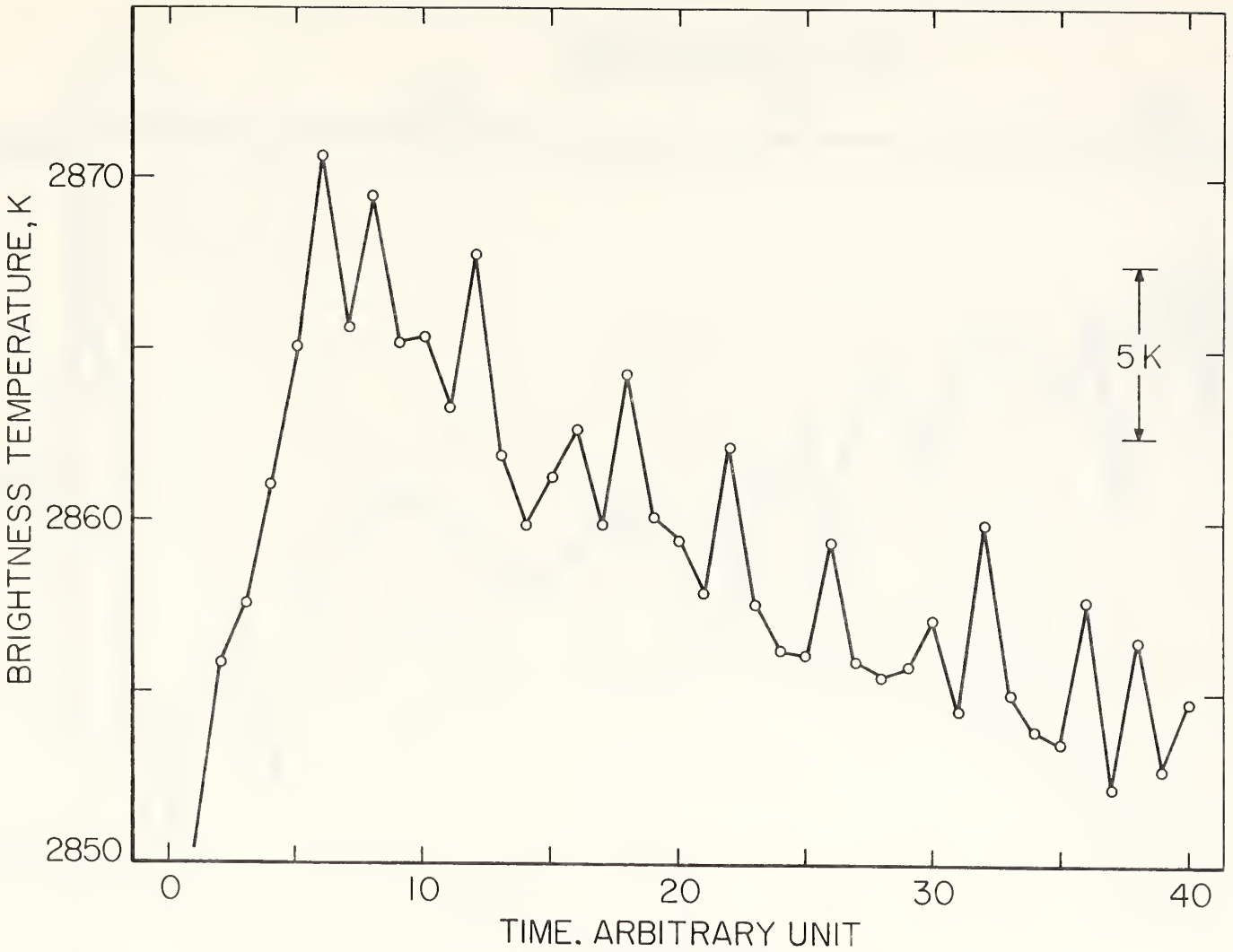

Figure 1. Variation of surface brightness temperature of tantalum specimen as a function of time during melting (1 time unit = 2.5 ms).

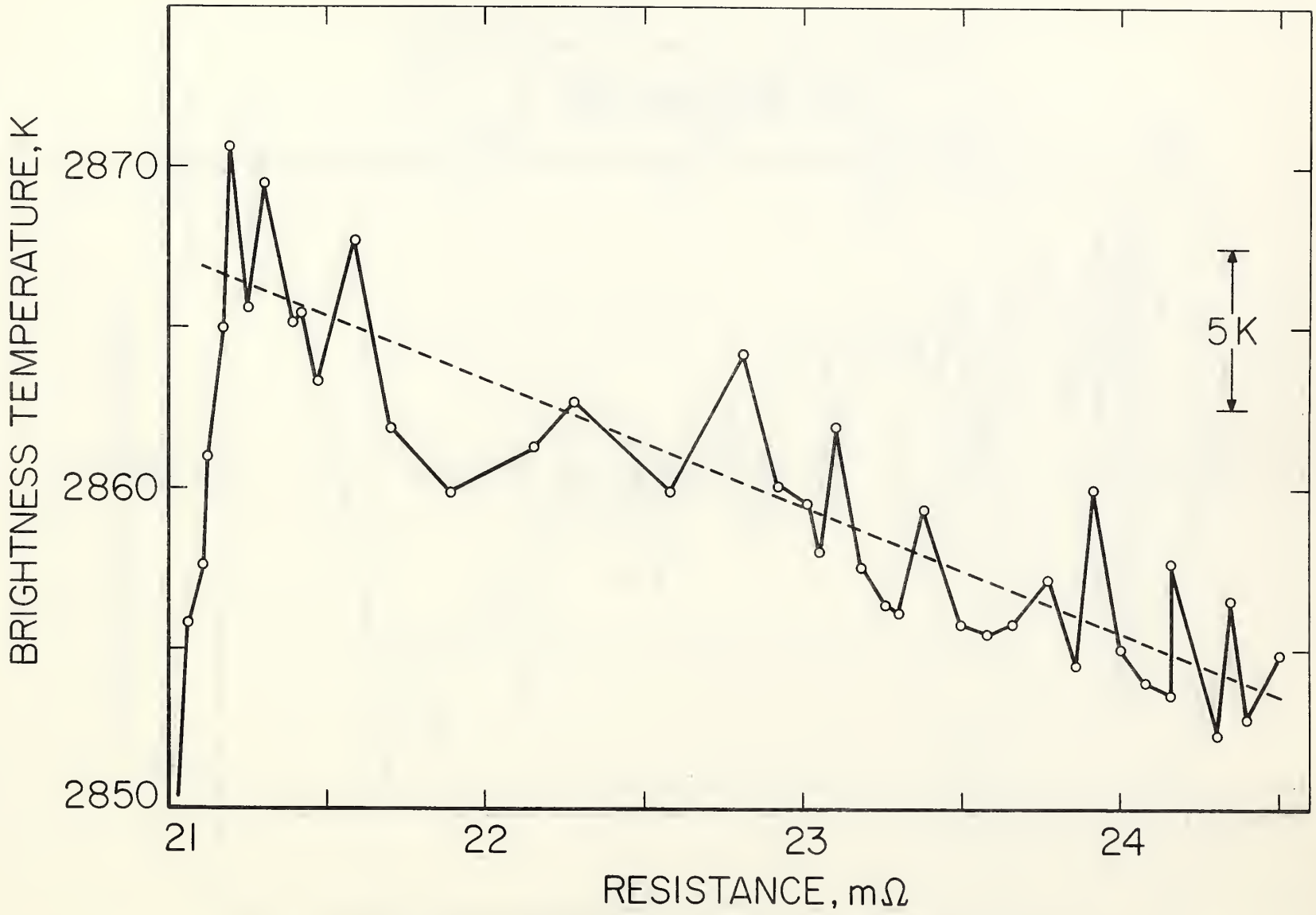

Figure 2. Variation of surface brightness temperature of tantalum specimen as a function of its resistance during melting.

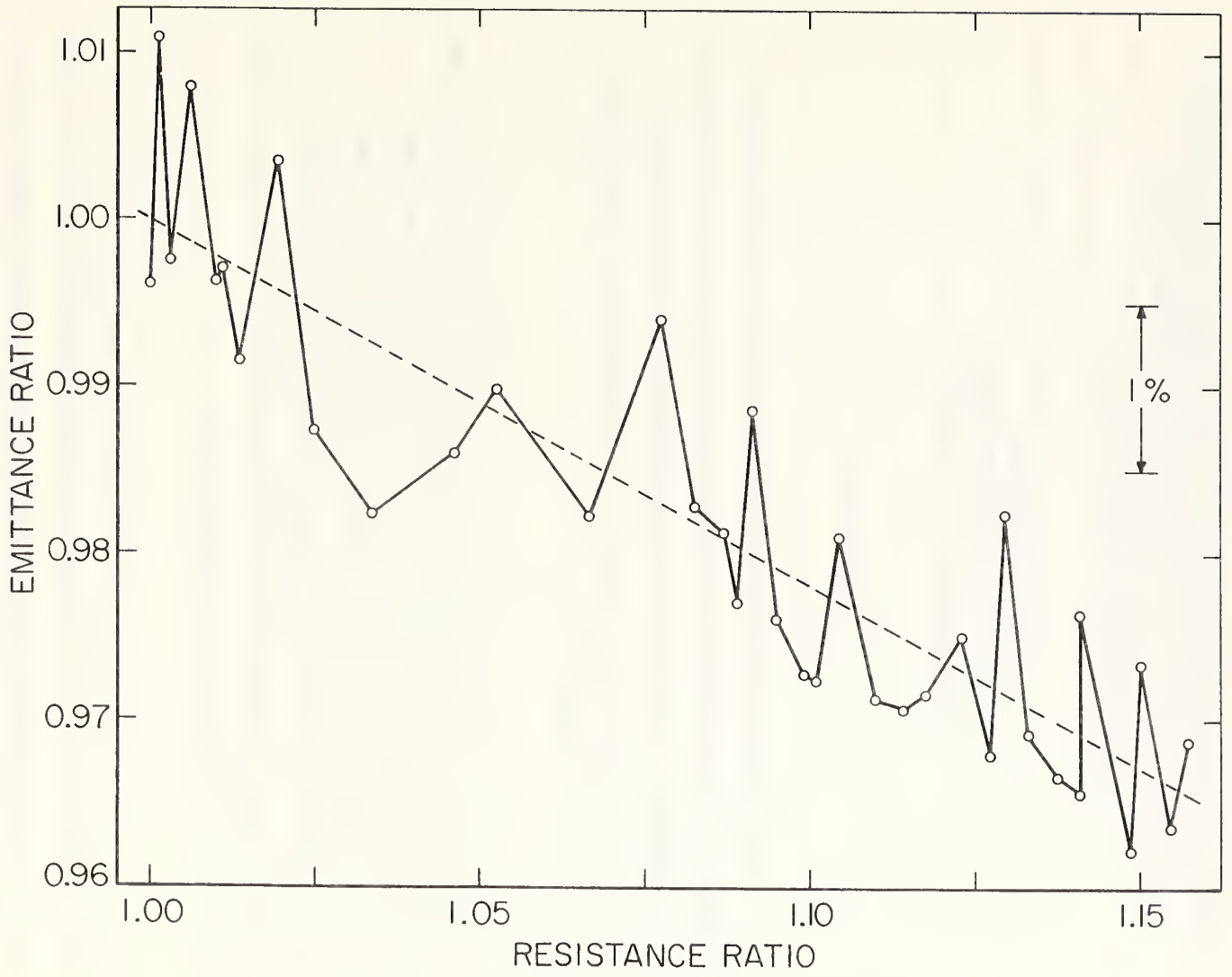

Figure 3. Variation of normal spectral emittance ratio, $\varepsilon/\varepsilon_s$, of tantalum as a function of its resistance ratio, R/R_s, during melting.

Chapter 9

A PULSE HEATING METHOD FOR THE MEASUREMENT OF MELTING POINT OF ELECTRICAL CONDUCTORS (THIN WIRES) ABOVE 2000 K*

Ared Cezairliyan
National Bureau of Standards
Washington, D. C. 20234

ABSTRACT

A pulse heating method is described for the measurement of melting point of electrical conductors at high temperatures (above 2000 K) which are in the form of thin wires. The technique is checked by measuring the melting point of platinum. The results give 2044 ± 5 K on IPTS-1968.

In general, melting points of substances are determined using quasi steady-state techniques, where the specimen is either heated or cooled very slowly until a phase change is detected. These methods present difficulties at high temperatures (above 2000 K) due to increased heat transfer, chemical reactions, evaporation, loss of mechanical strength, etc.

---

* This work was supported in part by the Propulsion Division of the U. S. Air Force Office of Scientific Research under contract ISSA-69-0001.

In order to overcome most of these difficulties experiments may be performed in short times by heating the specimen rapidly to its melting point. A technique utilizing this approach was described in the literature [2]. The specimen was of tubular form (100 mm long, 6.4 mm outside diameter, 0.5 mm wall thickness) with a small hole in the wall at the middle of the specimen. The cylindrical specimen approximated blackbody conditions for optical (pyrometric) temperature measurements. The specimen was heated from room temperature to its melting point in less than one second by the passage of a high current (2000 A) through it. The maximum temperature attained was the melting point. The melting point obtained by this method was reproducible within 1 K (standard deviation of the mean). The tubular specimen had to be destroyed during each determination. The cost and difficulty of fabricating specimens used in the above study make it unsuitable for general use.

The objective of this note is to describe a high-speed method of measuring melting point of electrical conductors (with melting points above 2000 K) where the specimens are in the form of thin wires. The method is based on detecting melting of a specimen which is wound around a tube as the latter is heated rapidly in vacuum. The limitation of the measurements to temperatures above approximately 2000 K is imposed by the optimization in the operation of the high-speed pyrometer.

The basic circuitry of the measurement system, shown in Fig. 1, was similar to that described in the literature [1]. The specimen was a high purity (99.999 percent) platinum wire (diameter = 0.001 in

0.025 mm), which was wound (half turn) around a thin-wall molybdenum tube. The tube was electrically in series with the main power pulsing circuit. Two pulleys supported the wire. A 0.5 g weight was attached to each end of the wire to assure good contact between the wire and the tube. A schematic drawing showing the specimen and the tube assembly is presented in Fig. 2. The ends of the platinum wire were connected to a special electronic circuit which indicated the time of the opening of the circuit resulting from the melting of platinum. The break in the circuit took place at a point of contact with the tube as the latter was pulse heated. Duration of an experiment (heating of the specimen from room temperature to its melting point) was approximately 0.8 s. Heating rate of the tube at the melting point of platinum was approximately 2 K ms^{-1}. Temperature of the tube was measured with a high-speed photoelectric pyrometer [3], which permits 1200 evaluations of tube temperature per second. The pyrometer target was a small rectangular hole (1 mm x 0.5 mm) fabricated in the wall at the middle of the tube. Signals were recorded with a high-speed digital data acquisition system [1] which has a full-scale signal resolution of approximately one part in 8000 and time resolution of 0.4 ms. Temperature of the tube corresponding to the time of the break in the platinum wire gave the melting point of platinum.

The results of three experiments gave an average value of 2044.2 K for the melting point of platinum on the 1968 International Practical Temperature Scale [4] with an average deviation from the mean of the three amounting to 1.1 K. This compares favorably with the accepted value of 2045 K [4].

In each experiment, the contribution to the uncertainty in tempera-

ture resulting from the uncertainty in the "temperature-time of break" determination was 0.4 K. The standard deviation of individual temperature measurements in each experiment was less than 0.3 K. Correction due to the radial temperature gradient in the tube was less than 0.1 K. Maximum inaccuracy in temperature measurements at the melting point of platinum, which results from uncertainties in standard lamp, pyrometer calibration, blackbody quality, scattered light, etc., is estimated to be 4 K [1]. Error in the melting point due to alloying effect is negligible since the entire experiment was of very short duration.

Because of the complex nature of the experimental method, it was difficult to determine exactly, (1) the time constant for heat transfer between the tube and the specimen, and (2) the effect of the tension due to end weights on the melting point. Crude estimates indicated that this time constant could be approximately 0.1 ms, which corresponds to an error of approximately 0.2 K in the melting point. It is likely that in the experiments the lowering of the melting point due to tension in the specimen was approximately compensated by an opposite effect which resulted from the finite time constant associated with heat transfer between the tube and the specimen. One may conclude that the melting point of platinum, as determined in this study, is 2044 ± 5 K on IPTS-68.

The results of preliminary work presented in this note have demonstrated the feasibility of measuring the melting point of electrical conductors in the form of thin wires by a pulse heating method of subsecond duration.

References

1. Cezairliyan, A., M. S. Morse, M. A. Berman, and C. W. Beckett, J. Res. Nat. Bur. Stds. (U.S.), 74A (Phys. and

Chem.), 65 (1970).

2. Cezairliyan, A., M. S. Morse, and C. W. Beckett, Measurement of Melting Point and Electrical Resistivity (Above 2840 K) of Molybdenum by a Pulse Heating Method, in preparation.
3. Foley, G. M., High-Speed Optical Pyrometer, Rev. Sci. Instr., 41, 827 (1970).
4. International Practical Temperature Scale of 1968, Metrologia, 5, 35 (1969).

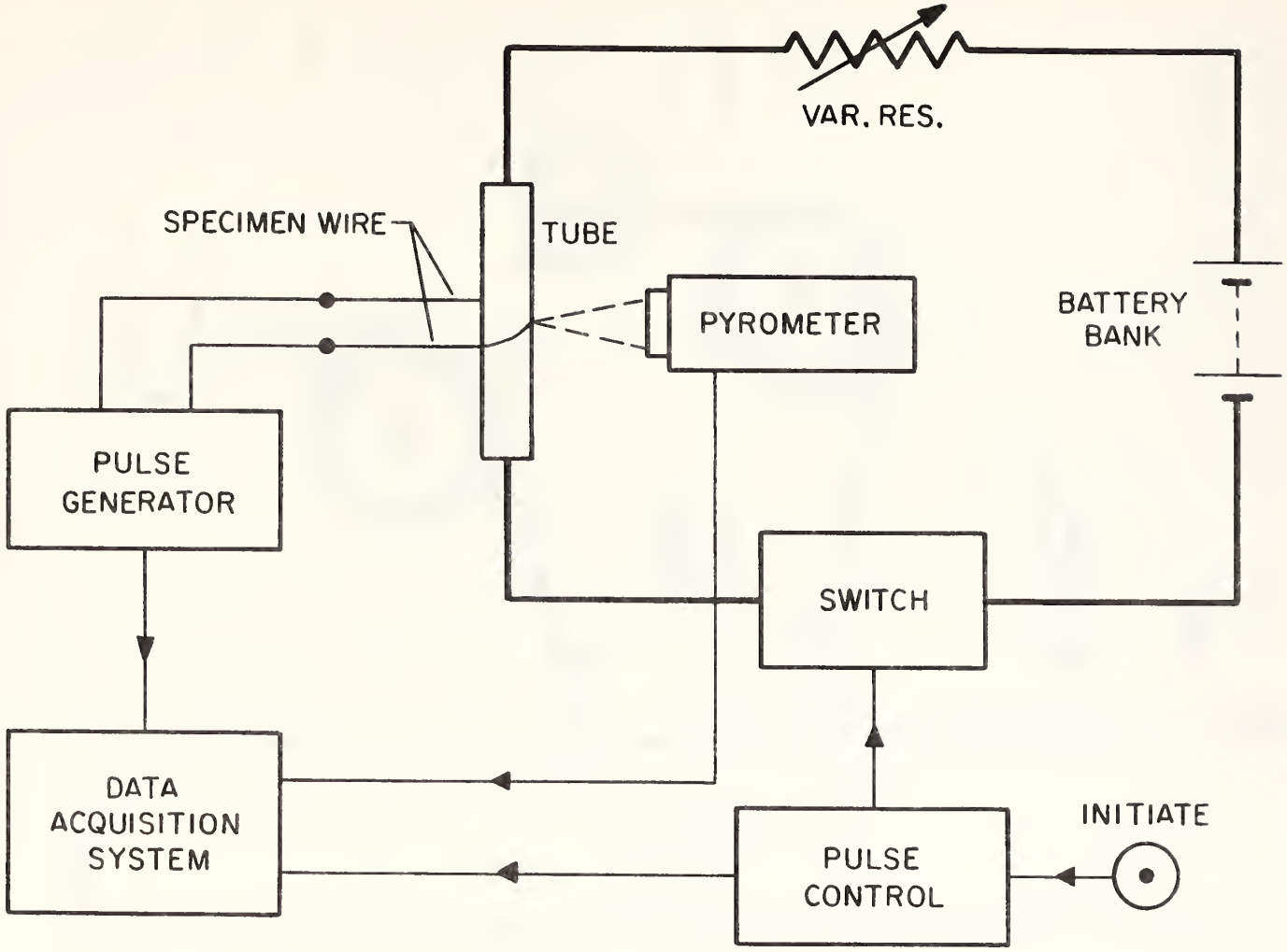

Figure 1. Functional diagram of the system for the measurement of melting point of electrical conductors (thin wires) above 2000 K.

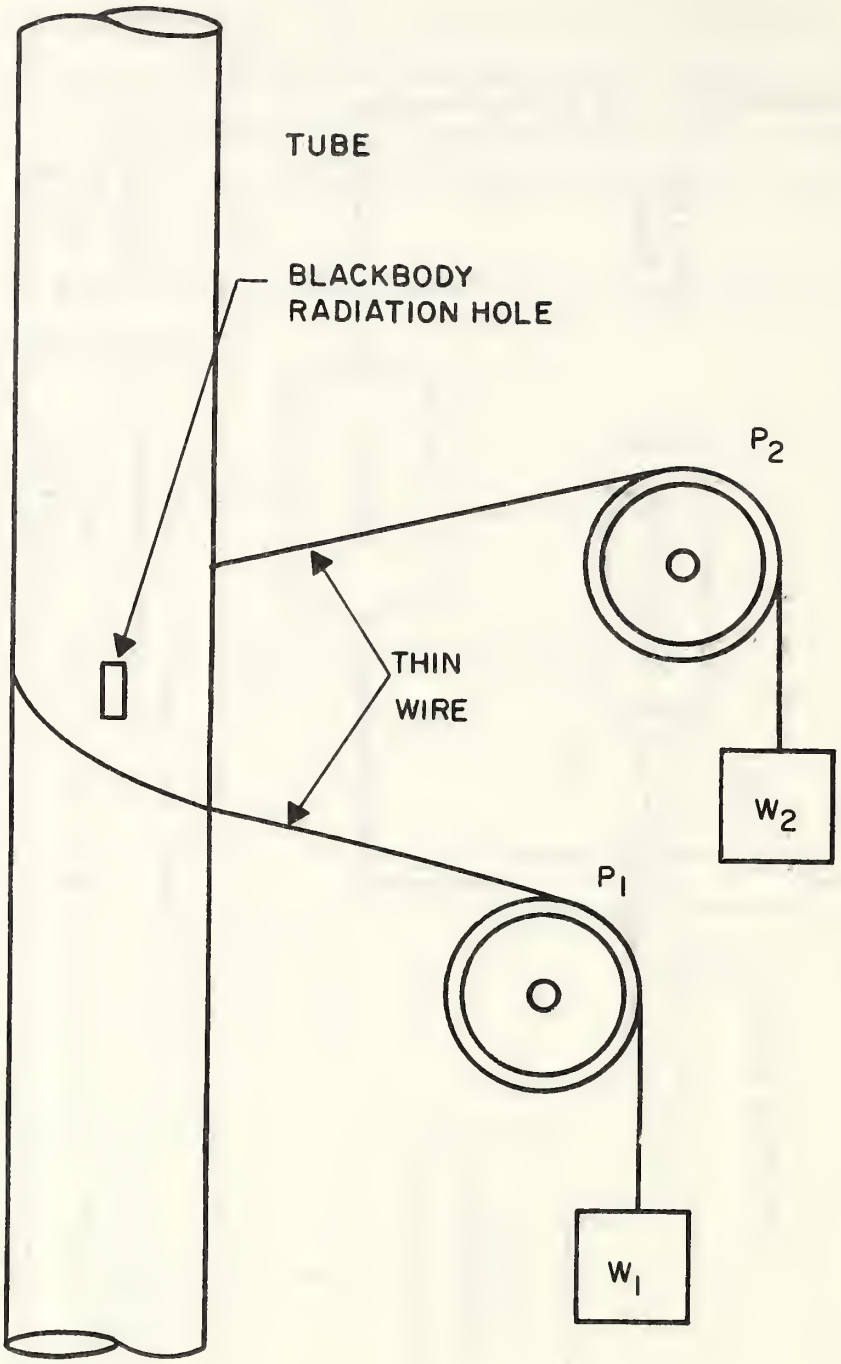

Figure 2. Schematic diagram of specimen and tube assembly.

Chapter 10

DESIGNING A TRANSPIRATION SEARCH FOR HIGHER BERYLLIA HYDRATES: IMPROVING THE SENSITIVITY BY EMPIRICAL COMPARISON WITH THE VOLATILITY OF GOLD

By

Thomas B. Douglas

Abstract

The reaction between BeO(c) and H_2O(g) is simplified by considering the formation of only $(BeO)H_2O$(g) and smaller amounts of $(BeO)_2H_2O$(g). From experimental data and by analogy, tentative values are assumed for enough parameters to determine the thermodynamic properties of the above system and of evaporating gold. On this basis the sensitivity of the basic thermodynamic properties of $(BeO)_2H_2O$ to error in any one of several parameters in transpiration experiments is computed. The adequacy of pyrometer-determined temperatures is found to be critical, but it is demonstrated that the serious consequences of temperature error can be considerably reduced in this case by transpiring gold simultaneously and requiring that the temperature of each experiment be properly related to the thermodynamic properties of liquid and gaseous gold. From the known and estimated thermodynamic properties of simple molecules containing gold, the conditions are estimated under which this use of gold is not invalidated by contaminants.

I. Introduction

A few years ago I pointed out that discrepancies between calculated and observed efficiencies of combustion of certain beryllium-containing fuels could be accounted for, at least in part, if some hitherto unrecognized bydrate of beryllia were formed in considerable amount. Several of my colleagues at NBS then used their expertise to estimate the numerical values of the molecular constants of a whole series of such "higher" hydrates of beryllia, which can be represented by the general formula $(BeO)_n H_2O$ [13].[1] Since calculations based on these parameter values showed that such new gas species might indeed be important ones under propulsion conditions, we undertook an experimental search for them by first redesigning our unusually precise transpiration apparatus [24] for the higher temperatures (to above 2000 K) which would certainly be necessary.

It was immediately evident that the most critical condition for the success of such measurements very probably lay in measuring the thermodynamic temperatures of reaction between BeO(c) and $H_2O(g)$ accurately enough. Toward this end we made detailed heat-transfer calculations to establish furnace designs with sufficiently flat temperature profiles, and also the detailed calculations summarized in this chapter to establish the temperature-measuring accuracy needed, as well as promising means of achieving it. One major consideration dictating high temperature accuracy was that one would essentially be looking for curvature in the vapor-pressure curve (say, of lnP vs. 1/T) attributable to the increasing contribution of a dimer (or higher) species as the temperature increased, but not measurable nor even detectable unless the pressure and temperature data have a high internal consistency.

The simplest method in principle to eliminate temperature determination as a source of error is to measure the (thermodynamic) temperature of each (isothermal) experiment sufficiently accurately. The temperatures of interest here are near or above 2000 K, and one would therefore naturally

---

[1] Numbers in brackets refer to references at the end of this chapter.

seek the required accuracy in their determination by optical pyrometer, since the International Practical Temperature Scale recognizes this as the most reproducible instrument for doing so in this temperature range.

However, the calculations described later in this chapter indicate that the best present-day pyrometer accuracy is hardly sufficient for the present purpose. But the calculations show also that one ought to be able to relate the different temperatures of different experiments well enough to give adequate accuracy to derived heats of formation of the higher-hydrate species sought, if one does so by comparison with the vapor-pressure curve of a substance such as gold.

The National Bureau of Standards has recently made available Standard Reference Material 745, which is gold wire whose vapor pressure over the temperature range 1300-2100 K is certified on the basis of measurements made in eleven different laboratories [25]. It should be emphasized, however, that the use of gold as a relative-temperature standard in the manner described in this chapter is largely free of the degree to which the temperatures of the vapor-pressure curve of the above "SRM-745" gold depart from the true thermodynamic temperature scale, and should be free of the systematic errors characteristic of different methods of measuring vapor pressure.

This experimental (transpiration) undertaking of ours on the $BeO-H_2O$ system has been postponed in favor of presently more urgent tasks, and its future status is unknown. For this reason it seems wise to report some of the results of our design calculations, in the belief that they may be of value and interest to anyone else who plans to study the $BeO-H_2O$ or an analogous system by similar means. I am well aware that the most convincing support for the conclusions from such a feasibility study come from actual performance behavior, and am sorry that we have no data of this sort to present now.

II. Simplified Picture of the Plan

The transpiration search is assumed to be for the gas species $(BeO)_n H_2O$ with $n > 1$, where the "monomer" (n=1) will almost certainly be the predominant species at the temperatures readily available experimentally. Reasonable estimates of the parameter values for all these species indicate that at the temperatures available ($\leq$ 2500 K) the "dimer" (n=2) will predominate over the sum of all higher hydrates ($n > 2$). Therefore the approach used here is to consider only the monomer and dimer and to ignore all higher hydrate species; besides, transpiration measurements alone cannot be expected to distinguish among the (numerous) thermodynamic parameters of different higher hydrates ($n > 1$) with any degree of reliability.

The existing data on the monomer (up to 1850 K, the highest temperature of such measurements reported) are not sufficiently precise to be used for more than preliminary estimates. Therefore, transpiration measurements from which it can be hoped to evaluate the dimer must simultaneously reevaluate the monomer. We have the two reactions

$$BeO(c) + H_2O(g) = BeO \cdot H_2O(g) \qquad (1)$$

and

$$2BeO(c) + H_2O(g) = (BeO)_2 \cdot H_2O(g) \ . \qquad (2)$$

The simplest plan is to consider measuring the system at three sufficiently different temperatures. Because the temperature coefficient of Reaction (2) will almost certainly be much greater than that of Reaction (1), the simplest approximately (not accurate) is to assume that at the two lowest temperatures (hereafter called T_1 and T_2) no dimer will be formed, but that at the highest temperature (T_3) measurable dimer accompanies the monomer. Hence, if an adequate $\Delta C_p(T)$ for Reaction (1) can be estimated, one may calculate from the observed amounts of BeO evaporated at T_1 and T_2 the amount <u>expected</u> at T_3 if no dimer were formed there either. The excess <u>observed</u> BeO at T_3 (over this amount) will then be a rough measure of the amount of higher hydrates formed at T_3. (In exemplary calculations of the type, taking the three temperatures as 1600, 1800, and 2000 K, this rough approximation reflected about one-third the assumed total of higher hydrates at T_3, and a larger fraction for $T_3 > 2000$ K.)

The tentatively estimated parameter values given in Section II predict such a small dimer/momomer ratio even at T_3 (if $T_3 \leq 2500$ K) that it is immediately obvious that the three thermodynamic temperatures T_1, T_2, and T_3 must be measured with relatively high absolute accuracy for the results to be meaningful as to whether any dimer is formed. Specific figures in relation to pyrometric accuracy will be discussed later. The alternative to measuring these temperatures pyrometrically that suggested itself is to evaporate gold simultaneously and in contact with the BeO, and to use the amount of gold evaporated in each experiment as a measure of the temperature. The assumption will be made that the necessary conditions have been met for preventing appreciable error through chemical reaction of the gold with contaminants. These necessary conditions are discussed in detail in Section VII of this chapter.

If a gold vapor-pressure thermometer is used in the usual sense, it will measure each temperature, independently of the other temperatures, from its experimentally determined vapor pressure at that temperature. This vapor-pressure value would introduce its own experimental uncertainties, one of which is the accuracy of temperature measurement when it was determined. Such an individual temperature, so determined, may easily be in error by 30 deg, as will be shown later.

However, the real goal is not to measure accurately the three individual temperatures T_1, T_2, and T_3, but rather the amount of the beryllia-hydrate dimer at some one temperature (or over a temperature range), or the parameters which determine that. As will be demonstrated, it turns out that the three vapor pressures of gold measured in the three postulated beryllia-hydrate experiments determine a relationship among T_1, T_2, and T_3 with much less uncertainty than that of any one of these temperatures in determining the resulting amount of beryllia-hydrate dimer.

The preceding statement can be illustrated dramatically by considering Reaction (1) and the reaction

$$Au(\ell) = Au(g) , \qquad (3)$$

and assuming for the moment that (a) these two reactions represent the only ones occurring, and that (b) $\Delta C_p = 0$ for both Reactions (1) and (3). Then we would have for these two reactions, respectively, the equilibrium constants (K' and k') given by

$$\ell n\ K_i' = -\frac{H'}{RT_i} + \frac{S'}{R} \tag{4}$$

and

$$\ell n k_i' = -\frac{h'}{RT_i} + \frac{s'}{R} \quad , \tag{5}$$

where H', S', h', s', and of course the gas constant R are constants. If we apply eqs (4) and (5) each at T_1, T_2, and T_3, we get six equations from which T_1, T_2, T_3, H', and h' may be eliminated (R, S', and s' also drop out) to give

$$\frac{\ell n\ K_3' - \ell n\ K_2'}{\ell n\ K_2' - \ell n\ K_1'} = \frac{\ell n\ k_3' - \ell n\ k_2'}{\ell n\ k_2' - \ell n\ k_1'} \tag{6}$$

Equation (6) may thus be solved for K_3 without knowledge of T_1, T_2, T_3, R, H', h', S', or s', and this calculated value of K_3 may be compared with the (greater) experimental value to give the very roughly approximate contribution at T_3 of the dimer beryllia hydrate, $(BeO)_2H_2O$.

The two simplifying assumptions stated in the preceding paragraph [(a) and (b) -- essentially, that vaporization yields only the ideal-gas monomer and with no change in heat capacity] are not, of course, exactly true, and the actual "corrections" were taken into account in the computations later reported in this chapter. Because these "corrections" are relatively minor ones, we may expect that the corresponding correction of the very simple relationship given by eq (6) will be rather minor, necessitating no highly accurate knowledge of the values of the various thermodynamic parameters compared with what would need to be known were it necessary to determine T_1, T_2, and T_3 independently of one another.

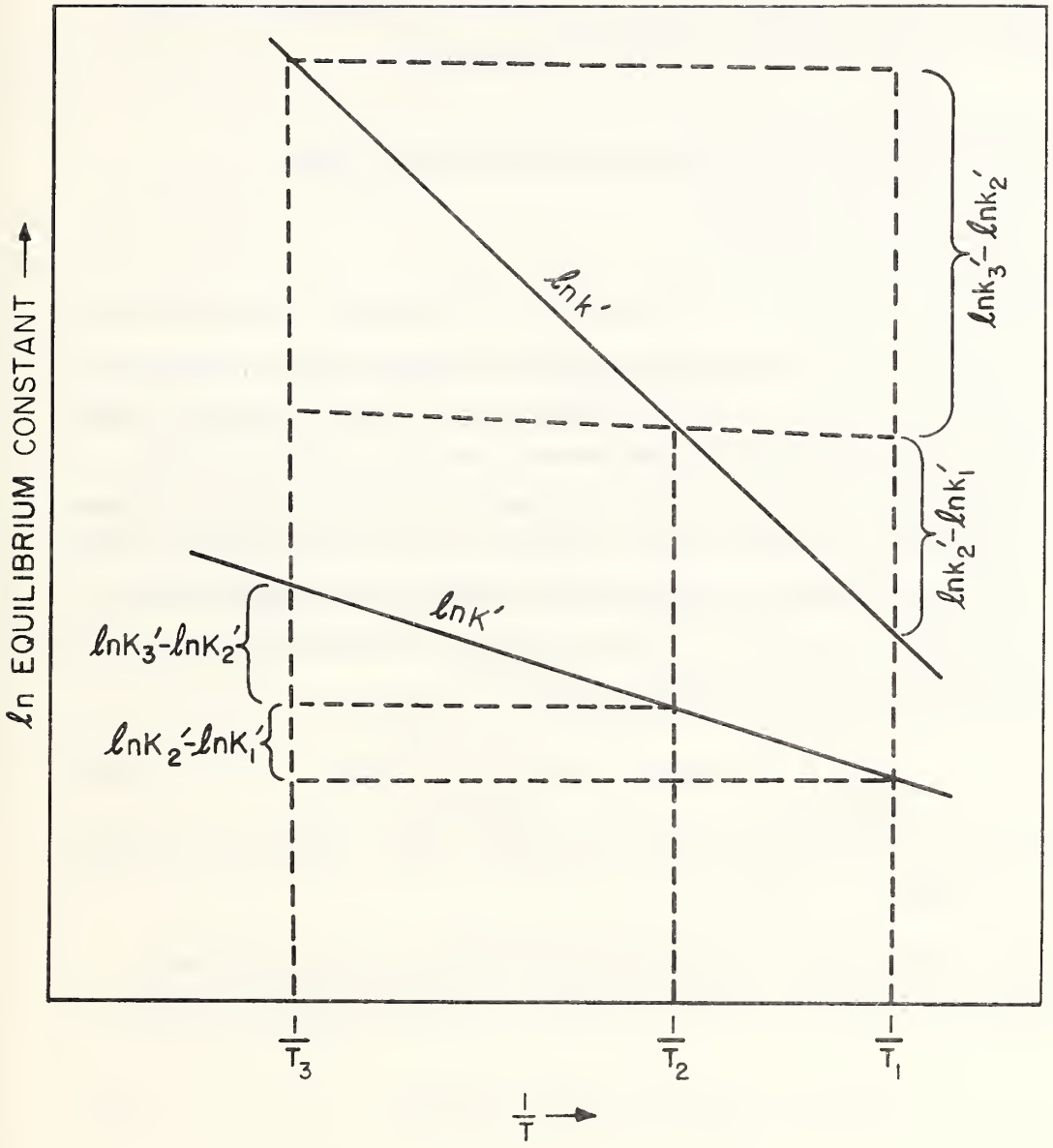

Figure 1. Illustration of the idealized graphical relation at three temperatures for the equilibrium constants of evaporation of two substances when each vapor is an ideal monomeric species and $\Delta C_p = 0$.

Incidentally, eq (6) is virtually self-evident from the diagramatic Fig. 1, whose straight lines follow from eqs (4) and (5). In actuality, the two straight lines in Fig. 1 become somewhat curved, so that each of the two members of eq (6) must actually be multiplied by a correction factor somewhat different from unity; the factors differ from each other, and furthermore are functions of the set $\{T_1, T_2, T_3\}$.

III. Tentative Estimated Thermodynamic-Parameter Values for the BeO-H_2O System

Grossweiner and Seifert [1], Young [2], and Stuart and Price [3] have studied the evaporation of BeO(c) into H_2O(g) by transpiration, altogether encompassing the temperature range 1340-1850 K. In this temperature range there is believed to be indirect evidence that the only gaseous hydrate formed to an appreciable extent is the "monomer" (by Reaction (1)). These three sets of experimental results are virtually in agreement (within their precision), and I shall adopt as mean parameter values describing these results the following (Second-Law) values of ΔH and log K for Reaction (1) at 1600 K (C.W.Beckett and T.B. Douglas, 1967):

$$H'_{1600} = 41.4 \text{ kcal}; \quad \log K'_{1600} = -3.926 \qquad (7)$$

(JANAF tables are available for BeO(c) and H_2O(g) [4].) Using eq (7), for Reaction (1) $\Delta S^{o}_{1600} = 7.911$ eu.

The general vaporization reaction hypothecated to cover the simultaneous formation of a whole series of gaseous "beryllia hydrates" may be written

$$n\text{BeO(c)} + H_2O(g) = (\text{BeO})_n\, H_2O(g), \qquad (8)$$

whose thermodynamic constants will be written with superscript n ($K^{(n)}$, $S^{(n)}$, etc.).

Though there must at present be some degree of arbitrariness, it is highly desirable to choose a set of molecular parameters which for n=1 fit the experimental data of eq (7). The earlier NBS estimates relied

heavily on analogy with the alkali hydroxides--Linear molecule; BeO distance, 1.40 Å; O-H distance, 0.96 Å; Fundamentals: OH stretch, 3500 cm^{-1}; OH bend, 350 cm^{-1}; BeO stretch [5],

$$\log \omega = 3.13335 - 0.05375\ n + 0.0507/n \quad cm^{-1}. \qquad (9)$$

To fit eq (7), these values require (for n=1) 950 cm^{-1} for each of the (4n-2) BeO-bend modes, and this value seems unreasonably high.

I modified the above set of molecular parameters somewhat. I chose the set, designed to fit eq (7) exactly for n=1, with consideration of the fact that Be is in the sequence of elements Li, Be, B, C in the first row of the Periodic Table, since information is available for some of the molecular constants of analogous bonds or groups containing B and C. For example, the groups BOH and COH are known to be non-linear, and it seems likely that BeOH may be so also (as assumed in the latest JANAF table for $Be(OH)_2(g)$ [4]). Nevertheless, I retained a linear molecule and the bond distances given above, because these assumptions probably make but minor difference, and because rotational calculations based on them had already been made and verified.

The vibrational fundamentals here adopted for $(BeO)_nH_2O$ are shown in Table 1.

Table 1

Tentative Molecular Constants for $(BeO)_n H_2O$ Assumed Here

Mode	Degeneracy n=n	n=1	n=2	n=3	Assumed (ω) (cm^{-1})	Analogies
OH stretch	2	2	2	2	3500	Numerous OH species
BeO stretch	2n	2	4	6	1350,1125,975,...[eq(9)]	---
HOBe bend	4	4	4	4	574	See footnote (a)
OBeO bend	2n	2	4	6	350	See footnote (b)
BeOBe bend	2n-2	0	2	4	140	See footnote (c)

(a) HONa, HORb, HOCs, approximately 325 cm^{-1} [6]; HOB, 961 cm^{-1} (Mack and Wilmot for HOBO [7]; White et al. [8] had earlier estimated 1250 cm^{-1} in HOBO); HOC, 1340 cm^{-1} Herzberg, 1945, for CH_3OH [9]).

(b) FBeF, 320 cm^{-1} (Snelson [10]).

(c) White et al. [11] found that a bend mode in Li_2O between 100 and 180 cm^{-1} gave Second- and Third-Law agreement, and they adopted the mean, 140 cm^{-1}, as an estimate for this molecule. Since there are no BeOBe bending modes for the monomer (n=1), the value in Table 1 is independent of eq (7).

It may be noted that the ionic model would predict a linear MOH bond. Furthermore, the electronegativity varies smoothly from Li to C: Li, 1.0; Be, 1.5; B, 2.0; C, 2.5 (Pauling [12]). The HOC bonds are considerably covalent, and hence the bond orbitals there are highly directed, as confirmed by the (observed) highly bent HOC groups in the alcohols.

The JANAF tables for BeO(c) and H_2O(g) [4], plus Table 1 above, give for Reaction (8) the values in Table 2.

Table 2

Some Entropy Changes Calculated for Equation (8), Assuming Table 1

n	ΔS^{o}_{1600} (eu)
1	7.907
2	17.178
3	25.947
4	35.028

There remains to formulate some reasonable estimate, for Reaction (8), of $\Delta H^{(n)}(T)$ that is consistent with eq (7). The heat of formation (or the dissociation energy) of an unknown molecule is usually the most difficult parameter to estimate with sufficient accuracy, and latitude will be allowed for this fact. In 1966 I found [13], using the latest JANAF tables then available except in the case of Be_2OF_2 [14], the apparent Be-O bond energies, calculated from heats of formation at 298 K, that are listed in Table 3.

Table 3

Apparent Be-O Bond Energies in Some Gaseous Beryllium Molecules, Calculated From Thermochemical Data

Molecule	Be-O Bond Energy (kcal/mole)
$(BeO)_2$	94
$(BeO)_3$	111
$(BeO)_4$	116
$(BeO)_5$	120
$(BeO)_6$	122
Be_2OF_2	120
$Be(OH)_2$	119

(The values for the polymers of BeO, assumed to be rings, originated from unrelated Second-Law values determined mass-spectrometrically. Assuming that the lower polymers of BeO reflect strain energy, it appeared that the Be-O bond energy in a non-ring molecule could reasonable be assumed nearly constant at about 120 kcal/mole.)

Taking the O-H bond energy the same as for $H_2O(g)$ at 1600 K and letting x be the mean BeO bond energy (in kcal/mole at 1600 K), there was obtained for $(BeO)_n H_2O$

$$\Delta H_{1600}^{(n)} = (279.56-2x)n \text{ kcal/mole} . \qquad (10)$$

Equations (7) and (10) give

$$x = 119.08 \quad \text{for } n = 1, \qquad (11)$$

and this value is adopted here for n = 1, but is here allowed to vary (as a parameter) by up to +4 kcal/mole for n > 1. Since the equilibrium constants for Reaction (8) are the quantities of greatest practical interest, this latitude in x can absorb the uncertainties of the ΔS^o_{1600} values of Table 2 to a certain extent, as will be shown by example later.

As to $\Delta C_p^{(n)}(T)$ for Reaction (8), the JANAF tables [4] give $C_p(T)$ accurately for $H_2O(g)$ and supposedly with fair accuracy for BeO(c); and $C_p^{(n)}(T)$ for the hydrate n can supposedly be calculated with fair reliability from Table 1, since $C_p^{(n)}(T)$ is near equipartitional for $T \geq 1600$. The result for n=1 was formulated as

$$\Delta C_p^{(1)} = 3.6 - 0.0023\ T \text{ cal/mole-K}, \qquad (12)$$

which fits the values so derived within 0.2 cal/mole-K between 1600 and 2400 K. For the calculations presented here the simplifying (but inaccurate) assumption was made that

$$\Delta C_p^{(2)}(T) = 0\ , \qquad (13)$$

and the estimated values of $\Delta H^{(2)}$ and $\Delta S^{o(2)}$ were adjusted to the middle of the temperature range to be considered. This unnecessary approximation is not serious, since it would be an achievement to establish reliably the presence of the dimer in appreciable amount at <u>any</u> temperature below 2500 K. Equation (12) for the monomer can, however, introduce appreciable uncertainty into the calculated abundance of the dimer if, as expected, the latter abundance is relatively small; and this question was explored in the calculations presented in Section VI.

It is of interest to see what results the parameter values outlined in this section predict for various temperatures. We shall use $K^{(n)}$ (dimensionless) to represent K_p for Reaction (8) and a specific value of n. Since transpiration measurements measure the mass of BeO held in the form of all the gaseous hydrate species present, and since this is also the quantity of practical (propulsion) interest, we should compare values of

$nK^{(n)}$ at a given temperature (see Reaction (8)). Table 4 was calculated (not neglecting ΔC_p for n > 1). (The results for 3700 K involve liquid BeO, and the corresponding thermal functions were taken from a JANAF table [4].)

Table 4

Calculated Equilibrium Constants K_p for Representative Reactions of (8) (x=119.08 kcal/mole for n=1;= value tabulated for n > 1. See Equations (10 and (11).)

$$[2K^{(2)}+3K^{(3)}+4K^{(4)}]/K^{(1)}$$

T(K)	$K^{(1)}$	(x-119.08)kcal/mol :0	1	2	3	4
1600	$1.183(10^{-4})$	0.0005	0.0017	0.0058	0.0205	0.0723
1800	$5.016(10^{-4})$	0.0020	0.0061	0.0186	0.0571	0.1755
2000	$1.585(10^{-3})$	0.0062	0.0169	0.0465	0.1282	0.3542
2300	$6.097(10^{-3})$	0.023	0.056	0.136	0.331	0.82
2500	$1.246(10^{-2})$	0.0465	0.105	0.240	0.552	1.30
3700	$8.891(10^{-2})$	0.319	0.582	1.080	2.054	4.030

Calculations were made for 3700 K because the opinion has been expressed that if the ratio represented in the last five columns of this table is, at this temperature, as great as 3 or 4, the higher hydrates of beryllia (n > 1) would be of great propulsion interest, but that if this ratio is unity or less, there would be much less interest [15].

Lest someone be tempted to forget their origin and use or cite them without due qualification, the numerical values of molecular constants and heats of formation assumed in this and subsequent sections of this chapter should be regarded as highly tentative and capable of considerable refinement. These values seem to be a reasonable basis for estimating the orders of magnitudes of observable quantities, and should prove servicable in this way if their uncertainties are not misrepresented.

IV. Definitions of Symbols, and "Normal" Values Assumed for the Computer Calculations

Parameter values for the beryllia hydrates have been derived and discussed in Section III. Several references are available for gold: All the thermodynamic properties [16, 17]; new experimental C_p measurements on Au(ℓ) [18]; properties of Au_2 from mass spectrometry [19, 20]. Monatomic gold has low-lying electronic states; the following equation fits the calculated values of C_p to within about 0.6% between 1300 and 1900 K, and was adopted:

$$\text{Au(g): } C_p/R = 0.5702 + 7.325(10^{-4})\ T + 1286.5/T\ . \qquad (14)$$

For reference we write the reaction

$$2\text{Au}(\ell) = \text{Au}_2(g)\ . \qquad (15)$$

Table 5 lists and defines the symbols subsequently used, and gives their "normal" values adopted in the calculations of Section VI.

Table 5

Symbols Used, and "Normal" Values Selected

Symbol	Meaning	Units	"Normal Value"	Remarks
h	ΔH_{1700} of Reaction (3)	kcal	81.77	See footnote (a).
C_ℓ	C_p of Au(ℓ) at all T's	cal/mole-K	7.953	From [18]; [17] uses 7.0.
S_ℓ	S°_{1337} of Au (ℓ)	eu/mol	23.342	See footnote (b).
D	Dissoc'n energy of Au_2 at 0 K	kcal/mol	52	See footnote (c).
ω	Vib. fundamental of Au_2	cm^{-1}	191	[19] cites 190.9 as obs.
r	r_e of Au_2	Å	2.68	See footnote (d).
H′	ΔH_{1600} of Reaction (8), n=1	kcal	41.4	Eq (7)
H″	ΔH_{2000} of Reaction (8), n=2	kcal	73.4	x=121.08; see footnote (e).
S′	ΔS°_{1600} of Reaction (8), n=1	eu	7.911	Eq (7)
S″	ΔS°_{2000} of Reaction (8), n=2	eu	16.41	Table 2 corrected to 2000 K
a;b	ΔC_p=a+bT:Reaction (8), n=1	ΔC_p in cal/mol-K	3.6;-0.0023	Eq (12)
x	Be-O bond energy at 1600 K	kcal/mol	119.08 (n=1); 121.08 (n=2)	
k'_i	Equil.const. of (3) at T_i	atm		The values are
k''_i	Equil.const. of (15) at T_i	atm		those corre-
k_i	$\equiv k'_i + 2k''_i$	atm		sponding to
K'_i	Equil.const. of (8)(n=1) at T_i	None		the other
K''_i	Equil.const. of (8)(n=2) at T_i	None		values in this
K_i	$\equiv K'_i + 2K''_i$	None		column.
T_1	Temperatures of	K	1700	
T_2	the 3 expts. detrmd.	K	2000	
T_3	from k_1, k_2, k_3	K	2300	

Footnotes to Table 5

(a) [17] gives 87.3 (±0.3) + 6.998-12.430 = 81.87; [21] gives 87.5 + 6.998-12.820 = 81.68 based on the weighted mean of several very recent investigations.

(b) For $S^\circ_{298.15}$ of Au(c): [17] gives 11.31 ±0.05 ; [18] give 11.319 ±0.059 based on the same data; G.T. Furukawa also has a carefully evaluated value (monograph).

(c) Mean of 51.5 ±2.2, 53.0 ±2.3, and 51.7 ±2.4 by various investigators [20].

(d) Ruamp (see [20]) gave 2.50; the value given is that preferred by [20], and the value of D adopted is consistent with this.

(e) The choice of a mean Be-O bond energy 2 kcal/mol greater for the dimer than for the monomer is arbitrary and probably has no substantial theoretical basis. This choice was made so as to involve a substantial ratio of dimer to monomer at T_3 (see Table 4) and so provide a reasonable chance of establishing that $K''_3 > 0$, within experimental error, in the hypothetical (computer) "experiments" of Section VI.

V. Equations for the Computer Calculations

Using the symbols and units given in Table 5, the numerical equations expressing the partial pressures of Au(g) and Au_2(g) (k_i' and k_i'' respectively) at T_i = 1600 - 2500 K are as follows:

$$\ell n\, k_i' = \frac{-503.228h + 10310.8 - 855.49C_\ell}{T_i} + \left(0.5702 - 0.50323C_\ell - \frac{1286.5}{T_i}\right) \ell nT_i$$

$$+ 3.6625(10^{-4})T_i + 20.7601 + 4.12518C_\ell - 0.503228\, S_\ell \qquad (16)$$

$$\ell nk_i'' = \frac{-1006.456h + 503.228D - 1710.98C_\ell + 20621.6}{T_i}$$

$$-\left(0.3596 + 1.00646C_\ell + \frac{2573}{T_i}\right) \ell nT_i + 7.325(10^{-4})\, T_i$$

$$-\ell n\,[1-\exp(-1.43879\omega/T_i)] + 37.6222 + 2\ell nr$$

$$+8.25036C_\ell - 1.00646\, S_\ell \qquad (17)$$

(These equations assume that the ground electronic states of Au and Au_2 have multiplicities of 2 and 1, respectively. There seems to be no reason by analogy to expect Au_2 to have any higher value.)

As stated earlier, the purpose of eqs (16) and (17) is to substitute an experimental value for k_i ($\equiv k_i' + 2k_i''$) and solve for the corresponding value of T_i. Rather than do so by iteration, a table of ℓnk_i vs. T_i was generated for T_i = 1600-2500 K in steps of ΔT_i = 20 K. Six additional tables (spot-checked by hand) were generated by varying h, C_ℓ, S_ℓ, D, ω, and r separately by small amounts from the values listed in Table 5, in order to test the sensitivity to the values of these parameters. (The numerical effects are shown in Section VI.)

The 20-kelvin spacing is fully adequate for 3-point interpolation. If the value of ℓnk_i is -A, -B, and -C at temperature T_o-20, T_o, and T_o + 20, respectively, and if -X is the value of ℓnk_i for which it is desired to

interpolate for T, this value of T is given by

$$T = T_o + \frac{A-C-\sqrt{(A-C)^2 - 8(B-X)\ (A-2B+C)}}{0.1(A-2B+C)} \quad . \tag{18}$$

Equations were set up for $K_i'(T_i)$ and $K_i''(T_i)$ using the symbols and units of Table 5. K_i' and K_i'' were then eliminated by introducing K_i as defined ($\equiv K_i' + 2K_i''$). From the three equations obtained by setting T_1, T_2, and T_3 for T_i, H′ and S′ were eliminated to give

$$T_1(T_3-T_2)\ (\theta_1 - \varphi_1) - T_2(T_3-T_1)(\theta_2-\varphi_2) + T_3(T_2-T_1)(\theta_3 - \varphi_3) = 0 \ , \tag{19}$$

where

$$\varphi_i \equiv \frac{805.165a + 6.4413(10^5)b}{T_i} + 0.50323\ a\ell nT_i + 0.25161bT_i$$

$$- 4.21593\ a - 805.165\ b \tag{20}$$

and

$$\theta_i \equiv \ell n[K_i - 2\ \exp\ (- \frac{503.23H''}{T_i} + 0.50323S'')] \ . \tag{21}$$

Using the values of T_1, T_2, and T_3 determined by k_1, k_2, and k_3 as described above, eq (19) can then be solved by iteration for H′′ or S′′ without knowledge of H′ and S′ but having measured K_1, K_2, and K_3.

Mathematically, H′′ and S′′ could be solved for separately by using a fourth temperature, but in view of the uncertainties in the data and parameters the more refined result would hardly be significant. While it is desired to find K_1'', K_2'' , and K_3'', the assumption of different values of S′′ (or H′′) when solving for H′′ (or S′′) must give somewhat different values for K_1'', K_2'', and K_3'', but least different for the largest and most important K_3'', as illustrated in the calculations of Section VI.

VI. Results and Discussion

Before showing the results of hypothetical computer "experiments" at (or near) 1700, 2000, and 2300 K, it will be of interest to calculate

the partial pressures of Au, Au_2, $BeO \cdot H_2O$, and $(BeO)_2H_2O$ at these temperatures, and from them the masses of Au and BeO condensed for weighing in the transpiration experiments. These results are given in Table 6.

Table 6

Approximate Magnitudes in Transpiration Measurements that Evaporate Both Au and BeO

T(K)	Au(mg/liter)	BeO(mg/liter)*	Apparent Vapor Pressure of Au(torr)
1700	0.027	0.046	0.015
2000	0.87	0.25	0.55
2300	10.7	0.92	7.8

*$H_2O(g)$ at 1 atm pressure

It seems likely that flow rates can be high enough (with virtual equilibrium) for as much as 100 liters of transpired gas per experiment to be practical. Table 6 then shows a possible problem, in weighing the BeO with considerable accuracy, only at 1700 K, and then possibly only if the receiver itself is BeO and therefore presents a large indistinguishable tare that would reduce the precision. If the gold is dissolved from its container (say, by aqua regia), large amounts could be recovered and weighed as the free metal. (Incidentally, a vapor pressure of 8 torr, as shown for 2300 K in Table 6, is well suited to the transpiration method.) As to small amounts, the NBS Analytical Chemistry Division has stated [22] that gold (in 6N HCℓ solution) can be determined by a colorimetric or fluorescent method to 1 or 2% accuracy if the total gold is 0.01 mg, or to about 1% routinely (and possibly to 0.5%, but probably not to 0.1%) if the total gold is as much as 1 mg. ("Known" standard solutions of gold are used.) (Radioactive methods of determining metallic gold in small amounts also are available, but have not been investigated by the author.)

Following the procedure outlined in Section V, a computer run was carried out which consisted of the iterative solution of eq (19) for H'' for 16 separate hypothetical "experiments," and the results are given in Tables 7 and 8. In each such experiment a different set of values of the

independent parameters in Table 5 was assumed. As indicated in Table 7, in the first experiment the parameters in the second column (which may be considered as the independent variables) were all assigned their "normal" values given in Table 5, and in each of the succeeding experiments the one parameter in the second column (except two parameters in the last experiment) was taken different from its "normal" value by the amount (in the units of Table 5) shown in the third column. The last four columns of Table 7 give the values of T_1, T_2, and T_3 corresponding to the values k_1, k_2, and k_3, respectively, as well as the value of H'' found to satisfy eq (19). (Altogether this involved setting up and evaluating the left-hand side of eq (19), using eqs (20) and (21), about 500 times, and required about one minute of UNIVAC 1108 computer time.) Note that the only parameters assumed to be measured in the transpiration experiments are k_1, k_2, k_3, K_1, K_2, and K_3; in these computer experiments these "experimental" values have been taken to be those indicated in Table 7.

Table 7

Results of Computer Experiments in Each of Which One Parameter is Assumed to be in Error by the Stated Amount (See also Table 8.)

Expt. No.	Parameter Varied	Variation from "normal"	T_1	T_2	T_3	H''
1	None	---	1700.000	2000.000	2300.000	73.4009
2	h	+1 kcal	1720.830	2024.851	2329.059	74.3237
3	C_ℓ	-1 cal mol^{-1} K^{-1}	1691.512	1987.525	2281.403	72.1899
4	S_ℓ	-0.3 eu	1689.447	1985.200	2280.107	72.6343
5	D	+3 kcal mol^{-1}	1699.740	1999.052	2297.594	73.0737
6	ω	-20 cm^{-1}	1699.980	1999.908	2299.711	73.3471
7	r	-0.2 Å	1700.026	2000.122	2300.379	73.4692
8	k_1	+1%	1700.698	2000.000	2300.000	73.7427
9	k_2	+1%	1700.000	2000.974	2300.000	72.6343
10	k_3	+1%	1700.000	2000.000	2301.296	73.9673
11	S''	+2 eu mol^{-1}	1700.000	2000.000	2300.000	78.6958
12	K_1	+1%	1700.000	2000.000	2300.000	72.7954
13	K_2	+1%	1700.000	2000.000	2300.000	75.3052
14	K_3	+1%	1700.000	2000.000	2300.000	72.4927
15	a	-1 cal mol^{-1} K^{-1}	1700.000	2000.000	2300.000	72.6147
16	a and b	(a = b = 0)	1700.000	2000.000	2300.000	74.3384

Table 8 presents the results of Table 7 in other forms. In Table 8 there are three blocks of three columns each. In the first block "δX" reproduces the respective variations of the third column of Table 7, and "δH" gives the variation of H'' (last column of Table 7) from the "normal" value (73.4 kcal). "δT_3" gives the variation of T_3 from the "normal" value (2300 K) which would produce the same variation in H'' (i.e., $\delta H''$) if T_1, T_2, and all other input parameters had their "normal" values, and was obtained by multiplying $\delta H''$ by the value of $\partial T_3/\partial H''$ (1.296/0.567) indicated by Experiment 10. The values of δX in the first block were chosen to be generous estimates of the present uncertainties in the various parameters. However, the δX values of the second block are more careful estimates of these uncertainties, and the δX values of the third block were roughly estimated as minimal uncertainties in the parameter values thought reasonably attainable by more accurate remeasurement of the individual parameters. The last two lines give the square root of the sum of the squares for each of several columns: The value on the first line is designed to measure the overall statistical uncertainty in measuring H'', and that on the second line reflects only the statistical uncertainty in H'' arising from measuring T_1, T_2, and T_3 by the "gold thermometer."

Table 8

Results of Computer Experiments in Each of Which one Parameter is Assumed to be in Error by the Stated Amount. (See also Table 7.)

Expt No.	Computer Run (Table 7)			Based on Present Est. Uncertainties			Based on Minimal Uncertainties Est., Easily Attainable		
	δX	$\delta H''$	δT_3	δX	$\delta H''$	δT_3	δX	$\delta H''$	δT_3
1	0	0	0	---	---	---	---	---	---
2	+1	+0.924	+2.112	0.5	0.46	1.06	0.5	0.46	1.06
3	-1	-1.210	-2.743	0.5	0.60	1.37	0.15	0.18	0.41
4	-0.3	-0.766	-1.751	0.15	0.38	0.88	0.1	0.25	0.59
5	+3	-0.326	-0.745	2.5	0.27	0.62	2.5	0.27	0.62
6	-20	-0.053	-0.121	10	0.03	0.06	10	0.03	0.06
7	-0.2	+0.069	+0.158	0.2	0.07	0.16	0.2	0.07	0.16
8	+1%	+0.343	+0.784	0.5%	0.17	0.39	0.5%	0.17	0.39
9	+1%	-0.766	-1.751	0.5%	0.38	0.88	0.1%	0.08	0.18
10	+1%	+0.567	+1.296	0.5%	0.28	0.65	0.1%	0.06	0.13
11	+2	+0.696*	+1.591*	2	0.70*	1.59*	2	0.70*	1.59*
12	+1%	-0.605	-1.383	2%	1.21	2.77	1%	0.60	1.38
13	+1%	+1.905	+4.354	0.4%	0.76	1.74	0.2%	0.38	0.87
14	+1%	-0.907	-2.073	0.1%	0.09	0.21	0.1%	0.09	0.21
15	-1	-0.785	-1.794	0.5	0.39	0.90	0.3	0.23	0.54
16	(a=b=0)	+1.338	+3.059	---	---	---	---	---	---
$\sqrt{\Sigma\delta^2}$		3.43	7.8		1.93	4.4		1.22	2.8
$\sqrt{\Sigma\delta^2}$	(expts. 2-10 only)	2.01	4.6		1.02	2.3		0.65	1.5

*For 2300 K only

The computed value for H'' for Experiment 1 (Table 7) is a check on the computer program, as the parameter values used should give 73.4. The program was required to interpolate between 65 and 85 (negative arguments of logarithms must be avoided to avoid spurious results and false solutions of functions being iterated!), and the finite spacing of the final iteration of this program can give an error in H'' as great as ±0.0024 kcal. (The value found for Experiment 1, 73.400879, was shown to be the exact value which the program should have selected in this case.)

In view of the independence of eq (6) of any assumed value of $\underline{h}$ (the heat of vaporization of gold), the result of Experiment 2 ($\delta H'' = 0.924$ kcal for $\delta h = 1$ kcal) was somewhat surprising. (The results for Experiments 2 and 8 were "hand-checked" by showing them to satisfy eq (19).) However, note from Table 7 the last four entries for Experiment 2: a 1 kcal error in $\underline{h}$ thus creates errors of from 21 to 29 K in T_1, T_2, and T_3, but the corresponding error in H'' is only about 0.9 kcal, and from Table 8 this is seen to be equivalent to an error of only 2 K in T_3 were T_1 and T_2 measured with no error. This is a dramatic illustration of the relative insensitivity of H'' to large errors in T_1, T_2, and T_3 if these errors are "properly" related by using this kind of "gold thermometer," as discussed in Section II.

The three sets of uncertainties in Table 8 were not arrived at very critically, and are subject to revision; furthermore, the assumption that they should be considered independent and without bias of sign is not strictly true. Nevertheless, the overall estimates of uncertainty in H'' in the penultimate line of the table are worth considering.

These values of 3.43, 1.93, and 1.22 correspond to errors in K_3'' by factors of 2.1, 1.5, and 1.3, respectively, and by somewhat larger factors at lower temperatures.

Of the values of H'' in Table 7, that for Experiment 11 differs from the "normal" value by what is by far the largest amount (5.296 kcal), but this is because of the abnormally large value of S'' assumed in this one experiment. This corresponds to a value of K_3'' lower by only 16%, corresponding to the first starred entry in Table 8.

The question arises as to how the error using this kind of "gold thermometer" compares with the error expected to arise if the three temperatures T_1, T_2, and T_3 are measured instead by a pyrometer [eq (19) can still be used to determine H'' or S'' if the other of these two is assumed]. The uncertainty in a temperature measured by pyrometer has been estimated as approximately $(T/1000)^2$ [23]. If the uncertainties in measuring 1700, 2000, and 2300 K are calculated in this way and then converted to the basis of δT_3 as defined in Table 8, the square root of the sum of the squares is 9.5 K, which is much larger than the corresponding values 4.6, 2.3, and 1.5 K in the last line of Table 8. However, this comparison is somewhat unfair to the pyrometric method, for these pyrometric errors probably reflect considerable systematic error that would tend to cause the errors in T_1, T_2, and T_3 to have the same sign and to cancel somewhat in the present application of determining H'' [or K'' (T)], as discussed above in the case of Experiment 2. I have not attempted to estimate the extent of this cancellation.

The conclusion of this feasibility study is that a "gold vapor-pressure comparison thermometer," used in the way described here, is probably superior to all except the most favorable pyrometric alternative. In a sense, this "gold thermometer" method transfers many of the measuring problems of the BeO-H_2O system to the more tractable gold system. It should be noted in this connection that the necessary parameters of gold (h, C_ℓ, S_ℓ, D, ω, and r) have so far been determined on the separate gold species, so that their uncertainties depend far less on temperature than the transpiration measurements proposed for the BeO-H_2O system. In fact, this is so markedly true that it is doubtful whether the NBS transpiration technique, despite its refinement, could do better by gross application to gold alone, where the different gold species would not be measured separately.

VII. Effect of Contaminants on the Apparent Vapor Pressure of Gold

The conditions under which the use of gold as described in Sections II - VI is valid were alluded to in Section II, and are considered in this section.

The original plan for monitoring by gold the temperatures of transpiring $H_2O(g)$ over BeO(c) was to pass the steam (pure or diluted) over liquid gold contained in a tube of solid beryllia, so that the temperature would surely be identical for the reaction of steam with the beryllia and for the evaporation of gold. It is clear that the thermodynamic activities of the liquid and gaseous phases of gold must be unchanged in the presence of the other substances if the stoichimetrically measured vapor-pressure, temperature relation for pure gold is to be valid here. The chemical inertness of gold with respect to forming new condensed-phase compounds of gold is well known, especially in the case of substances as thermodynamically stable as BeO(c) and H_2O, and the assumption that BeO(c) does not dissolve appreciably in Au(ℓ) at the temperatures in question seems reasonable. However, it was pointed out to me [23] that my initial tentative assumption that no appreciable proportion of gold in the gas phase would be present as gold compounds was a dangerous one and, in view of the high published dissociation energies of a few diatomic gold species (of the order of 3eV), very possibly an untenable one.

We shall take 1700, 2000, and 2300 K as representative temperatures at which to estimate the fraction of the gas-phase gold not present as Au(g) or $Au_2(g)$, these two species being accounted for in the treatment of the preceding sections. Since polyatomic species tend to be entropically unstable at high temperatures, consideration will be limited to the diatomic gaseous species of gold with the other elements present (AuO, AuH, AuC, and AuBe) except including AuOH. (The AuC is included because of the anticipation that the liquid gold will need to be isolated from the H_2O, but may possibly be containable in graphite; also, CO and CO_2 are common gaseous contaminants.) Furthermore, insofar as the dissociation energy of a molecule seems definitely uncertain, a value on the high side may be assumed. This bias may add some weight to the final conclusions that the gold may be in the presence of BeO(c),

graphite, or common gases at attainably low pressures, but definitely not in the presence of $H_2O(g)$ at a pressure of the order of 1 atm.

The calculation of the relative abundance of various species later in this Section is based on the thermodynamic properties listed in Table 9. For this purpose no distinction is made between D_0, the dissociation energy at 0 K and that at 298 K.

Table 9

Assumed Dissociation Energies and Free-Energy Functions for Various Species

Species & State	D_0(ev) Value	Source	$-(G^o-H^o_{298})/T$ (cal $mol^{-1}K^{-1}$) 1700K	2000K	2300K	Source
Au(c,ℓ)	3.8	See Table 5, Footnote a.			19.9	[27]
Au(g)	0	-	47.7	48.4	49.0	[17]
$Au_2(g)$	2.26	See Table 5.				-
$O_2(g)$	5.1	[4,26]	56.0		58.1	[4]
$H_2O(g)$	9.5	[4,26]	53.2	54.5	55.8	[4]
OH(g)	4.4	[4,26]	50.5	51.5	52.4	[4]
$H_2(g)$	4.5	[4,26]	37.6		39.6	[4]
$CO_2(g)$	16.5	[4,26]			64.5	[4]
CO(g)	11.1	[4,26]			56.0	[4]
AuH(g)	3.3	[26] gives 3.2 ± 0.1	57.1	58.1	59.1	Molecular constants from [28]
AuOH(g)	(7.8)	See discussion below	(74.7)	(76.0)	(77.2)	See discussion below
AuC(g)	(4.45)	" " "	(69.3)	(70.5)	(71.6)	" " "
AuO(g)	(3.5)	" " "	(67.6)	(68.8)	(69.9)	" " "
H(g)	0	-	31.9	32.6	33.2	[4]
O(g)	0	-	43.1	43.8	44.4	[4]
C(graphite)	7.4	[4,26]	4.8	5.5	6.1	[4]
AuBe(g)	(3.3)	[26] gives 2.9±0.4	(69.3)	(70.5)	(71.6)	Assumed same as for AuC(q.v.)
Be(c)	3.4	[4]				-
Be(g)	0	-	37.1	37.8	38.4	[4]
BeO(c)	12.2	[4]	12.1	13.7	15.1	[4]

1. The Dissociation Energies of AuC(g), AuO(g), and AuOH(g)

No experimental value for AuC is available, but 4.45 eV was estimated as an upper limit from those of C_2 and Au_2 (6.25±0.2 smf 2.30± 1 eV, respectively [26]; average, 4.3±0.3 eV). According to Pauling [12], the electronegativities of Au and C are nearly the same (2.4 and 2.5, respectively), a fact which would give a nearly additive dissociation energy for the heteronuclear diatomic molecule for closed shells, which is of course not the case here. (However, the carbide molecule PtC has been reported to have the surprisingly large value of 6.5± eV [26].)

It has been reported [29] that in the temperature range 1200° - 1400°C gold metal has a higher volatility in H_2 than in O_2, N_2, CO, or CO_2 [at the same pressure]. Using data from Table 9, this fact leads to $D_0(AuO) < 3.5$ eV. 3.5 eV has been chosen (as an upper limit).

Looking for trends among the dissociation energies of the monomeric gaseous fluorides, chlorides, and hydroxides of Li, Na, and K [4] and that of AuCl, 3.5 eV [26], it was concluded that D_0 of AuOH (to Au and OH) probably lies between 2.8 and 4.0 eV; the average, 3.4 eV, was assumed. The uncertainty in this value is, of course, very considerable.

(A recent paper [30] (containing many references to earlier works) may be consulted concerning the dissociation energies of many other diatomic molecules containing gold.)

2. The Fundamental Molecular Constants of the Ground States of AuC(g), AuO(g), and AuOH(g)

The general numerical equation for the Gibbs free-energy function (in cal $mol^{-1}K^{-1}$) of the ground electronic state of a diatomic molecule at T(K) is, in the rigid-rotor harmonic-oscillator approximation,

$$-(G^\circ - H^\circ_{298.15})/T = 4.5756 \log_{10} [g_e A_1 A_2 (A_1 + A_2)^{1/2} T^{7/2} r^2$$

$$-4.5756 \log_{10} \sigma (1-10^{-0.62486\omega/T}) +2.8591 \omega/T (10^{0.0020958\omega} - 1)$$

$$+2073.7/T - 13.6192 , \qquad (22)$$

where g_e is the statistical weight of the ground electronic state, A_1 and A_2

are the two atomic weights, r is the equilibrium internuclear distance in 10^{-8} cm, σ is the symmetry number, and ω is the vibrational fundamental in cm^{-1}.

The molecular constants assumed for the present purpose are as follows: AuC: g_e,4(??); ω, 250 cm^{-1}; r, 2.11 (being the sum of the single-bond radii of Au (see Table 5) and C [12]. AuO: g_e, 2(is 2 for AgO);ω,350 (ω = 493.2 for Ag_2O [28]; r, 2.00 (being the sum of the single-bond radii of Au(see Table 5) and O [12]). AuOH: g_e 1; ω: 300, 1300, and 3500; Au-O-H angle, 110°; Au-O distance, 1.99; O-H distance, 0.96 (hence $I_x I_y I_z$= 3055, in atomic-weight units and 10^{-8} cm).

3. Reactivity of Au(ℓ) with H_2O(g) at 1 Atm. Pressure

Using the foregoing thermodynamic values, the following partial pressures were calculated for the three representative temperatures of interest (Table 10).

Table 10.

Calculated Vapor Composition of Au(ℓ) - H_2O(g, 1atm). (The chemical symbol of the species is used for its partial pressure in atm.)

T (K)	Au	AuH	AuOH	H	OH	H_2O	$\frac{AuH + AuOH}{AuH + AuOH + Au}$
1700	1.9×10^{-5}	3.6×10^{-5}	1.7×10^{-6}	$2.6(10^{-5})$	$6.1(10^{-5})$	1	0.66
2000	7.2×10^{-4}	5.7×10^{-4}	4.5×10^{-5}	$4.0(10^{-4})$	$9.3(10^{-4})$	1	0.46
2300	1.0×10^{-2}	4.4×10^{-3}	4.8×10^{-4}	$2.9(10^{-3})$	$6.8(10^{-3})$	1	0.33

It is immediately concluded from the last column of Table 10 that the presence of H_2O(g) at any practical pressure enhances the volatility of the gold to such an extent as to make correction for gold species other than Au (and Au_2) uncertain and impractical. Hence the gold, if used to monitor the temperature in the manner proposed, must be contained in a separate tube which is dry but in close thermal contact with the tube in which the BeO-H_2O reactions occur.

4. Reactivity of Au(ℓ) with Graphite

The ratio of the partial pressure of AuC(g) to that of Au(g) was calculated to be 1.1×10^{-5} at 1700K, 2.0×10^{-4} at 2000K, and 1.7×10^{-3} at 2300K.

According to these figures, the gold could be evaporated by transpiration in a separate (presumably parallel) dry graphite tube without serious interference from the AuC(g) formed. However, these results are based on a purely estimated dissociation energy of AuC; if the dissociation energy were 1 eV greater, the effect would be serious.

A note of caution regarding the evaporation of liquid gold in graphite is to be found in the work of Ackerman, Stafford, and Drowart [31], who vaporized this metal from Knudsen effusion cells in the temperature range 1550-1780 K. Using graphite containers, the intensity of the gas species Au decreased steadily with time, and after such an experiment a ball of gold was found to be covered with a heavy layer of graphite, in contrast with the results of Rossman and Yarwood [32]. This lack of equilibrium of Ackerman et al. may have been associated with unnecessary temperature gradients; it is to be noted also that they had no flow of gas across the gold.

5. Reactivity of Au(ℓ) with BeO(c)

The vapor-phase partial pressures shown in Table 11 were calculated.

Table 11

Calculated Vapor Composition over Au(ℓ) - BeO(c). (The chemical symbol of the species is used for its partial pressure in atm.)

T (K)	AuBe	AuO	Be	O	Au	$\frac{AuBe+AuC}{AuBe+AuO+Au}$
1700	4×10^{-10}	3×10^{-10}	8×10^{-12}	8×10^{-11}	1.9×10^{-5}	4×10^{-5}
2000	1.9×10^{-7}	1.5×10^{-7}	3×10^{-9}	4×10^{-8}	7.2×10^{-4}	4.7×10^{-4}
2300	1.8×10^{-5}	1.4×10^{-5}	3×10^{-7}	4×10^{-6}	1.0×10^{-2}	3.2×10^{-3}

According to the last column of Table 11, gold in a dry tube of BeO could be transpired by an inert gas with less error up to 2300 K from Au-containing species arising from the BeO than from other sources.

6. Reactivity of Au(ℓ) with Common Gaseous Contaminants

The most serious effects can be shown to occur at the highest temperature used, so calculations have been limited to 2300 K. Table 12 lists several reactions involving equilibria between liquid gold and different common contaminating gases. At 2300 K the vapor pressure of pure gold is about 0.01 atm; in the table is given the partial pressure of the specified contaminating gas necessary to give a partial pressure of 0.3% of 0.01 atm. for the total Au-containing species other than Au and Au_2.

Table 12

Equilibria Between Au(ℓ) and Several Gases at 2300 K

Equilibrium	K_p (in atm)	If Σ AuX/Au = 0.003	
		Gas	Its pressure (atm)
$2\ Au(\ell) + O_2(g) = 2\ Au\ O(g)$	5.1×10^{-4}	O_2	1.8×10^{-6}
$2\ Au(\ell) + H_2(g) = 2\ Au\ H(g)$	3.0×10^{-4}	H_2	3.1×10^{-6}
$2\ Au(\ell) + H_2O(g) = AuH(g)+AuOH(g)$	5.6×10^{-5}	H_2O	4.0×10^{-6}
$Au(\ell) + CO_2(g) = AuO(g) + CO(g)$	4.0×10^{-4}	CO_2	2.2×10^{-6}
$2\ Au(\ell) + CO(g) = AuO(g) + AuC(g)$	3.0×10^{-14}	CO	8×10^{3}
$Au(\ell) + CO(g) = AuO(g) + C(graph)$	1.8×10^{-9}	CO	2×10^{4}
$2\ Au(\ell) + CO_2(g) = 2\ AuO(g)+ C(graph)$	6.8×10^{-13}	CO_2	1.3×10^{3}

According to the last column of Table 12, a partial pressure of O_2, H_2, H_2O, or CO_2 of about $2(10^{-6})$ atm will cause an enhanced evaporation of gold at 2300 K by 0.3%, and $2(10^{-5})$ atm will give a figure of 1%. According to Table 8, "Experiment 10," an uncorrected enhancement of 1% at 2300 K is equivalent to an error in measuring this temperature of only 1.3 K, and according to Section VI this error would be tolerable in combination with other existing errors. It is concluded, therefore, that the partial pressure of each of these four gases must be reduced to a level of about 2×10^{-5} atm. CO, on the other hand, appears to do no harm.

VIII. References

[1] L. I. Grossweiner and R. L. Seifert. J. Amer. Chem Soc. 74, 2701 (1952).

[2] W. A. Young, J. Phys. Chem. 64, 1003 (1960).

[3] W. I. Stuart and G. H. Price, J. Nucl. Materials 14, 417 (1964).

[4] JANAF Thermochemical Tables; Clearinghouse. U.S. Dept. of Commerce. Springfield, Va., 1965 (and addenda issued in later years).

[5] S. Abramowitz, NBS (private communication).

[6] N, Acquista, S. Abramowitz, and D. R. Lide, Jr., J. Chem. Phys. 49. 780 (1968), and later papers.

[7] J. L. Mack and G. B. Wilmot, CPIA Publication No. 173, Vol. I, p. 59, Aug. 1968 (Proceedings of the Sixth ICRPG Thermochemistry Working Group Meeting. Mar. 25-27, 1968).

[8] D. White, D. E. Mann, P. N. Walsh, and A. Sommer, J. Chem. Phys. 32, 488 (1960) (see p. 491).

[9] G. Herzberg, "Infrared and Raman Spectra," D. Van Nostrand Co., New York, 1945, p. 335.

[10] A. Snelson, CPIA Publication No. 54 U, p. 97, Aug. 1964 (Proceedings of the Second ICRPG Thermochemistry Working Group Meeting, June 3-4, 1964).

[11] D. White, K. S. Seshadri, D. F. Dever, D. E. Mann, and M. J. Linevsky, J. Chem. Phys. 39, 2463 (1963).

[12] L. Pauling, "The Nature of the Chemical Bond," 3rd edition, Cornell Univ. Press, Ithaca, N.Y., 1960, p. 93.

[13] T. B. Douglas, CPIA Publication No. 108, Volume I, p. 27, June 1966 (Proceedings of the Fourth ICRPG Thermochemistry Working Group Meeting, Mar. 16-18, 1966).

[14] J. Efimenko, NBS Report 8186, NBS, Washington, D. C., 1 Jan. 1964, p. 103.

[15] A. Camp (private communication to the author, Apr. 24, 1969).

[16] D. R. Stull and G. C. Sinke, "Thermodynamic Properties of the Elements," ACS Monograph 18, Amer. Chem. Soc., Washington, D.C., 1956, pp. 18,97,98.

[17] R. Hultgren, R. L. Orr, P. D. Anderson, and K. K. Kelley, "Selected Values of Thermodynamic Properties of Metals and Alloys," John Wiley and Sons, Inc., New York, 1963, pp. 38-42.

[18] J. W. Tester, R.C. Feber, and C. C. Herrick, J. Chem. & Eng. Data 13, 419 (1968).

[19] P. Schissel, J. Chem. Phys. 26, 1276 (1957).

[20] M. Ackerman, F. E. Stafford, and J. Drowart, J. Chem. Phys. 33, 1784 (1960).

[21] R. C. Paule, NBS (private communication. May 1969).

[22] R. W. Burke, NBS (private communication to the author, May 12, 1969).

[23] C. W. Beckett. NBS (private communication).

[24] R. F. Krause, Jr., and T. B. Douglas. J. Phys. Chem. 72. 475 (1968); ibid. 72, 3444 (1968).

[25] R. C. Paule and J. Mandel, NBS Special Publication 260-19, Washington, D. C., January 1970

[26] A. G. Gaydon, "Dissociation Energies and Spectra of Diatomic Molecules," Chapman and Hall. Ltd., London. 1968, 3rd edition. Chap. 12

[27] D. R. Stull and G. C. Sinke, "The Thermodynamic Properties of the Elements," ACS Monograph Series, Amer. Chem. Soc., Washington, D. C. 1956.

[28] G. Herzberg, "Molecular Spectra and Molecular Structure: I. Diatomic Molecules," Prentice-Hall, Inc., New York, 2nd edition, 1950.

[29] G. N. Lewis. M. Randall, K. E. Pitzer, and L. Brewer, "Thermodynamics," McGraw-Hill Book Co., New York, 2nd edition, 1960. p. 548, Problem 33-10.

[30] K. A. Gingerich and H. C. Finkbeiner, J.Chem. Phys. 52, 2956 (1970).

[31] M. Ackerman, F. E. Stafford, and J. Drowart. J. Chem. Phys. 33, 1784 (1960)

[32] M. G. Rossman and J. Yarwood, Brit. J.Appl. Phys. 5, 7 (1954).

Chapter 11

REVIEW OF THE CHEMICAL THERMODYNAMIC PROPERTIES OF SELECTED HALIDES AND OXY-HALIDES OF NIOBIUM

K. L. Churney

A. Introduction

During the course of revision of the thermodynamic properties listed in NBS Circular 500, Series I, for the element niobium, it became apparent that a careful study of the halides and oxy-halides of niobium would yield useful suggestions about the interrelations of thermodynamic properties of the lower fluorides and oxy-fluorides of molybdenum. In the latter case, relatively little is known. In the case of niobium more is known; for the chlorides, at least, considerable information is available. The analogous behavior of the lower halides of niobium, tantalum, molybdenum, tungsten, and rhenium has already been noted [1].

In the following section, data is evaluated for NbF_5, niobium chlorides and oxy-chlorides, and $NbBr_5$. Use has been made of the heat of formation selected for Nb_2O_5(s) of $\Delta Hf° = -454.0 \pm 1$ kcal/mol, the Nb_2O_5 low temperature heat capacity measurements of King [2] and the high temperature heat contents of Orr [3]. Thermodynamic values for Nb(s) are taken from Hultgren [4] and for other elements (or compounds not containing niobium) from Wagman et al. [5] or the JANAF Thermochemical Tables [6].

Organization of the material in section B is as follows:

- 1a: low temperature heat capacity measurements
- 1b: high temperature heat capacities or enthalpy increment measurements
- 1c: vapor pressure measurements, structures, etc.
- 2: enthalpy of formation measurements
- 3: discussion of selection of thermodynamic values.

Omission of a section indicates no measurements have been reported to our knowledge.

B. Thermodynamics

NbF_5

1a,b. Brady, Myers, and Claus [7] have measured the heat capacity of NbF_5(s) from 50 to 320 K and H(T)-H(298.15) from 350.7 K (triple point) to 550 K. Using an extrapolation to 0 K involving a Debye function of 6 degrees of freedom (θ_D=170 K) and an Einstein function of 8 degrees of freedom (ν=247 cm^{-1}) gives the value of $S°(298) = 38.3 \pm 2$ e.u., $H°(298)-H°_0$ of 5.704 kcal/mol. $Cp°(298,solid)$ was taken to be 32.2 cal/mol-K and ΔH_{fusion}(350.7 K) 2.920 ± .015 kcal/mol.

lc. Vapor pressure measurements have been reported by Ruff and Schiller [8] (458-590 K) Junkins et al. [9] (390-623 K), and Fairbrother and Frith [10] (341-505 K). The vapor pressures determined by Ruff and Schiller are higher than those of the other investigators. This might be caused by hydrolysis of NbF_5 (see [10](or the observed reaction of $NbF_5(g)$ with the oil in the manometer of Ruff and Schiller. The triple points determined by the latter two investigators, 352.1 ± 0.2 K [9] and 353.2 K [10], agree reasonably well with those determined by Brady et al. [7] but the enthalpy of fusion determined by Junkins et al. [9] (8.6 ± 0.5 kcal) does not.

Electron diffraction studies of $NbF_5(g)$ by Romanov and Spiridanov [11] show that at low temperatures (~ 300 K), the vapor consists of tetramers. This is essentially the structure found for $NbF_5(s)$ by Edwards [12a] and is similar to that found for $MoF_5(s)$. At higher temperatures (~ 560 K) Romanov and Spiridanov [11] find the vapor consists of essentially monomers made up of trigonal bypyramids with a mean Nb-F distance of 1.88 ± .02 A°. The high viscosity of $NbF_5(\ell)$ [12b] indicates appreciable association in the liquid phase.

Raman and infrared studies of $NbF_5(\ell)$ and $NbF_5(s)$ have been reported by Blanchard [13], Selig et al. [14], Beattie et al. [15], and are discussed by Oulette et al. [16]. Calculation of the thermal functions of $NbF_5(g)$ based on the vibrational frequency assignment of Oulette et al. [16]* (D_{3h}) and moments of inertia using a Nb-F distance of 1.88 A° (11) gives values of S°, Cp°, and $H°-H_0^\circ$ at 298.15 K for $NbF_5(g)$ monomer of 76.9 e.u., 23.2 cal/mol-K, and 4.487 kcal respectively. Use of these thermal functions and the thermal functions of Brady et al. [7] for $NbCl_5(s)$ yields values of ΔH_0° (sublimation) with the vapor pressure data of Fairbrother and Frith [10] of 18.92 ± .28 kcal/mol. The corresponding value obtained from the equation** given by Junkins and Farrar over the temperature interval 457-505 K is 18.92 ± .11 kcal/mol. A second law fit of the vapor pressure data of Fairbrother and Frith using a value of -9.3 cal/mol-K for ΔCp gives $\Delta H_{subl}(445.6)$ of 12.61 ± .23 kcal/mol and $\Delta S_{subl}(445.6)$ of 24.8 ± 1.0 e.u. A comparison of the second and third law calculations is given below:

		$\Delta H_{subl}(298.15)$	$\Delta S_{subl}(298.15)$
Second Law	(Fairbrother & Frith)	16.94 ± 0.23 kcal/mol	37.0 ± 1 e.u.
Third Law	(Fairbrother & Frith)	17.68 ± 0.28*	38.7 ± 2 e.u.
	(Junkins, Farrar)	17.68 ± 0.11*	38.7 ± 2 e.u.

---

*ν_8 is estimated to be 400 ± 50 cm^{-1}. An uncertainty of 0.1 kcal was added to ΔH_0°.

**$\ln P_{mm} = 51.3101 - 8716/T - 4.41 \ln T$.

2. The heat of formation of $NbF_5(s)$ at 298.15 K has been determined by direct reaction of $F_2(g)$ with Nb(s) by Greenberg, Natke, and Hubbard [17], to be -433.50 ± 0.2 kcal/mol. A less accurate value was determined by Meyers and Brady [18] from heats of solution of $NbF_5(s)$ and estimates of the enthalpy of the formation of the products by 3 different reactions (-439 ± 8, -423 ± 10 and -435 kcal/mol).

3. We select for $\Delta Hf°$ ($NbF_5(s)$, 298) the value of Greenberg et al. [17], -433.5 ± 0.2 kcal/mol, and for Cp°, S° and $H°-H_0^\circ$ at 298.15 those values obtained from the work of Brady et al. [7]. The small discrepancy between the second and third law vapor pressure calculations appears to be due to the extrapolation of the low temperature heat capacity from 50 K to 0 K. (S°(50 K) - S°(0 K) = 4.27 e.u.). We select $\Delta H^\circ_{sub1}(298.15)$ to be 17.68 ± .28 kcal/mol to yield $\Delta Hf°$ for $NbF_5(g)$ at 298.15 of -415.8 ± .4 kcal/mol.

$NbCl_5$

1b. The only values of H°(T)-H°(298.15) were determined by drop calorimetry by Kenshea et al. [19] from 298.15 K to 600 K; saturation enthalpies (i.e., no value was available for T(dV/dT)p) were determined from 600 to 804 K. An 0.02% oxygen impurity in the sample, presumably present as $NbOCl_3$, was removed by sublimation of $NbCl_5(s)$, 99.95% free of metals, in a stream of He saturated with $SOCl_2(g)$. Samples were sealed in quartz ampoules.

1c. Vapor pressure measurements have been reported by the following workers and are summarized according to the temperature range and method of measurements: Opykhtina and Fleischer [20], 373-514 K, transpiration; Tarasenkov and Komandin [21], 296-506 K, static, 504-520 K boiling point; Alexander and Fairbrother [22], 403-528 K, static; Ainscough et al. [23], 516-528 K, boiling point, t'Hart and Meyer [24], 544-715 K, static; Nisil'son et al. [25]; and Johnson et al. [26], 504-800 K, boiling point.

Numerous determinations of the triple point of $NbCl_5$ have been made in conjunction with various types of studies and are summarized below:

Investigator	Triple Point (K)	Method
Kenshea et al. [19], 1968	478.9 ± 0.5	visual
Opykhtina et al. [20], 1937	~ 485	vapor pressure
Tarasenkov et al. [21], 1940	~ 488	vapor pressure, visual
Alexander et al. [22], 1949	482.7 ± 0.5	vapor pressure, melting point
Ainscough et al. [23], 1957	476.6 ± 0.2	vapor pressure, melting point
Nisil'son et al. [25], 1965	477.7	melting point (phase study of $NbCl_5$-$AlCl_3$)
Meyer et al. [27], 1961	480.0 ± 0.3	melting point (phase study of $NbCl_5$-$NbOCl_3$)
Schäfer et al. [28], 1951	477.9 ± 0.2	melting point (phase study of $NbCl_5$-$TaCl_5$)
Schäfer et al. [29], 1952 Schäfer et al. [30], 1960	477.9 ± 0.2	Reanalysis of vapor pressure data [20-23] and from [28]
Palkin et al. [31], 1959	479.2	melting point (phase study of $NbCl_5$-KCl)
Nisil'son et al. [32], 1958	477.7	melting point (phase study of $NbCl_5$-$TiCl_4$)
Sheka et al. [33], 1959	477.7	melting point (phase study of $NbCl_5$-$POCl_3$)
Johnson et al. [34], 1970	478.5 ± 1.5 K	dilatometry
Nisil'son et al. [35], 1964	477.4 (± 1.5 K)	dilatometry

The differences in the various determinations in triple points can be explained in part by varying amounts of impurities, principally $NbOCl_3$, present in $NbCl_5$. Complete removal of $NbOCl_3$ from $NbCl_5$ cannot be accomplished by sublimation or distillation [27] but only by distillation in $SO\ Cl_2$ [19,28,30] which causes the conversion of $NbOCl_3$ to $NbCl_5$.

On this basis, the samples used by Kenshea et al. [19], the same as that used by Johnson et al. [26,34], and Schäfer et al. [28] are presumed to contain less $NbOCl_3$ than that used in earlier experimental work. The triple point is taken to be 478.9 K.

According to the work of Meyer et al. [27], $NbOCl_3$ forms a eutectic with $NbCl_5$ at 5.6 ± 0.2 mol % $NbOCl_3$ and 476.5 ± 0.1 K. The upper bound (by extrapolation from 3.5 mole % $NbOCl_3$*) of the triple point of $NbCl_5$ assuming ideal solutions, was calculated to be 480 K. For $NbOCl_3$ concentrations larger than 5.6 mole % the liquidus curve rises steeply. The melting points of $NbCl_5$ containing 1.8 to 3.6 mole % $NbOCl_3$ made by t'Hart and Meyer [24] fall on the liquidus curve proposed by Meyer, Oosterom, and Van Oeveren [27]. t'Hart and Meyer found the melting point at 1.8 mole % $NbOCl_3$ to be 478.9 ± 0.2 K. Because this implies that the triple point of $NbCl_5$ is greater than 478.9 K we have increased the uncertainty for the triple point of ± 0.5 K given by Kenshea et al. [19] to ± 1 K. This uncertainty brackets the more recent determinations.

The vapor pressure of $NbCl_5(\ell)$ as calculated by the equation given by Johnson et al. [26], Peq,** was compared with the relevant measured pressures, Pobsv, of other workers. The results are discussed in terms of ΔP (i.e., Peq-Pobsv), Δ1nP (i.e. 1nPeq-1n Pobsv), and S (i.e. $[\Sigma(\ln Peq - \ln Pobsv)^2/N]^{1/2}$ where N is the number of Pobsv).

Investigator	Comments***
Opykhtina et al. [20]	From 474-514 K, ΔP and Δ1nP are negative, except for lowest point. ΔP varies from -.05 to -.13, S = .16.
Tarasenkov et al. [21 static method	From 490-506 K, ΔP and Δ1nP are negative, except for lowest point. ΔP is about constant and equal to -2.5×10^{-2}. S = 5×10^{-2}.
boiling point	From 504-509 K, ΔP (and Δ1nP) are negative; 512-517 K, ΔP is positive; 518-520 K ΔP is negative. S = 3×10^{-2}.
Alexander et al. [22]	From 483-528 K, Δ1nP is about constant and equals + 0.17. S = 0.17.
Ainscough et al. [23] (equation)	From 516-528 K, ΔP is about constant and equals 1.5×10^{-2}. S = 1.5×10^{-2}. Based on 14 points calculated from their equation.

*Assuming a heat of fusion of 8.3 ± 0.4 kcal.

**Peq: $\log_{10} P(atm) = 6.11621 - \frac{5.42391 \times 10^3}{T} + \frac{2.10052 \times 10^6}{T^2} - \frac{0.48558 \times 10^9}{T^3}$

***Pressures are expressed in atmospheres.

Investigator	Comments
t'Hart et al. [24]	Measurements were made on samples 1-3 containing 1.8, 2.9, and 3.6 mole % $NbOCl_3$, respectively. No significant differences in vapor pressures between samples was noted. From 544 K to 713 K, $\Delta \ln P$ is positive and equals about 2×10^{-2}. Above 680 K $\Delta \ln P$ increases to $+ 3$ to 4×10^{-2}. $S = 2.4 \times 10^{-2}$, 2.9×10^{-2} for samples 1-3, respectively.
Kenshea et al. [19] (see eq. in ref [26]	Equation derived in Σ' plot analysis. From 475-600 K $\Delta \ln P$ increases from -4×10^{-2} to $+ 3 \times 10^{-2}$. $S = 2 \times 10^{-2}$.
Johnson et al. [26]	Data used to derive equation. From 500-800 K, no systematic difference in $\Delta \ln P$ if found. $S = 7 \times 10^{-3}$.

The vapor pressures of Opykhtina et al. are, on the average 16% higher while those of Alexander et al. are 17% lower than those of Johnson et al. In neither case is the reason for this discrepancy evident.* Except for the static measurements of Tarasenkov, which are some .025 atm higher than those of Johnson et al., all the vapor pressures are lower than those of Johnson et al. which is in agreement with the idea that the sample used by Johnson et al. had less impurity. The equation used in the Σ' plot analysis by Kenshea et al., which is based on their analysis of the vapor pressure measurement of all the other workers [20-24,26] differs by a small but significant amount from that given by Johnson et al. [26].

Alexander et al. [22] reported a transition point of $NbCl_5(s)$ at 456 K based upon both visual observations and a "break" in the vapor pressure curve at this temperature. The analysis of the vapor pressure curves of Opykhtina et al. [20], Tarasenkov et al. [21], and Alexander et al. [22] made by Schäfer et al. [28] did not support the existence of a "break" in the vapor pressure curve. Neither Ainscough et al. [23] or Kenshea et al. [19] found evidence for the transition. We assume that no transition occurs at this temperature.

---

*In the case of Alexander et al., the presence of $NbOCl_3$ would not account for the discrepancy, since their vapor pressures are lower than those determined for the $NbOCl_3(s)$, liquid ($NbCl_5$, $NbOCl_3$), gas equilibrium at the same temperatures by Meyer et al. [27].

A Σ' analysis carried out by Kenshea et al. [19] using the various vapor pressure measurements up to 600 K yielded $H°(gas) - H°(solid) = 22.41 \pm .06$ kcal and $S°(gas) - S°(solid) = 45.40 \pm 0.11$ e.u. at 298.15 K. From the former they calculated $S°(s) = 45.4$ e.u. which appears to be low. The gases were assumed to be ideal and the work of Opykhtina et al. [20] and Alexander et al. [22] were not used. The free energy functions for the gas were those derived by Nagajarin [36] based on the vibrational frequency assignment of Gaunt et al. [37].

The assignment of Gaunt et al., as well as Carlson et al. [38]*, are based upon the interpretation of the observed Raman and infrared absorptions in solid $NbCl_5$ and $NbCl_5$ dissolved in CCl_4 and CS_2 in terms of monomeric $NbCl_5$ with D_{3h} symmetry established by electron diffraction D_{3h} [40] for $NbCl_5(g)$. Actually single crystal X-ray diffraction of solid $NbCl_5$ [41] shows the presence of dimers consisting of distorted octahedra sharing a common edge. Further, there is evidence to support the presence of dimeric $NbCl_5$ in organic solvents [42,43] and liquid $NbCl_5$ [34]. The density of $NbCl_5(g)$ along the saturation curve [34,35] is consistent with the presence of monomeric $NbCl_5$ [26]. Recently, Werder et al. [44] have repeated the Raman and infrared spectroscopy on $NbCl_5(s)$, $NbCl_5$ dissolved in organic solvents, and on $NbCl_5$ in low temperature matrices. Vibrational assignments have been made for both monomer and dimer of $NbCl_5$; those of the monomer differ considerably from previous assignments. (see also [45,46])

Corrections were applied to the Σ' analysis Kenshea et al. [19] for the difference in free energy functions based on the work of Werder et al [44] and gas imperfection corrections (and also that due to the volume of the solid phase) using the data of Johnson et al. [26,34]. Due to the fact that the bulk of the accurate vapor pressure data is for liquid $NbCl_5$, the Σ' analysis was also corrected for the difference up to 600 K between the vapor pressure equation used by Kenshea et al. [19] (cited in [26]) for the liquid from that given by Johnson et al. [26]. This yields the following results:

	Kenshea et al. [19]	Corrected Results
$H°(gas)-H°(solid)$	22.41 ± .06 kcal/mol	23.1 (± .2)** kcal/mol
$S°(gas)-S°(solid)$	45.40 ± .11 e.u.	46.9 (± .3) e.u./mol

One obtains an entropy for $NbCl_5(s)$ of 48.6 or 50.3 e.u. which are closer to the Latimer estimate given by Kenshea et al. [19].

---

*Krynauw et al. [39] give thermodynamic functions based on Carlson's assignment.

**We assume the uncertainties are essentially triple those given by Kenshea et al. [19].

2. Heats of formation at 298.15 K of $NbCl_5(s)$ have been determined by reaction of liquid chlorine with niobium metal by Gross et al. [47], by solution of niobium metal and $NbCl_5(s)$ in HF(aq) by Schäfer et al. [30], by solution of $NbCl_5(s)$ and $Nb_2O_5(s)$ in $H_2O(\ell)$ by Shchukarev et al. [48]. The heat of formation of $NbCl_5(g)$ at 680 K has been determined by Retznitskii [49] by reaction of niobium metal with $Cl_2(g)$. The results of Schäfer et al. and Shchukarev et al. were recalculated to conform to the accepted heat of formation of HCl (aq) [5] and in the case of Schäfer et al. the heats of dilution of HF(aq) [5]. The results of Shchukarev were corrected for the heat of formation of $Nb_2O_5(s)$ given in section A. The results of Retznitskii are corrected to 298.15 K using the thermal functions of Werder et al. [44] for $NbCl_5(g)$, of Stull et al. [6] for $Cl_2(g)$ and Hultgren et al. [4] for Nb(s). Calculation of $NbCl_5(s)$ is made using $H°(gas) - H°(solid)$ given by Kenshea et al. [19] and the corrected values given in the previous section. The results are summarized below:

		$\Delta Hf°$, $NbCl_5(s)$, kcal/mol	
Investigator	Reactions used	Cited	Recalculated
Gross et al. [47]	$Nb(s)+\frac{5}{2}Cl_2(\ell)\rightarrow NbCl_5(s)$	-190.6±0.3	-190.6±0.4
Schäfer et al. [30]	$Nb(s), NbCl_5(s)+HF(aq)$	-190.5±1.2	-190.3±1.6
Shchukarev et al. [48]	$NbCl_5(s), Nb_2O_5(s)+H_2O(\ell)$	-193.7±0.7	-192.9±1.7
			kcal/mol
Retznitskii [49]	$Nb(s)+\frac{5}{2}Cl_2(g)\rightarrow NbCl_5(g)$	$\Delta Hf°(680)$	= -169.1±1
		$\Delta Hf°(298.15)$	= -168.02±1
	$Nb(s)+\frac{5}{2}Cl_2(g)\rightarrow NbCl_5(s)$	$\Delta Hf°(298.15)$	= -190.4±1.1[a]
		$\Delta Hf°(298.15)$	= -191.1±1.1[b]

[a] calculated using $\Delta H°_{subl.}$ (298.15 K) given by Kenshea et al. [19].

[b] calculated using $\Delta H°_{subl.}$ (298.15 K) given in previous section.

1b. Addition: After the analysis summarized in section 1b. was completed, the vapor pressure measurements of solid $NbCl_5(s)$ by Schäfer and Pölert [51] were brought to our attention. Their analysis, which includes other measurements of the vapor pressure of $NbCl_5(s)$, yields H°(gas)-H°(solid) of 22.9 ± 0.6* kcal and S°(gas) - S°(solid) of 46.3 ± 1.0* e.u.

3. We select $\Delta Hf°$ ($NbCl_5(s)$, 298.15 K) = -190.6 ± 0.4 kcal/mol based on the work of Gross et al. [47]. The close agreement of the work of Schäfer et al. [30] supports this choice well within their uncertainty limits. The lower bound of the value given by Shchukarev et al. almost agrees with this selection provided one uses the expanded uncertainty limit for their value we have assigned. We feel that the uncertainties in the changes in states (as published) measured by Shchukarev et al. [48] do not warrant giving much weight to this otherwise careful experiment. Use of this selected heat of formation for $NbCl_5(s)$ plus $\Delta H°_{subl}$(298.15 K) derived either from Kenshea et al. [19] or our correction of their value gives -168.2 ± 0.5 or -168.9 ± 0.5 kcal/mol, respectively, for the heat of formation of $NbCl_5(g)$ at 298.15 K. Both agree well with the value obtained by Retznitskii [49] within the combined uncertainty limits as well with each other. Pending a complete reevaluation of the Σ' analysis given by Kenshea et al. (which now seems warranted because of the measurements on $NbCl_5(s)$ made by Schäfer and Pölert [51]), we select $\Delta Hf°(NbCl_5(g), 298.15)$ = -168.2 ± 0.5 kcal/mol. The values of $H°(298.15) - H°_0$, S°, and Cp° are taken to be 6.37 kcal/mol, 95.7 e.u., and 28.9 cal/mol-K for $NbCl_5(g)$ based on the thermodynamic functions given by Werder et al. [44]. The heat capacity of $NbCl_5(s)$ at 298.15 K is taken from Kenshea et al. [19] and the entropy of $NbCl_5(s)$, based on S°(gas) - S°(solid) = 45.4 ± 0.22 e.u. and the entropy of $NbCl_5(g)$, is selected to be 50.3 ± 0.3 e.u.

$NbCl_4$

1c. Vapor pressure measurements of $NbCl_4(s)$ have been made by Schäfer and Bayer [52] at four temperatures (577-647 K). $NbCl_4(s)$ was made by reacting excess $NbCl_5(g)$ with Nb(s); the unreacted $NbCl_5(g)$ was sufficient to prevent the decomposition of $NbCl_4(s)$ into "$NbCl_3(s)$" and $NbCl_5(g)$ (see below).

*Average deviation using various authors' measurements.

The presence of $NbCl_4$ was established by the fact that the vapor contents of the vessel dissolved in 2NHCl to give a deep blue color (see [53]). It was assumed the $NbCl_4(g)$ was monomeric and that $NbCl_4(s)$ is insoluble in $NbCl_5(\ell)$. The authors fit the results with the equation

$$\log_{10} P(\text{mm Hg}) = 12.30 - 6.87 \times 10^3/T$$

We obtained by least squares* the following:

$$\log_{10} P(\text{mm Hg}) = 11.9 \pm 1.3 - (6.64 \pm 0.8) \times 10^3/T$$

Thus, at 614 K (the centroid of the measurements) we obtain

$$\Delta H^\circ_{vap} = 30.4 \pm 7.5^{**} \text{kcal/mol at 614 K}$$

$$\Delta S^\circ_{vap} = 41.3 \pm 6 \text{ e.u. at 614 K.}$$

Using the estimate of Schäfer and Kahlenberg [53] of the heat capacity of $NbCl_4(s)$,*** $NbCl_4(g)$, one obtains

$$\Delta H^\circ_{vap}(298.15) = 32.2 \pm 7.5 \text{ kcal/mol}$$

$$\Delta S^\circ_{vap}(298.15) = 45.1 \pm 6 \text{ e.u.}$$

The structure of $NbCl_4(s)$ has been studied by McCarley et al. [54,55], Schäfer et al. [56], Schnering et al. [57] and Frére [58]. Discussions of the structure [59,1] indicate that it is similar to the CdI_2 structure with Nb atoms inserted into the octahedral interstices of hexogonal close-packed chlorine atoms. Metal to metal bonding occurs between alternate pairs of Nb atoms to give strings of atoms with a repeat unit of Nb_2Cl_8.

---

*We assumed the error in P is proportional to P and the weights are inversely proportional to the square of the percent error in P given by the authors; results are in terms of standard deviations.

**Twice the standard deviation.

***The former was equated with Cp for $ZrCl_4(s)$, the latter by estimation from $SiCl_4$, $TiCl_4$.

2. Schäfer and Kahlenberg [53] determined a value of -24.5 ± 0.6 kcal/mol for the enthalpy change at 298.15 K for the reaction

$$NbCl_4(s) + \frac{1}{2} Cl_2(g) = NbCl_5(s)$$

by dissolving $NbCl_5(s)$ and $NbCl_4(s)$ in HF(aq) solutions. Using the value selected for $\Delta Hf°$ of $NbCl_5$, one obtains for $\Delta Hf°$ $NbCl_4(s)$ = -166.0 ± 1.0 kcal/mol. Ainscough, Holt, and Trowse [60] have studied the reaction of Nb(s) with mixtures of $H_2(g)$ and HCl(g) at 1073 and 1173 K. The products of the reaction, either $NbCl_4(g)$ or $NbCl_5(g)$, were not identified experimentally. Apriori estimates of the equilibrium of $NbCl_4(g)$ with Nb(s) and $NbCl_5(g)$ suggests that at these temperatures the predominant species is $NbCl_4(g)$ (about 96%). Use of an estimate of the entropy of $NbCl_4(g)$ at 1000 K was also in agreement with the idea that the only important reaction is:

$$Nb(s) + 4HCl(g) \rightarrow NbCl_4(g) + \frac{1}{2} H_2(g)$$

From their data we calculate that at 1121 K $\Delta Hf°$ ($NbCl_4(g)$) equals -129.3 ± 8 kcal/mol using a value of $\Delta S°$ derived from their data of -27.8 ± 8 e.u. or $\Delta Hf°$ = -136.3 ± 5 kcal/mol using an estimate of $\Delta S°$ of -34.1 ± 5 e.u. based on S° for HCl(g) [6], $H_2(g)$ [6], Nb(s) [4], and the calculated S° for $NbCl_4(g)$ using vibrational frequency estimates of Ainscough et al. [60]. These yield values of $\Delta Hf°$ $NbCl_4(g)$ at 298.15 K of -127.6 ± 8 kcal/mol and -135.6 ± 5 kcal/mol, respectively. From the previous heat of formation and vaporization of $NbCl_4(s)$ one obtains the value -137.4 ± 8 kcal/mol for the heat of formation of $NbCl_4(g)$.

3. We take for $\Delta Hf°$ ($NbCl_4(s)$, 298.15 K) the value of -166.0 ± 1 kcal/mol and for $\Delta Hf°$ $NbCl_4(g)$, 298.15 K) the value of -133.8 ± 8 kcal/mol. The entropy and heat capacity of $NbCl_4(g)$ are based on the estimates of the vibrational frequencies given by Ainscough et al. [60] and are taken to be $S°_{NbCl_4(g)}$ = 86 ± 3 e.u. and Cp° = 23.1 ± 2 cal/mol-K. An estimate of $S_{NbCl_4(s)}$ can be obtained from the above with the entropy of vaporization of 41 ± 5 e.u. The latter appears to be a bit low ; the estimate of S° = 44 e.u. given by Schäfer and Kahlenberg [30] seems more reasonable. 44 ± 3 e.u. is estimated for S° of $NbCl_4(s)$. Cp° is estimated to be 28.6 ± 1 cal/mol-K by analogy with $ZrCl_4(s)$ (suggested by Schäfer and Kahlenberg [30].

$NbCl_3$

1c. Schäfer and Dohman [61] have investigated the decomposition of $NbCl_4(s)$ into $NbCl_5(g)$ and "$NbCl_3$" and established that $NbCl_3$ consists of a single phase whose composition varies from $NbCl_{3.13}$ to $NbCl_{2.67}$. A single crystal X-ray examination of $Nb_3Cl_8(s)$ ($NbCl_{2.67}$) by Schnering,

Wöhrle, and Schäfer [62] shows that it forms a CdI_2-type layer lattice with the Cl atoms hexagonally close - packed and sufficient Nb atoms to occupy 3/4 of the octahedral interstices. The resulting structure forms trigonal clusters of Nb atoms having a structure similar to that of $Zn_2M_3O_8$ [57,59,63a]. The composition variation from Nb/Cl = 1:2.67 to 1:3.13 may be regarded as a solid solution of $NbCl_4$ and Nb_3Cl_8 in which Nb_3 triplets of the Nb_3Cl_8 structure are statistically replaced by the Nb-Nb pairs of Nb_2Cl_8 [63b]. The phase region between $NbCl_{3.13}$ and $NbCl_4$ is regarded as heterogeneous [59].

Schäfer and Liedmeier [64] have determined the enthalpy of reaction at 298.15 K by solution calorimetry of

$$\frac{1}{3}\ Nb_3Cl_8(s) + \frac{7}{6}\ Cl_2 \rightarrow NbCl_5(s)$$

for which they obtain -62.37 ± 0.36 and -61.60 ± 0.56 kcal/mol for two different samples of $Nb_3Cl_8(s)$. They adopt the value of -61.9 ± 0.6 kcal/mol on the basis that the second value (-61.60) was for a more crystalline sample than the first. Using the value for the heat of formation of $NbCl_5(s)$ (-190.6 ± 0.4 kcal/mol) one obtains $\Delta Hf°$ $Nb_3Cl_8(s)$ = -128.6 ± 1.0 kcal/mol. Schäfer and Liedmeier [64] also determined the enthalpy of reaction for

$$NbCl_{3.18}(s) + 0.91\ Cl_2(g) \rightarrow NbCl_5(s)$$

of -44.63 ± 1.1 kcal/mol which gives $\Delta Hf°$ = -146.0 ± 1.5 kcal/mol for $NbCl_{3.18}$ (they quote -145.9 kcal/mol based on -190.5 kcal/mol for $\Delta Hf°$ of $NbCl_5(s)$). Assuming that the compound they dissolved in acid was 0.9425 $NbCl_{3.13}$ + .0575 $NbCl_4$ one obtains the heat of formation of $NbCl_{3.13}$ of -144.7 ± 1.5 kcal/mol. Linear interpolation between the heats of formation $NbCl_{2.67}$ and $NbCl_{3.18}$ gives -144.3 ± 1.5 kcal/mol. We take the former value.*

As Schäfer and Kablenberg [53] have pointed out, the validity of the decomposition pressure study carried out by Schäfer, Bayer, and Lehman [65] for the decomposition of $NbCl_4(s)$ to form $NbCl_5(g)$ and "$NbCl_3(s)$" is in doubt since it was carried out prior to the work of Schäfer and Dohmann [61]. From the decomposition pressure of $NbCl_5(g)$ over $NbCl_4(s)$ and $NbCl_3(s)$ the former authors obtained an enthalpy and entropy of reaction at 532 K of $\Delta H°$ = 28.3 ± 0.4 kcal and $\Delta S°$ = 47.0 ± 0.6 e.u. for the reaction

$$2NbCl_4(s) \rightarrow NbCl_5(g) + NbCl_3(s)$$

---

*The value -143.6 kcal/mol for $\Delta Hf°$ of $NbCl_{3.13}$ given by the authors could not be verified.

Recalculation of these results using the more accurate vapor pressure equation for solid $NbCl_5$ given by Schäfer and Pölert [51] and liquid $NbCl_5$ given by Johnson et al. [26] plus correction for the vapor pressure of $NbCl_4(s)$ confirms the suspicion of Schäfer, Bayer and Lehman [65] that the solubility of $NbCl_4(s)$ in $NbCl_5(\ell)$* would have an appreciable affect on their results. Recalculation, omitting their data for $NbCl_5(\ell)$, gives for the previous reaction at 532.9 K $\Delta Hf°$ -32.1 ± 0.9 kcal/mol and $\Delta S°$ = 62.7 ± 2.0 e.u. Correction of these results to 298.15 K using the estimated heat capacities of $NbCl_4(s)$ and "$NbCl_3(s)$" given by Schäfer and Kahlenberg [30] on the assumption that "$NbCl_3(s)$" actually had the composition Nb:Cl = 1:3 gives $\Delta Hf°$, $NbCl_3(s)$, = -129.1 ± 4.5 kcal/mol. Linear interpolation between the values determined calorimetrically for $\Delta Hf°$ of $NbCl_{3.13}$ and $NbCl_{2.67}$ gives $\Delta Hf°$, $NbCl_3(s)$ = -140.1 ± 1.5 kcal/mol. The difference of 11 ± 6.0 kcal/mol confirms the suggestion by Schäfer and Kahlenberg [30] that the results of the study by Schäfer, Bayer, and Lehmann must be discarded because the composition of the "$NbCl_3(s)$" phase was unknown.**

Use of the decomposition pressure of $NbCl_5(g)$ over $NbCl_{3.13}(s)$ and $NbCl_4(s)$ cited by Schäfer and Kahlenberg [30] (from the data of Schäfer and Dohmann [61]) gives a value of $S°_{NbCl_{3.13}}(s)$ of 35 ± 5 e.u. which is in good agreement with the estimate of 36 ± 2 e.u. given by Schäfer and Kahlenberg [30]. This is based on the heats of formation taken previously and the estimated heat capacities of $NbCl_4(s)$, $NbCl_{3.13}(s)$ [30], the heat of formation of $NbCl_5(g)$ (see previous section) and $NbCl_5(g)$ thermal functions of Werder et al. [44] and the value of S° for $NbCl_4(s)$ given in the previous section.

3. For $NbCl_{3.13}(s)$, we take $\Delta Hf°(298.15)$ equal to -144.7 ± 1.5 kcal/mol and $S°(298.15)$ = 35 ± 5 e.u. $Cp°(298.15)$ was estimated to be 23±2 cal/mol-K based on the estimate given by Schäfer and Kahlenberg [30]. For $NbCl_{2.67}(s)$, we take $\Delta Hf°(298.15)$ equal to -128.6 ± 1.0 kcal/mol S° is estimated to be 31 ± 2 e.u. and Cp° = 21 ± 1 cal/mol-K on the assumption that $\Delta S°$ and $\Delta Cp°$ are zero for the reactions:

$$1.33\ NbCl_{3.13}(s) = 0.87\ NbCl_{2.67} + 0.46\ NbCl_4(s)$$

$$1.17\ NbCl_{2.67}(s) = NbCl_{3.13}(s) + 0.17\ Nb(s)$$

---

*$NbCl_5(s)$ or $NbCl_5(\ell)$ vapor pressure was used to determine the decomposition pressure of $NbCl_5$.

**Equilibrium conditions may not have been attained.

$NbCl_4(g)$, $NbCl_3(g)$ Addition

A study of the equilibria of Nb(s) and $NbCl_5(g)$ in the temperature range 1100-1700 K by transpiration measurements and mass spectrometry made by Kenshea and Cubiciotti [50] was called to our attention after the previous analysis was completed. Mass spectrometry indicated the principal vapor components were $NbCl_5(g)$, $NbCl_4(g)$ and $NbCl_3(g)$. Their analysis yielded a value of $\Delta H°(298.15\ K)$ for the following reaction of 23 ± 8 kcal/mol

$$\frac{1}{4}\ Nb(s) + NbCl_4(g) = \frac{4}{3}\ NbCl_3(g)$$

Using the previously selected values for the heat of sublimation and formation of $NbCl_4(g)$ at 298.15 K we obtain -86 ± 8 kcal/mol for the heat of formation of $NbCl_3(g)$. This result and our value of $\Delta Hf°$ for $NbCl_4(g)$ agree well with the values determined by the above investigators.

Nb_6Cl_{14}

2. Schäfer and Liedmeier [64] determined the enthalpy of reaction at 298.15 K of

$$NbCl_2(s) + 1.5\ Cl_2(g) = NbCl_5(s)$$

to be + 93.44 ± 0.2 kcal/mol. On the basis of the later work of Simon, Schnering, Wöhrle, and Schäfer [66] which indicates a composition of Nb:Cl = 1:2 consists of a mixture of 1/7 (Nb_6Cl_{14} + Nb), we obtain using the latter's formulation

$$Nb_6Cl_{14}(s) + Nb(s) + 10.5\ Cl_2(g) = 7NbCl_5(s);\ \Delta H°(298) = -654.1 \pm 1.4$$
$$Nb(s) + 2.5\ Cl_2(g) = NbCl_5(s);\ \Delta H°(298) = -190.6 \pm 0.4$$

$$Nb_6Cl_{14}(s) + 8\ Cl_2(g) = 6\ NbCl_5(s);\ \Delta H°(298) = -463.5 \pm 1.8$$

or a heat of formation of $Nb_6Cl_{14}(s)$ of -680.1 ± 5.4 or $NbCl_{2.33}(s)$ of -113.4 ± 0.9 kcal/mol. An estimate for the entropy and heat capacity of $NbCl_{2.33}(s)$ by assuming that $\Delta S°$ and $\Delta Cp°$ are zero for the reaction:

$$2\frac{1}{3}\ NbCl_{2.67} + \frac{1}{3}\ Nb = 2\frac{2}{3}\ NbCl_{2.33}$$

yields S° = 28 ± 2 e.u. and Cp° = 19 ± 1 cal/mol-K. The crystal structure of $Nb_6\ Cl_{14}$ consists of a cage made up of 6 Nb atoms lying at the apices of a slightly flattened octahedron and 12 Cl atoms acting as bridges and lying on the octahedral edges. Six Cl atoms are attached centrifugally to each Nb atom and are shared with other (Nb_6Cl_{12}) cores. In addition 2 of the bridging Cl atoms are shared with adjacent cores so the formula may be written as $[(Nb_6Cl_{10}Cl_{2/2})Cl_{6/2}]$.

1b. Vapor pressure measurements of $NbOCl_3$ have been reported by Morozov and Korshunov [67], Schäfer and Kahlenberg [68], Gloor and Wieland [69], Fairbrother, Cowley, and Scott [70], Meyer, Oosterom, and Van Oeveren [27], t'Hart and Meyer [24,71], Suzuki, Matsushima, Saeki [72]. It has been established on the basis of vapor density measurements [69,73] that $NbOCl_3(g)$ consists principally of monomers in the gas phase and that, depending upon the temperature, larger or smaller amounts of $NbCl_5(g)$ are present [67-72]. Along with $NbOCl_3(s)$ $Nb_2O_5(s)$ has been identified in the solid phase by X-ray diffraction in the temperature range 600-700 K [70,71]. In some vapor pressure experiments a crystalline blue compound has been observed in this temperature range which contains a very small percentage of chlorine [11]. Schäfer, Sibbing, and Gerken [74] have shown in a preparative study that at 800 K or above $Nb_2O_5(s)$ reacts with $NbCl_5(g)$ to produce $Nb_3O_7Cl(s)$ as shown by chemical analysis as well as the course of the reaction pressure. This compound is colorless in the presence of $O_2(g)$ or $Cl_2(g)$ but is blue in their absence. Analysis of a grey powder left on sublimation of $NbOCl_3(s)$ by Schukarev, Smirnova, and Shemyakina [75] yielded a new compound corresponding to the formula $Nb_4O_9Cl_2(s)$ (determined by chemical analysis--the Debye diagram differed from $Nb_2O_5(s)$ or $Nb_3O_7Cl(s)$). The authors suggest the residue might be formed as the result of high temperature hydrolysis as opposed to disporportionation of $NbOCl_3(s)$.

For reasons that are not apparent the total pressure over $NbOCl_3(s)$ of Morozov and Korshunov [67] and Fairbrother, Cowley, and Scott [70] are not in reasonable agreement with the work of the other workers and were not considered further. The results of remaining workers are summarized below in terms of the formula: $\log_{10}P(atm) = +A - B/T$

	A	B	
Schäfer et al. [68]	10.162	6,150	(573-605K)
Gloor et al. [69]	10.652	6,433	(475-605K)
t'Hart et al. [24]*	10.386±0.104	6,290±66	(510-670K)
Suzuki et al. [72]	11.05	6,667	(498-602K)

Since Schäfer et al. [68] did not experimentally determine the amount of $NbCl_5(g)$, further use of their results was not considered. Correction for $NbCl_5(g)$ was made by Gloor et al. [69] by optical methods and by t'Hart et al. [71] and Suzuki et al. [72] by making vapor pressure measurements in the two phase region $NbOCl_3(s)$, $NbCl_5(g)$, $NbOCl_3(g)$. The results obtained are summarized in terms of the formula $\log_{10}P(NbOCl_3,atm) = A - B/T$, $\Delta S°$and $\Delta H°$of sublimation as follows:

	A	B	Temperature Range
Gloor et al.	10.719	6,478	503-609K
t'Hart et al.	10.102±0.91	6,150±58	610-670K
Suzuki et al.	10.47	6,349	498-602K

	$\overline{T}$	$\Delta H°(\overline{T})$	$\Delta S°(\overline{T})$	$\Delta H°(298)$	$\Delta S°(298)$
	K	kcal/mol	e.u.	kcal/mol	e.u.
Gloor et al.	550K	29.6	49.0	31.3	53.2
t'Hart et al.	640K	28.14±.3	46.22±.4	30.4±.6	51.3±1
Suzuki et al.	550K	29.1	47.9	30.8	52.1

Correction of $\Delta H°$and $\Delta S°$sublimation from the midpoint temperature, $\overline{T}$, of each set of measurements was made using thermal functions for $NbOCl_3(g)$ calculated using the vibrational frequency assignments (C_{3V}) given by Beattie, Ozin, and Livingston [76] (see also Djordjevic [77], Brown [78], and Schultz and Stafford [79]). In order to obtain the moments of inertia, the Nb-Cl distance was assumed to be 2.29A° (the same as in $NbCl_5$). This is partly justified since the "nonbonding"Nb-Cl distance derived in the

*These authors use the lower pressure-temperature measurements of Meyer, Oosterom, and Van Oeveren [27] in their analysis of the reaction $5NbOCl_3(g) = NbCl_5(g) + Nb_2O_5(s)$ in [71].

single crystal X-ray work of Sands and Zalkin [80] is 2.24A° which is nearly identical to the 2.25A° in $Nb_2Cl_{10}(s)$. The Nb = O distance was estimated on the basis of electron diffraction studies of $VOCl_3(g)$ (see Palmer [81]) to be about 1.73A°. The heat capacity of $NbOCl_3(s)$ was assumed to be equal to that of $ZrCl_4(s)$ (see [68]).

2. Heats of formation at 298 K of $NbOCl_3(s)$ have been determined by Shchukarev et al. [75] and Schafer et al.[68] by solution calorimetry to be -212.2 ± 1.0 kcal/mol and -210.2 ± 0.7 kcal/mol, respectively.

3. We have taken for $\Delta H°(NbOCl_3(s), 298)$ the value -210.2 ± 1.0 kcal/mol. Using 30.4 ± 0.6 kcal/mol for heat of sublimation of $NbOCl_3(s)$ one obtains for $\Delta H°(NbOCl_3(g), 298.15)$ a value of -179.8 ± 1.6 kcal/mol. Using the thermal functions for $NbOCl_3(g)$ discussed previously one obtains $S°(NbOCl_3(g), 298)$ = 85.6 ± 1 e.u., $Cp°(NbOCl_3(g), 298.15)$ = 28 ± 1 cal/mol-K (estimated), and in combination with an entropy of sublimation of 51.3 ± 1 e.u. for $NbOCl_3(s)$, $S°(NbOCl_3(s), 298.15)$ = 34.3 ± 2 e.u.

Attempts to confirm the thermal functions of $NbOCl_3(g)$ by comparison of calculated and observed results for the equilibrium $5NbOCl_3(g) = 3NbCl_5(g) + Nb_2O_5(s)$, presumed to be occurring in the vapor pressure measurements of $NbOCl_3(s)$, were unsuccessful. The results of the calculations are listed below:

	Calculated Results*			"Observed" Results			
$\overline{T}$	$\Delta G°$	$\Delta H°$	$\Delta S°$	$\Delta G°$	$\Delta H°$	$\Delta S°$	Investigator
K	kcal	kcal	e.u.	kcal	kcal	e.u.	
640	5.6	-59±10	-10.2±4	9.75	-43.0±1.4	-82.5±2.2	[9]
550	-1.8	-59±10	-103±4	6.39	-84	-164	[3]
				4.7	-18	-42	[7]

Which of the various possible reasons is responsible for the various differences is not readily apparent.

2. Schäfer and Liedmeyer [82] have measured the heat of reaction at 298.15 K of

$$NbOCl_2(s) + \frac{1}{2} Cl_2(g) = NbOCl_3(g)$$

---

*See previous sections for $Nb_2O_5(s)$, $NbCl_5(g)$ thermal functions, etc.

From their value of 25.14 ± 0.7 kcal/mol and the value of $\Delta Hf°$ $NbOCl_3(s)$ of -210.2 ± 1 kcal/mol one obtains $\Delta Hf°$ $NbOCl_2(s)$ = -185 ± 1.7 kcal/mol.

$NbBr_5$

1b. Vapor pressure measurements have been made by Alexander and Fairbrother [22] (static method; 481 K - 635 K) and by Berdonosov, Lapitskii, and Bakov [83] (static method using tracers; 478 K - 623 K). The latter used a method which determined the density of the gas and required the assumption that the gas was monomeric and ideal. The good agreement of the measurements with the former confirm these assumptions. The results of the latter are:

	$\overline{T}$	$H°(gas)-H°(cond)$	$S°(gas)-S°(cond)$
	K	kcal/mol	e.u.
$NbBr_5(s)$	500	26.46±0.72	44.08±1.2
$NbBr_5(\ell)$	574	19.89±0.67	31.59±1.1

The calculated triple point of $NbBr_5$ from the vapor pressure equations, 527±1.5 K, agrees well with values determined visually, 528±2 K, and by cooling curves, 527±1 K. Their value is somewhat lower than that obtained by Alexander and Fairbrother [22], 540.7 ± 1 K, but is in good agreement with that obtained by Nisil'son and Sokolova [84], 528 K. Electron diffraction studies of $NbCl_5(g)$ have been carried by Skinner and Sutton [40] and Spiridanov and Romanov [85]. Both are in excellent agreement; the vapor consists of a trigonal bypyramid with the Nb-Br distance of 2.46 ± 0.03A°. No single crystal X-raydiffraction studies of $NbBr_5(s)$ have been made. (Interpretations of powder diffraction data disagree--see [41], [86], [87], [88]). The infrared red spectrum of $NbBr_5(g)$ has been measured by Walton et al. [89] but no vibrational frequency assignment has been made.

2. The heats of formation of $NbBr_5(s)$ have been determined by Shchukarev et al. [90], Schäfer and Heine [91], and Gross et al. [92]. Schukarev et al. [90] determined by solution calorimetry the value for $\Delta Hf°(NbBr_5(s))-\Delta Hf°(Nb_2O_5(s))$ = +91.81 ± 0.9 kcal at 298.15 K. Correcting their results for the new value of $\Delta Hf°$(HBr, ag) [5] and the heat of formation of $Nb_2O_5(s)$ selected previously gives $\Delta Hf°(NbBr_5(s)$, 298.15) = -135.9 ± 1.5 kcal/mol. Schäfer and Heine [91] determined by solution calorimetry the value for $\Delta Hf°(NbBr_5(s)$, 298)-$\Delta Hf°(NbCl_5(s)$,298) = +54.78 ± 0.5 kcal/mol at 298.15 K. Using the value of $\Delta Hf°$ $NbCl_5(s)$ selected previously gives $\Delta Hf°(NbBr_5(s)$,298.15) = -135.8 ± 1.0 kcal/mol.

Gross et al. [92] determined the heat of formation of $NbBr_5(s)$ by direct reaction of $Br_2(\ell)$ with Nb(s) at 110°C. Using an assumed value for the heat capacity of $NbBr_5(s)$ of 34 cal/mol-K, they obtain $\Delta Hf° = -132.85 \pm 0.4$ kcal/mol.

3. We select $\Delta Hf°(NbBr_5(s)) = -132.9 \pm 0.4$ kcal/mol.

References

[1] Keppert, D. L., Vrieze, K., "Halides Containing Multicentered Metal-Metal Bonds", Chapter in "Halogen Chemistry", Vol. 3, Viktor Gutman, Editor, Academic Press (New York, 1967).

[2] King, E. G., J. Am. Chem. Soc. 76, 3289 (1954).

[3] Orr, R. L., J. Am. Chem. Soc. 75, 2808 (1953).

[4] Hultgren, R., Orr, R. L., Anderson, P. D., and Kelley, K. K., "Selected Values of Thermodynamic Properties of Metals and Alloys", John Wiley and Sons (New York, 1963).

Hultgren, R., Orr, R. L., and Kelley, K. K., "Supplement to Selected Thermodynamic Properties of Metals and Alloys", Lawrence Radiation Laboratory, Univ. of California, Berkeley, California.

[5] Wagman, D. D., Evans, W. H., Halow, I., Parker, V. B., Bailey, S. M., and Schumm, R. H., NBS Tech. Notes 270-3 and 270-4.

[6] Dow Chemical Company, JANAF Thermochemical Tables, PB-168-170. (Clearinghouse for Federal Scientific and Technical Information, Springfield, Virginia, 1965).

[7] Brady, A. P., Myers, O. E., and Claus, J. K., J. Phys. Chem. 64, 588 (1960).

[8] Ruff, O., and Schiller, C., Z. anorg. u. allgem. chem. 72, 329 (1911).

[9] Junkins, J. H., Farrar, R. L., Jr., Barber, E. J., and Bernhardt, H. A., J. Am. Chem. Soc. 74, 3464 (1952).

[10] Fairbrother, F., and Frith, W. C., J. Chem. Soc. 3051 (1951).

[11] Romanov, G. V., Spiridanov, V. P., Vestn. Mosk. Univ. Khim. 23, 7 (1968).

[12a] Edwards, J. A., J. Chem. Soc. 3714 (1964).

[12b] Fairbrother, F., Grundy, K. H., and Thompson, A., J. Chem. Soc. 761 (1965).

[13] Blanchard, S., J. Chem. Phys. 62, 919 (1965).

[14] Selig, H., Reis, A., and Gasner, E. L., J. Inorg. Nucl. Chem. 30, 2087 (1968).

[15] Beattie, I. R., Livingstone, K. M., Ozin, G. A., and Reynolds, D. J., J. Chem. Soc. (A) 963 (1969).

[16] Oulette, T. J., Ratcliffe, C. T., and Sharp, D. W. A., J. Chem. Soc. (A) 2351 (1969).

[17] Greenberg, E., Natke, C. A., and Hubbard, W. N., J. Phys. Chem. 69, 2089 (1965).

[18] Myers, O. E., and Brady, A. P., J. Phys. Chem. 64, 591 (1960).

[19] Kenshea, F. B., Cubicciotti,D., Withers, G., and Eding, H., J. Phys. Chem. 72, 1272 (1968).

[20] Opykhtina, M. A., Fleischer, N. A., Zhur. Obshch. Khim. 7, 2016 (1937).

[21] Tarasenkov, D. N., and Komandin, A. V., Zhur. Obshchei Khim. 10, 1319 (1940).

[22] Alexander, K. M., and Fairbrother, F., J. Chem. Soc. S223 (1949).

[23] Ainscough, J. B., Holt, R. J. W., and Trowse, F. W., J. Chem. Soc. 1034 (1957).

[24] t'Hart, W., Meyer, G., Rec. trav. chim. 84, 1155 (1965).

[25] Nisil'son, L. A., Rustil'nik, A. I., Gavilov, O. R., and Rodin, V. A., Zhur. Neorg. Khim. 10, 2339 (1965).

[26] Johnson, J. W., Silva, W. J., and Cubicciotti, D., High Temp. Sci. 2, 20 (1970).

[27] Meyer, G., Oosterom, J. F., van Oeveren, W. J., Rec. trav. chim. 80, 502 (1961).

[28] Schäfer, H., and Pietruck, C., Zeit. anorg. u. allgem. Chem. 267, 174 (1951).

[29] Schäfer, H., Bayer, L., and Lehman, H., Zeit. anorg. u. allgem. Chem. 268, 268 (1952).

[30] Schäfer, H., and Kahlenberg, F., Z. anorg. u. allgem. Chem. 305, 291 (1960).

[31] Palkin, A. P., and Chikanov, N. D., Russ. J. Inorg. Chem. 4, 407 (1959).

[32] Nisil'son, L. A., and Perekhrest, G. L., Zhur. Neorg. Khim. 3, 2150 (1958).

[33] Sheka, I. A., Voitovich, B. A., and Nisil'son, L. A., Russ. J. Inorg. Chem. 4, 1803 (1959).

[34] Johnson, J. W., Cubicciotti, D., High Temp. Sci. 2, 9 (1970).

[35] Nisil'son, L. A., Pustil'nik, A. I., and Sokolova, T. D., Russ. J. Inorg. Chem. 9, 574 (1964).

[36] Nagajarin, G., Bull. Soc. Chim. Belges. 71, 324 (1963).

[37] Gaunt, J., and Ainscough, J. B., Spectrochim. Acta 10, 52 (1957).

[38] Carlson, G. L., Spectrochim. Acta 19, 1291 (1963).

[39] Kyrnauw , G. N., Pistorius, C. W. F. T., and Pistorius, M. C., Z. Phys. Chem. (Frankfurt) 43, 213 (1964).

[40] Skinner, H. A., and Sutton, L. E., Trans. Faraday Soc. 36, 668 (1940).

[41] Zalkin, Z., and Sands, D. E., Acta Crystallogr. 11, 615 (1958).

[42] Kepert, D. L., Nyholm, R. S., J. Chem. Soc. 2871 (1965).

[43] Bader, R. F., and Westland, A. D., Canad. J. Chem. 39, 2306 (1961).

[44] Werder, R. D., Fry, R. A., and Gunthard, Hs. H., J. Chem. Phys. 47, 4159 (1967).

[45] Walton, R. A., Brisdon, B. J., Spectrochim. Acta 23A, 2489 (1967).

[46] Beattie, I. R. Gilson, T. R., and Ozin, G. A., J. Chem. Soc. (A) 2765 (1968).

[47] Gross, P., Hayman, C., Levi, D. L., and Wilson, G. L., Trans. Faraday Soc. 56, 318 (1960).

[48] Shchukarev, C. A., Oranskaya, M. A., Shemyakina, T. S., Russ. J. Inorg. Chem. 5, 1036 (1960).

[49] Retznitskii, L. A., Russ. J. Inorg. Chem. 41, 787 (1967).

[50] Kenshea, F. J., and Cubicciotti, D., J. Phys. Chem. 73, 3054 (1969).

[51] Schäfer, H., Pölert, W., Z. anorg. u. allgem. Chem. 353, 78 (1967).

[52] Schäfer, H., and Bayer, L., Z. anorg. u. allgem. Chem. 277, 140 (1954).

[53] Schäfer, H., Goser, C., and Bayer, L., Z. anorg. u. allgem. Chem. 265, 258 (1961).

[54] McCarley, R. E., and Boatman, J. C., Inorg. Chem. 2, 547 (1963).

[55] McCarley, R. E. and Torp, B. A., Inorg. Chem. 2, 540 (1968).

[56] Schäfer, H., Scholz, H., and Gerkin, R., Z. anorg. u. allgem. Chem. 331, 154 (1964).

[57] Schnering, H. G., and Wöhrle, K., Angew. Chem. 75, 684 (1963).

[58] Frére, P., Ann. chim. Paris 7, 85 (1962).

[59] Schäfer, H., and von Schnering, H. G., Angew. Chem. 76, 833 (1964).

[60] Ainscough, J. B., Holt, R. J. W., and Trowse, F. W., IGR-TN/S-804, 11 pp. (1958).

[61] Schäfer, H., Dohman, K., Z. anorg. u. allgem. Chem. 300, 1 (1959).

[62] von Schnering, H. G., Wöhrle, H., and Schäfer, H., Naturwiss. 48, 159 (1961).

[63a] Cotton, H. A., and Wilkinson, G., "Advanced Inorganic Chemistry", Interscience Publishers (New York, 1966).

[63b] Fairbrother, F., "The Chemistry of Niobium and Tantalum", Elvesier Publishing Co. (New York, 1967).

[64] Schäfer, H., and Liedmeier, F., J. Less-Common Metals 6, 307 (1964).

[65] Schäfer, H., Bayer, L., and Lehmann, H., Z. anorg. u. allgem. Chem. 268, 268 (1952).

[66] Simon, A., Schnering, H. G., Wöhrle, H., and Schäfer, H., Z. anorg. u. allgem. Chem. 339, 155 (1965).

[67] Morozov, I. S., Korshunov, B. G., Akad. Nauk. SSSR, Inst. Obschei Neorg. Khim. 2, 102 (1955).

[68] Schäfer, H., Kahlenberg, F., Z. anorg. u. allgem. Chem. 305, 327 (1960).

[69] Gloor, M., and Wieland, K., Helv. Chim. Acta 44, 1098 (1961).

[70] Fairbrother, F., Cowley, A. H., and Scott, N., J. Less-Common Metals 1, 206 (1959).

[71] t'Hart, W., and Meyer, G., Rec. trav. chim. 86, 1191 (1967).

[72] Suzuki, T., Matsushima, T., and Saeki, Z., Trans. Natl. Research Inst. Metals (Tokyo) 6, (5), 222-5(1964) (Eng.) Published in Denki-Kagaku 32, 671 (1964).

[73] Deville, H. S.-C., and Troost, L., C. R. Lebd. Seáces Acad. Sci. 64, 294 (1897).

[74] Schäfer, H., Sibbing, E., and Gerken, R., Z. anorg. u. allgem. Chem. 307, 11 (1961). see also Schäfer, H., Sibbing, E., Z. anorg. u. allgem. Chem. 305, 341 (1960).

[75] Shchukarev, S. A., Smirnova, E. K., Shemyakina, T. S., and Ryabov, A. N., Russ. J. Inorg. Chem. 7, 626 (1962).

[76] Beattie, I. R., Livingstone, K. M. S., Reynolds, D. J., and Ozin, G. A., J. Chem. Soc. (A) 1210 (1970).

[77] Djordjevic, C., Spectrochim. Acta 21, 301 (1965).

[78] Brown, D., J. Chem. Soc. 4944 (1964).

[79] Schultz, C. O., and Stafford, F. E., J. Phys. Chem. 72, 4686 (1968).

[80] Sands, D. E., Zalkin, A., and Elson, R. E., Acta Cryst. 12, 21 (1959).

[81] Palmer, K. J., J. Am. Chem. Soc. 60, 2360 (1938).

[82] Schäfer, H., and Liedmeier, F., Z. anorg. u. allgem. Chem. 329, 225 (1964).

[83] Berdonosov, S. S., Lapitskii, A. V., and Bakov, E. V., Russ. J. Inorg. Chem. 10, 173 (1965).

[84] Nisil'son, L. A., and Sokolova, T. D., Russ. J. Inorg. Chem. 9, 1117 (1964).

[85] Spiridonov, V. P., and Romanov, G. V., Vestn. Mosk. Univ. Ser. II 21, 109 (1966).

[86] Berdonosov, S. S., Lapitskii, A. V., Berdonosova, D. G., and Ulasov, L. G., Russ. J. Inorg. Chem. 8, 1315 (1963).

[87] Rolsten, R. F., J. Phys. Chem. 62, 126 (1958).

[88] Dorschner, R., Dehaud, J., Bull. Soc. Chim. France 2056 (1967).

[89] Walton, R. A., and Brisdon, B. J., Spectrochim. Acta 23A, 2489 (1967).

[90] Shchukarev, S. A., Smirnova, E. K., Vasil'kova, I. V., and Borokova, N. I., Russ. J. Inorg. Chem. 7, 625 (1962).

[91] Schäfer, H., and Heine, H., Z. anorg. u. allgem. Chem. 352, 258 (1967).

[92] Gross, P., Hayman, C., Levi, D. L., and Wilson, G. L., Trans. Faraday Soc. 58, 890 (1962).

USCOMM-NBS-DC

UNCLASSIFIED

Security Classification

DOCUMENT CONTROL DATA - R & D

(Security classification of title, body of abstract and indexing annotation must be entered when the overall report is classified)

1. ORIGINATING ACTIVITY (Corporate author)

National Bureau of Standards
Washington, D. C. 20234

2a. REPORT SECURITY CLASSIFICATION

UNCLASSIFIED

2b. GROUP

3. REPORT TITLE

INTERIM REPORT ON THERMODYNAMICS OF CHEMICAL SPECIES IMPORTANT TO ROCKET TECHNOLOGY.

4. DESCRIPTIVE NOTES (Type of report and inclusive dates)

Scientific Interim

5. AUTHOR(S) (First name, middle initial, last name)

Thomas B. Douglas
Charles W. Beckett

6. REPORT DATE

1 July 1970

7a. TOTAL NO. OF PAGES

221

7b. NO. OF REFS

254

8a. CONTRACT OR GRANT NO.

ISSA 69-001

b. PROJECT NO.

9750-01

c. 61445014

d. 681308

9a. ORIGINATOR'S REPORT NUMBER(S)

NBS Report 10326

9b. OTHER REPORT NO(S) (Any other numbers that may be assigned this report)

AFOSR 70-2395TR

10. DISTRIBUTION STATEMENT

2. This document is subject to special export controls and each transmittal to foreign governments or to foreign nationals may be made only with prior approval of the AFOSR (SRGO).

11. SUPPLEMENTARY NOTES

TECH, OTHER

12. SPONSORING MILITARY ACTIVITY

Air Force Office of Scientific Research
1400 Wilson Boulevard
Arlington, Virginia 22209

13. ABSTRACT

The heat of formation of ClF, measured in a flame calorimeter, favors 32 kcal/mol for the dissociation energy of F_2. A transpiration search near 1200 K for gaseous reaction between HF (up to 3/4 atm) and AlF_3 indicates low stability for $HAlF_4$. Selected thermodynamic properties of niobium compounds from an up-to-date critical literature review are discussed and tabulated. The heat capacity, electrical resistivity, and hemispherical total and normal spectral emittances of tantalum (including the emittance change on melting) were measured 1900-3200 K by a high-speed pulse technique, which is also adapted to measuring the melting points of thin-wire conductors above 2000 K. Detailed calculations, made in a feasibility study of seeking unknown beryllia hydrates by transpiration, show promise of increasing the temperature-measuring consistency above 2000 K by comparing with the volatility of gold. The heat capacity, enthalpy, and heat of fusion of barium were measured 18-1173 K (these show several anomalies), leading to previously missing thermodynamic functions; the latter permitted for the first time a third-law analysis of published vapor pressures of this metal. Atomic barium, deposited in solid-argon matrices containing isotopic varieties of O_2, yielded two infrared stretching frequencies of BaO_2; that due to the O-O group suggests that the molecule has essentially the ionic structure $Ba^+ O_2^-$.

DD FORM 1 NOV 65 1473

UNCLASSIFIED

Security Classification

KEY WORDS	LINK A		LINK B		LINK C	
	ROLE	WT	ROLE	WT	ROLE	WT
Thermodynamic Properties						
Thermochemistry						
Rocket Technology						
Critical Data Reviews						
High-Speed Measurements						
Matrix-Isolation Infrared Spectroscopy						
Transpiration						
Heat-Capacity Calorimetry						
Barium Metal						
Chlorine Monofluoride						
Barium Dioxide Molecule						
Tantalum						
Niobium and Its Compounds						
Melting Points of Electrical Conductors						
Hydrogen Fluoroaluminate						
Dissociation Energy of Fluorine						

NBS TECHNICAL PUBLICATIONS

PERIODICALS

JOURNAL OF RESEARCH reports National Bureau of Standards research and development in physics, mathematics, chemistry, and engineering. Comprehensive scientific papers give complete details of the work, including laboratory data, experimental procedures, and theoretical and mathematical analyses. Illustrated with photographs, drawings, and charts.

Published in three sections, available separately:

• Physics and Chemistry

Papers of interest primarily to scientists working in these fields. This section covers a broad range of physical and chemical research, with major emphasis on standards of physical measurement, fundamental constants, and properties of matter. Issued six times a year. Annual subscription: Domestic, $9.50; foreign, $11.75*.

• Mathematical Sciences

Studies and compilations designed mainly for the mathematician and theoretical physicist. Topics in mathematical statistics, theory of experiment design, numerical analysis, theoretical physics and chemistry, logical design and programming of computers and computer systems. Short numerical tables. Issued quarterly. Annual subscription: Domestic, $5.00; foreign, $6.25*.

• Engineering and Instrumentation

Reporting results of interest chiefly to the engineer and the applied scientist. This section includes many of the new developments in instrumentation resulting from the Bureau's work in physical measurement, data processing, and development of test methods. It will also cover some of the work in acoustics, applied mechanics, building research, and cryogenic engineering. Issued quarterly. Annual subscription: Domestic, $5.00; foreign, $6.25*.

TECHNICAL NEWS BULLETIN

The best single source of information concerning the Bureau's research, developmental, cooperative and publication activities, this monthly publication is designed for the industry-oriented individual whose daily work involves intimate contact with science and technology—*for engineers, chemists, physicists, research managers, product-development managers, and company executives.* Annual subscription: Domestic, $3.00; foreign, $4.00*.

* Difference in price is due to extra cost of foreign mailing.

NONPERIODICALS

Applied Mathematics Series. Mathematical tables, manuals, and studies.

Building Science Series. Research results, test methods, and performance criteria of building materials, components, systems, and structures.

Handbooks. Recommended codes of engineering and industrial practice (including safety codes) developed in cooperation with interested industries, professional organizations, and regulatory bodies.

Special Publications. Proceedings of NBS conferences, bibliographies, annual reports, wall charts, pamphlets, etc.

Monographs. Major contributions to the technical literature on various subjects related to the Bureau's scientific and technical activities.

National Standard Reference Data Series. NSRDS provides quantitative data on the physical and chemical properties of materials, compiled from the world's literature and critically evaluated.

Product Standards. Provide requirements for sizes, types, quality and methods for testing various industrial products. These standards are developed cooperatively with interested Government and industry groups and provide the basis for common understanding of product characteristics for both buyers and sellers. Their use is voluntary.

Technical Notes. This series consists of communications and reports (covering both other agency and NBS-sponsored work) of limited or transitory interest.

Federal Information Processing Standards Publications. This series is the official publication within the Federal Government for information on standards adopted and promulgated under the Public Law 89–306, and Bureau of the Budget Circular A–86 entitled, Standardization of Data Elements and Codes in Data Systems.

Order NBS publications from:

Superintendent of Documents
Government Printing Office
Washington, D.C. 20402


DEPARTMENT OF COMMERCE
NATIONAL BUREAU OF STANDARDS